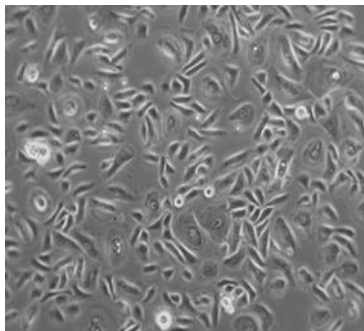
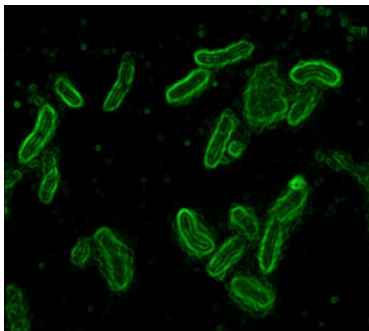


DEVELOPMENT AND EVALUATION OF ENGINEERED BACTERIOPHAGE ENDOLYSINS FOR INACTIVATION OF GRAM-NEGATIVE BACTERIA



Maarten Walmagh

Proefschrift voorgedragen tot
het behalen van de graad van Doctor
in de Bio-ingenieurswetenschappen

Januari 2013

Cover illustrations:

Left: *Pseudomonas aeruginosa* PAO1 cells with green jacket due to OBP₁₋₁₁₇-EGFP cell wall binding

Center: Confluent grown human keratinocytes derived from neonatal foreskin

Right: *Caenorhabditis elegans* nematode SS104

©2013 KU Leuven, Groep Wetenschap & Technologie, Arenberg Doctoraatschool, W. de Croylaan 6, 3001 Heverlee, België

Alle rechten voorbehouden. Niets uit deze uitgave mag worden vermenigvuldigd en/of openbaar worden gemaakt door middel van druk, fotokopie, microfilm, elektronisch en op welke andere wijze ook zonder voorafgaande schriftelijke toestemming van de uitgever.

All rights reserved. No part of this publication may be reproduced in any form of print, photoprint, microfilm, electronic or any other means without written permission from the publisher.

ISBN 978-90-8826-281-4

D/2913/11.109/8

DEVELOPMENT AND EVALUATION OF ENGINEERED BACTERIOPHAGE ENDOLYSINS FOR INACTIVATION OF GRAM-NEGATIVE BACTERIA

Maarten WALMAGH

Promotor:

Prof. Rob Lavigne, KU Leuven

Leden van de examencomissie:

Prof. Maurice De Proft, KU Leuven

Prof. Chris Michiels, KU Leuven

Prof. Bruno Goddeeris, KU Leuven

Prof. Christophe Courtin, KU Leuven

Prof. Henri De Greve, VUB, Brussels

Dr. Laurent Debarbieux, Institut Pasteur, Paris

Proefschrift voorgedragen tot het
behalen van de graad van Doctor
in de Bio-ingenieurswetenschappen

Januari 2013

Table of contents

Dankwoord	I
Summary	III
Samenvatting	V
List of abbreviations	VIII
List of publications	IX
Chapter 1 Introduction and background	1
1.1 General introduction	1
1.2 Bacteriophage-encoded peptidoglycan hydrolases	2
1.2.1 History on bacteriophage-encoded peptidoglycan hydrolases	3
1.2.2 Natural role of peptidoglycan hydrolases in bacterial lysis mechanisms	5
1.2.3 Structural composition of phage endolysins	9
1.3 Gram-negative outer membrane as a natural barrier for external agents	17
1.3.1 Structure and diversity of lipopolysaccharide	17
1.3.2 Outer membrane-based resistance mechanisms	24
1.3.3 Possible strategies to overcome the outer membrane barrier	27
1.4 Antimicrobial peptides	32
1.4.1 Structure of antimicrobial peptides	32
1.4.2 Mode of action of antimicrobial peptides	33
1.4.3 Optimizing activity of antimicrobial peptides	40
Chapter 2 Aims and study objectives	41
Chapter 3 Materials and methods	43
3.1 Bacterial strains and <i>Caenorhabditis elegans</i> SS104	43
3.2 Cloning, recombinant large scale expression and protein purification	44
3.2.1 Cloning methodology	50
3.2.2 Recombinant large scale expression and purification protocols	52
3.3 Biochemical and biophysical assays	54
3.3.1 Peptidoglycan degrading or muralytic assay	54
3.3.2 Fluorescence binding assay	55
3.3.3 Surface Plasmon Resonance	56
3.4 In vitro assays	56
3.4.1 In vitro antibacterial assay	56
3.4.2 In vitro biofilm assay	57
3.4.3 In vitro human keratinocyte assays	58
3.5 In vivo <i>Caenorhabditis elegans</i> assays	59
3.5.1 Cytotoxic effects of compounds on <i>C. elegans</i>	59
3.5.2 <i>C. elegans</i> infection and survival assays	59
Chapter 4 Preface: selecting most promising Gram-negative phage endolysins	61
Chapter 5 Characterization of six novel, single-domain endolysins from Gram-negative infecting bacteriophages	65
5.1 In silico structural analysis of six novel, single-domain endolysins	66
5.2 Biochemical properties of six novel, single-domain endolysins	68
5.2.1 pH-dependency	68
5.2.2 Quantification of muralytic activity	69
5.2.3 Stability at 4°C and 50°C	71

5.3 <i>In vitro</i> antibacterial activity	72
5.4 Discussion	74
Chapter 6 Characterization of modular bacteriophage endolysins from <i>Myoviridae</i> phages OBP, 201φ2-1 and PVP-SE1	77
6.1 Modularity feature in OBPgp279, 201φ2-1gp229 and PVP-SE1gp146	78
6.1.1 <i>In silico</i> domain prediction in OBPgp279, 201φ2-1gp229 and PVP-SE1gp146.....	78
6.1.2 The predicted peptidoglycan binding domains in OBPgp279, 201φ2-1gp229 and PVP-SE1gp146	80
6.2 Biochemical properties of OBPgp279, 201φ2-1gp229 and PVP-SE1gp146	83
6.2.1 Substrate specificity.....	83
6.2.2 Quantification of muralytic activity	84
6.2.3 Activity after heat treatment.....	87
6.3 <i>In vitro</i> antibacterial activity	88
6.4 Discussion	90
Chapter 7 N-terminal single and double fusion modifications of OBPgp279 and PVP-SE1gp146	97
7.1 Introduction.....	97
7.1.1 Hydrophobic peptides: pentapeptide and ArtiMW1 peptides.....	97
7.1.2 Polycationic peptide: PK peptide.....	99
7.1.3 Combining the best of both: amphipathic peptides.....	99
7.2 Cloning, expression and purification of N-terminally fused OBPgp279 and PVP-SE1gp146 variants	100
7.3 <i>In vitro</i> antibacterial activity of N-terminal OBPgp279 and PVP-SE1gp146 fusion variants ..	102
7.4 Cloning, expression and purification of N-terminal double fusion variants of OBPgp279 and PVP-SE1gp146	105
7.5 <i>In vitro</i> antibacterial activity of N-terminal double fusion variants of OBPgp279 and PVP-SE1gp146.....	107
7.6 Discussion	109
Chapter 8 Evaluation and optimization of PK peptide fusion approach.....	113
8.1 Introduction.....	113
8.2 Influence of N-terminal PK peptide fusion on endolysin characteristics.....	113
8.2.1 Influence on expression yield	113
8.2.2 Influence on muralytic activity	115
8.2.3 Influence on pH-dependency	116
8.2.4 Influence on activity of OBPgp279 and PVP-SE1gp146 after heat treatment.....	117
8.2.5 Influence on <i>in vitro</i> antibacterial activity.....	118
8.3 Biofilm-degrading potential of PK peptide fusion approach	121
8.4 Strategies to optimize the PK peptide fusion approach... ..	123
8.4.1 By switching the PK peptide to the C-terminal end of OBPgp279 and PVP-SE1gp146	123
8.4.2 By extension of linker length between N- or C-terminal PK peptide and endolysin....	128
8.5 Discussion	133
Chapter 9 Antibacterial potential and cytotoxicity of PK-fused endolysin on an <i>in vitro</i> human keratinocyte infection model	137
9.1 A keratinocyte monolayer as alternative <i>in vitro</i> model	137
9.2 Cytotoxicity assessment on growing human keratinocytes	137
9.3 Antibacterial efficacy on a keratinocyte infection model	140

9.4 Discussion	142
Chapter 10 Antibacterial potential and cytotoxicity of PK fusion endolysins on an <i>in vivo Caenorhabditis elegans</i> nematode model	147
10.1 <i>C. elegans</i> as model organism for bacterial pathogenesis.....	147
10.2 Cytotoxicity assessment on <i>C. elegans</i>	148
10.3 <i>In vivo</i> antibacterial efficacy on <i>C. elegans</i>	150
10.3.1 Selection of appropriate <i>P. aeruginosa</i> strain for infection of <i>C. elegans</i> SS104	150
10.3.2 Survival of <i>P. aeruginosa</i> PA14-infected <i>C. elegans</i> upon endolysin treatment	151
10.4 Discussion	153
Chapter 11 General conclusions and future perspectives	157
11.1 From fundamental conclusions and perspectives.....	157
11.1.1 Modular versus single-domain endolysins of Gram-negative infecting phages.....	157
11.1.2 Extending the base of the endolysin pyramid	158
11.1.3 Structural analysis of characterized endolysins and their interactions.....	159
11.2 ...to application-oriented conclusions and perspectives	159
11.2.1 PK peptide fusion as ideal starting point to tackle the outer membrane <i>in vitro</i>	159
11.2.2 Biofilm-degrading potential of PK peptide fusion approach	161
11.2.3 Safety and antibacterial efficacy in keratinocyte and <i>C. elegans</i> infection models ...	162
11.2.4 Taking the PK peptide fusion approach to a next level	164
11.2.5 Issues in future development of PK fusion approach.....	164
11.3 Widening the possibilities: from phage therapy to natural predators	167
References	171

Dankwoord

“Pff”. Op deze zucht heb ik mij regelmatig betrappt de afgelopen vier jaar als doctoraatstudent. Ze verborg vaak de teleurstelling omwille van een zoveelste mislukt experiment, de logica of inspiratie die even zoek was of een paper die maar niet aanvaard werd ondanks al het harde werk. Gelukkig was er ook regelmatig een motiverende “Yes” te horen, na een onverwacht positief resultaat of een nieuw verworven kijk op de dingen. Naarmate het doctoraat vorderde nam de “Yes” meer en meer de overhand van de “Pff”, en de volgende mensen hebben hier een belangrijke bijdrage aan gehad.

Allereerst een bijzondere dank aan mijn toegewijde en enthousiaste promotor Prof. Rob Lavigne van wie ik heel veel heb bijgeleerd op professioneel vlak en wiens deur altijd open stond voor advies, kritische discussies, brainstorming of dagelijkse babbeltjes. Ging het wat minder tijdens die vier jaren onderzoek dan was hij er om mij te blijven motiveren en aan te moedigen. Iemand op wie je altijd kon terugvallen, een rots in de branding.

Uiteraard moet ik hier ook Dr. Yves Briers vermelden omdat hij degene was die mij vijf jaar geleden met heel veel enthousiasme en fascinatie heeft geïntroduceerd in the endolysine-onderzoek, mij mijn eigen weg heeft laten zoeken hierin met zijn “ups” en “downs”, en vele uren heeft gestoken in het kritisch becommentariëren van mijn doctoraatschrijfsels. Een welgemeende dankuwel hiervoor, Yves, jouw ervaring en inzicht waren van goudwaarde voor mijn onderzoek.

Mijn assessoren, Chris Michiels en Bruno Goddeeris, en de andere leden van mijn examencommissie wil ik bedanken voor hun bereidheid om in mijn doctoraatsjury te zetelen en deze zware kloef te doorworstelen. Met hun opmerkingen en suggesties tilden zij dit manuscript tot een hoger niveau. Voor de financiële steun als specialisatiebursaal zou ik graag IWT Vlaanderen willen bedanken.

Een niet te onderschatten factor tijdens die vier jaar waren de vele terrasjes, BBQ's, feestjes en sportieve momenten (handbal, netbal, frisbee, korfbal, honkbal, bowling...) die ik samen beleefde met mijn collega labogenootjes en die er voor zorgden dat het altijd voelde als thuiskomen in ons labo. Bart, Wesley, Andrew, Stijn, Elke, Gert en Anneleen, jullie zijn mij met succes voorgegaan en verkennen nu andere horizonten. Marleen, Barbara en Chris, jullie als laboranten wil ik bedanken voor de administratieve en technische ondersteuning tijdens mijn doctoraat. Dank ook aan alle doctoraatsstudenten (Elke, Joleen, Dieter, Anneke, Jessica, Birgit, Jeroen DS, Sofie, Bob, Elisabete, Hugo, Barbara en Diana) en post-docs (Pieter-Jan, Yves en Anne-Sophie) voor het creëren van die fantastische labo-atmosfeer. Zonder jullie had ik het zeker geen vier jaar volgehouden.

Samen met mijn jaargenoten Katrien, Evelien en Jeroen W. hebben we vele watertjes doorzwommen om te komen waar we nu staan: van de kandidatuurjaren als frisse groentjes, de proclamatie als fiere bio-ingenieurs tot het behalen van onze doctoraatstitel. Ik wil jullie alle drie bedanken voor alle vreugdevolle momenten die we samen beleefden tijdens die negen jaar. Ook voor jou, Jeroen W., is het einde bijna in zicht. Nog even doorbijten, senior PhD!

Ik mag hier zeker niet mijn thesisstudentjes Javier, Beker, Jan en Victor vergeten die ik met veel passie en plezier voor het vak heb begeleid en warm gemaakt voor wetenschappelijk onderzoek. Hun enthousiasme, humor en inzet maakten er een geweldige samenwerking van. Jullie mogen fier zijn op de belangrijke bijdrage die jullie aan dit eindwerk leverden. Hopelijk heb ik ook mijn steentje bijgedragen aan jullie ontwikkeling tot kritische wetenschappers. Het ga jullie goed in jullie verdere professionele carrière.

Rob moedigt als geen ander de samenwerking met andere labo's aan. Opbouwen van inzicht en expertise in andere technieken en domeinen is iets wat elke wetenschapper drijft of moet drijven. De mogelijkheden tot samenwerking met prof. Michiels (Centrum voor Levensmiddelenmicrobiologie, Leuven), Dr. Pirnay (Lab MCT, Neder-Over-Heembeek, Brussel) en prof. Hernalsteens (GEVI, VUB, Brussel) boden een meerwaarde voor mijn onderzoek en voor mijn professionele ontwikkeling. Ik wil hun en alle medewerkers in deze labo's dan ook bedanken voor hun gastvrijheid, het beschikbaar stellen van hun materiaal en de overdracht van hun expertise.

Mijn ouders en mijn broer hebben mij al die jaren als student met veel enthousiasme blijven steunen. Ik ben ontzettend blij dat jullie al die jaren in mij bleven geloven. Jullie hebben mij deels gevormd tot wat ik nu ben en daar mogen jullie terecht fier op zijn. Ten slotte draag ik dit eindwerk speciaal op aan twee supertoffe die recent zijn heen gegaan: mijn Bomma en Bompa. Jammer dat jullie als fiere grootouders er niet meer bij zijn op de publieke verdediging om te zien wat jullie kleinzoon al die jaren heeft uitgespookt daar in het verre Leuven. Al ben ik er van overtuigd dat jullie van daarboven deze mijlpaal in mijn leven gelukkig gadeslaan. Het ga jullie goed.

Negen jaar student zijn, een belangrijk deel van je leven, eentje met onvergetelijke momenten. Met het behalen van dit doctoraat sluit ik deze periode met grote voldoening af. Een nieuw leven gaat nu voor mij open, een stap in het onzekere, maar met de nodige bagage om er iets moois van te maken.

Maarten,
Januari 2013

Summary

Bacteriophages, viruses infecting bacteria, disrupt the bacterial cell wall at the end of their replication cycle to release newly produced virions. The major constituent of the bacterial cell wall is the peptidoglycan. To degrade this rigid layer, bacteriophages encode peptidoglycan hydrolases, called endolysins, that hydrolyze specific bonds in the peptidoglycan. This dissertation specifically focuses on endolysins, isolated from phages infecting Gram-negative bacterial species, including *Pseudomonas aeruginosa*, *Salmonella* Typhimurium, *Escherichia coli*, *Klebsiella pneumoniae* and *Citrobacter rodentii*. Most of these bacteria are opportunistic pathogens that are of increasing concern in hospitals due to their high intrinsic and acquired antibiotic resistance.

In a first part of this study, we extend the pool of available endolysins from Gram-negative origin and analyze their potential and applicability as alternative antibacterial agents for antibiotics to combat these Gram-negative pathogens. The Gram-negative outer membrane prevents exogenously applied endolysins from reaching the peptidoglycan layer and protects bacteria against their lytic activity. We therefore evaluate in the second part of this dissertation an approach that allows the endolysin to efficiently destabilize the outer membrane and subsequently reach the peptidoglycan. This approach consists of the fusion of a set of outer membrane-permeabilizing antimicrobial peptides to the endolysin to allow for an autonomous interaction with the outer membrane. To sketch the background, this dissertation starts with an overview of the literature concerning bacteriophage endolysins (history and structural diversity), antimicrobial peptides (types and mode of action) and outer membrane diversity present among Gram-negative bacteria.

From an *in silico* analysis of fully sequenced phage genomes, a selection of fifteen interesting candidate endolysins is made (Chapter 4). Six single-domain (Chapter 5) and three modular (Chapter 6) endolysins with the highest maximal muralytic activity under physiological conditions, are selected for extensive characterization on biochemical (pH-dependency, enzymatic activity, activity upon heating) and antibacterial level. In this way, we aim to prove their lytic role and to reveal enzyme-specific characteristics interesting from an application perspective. *In silico*, the single-domain endolysins consist of a catalytic domain, whereas the modular ones feature an N-terminal peptidoglycan binding domain and a C-terminal catalytic domain, hitherto a unique property present in a few endolysins from Gram-negative origin. In addition, the predicted peptidoglycan binding domains are experimentally verified.

The modular endolysins in this study are shown to be enzymatically more active than the single-domain endolysins, an observation that was translated into their *in vitro* antibacterial activity. Of all tested endolysins, the modular endolysin from *Pseudomonas fluorescens* phage OBP, OBPgp279, shows the highest muralytic and antibacterial activity, followed by PVP-SE1gp146, the endolysin from *Salmonella* Enteritidis phage PVP-SE1. The peptidoglycan

binding domain present in modular endolysins accounts for their strong lytic action since the contribution of this domain (38 to 56 %) to the total enzymatic activity is considerable. In addition, the enzymatic activity is consistent for the different Gram-negative bacterial species due to their conserved peptidoglycan (A1 γ chemotype). This characterization also revealed various interesting biochemical properties. OBPgp279 shows intrinsic antibacterial activity on *P. aeruginosa* PAO1 (± 1 log unit), probably by destabilizing the *Pseudomonas* outer membrane. PVP-SE1gp146 remains active up to temperatures of 90°C with 60 % residual enzymatic activity after 40 minutes. This last property makes the enzyme a potential candidate as antibacterial component in hurdle technology for food preservation.

At the start of the second part, OBPgp279 and PVP-SE1gp146, the two most promising endolysins, are selected to evaluate the proposed fusion approach for passage of the outer membrane (Chapter 7). The N-terminal fusion of a polycationic PK peptide (KRKKRKKRK) composed of lysine and arginine residues, turns out to be the most effective fusion to improve the antibacterial activity of both endolysins. The highest activity is reached for *P. aeruginosa* with maximal 2.61 log units. Addition of minor EDTA concentrations enhances activity and extends the activity range with *E. coli* (maximal 1.70 log units) and *S. Typhimurium* (maximal 0.91 log units). This fused PK peptide is believed to compete with the Achilles' heel of the outer membrane: the stabilizing divalent cations. A double N-terminal fusion of this promising PK peptide with other antimicrobial peptides only increases the antibacterial activity of OBPgp279 against *E. coli* to maximal 2.22 log units (for PP-PK double fusion), but is detrimental for the activity against other Gram-negative species. Analysis for the impact of the N-terminal PK fusion on endolysin characteristics reveals a protein-dependent inhibition of the enzymatic activity (with 52 to 94 %), a reduced heat resistance and a switch in pH-dependency to slightly more alkaline values (Chapter 8). Due to a more hydrophobic outer membrane, the antibacterial efficacy of the PK fusion is limited for Enterobacteriaceae. Additionally, the PK fusion also confers biofilm-degrading activity to PVP-SE1gp146. Extension of the linker length between the PK peptide and endolysin partly reconstitutes the reduced muralytic activity due to the PK peptide fusion, leading to an improved antibacterial activity against Pseudomonads and Enterobacteriaceae. Switching the PK peptide to the C-terminal end does not improve activity. These data nicely illustrate that endolysins can be turned into effective anti-Gram-negative compounds by an N-terminal fusion approach and subsequent optimization of the linker length.

In the last part, we evaluate the PK-fused endolysin approach on an *in vitro* human keratinocyte monolayer and an *in vivo* *Caenorhabditis elegans* model. PK-PVP-SE1gp146 is able to protect the keratinocyte monolayer from a *P. aeruginosa* PA14 infection (Chapter 9). In addition, PK-PVP-SE1gp146 improves the survival of PA14-infected *C. elegans* with 60 % after five days of treatment (Chapter 10). These results prove the *in vitro* and *in vivo* applicability of the PK-fused endolysin approach against *P. aeruginosa*, offering promising perspectives towards prophylactic and therapeutic applications in human health and veterinary and towards microbial decontamination purposes in the food industry.

Samenvatting

Bacteriofagen, virussen die specifiek bacteriën infecteren, moeten de celwand van hun bacteriële gastheer doorbreken op het einde van hun vermenigvuldigingscyclus om de nieuwgevormde faagvirions vrij te zetten. De belangrijkste component binnen de bacteriële celwand vormt de rigide peptidoglycaanlaag. Om deze laag te doorbreken coderen bacteriofagen voor peptidoglycaanhydrolasen, ook wel endolysines genoemd, die specifieke verbindingen in het peptidoglycaan doorbreken. Dit doctoraat focust zich uitsluitend op endolysines afkomstig uit bacteriofagen die verschillende gramnegatieve bacteriële species infecteren, waaronder *Pseudomonas aeruginosa*, *Salmonella Typhimurium*, *Escherichia coli*, *Klebsiella pneumoniae* en *Citrobacter rodentii*. De meeste van deze bacteriën zijn opportunistische pathogenen die in ziekenhuizen een zorgwekkende bedreiging vormen door hun intrinsieke en verworven antibioticaresistentie.

In een eerste luik van dit doctoraat breiden we de pool van gekarakteriseerde endolysines met een gramnegatieve achtergrond uit en analyseren we hun potentieel en inzetbaarheid als mogelijk alternatief voor antibiotica om deze gramnegatieve pathogenen te bestrijden. De gramnegatieve buitenmembraan verhindert de toegang van exogeen toegevoegde endolysines tot de peptidoglycaanlaag en beschermt de bacterie tegen hun lytische activiteit. Daarom evalueren we in het tweede deel van dit doctoraat een benadering die het endolysine toelaat om de buitenmembraan efficiënt te destabiliseren en het peptidoglycaan te bereiken. Deze benadering is gebaseerd op de fusie van een reeks buitenmembraanpermeabiliserende antimicrobiële peptiden aan het endolysine zodat het zelfstandig kan interageren met de buitenmembraan. Om de achtergrond te schetsen start dit doctoraat met een literatuuroverzicht betreffende bacteriofaagendolysines (hun geschiedenis en structurele diversiteit), antimicrobiële peptiden (hun indeling en werkingsmechanismen) en buitenmembraandiversiteit tussen gramnegatieven onderling.

Via een bio-informatische analyse van volledig gekarakteriseerde faaggenomen wordt een selectie gemaakt van vijftien interessante kandidaatendolysines (Hoofdstuk 4). Zes één-domein (Hoofdstuk 5) en drie modulaire endolysines (Hoofdstuk 6) met de sterkste maximale muralytische activiteit onder fysiologische condities worden uitvoerig gekarakteriseerd zowel bio-informatisch, als op biochemisch (pH afhankelijkheid, enzymatische activiteit en activiteit na hittebehandeling) en antibacterieel niveau. Op deze manier streven we om hun lytische rol te bewijzen en protein-specifieke karakteristieken bloot te leggen die interessant kunnen zijn voor verdere toepassingen. *In silico* bevatten de gekarakteriseerde één-domein endolysines enkel een katalytisch domein, terwijl de modulaire endolysines bestaan uit zowel een N-terminaal peptidoglycaanbindend domein als een C-terminaal katalytisch domein. Deze modulariteit is een unieke eigenschap die maar bij enkele endolysines van gramnegatieve bacteriën voorkomt. De voorspelde peptidoglycaanbindende domeinen worden daarenboven experimenteel geverifieerd.

De modulaire endolysines uit deze studie zijn op enzymatisch vlak actiever dan de één-domein endolysines, een observatie die zich ook vertaalt in hun *in vitro* antibacteriële activiteit. Van alle geteste endolysines vertoont het modulaire endolysine OBPgp279, afkomstig van de *Pseudomonas fluorescens* faag OBP, de sterkste enzymatische en antibacteriële activiteit, gevolgd door PVP-SE1gp146, het endolysine van de *Salmonella* Enteritidis faag PVP-SE1. Het peptidoglycaanbindend domein aanwezig in modulaire endolysines biedt een aanzienlijke bijdrage (38 tot 56 %) tot de totale activiteit. Bovendien is voor verschillende gramnegatieve species de enzymatische activiteit gelijk omdat hun peptidoglycaan (A1γ chemotype) sterk geconserveerd is. Deze karakterisering onthult verder ook verscheidene interessante biochemische eigenschappen. OBPgp279 vertoont intrinsieke antibacteriële activiteit tegen *P. aeruginosa* PAO1 (± 1 log unit), waarschijnlijk doordat het de *Pseudomonas* buitenmembraan destabiliseert. PVP-SE1gp146 blijft gedeeltelijk actief na een verhitting tot een temperatuur van 90°C met een 60 % overgebleven enzymatische activiteit na 20 minuten incubatie. Dit laatste kenmerk maakt het enzym geschikt voor gebruik als antibacteriële component in de zogenaamde “hurdle”-technologie bij het bewaren van voeding.

Aan de start van het tweede luik van dit doctoraat worden OBPgp279 en PVP-SE1gp146 als meest beloftevolle endolysines gekozen om de vermelde fusiebenadering te evalueren waarmee we trachten de buitenmembraan te overbruggen (Hoofdstuk 7). De N-terminale fusie van een polykationisch (PK) peptide (KRKKRKKRK) bestaande uit lysine en arginine residue's blijkt de meest efficiënte fusie te zijn. De hoogste afdoding wordt bekomen voor *P. aeruginosa* met maximaal 2.61 logeenheden. De toevoeging van een kleine hoeveelheid EDTA verhoogt de activiteit en verbreedt de actieradius met *E. coli* (maximaal 1.70 logeenheden) en *S. Typhimurium* (maximaal 0.91 log eenheden). Het gefusioneerde PK peptide treedt hoogstwaarschijnlijk in competitie met de achilleshiel van de gramnegatieve buitenmembraan: de stabilizerende divalente kationen. Een dubbele N-terminale fusie van de beloftevolle PK peptide met andere antimicrobiële peptiden kan enkel de antibacteriële activiteit van OBPgp279 tegen *E. coli* versterken tot maximaal 2.22 logeenheden (voor de PP-PK dubbelfusie), maar is nefast voor de activiteit van het endolysine tegen andere gramnegatieve species. Analyse van de impact van de N-terminale PK fusie op de karakteristieken van al onze endolysines onthult een eiwitafhankelijke inhibitie van de enzymatische activiteit (met 52 tot 94 %), een verminderde hitteresistentie en een verschuiving van de pH-afhankelijkheid naar meer alkalische waarden (Hoofdstuk 8). Door de aanwezigheid van een hydrofober buitenmembraan is de antibacteriële efficiëntie van de PK fusie sterk gelimiteerd in geval van de Enterobacteriaceae. Verder geeft de PK fusie ook biofilmafbrekende activiteit aan PVP-SE1gp146. Verlenging van de linkerlengte tussen het PK peptide en het endolysine herstelt gedeeltelijk de verminderde enzymatische activiteit wat leidt tot een sterk verbeterde antibacteriële activiteit tegen Pseudomonaden en Enterobacteriaceae. Verwisseling van de PK peptide naar de C-terminale kant verbetert de activiteit niet. Deze resultaten illustreren de mogelijkheid om endolysines te transformeren

in efficiënte anti-gramnegatieve agentia door de PK-fusiestrategie en verdere optimalisatie van de linkerlengte.

In het laatste luik evalueren we de fusiebenadering enerzijds op een *in vitro* monolaag van humane keratinocyten en anderzijds op een *in vivo* *Caenorhabditis elegans* nematode model. PK-PVP-SE1gp146 kan de keratinocytmonolaag beschermen tegen een *P. aeruginosa* PA14 infectie op korte termijn (Hoofdstuk 9). Bovendien wordt de overleving van *C. elegans* nematoden die geïnfecteerd zijn met PA14 verhoogd met 27 %, voor PVP-SE1gp146, en met 60 % voor (PK-)PVP-SE1gp146, na vijf dagen behandeling (Hoofdstuk 10). Deze resultaten bewijzen de *in vitro* en *in vivo* toepasbaarheid van de fusiebenadering tegen *P. aeruginosa* en bieden bovendien beloftevolle perspectieven voor profylactische en therapeutische toepassingen in de mens- en dierengeneeskunde en voor microbiële decontaminatie doeleinden in de voedingsindustrie.

List of abbreviations

Amp ^r	<u>A</u> mpicillin- <u>R</u> esistance
AMP	<u>A</u> nti <u>M</u> icrobial <u>P</u> eptide
CHAP	<u>C</u> ysteine-, <u>H</u> istidine-dependent <u>A</u> minohydrolase/ <u>P</u> eptidase
CD	<u>C</u> ircular <u>D</u> ichroism
CD14	<u>C</u> luster of <u>D</u> ifferentiation 14
CFU	<u>C</u> olony <u>F</u> orming <u>U</u> nits
(k)Da	(kilo)Dalton
DNA	<u>D</u> eoxyribo <u>N</u> ucleic <u>A</u> cid
DSC	<u>D</u> ifferential <u>S</u> canning <u>C</u> alorimetry
EDTA	<u>E</u> thylene <u>D</u> iamine <u>T</u> etra <u>A</u> cetic acid
(E)GFP	(<u>E</u> nhanced) <u>G</u> reen <u>F</u> luorescent <u>P</u> rotein
FPLC	<u>F</u> ast <u>P</u> rotein <u>L</u> iquid <u>C</u> hromatography
GH19	<u>G</u> lycoside <u>H</u> ydrolase 19 family
Hep	<u>H</u> eptose
HEPES	4-(2- <u>H</u> ydroxy <u>E</u> thyl)-1- <u>P</u> iperazine- <u>E</u> thane <u>S</u> ulfonic acid
HEWL	<u>H</u> en <u>E</u> gg <u>W</u> hite <u>L</u> ysozyme
IPTG	<u>I</u> so <u>P</u> ropyl- β -D-1- <u>T</u> hio <u>G</u> alactopyranoside
Kdo	2- <u>K</u> eto-3- <u>D</u> eoxy <u>O</u> ctanoate
LIC	<u>L</u> igation <u>I</u> ndependent <u>C</u> loning
LB	<u>L</u> ysogeny <u>B</u> roth
LPS	<u>L</u> ipo <u>P</u> oly <u>S</u> accharide
LMW	<u>L</u> ow <u>M</u> olecular <u>W</u> eigh
MIC	<u>M</u> inimal <u>I</u> nhibitory <u>C</u> oncentration
MRSA	<u>M</u> ethicillin- <u>R</u> esistant <u>S</u> taphylococcus <u>aureus</u>
MH	<u>M</u> ueller- <u>H</u> inton
NAG or GluNAc	N-acetylglucosamine
NAM or MurNAc	N-acetylmuramic acid
NGM	<u>N</u> ematode <u>G</u> rowth <u>M</u> edium
OD _{xxxnm}	<u>O</u> ptical <u>D</u> ensity at xxx nm wavelength
OM	<u>O</u> uter <u>M</u> embrane
OMV	<u>O</u> uter <u>M</u> embrane <u>V</u> esicle
ORF	<u>O</u> pen <u>R</u> eadng <u>F</u> rame
PBS	<u>P</u> hosphate <u>B</u> uffered <u>S</u> aline
PG	<u>P</u> eptido <u>G</u> lycan
PK	<u>P</u> oly <u>K</u> ation
PP	<u>P</u> oly <u>P</u> eptide
RNA	<u>R</u> ibo <u>N</u> ucleic <u>A</u> cid
SAR	<u>S</u> ignal <u>A</u> rrest <u>R</u> elease
SDS-PAGE	<u>S</u> odium <u>D</u> odecyl <u>S</u> ulfate <u>P</u> oly <u>A</u> crylamide <u>G</u> el <u>E</u> lectrophoresis
Tris	<u>T</u> ris(hydroxymethyl)aminomethane
TAT	<u>T</u> rans- <u>A</u> ctivator of <u>T</u> ranscription
TLR4	<u>T</u> oll- <u>L</u> ike <u>R</u> eceptor 4

List of publications

Peer-reviewed articles

Walmagh M, Boczkowska B, Grymonprez B, Briers Y, Drulis-Kawa Z, Lavigne R (2012a) Characterization of five novel endolysins from Gram-negative infecting bacteriophages. *Appl Microbiol Biotechnol*. PMID:22832988

Walmagh M, Briers Y, Dos Santos SR, Azeredo J, Lavigne R (2012b) Characterization of modular bacteriophage endolysins from *Myoviridae* phages OBP, 201φ2-1 and PVP-SE1. *PLoS One* **7**: e36991

Briers Y, **Walmagh M**, Lavigne R (2011) Use of bacteriophage endolysin EL188 and outer membrane permeabilizers against *Pseudomonas aeruginosa*. *J Appl Microbiol* **110**: 778-785

Callewaert L, **Walmagh M**, Michiels CW, Lavigne R (2011) Food applications of bacterial cell wall hydrolases. *Curr Opin Biotechnol* **22**: 164-171

Patents

Azeredo J, Santos SR, Kluskens L, Lavigne R, **Walmagh M** (2012) Novel endolysin. Publication number: WO/2012/059545

Briers Y, Lavigne R, **Walmagh M**, Miller S (2011) New endolysin OBPgpLYS. Publication number: WO/2011/023702

Lavigne R, Miller S, Briers Y, Volckaert G, **Walmagh M** (2010) Antimicrobial agents. Publication number: WO/2010/149792

Introduction and background

1.1 General introduction

Multidrug-resistant Gram-negative bacteria cause serious and often fatal infections in animals and humans and are of considerable concern in the medical world, especially in hospital environments. The most prevalent infection sites in the human body are the urinary tract, the airways, the bloodstream and surgical wounds. Multidrug-resistant bacterial infections are hard to combat with most of the available antibiotics due to a combination of intrinsic (low outer membrane permeability, presence of efflux pumps, biofilm formation) and acquired (horizontal transfer of resistance genes, chromosomally-encoded gene mutations) resistance mechanisms. These acquired mechanisms lead to drug inactivation and target alteration. Annually, the four most prevalent antibiotic-resistant Gram-negative pathogens *Pseudomonas aeruginosa*, *Acinetobacter baumannii*, *Klebsiella pneumoniae* and *Escherichia coli*, cause the death of an estimated 25,000 patients in Europe alone (European Medicines Agency, 2011), of which 845 in Belgium (on a total of 11 million inhabitants). In 2008, the Belgian Federal Service for Health (FOD-volksgezondheid) estimated that hospital-acquired or nosocomial infections in Belgium hospitals cost a 100 million euro per year. *P. aeruginosa*, the most ubiquitous Gram-negative hospital-acquired pathogen, causes opportunistic infections in immune-compromised patients, such as burn wounds or cystic fibrosis patients. The second most emerging nosocomial Gram-negative pathogen in Intensive Care Units, *A. baumannii*, infects critically ill patients causing pneumonia, septicemia and nosocomial meningitis. This bacterium is known for its remarkable genome plasticity and ability to acquire resistance determinants leading to several recent multidrug-resistant outbreaks (Kempf & Rolain, 2012). Both *P. aeruginosa* and *A. baumannii* isolates can acquire resistance to almost all commonly used antibiotics, with only colistin and tigecycline left as last-line treatments. Recent reports of a major pathogenic *E. coli* O104:H4 outbreak in North-Germany in 2011 (Karch et al, 2012) and the appearance of New Delhi metallo- β -lactamase producing Enterobacteriaceae (*E. coli* and *K. pneumoniae*) in hospitals in India

(Taneja et al, 2010), Japan (Chihara et al, 2011), United Kingdom (Hornsey et al, 2011) and Cameroon (Dortet et al, 2012) reflect the urge for alternative and innovative treatments.

Bacteriophages, bacteria-infecting viruses, can be seen as a natural toolbox: they offer a whole arsenal of potential biotechnological tools, including RNA polymerases of phages T7 and SP6 used for tight controlled protein expression (Butler & Chamberlin, 1982; Tabor & Richardson, 1985), LPS-binding tail spike protein gp09 of phage P22 for endotoxin removal (Handa et al, 2010), exopolysaccharide depolymerases for biofilm degradation (Hughes et al, 1998), and peptidoglycan hydrolases that cause destruction of bacterial cell walls. It is only since the last decade that the potential interest in phage-encoded peptidoglycan hydrolases was tapped due to the urgent need for alternative antibacterial compounds to combat emerging multidrug-resistant bacterial pathogens. These peptidoglycan hydrolases, also called “*endo*”lysins as they naturally act from within the phage-infected bacterial host, are the main subject of this dissertation.

The literature review will start with an historic overview of the discovery of endolysins and their stepwise characterization, optimization and development into potential therapeutic compounds, with a special emphasis on their structural and enzymatic diversity (1.2). In the second part, this review goes into depth on the structural diversity present in the outer membrane of different Gram-negative species, and its barrier function which hampers the therapeutic application of endolysins. To close with, some possible strategies to tackle this outer membrane barrier are discussed (1.3). The literature review ends with a focus on the realm of the antimicrobial peptides, small molecules present in all life forms in nature, and highlights their diversity and mode of action on bacterial and eukaryotic membranes (1.4).

1.2 Bacteriophage-encoded peptidoglycan hydrolases

At the end of the bacteriophage replication cycle, the mature virion particles should be dispersed in the extracellular environment for further prey infection and phage propagation. During evolution, phages have developed different strategies to release their progeny from the cell interior. Most lytic phages encode specific peptidoglycan hydrolases, or endolysins,

that degrade the peptidoglycan layer of the infected bacteria from within (Young, 1992). Normally, the peptidoglycan layer gives structural integrity to the bacterial cell and is therefore assumed as the major determinant of cell shape (Vollmer et al, 2008a). When this peptidoglycan layer is broken, the bacterial cell cannot withstand the high internal osmotic pressure (5 atmosphere for Gram-negative bacteria and up to 50 atmosphere for Gram-positive bacteria) and will eventually burst (Nelson et al, 2012). Some small, single-stranded RNA or DNA phages are known to cause cell lysis by the inhibition of peptidoglycan biosynthesis using a single protein (single lytic factor). Phage ϕ X174, for example, encodes for lysis protein E which is an inhibitor of the MraY-catalyzed step in peptidoglycan biosynthesis (Bernhardt et al, 2001a). MraY is a membrane-bound translocase that catalyzes the formation of the lipid II precursor. Filamentous phages (for instance M13, fd or f1) are continuously extruded from the bacterial cells without killing them, probably by the aid of specific phage proteins that function as outer membrane export channel (Russel et al, 1997).

1.2.1 History on bacteriophage-encoded peptidoglycan hydrolases

Frederick Twort (in 1915), a British bacteriologist at the Brown institute in London, and Félix d’Herelle (in 1917), a French-Canadian microbiologist at the Pasteur institute in Paris, independently discovered small entities that were able to kill bacteria (Figure 1.1). d’Herelle named these invisible agents bacteriophages, after the Greek word “phagein” (“to eat”). For their independent discoveries, both Twort and d’Herelle are considered to be the founding fathers of bacteriophage research.



Figure 1.1: Felix d’Herelle (1873-1949, left) and Frederick Twort (1850-1922, right). The founding fathers of bacteriophage research.

By extraction of an active lytic agent from phage lysate, d'Herelle was the first (1921) to prove the presence of a phage-associated enzymatic molecule that is able to lyse bacterial cells independently from the replication action of the phage. Later, Vladimir Sertic (1929) was able to isolate what he called a "lysine d'une race de bactériophagie". The isolated "lysine" caused the formation of a specific zone surrounding *Escherichia coli* plaques in which cells possessed an altered morphology.

Back in those days, a lot of skepticism was present among microbiologist concerning the existence of such phage lysins, since it was difficult to prove that these lysins were responsible for cell lysis. It took a couple of decades to reassure the scientific world that lysins do exist and for the "lysine" hypothesis to gain ground. An important breakthrough came by the isolation of a lytic protein called "virolysin" in phage-infected *Staphylococcus aureus* lysates by Ralston and coworkers (1957), which turned out to be distinct from the bacterial host autolysins. The term "endo"lysin was first introduced by Jacob and Fuerst (1958) who showed that these enzymes were part of the multiplication machinery of the phage causing lysis of the bacterial cell envelope "from within" at the end of the lytic replication cycle. In addition, phages also possess tail-associated peptidoglycan hydrolases, called structural lysins, which are used for localized degradation of the cell wall "from without" at the beginning of the infection cycle (Moak & Molineux, 2004).

In the next couple of years, many other endolysins were discovered in phage/bacteria lysates from *Bacillus* (Murphy, 1957), *Streptococcus* (Reiter & Oram, 1963), *Lactococcus* (Tourville & Johnstone, 1966) and Enterobacteriaceae (Maass & Weidel, 1963) infecting phages. Due to progressing purification techniques like ammonium sulfate precipitation, gel filtration, calcium phosphate absorption (Doughty & Hayashi, 1962; Krause, 1958) and stabilization of reactive residues by sodium-tetrathionate-protecting groups (Fischetti et al, 1971), higher lysin purity was achieved.

Since in the last decade the prevalence of hospital-acquired multidrug-resistant pathogens increased, endolysins came more and more under the attention of scientists throughout the world as a possible alternative for commonly used antibiotics. In the beginning of the new millennium, Fischetti and coworkers proved for the first time the antibacterial efficacy of

exogenously added purified endolysin to a Gram-positive *Streptococcus* culture by “lysis from without” (Fischetti, 2001). From that moment on, endolysin research boomed worldwide with plenty of publications focusing on the potential use of endolysins from *Streptococcus pneumoniae* (Loeffler & Fischetti, 2003), *Staphylococcus aureus* (Rashel et al, 2007), *Bacillus anthracis* (Schuch et al, 2002) and *P. aeruginosa* (Briers et al, 2007b) bacteriophages as “enzymotics” or enzyme-based antibacterials (Veiga-Crespo et al, 2007).

1.2.2 Natural role of peptidoglycan hydrolases in bacterial lysis mechanisms

Three different mechanisms, summarized in Figure 1.2, are described so far in literature for release of phage-encoded endolysins in the periplasmic area of the bacterial cell: the endolysin-holin two component mechanism (1.2.2.1), the signal peptide-based secretion mechanism (1.2.2.2) and the “Signal-Arrest-Release” mechanism (1.2.2.3).

1.2.2.1 Endolysin-holin two component mechanism

The majority of the lytic double-stranded DNA phages make use of the endolysin-holin two component system for efficient lysis of the bacterial host. Holins (“hole”-formers) are small hydrophobic phage-encoded proteins that can accumulate in the inner membrane of the host cell during late protein synthesis after infection (Grundling et al, 2001). Expression of phage holins is tightly regulated. At a genetically programmed time point, they can aggregate into a pore-forming oligomeric complex (340 nm-1 μ m diameter width) through which the endolysins migrate to the peptidoglycan layer for completion of the host cell lysis (Young, 1992; Young & Blasi, 1995). The holin thus controls the length of the vegetative cycle and the burst size of the infection. Their primary sequence suggests a structure consisting of one or more helical transmembrane domains and a strongly charged, hydrophilic C-terminus (Young & Blasi, 1995). The remarkable timing of holin action is not yet fully understood, but oligomer formation is hypothesized to be under control of specific holin inhibitors (Blasi et al, 1990; Vukov et al, 2003) or to set off when critical holin concentrations are reached (Grundling et al, 2001). In a typical endolysin-holin system, the genes encoding the endolysin and the holin are encoded together in a tandem operon. Bacteriophage λ has been the prototype phage for extensive study of this lysin-holin system. The holin-encoding gene,

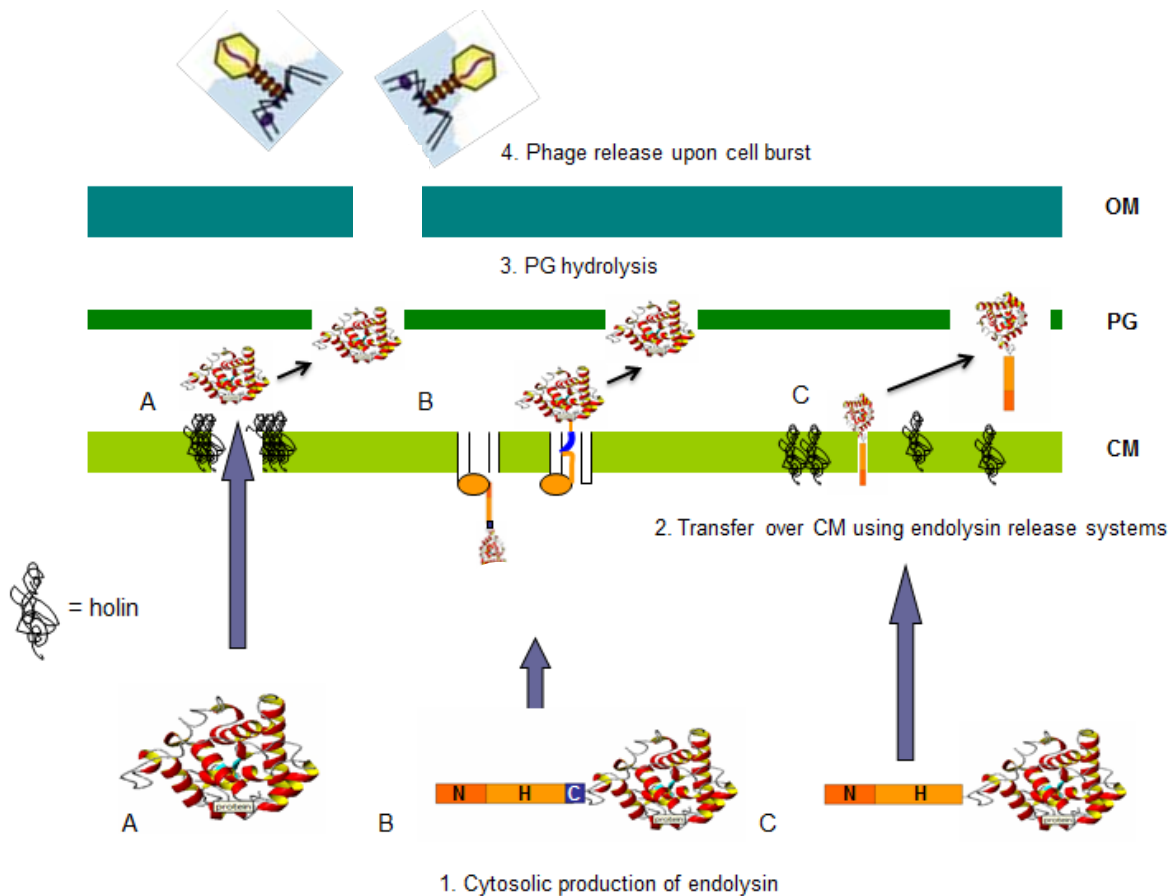


Figure 1.2: Schematic overview of endolysin-induced lysis mechanisms. Upon production in the host cytosol in the late stage of the phage replication cycle, phage endolysins are translocated over the bacterial cytoplasmic membrane by three different mechanisms. (A) The classical endolysin-holin two component system makes use of pore-forming holins to allow passage of the peptidoglycan-degrading endolysins through the cytoplasmic membrane of the bacterial host into the periplasm. The majority of double-stranded DNA phages makes use of such a mechanism. (B) Some phage endolysins possess an N-terminal, cleavable signal peptide sequence (N = positively charged region, H = hydrophobic region and C = catalytic region bearing the recognition site of signal peptidase), which helps these endolysins to be translocated over the cytoplasmic membrane by aid of the host Sec translocation system. At the end, the signal peptide is cleaved off from the endolysin by a membrane-bound peptidase enzyme. (C) Endolysins with an N-terminal SAR (signal-arrest-release) sequence lack the C-region in their signal sequence and remain tethered to the cytoplasmic membrane upon translocation by the Sec-machinery in an inactive form. The membrane-tethered molecules are then released in the periplasmic space by the aid of pinholins that form small pores in the cytoplasmic membrane, resulting in membrane depolarization and endolysin release. The active endolysins in the periplasm hydrolyze the peptidoglycan layer, subsequently leading to cell burst and phage virion release in extracellular environment. PG = peptidoglycan, CM = cytoplasmic membrane and OM = outer membrane. Adapted from Peeters (2009).

called S gene in phage λ , plays a major role in this system: it possesses a dual-start motif with two methionine residues (Met-Lys-Met-) and encodes for two almost identical proteins: the effector holin S105 (with three transmembrane domains) and the inhibitor anti-holin S107 which initially form non-functional hetero-oligomers in the inner membrane (Blasi et al, 1990). According to a simple two-step model for holin timing, the positively charged Lys-residue at position 2 in the N-terminal side of the S107 inhibitor prevents functional S105/S107 oligomer formation by interaction with the negatively charged cytoplasmic side of the inner membrane. Upon collapse of the membrane potential, this interaction gets abolished resulting in a quick S105/S107 oligomer rearrangement, functional hole formation and subsequent peptidoglycan degradation and cell lysis by the accumulated endolysin (encoded by the R gene). While many holins rely on this λ two step model, others like the *Staphylococcal aureus* CidA, a holin-like protein essential for programmed cell death, use other, yet unknown mechanisms that await further investigation (Rice & Bayles, 2008).

Holins are not only of phage origin. Holin-like structures are present in almost all types of bacteria, where they are hypothesized as an alternative secretion system for proteins without signal peptide (Desvaux et al, 2009). For example, TcdE, a holin-like protein discovered in *Clostridium difficile* mediates the release of exotoxins A and B in the extracellular environment (Govind & Dupuy, 2012).

1.2.1.2 Signal peptide based secretion mechanism

The idea that endolysins are only relying on holin action for transfer to the periplasmic area withstood for a long time, until Sao-Jose and coworkers (2000) reported the presence of an N-terminal, cleavable signal peptide in *Oenococcus oeni* phage fOg44 endolysin. This signal peptide acts as a secretion signal and is recognized by the bacterial Sec translocation system. The phage hijacks this Sec system to translocate its own endolysin over the inner membrane. During translocation, the N-terminal signal peptide is cleaved off by the action of a membrane-bound signal peptidase. Phages using this endolysin release system also encode holins. In this case, holins are not necessary for the endolysin export, but mediate dissipation of the proton motif force and subsequent membrane depolarization. This help seems crucial for proper activation of the previously translocated enzymes (Nascimento et al, 2008).

1.2.2.3 “Signal arrest release” (SAR) mechanism

Some phage endolysins, like the *Lyz* endolysin of the *E. coli* phage P1, the R²¹ endolysin of lambdoid phage 21 or the KMV45 endolysin of *P. aeruginosa* phage ϕ KMV, exhibit a signal sequence named SAR (Signal Arrest Release) at their N-terminal side, that mediates the translocation of the enzyme without being cleaved (Briers et al, 2011a; Xu et al, 2004). This SAR sequence is rich in positively charged (N-region) and weak hydrophobic (H-region) residues, but lacks a cleavage site (C-region), compared to a normal signal sequence (Figure 1.2). The SAR sequence is, similar to a normal signal sequence, recognized by the Sec translocation machinery of the host cell, resulting in tethering of the endolysin to the periplasmic side of the inner membrane in an inactive form. The membrane-tethered molecules are then released in the periplasmic space by the aid of pinholins that form small pores (< 2 nm), resulting in membrane depolarization. In the case of *Lyz* (Xu et al, 2005) and the endolysin of a recently discovered *Erwinia amylovora* phage ERA103, *Lyz*¹⁰³ (Kuty et al, 2010), enzyme activation appears by an intra-molecular disulfide isomerization (Figure 1.3).

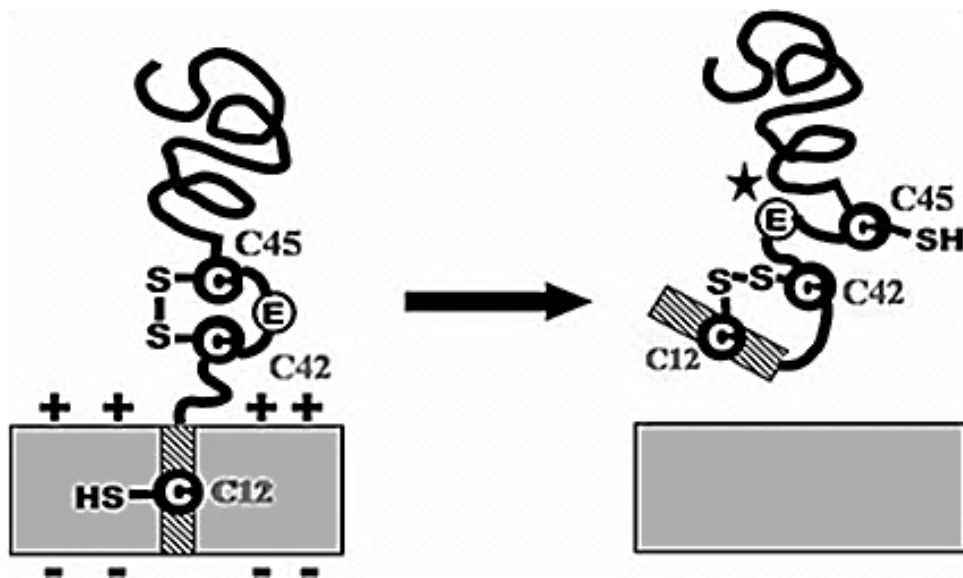


Figure 1.3: Disulfide caging mechanism for regulation of *Lyz*¹⁰³ activity. (Left) In an inactive form, *Lyz*¹⁰³ is tethered to the cytoplasmic membrane with its SAR domain (hatched part). In this form, a disulfide bond is present between Cys42 (C42) and Cys45 (C45) that cages the catalytic glutamate residue (E). (Right) When the SAR domain is released from the membrane, the SAR-containing Cys12 (C12) residue spontaneously attacks the caging disulfide bond at Cys42, forming a new disulfide bond that opens the cage. The catalytic glutamate residue is now released from the caging and the endolysin becomes active (from Kuty et al, 2010).

This spontaneous isomerization unblocks a specific cysteine residue in the catalytic part of *Lyz*, and releases a glutamate residue in the active site of phage ERA103 endolysin which is normally caged by a disulfide bond. The SAR endolysin R²¹ uses another activation mechanism: its SAR sequence refolds back into the body of the enzyme and repositions one specific residue in the catalytic site that effects the enzymatic activity (Sun et al, 2009). The high diversity of the regulatory strategies used for activation of endolysins reflects how important correct lysis timing is for optimal phage fitness.

1.2.3 Structural composition of phage endolysins

1.2.3.1 Structural diversity

In general, endolysins from Gram-positive infecting phages possess a modular, more than one domain structure with one or more cell wall (or peptidoglycan) binding domains at their C-terminal end and one or more catalytic domains at their N-terminal end (Fischetti, 2010). Figure 1.4 shows the three-dimensional structure of the modular endolysin Cpl-1 of *S. pneumoniae* phage Cp-1 (Fokine et al, 2008; Perez-Dorado et al, 2007). This endolysin bears a C-terminal muramidase as catalytic domain. The peptidoglycan binding part of Cpl-1 is composed of 6 repeating choline-binding motifs. Peptidoglycan binding domains with similar repeated motifs have also been found in other pneumococcal endolysins such as the recently crystallized endolysin Cpl-7 where the cell wall binding domain consists of three identical motifs (Bustamante et al, 2010; Perez-Dorado et al, 2007). Structurally, the endolysin of the *S. pneumoniae* infecting bacteriophage C1, PlyC, is an exception among endolysins of Gram-positive phages, as it has a multimeric conformation (Nelson et al, 2006). The PlyC holoenzyme consists of an enzymatically active PlyCA 'heavy chain' (50 kDa) and eight smaller cell wall binding PlyCB chains (8 kDa) that are proposed to form one complex (Nelson et al, 2006). The total complex is encoded by two separate genes embedded in a single operon.

In contrast, the majority of the endolysins originating from Gram-negative infecting phages have a single-domain structure consisting of a catalytic domain, like *E. coli* phage T4 lysozyme (Matthews & Remington, 1974). Only a few of these endolysins are predicted

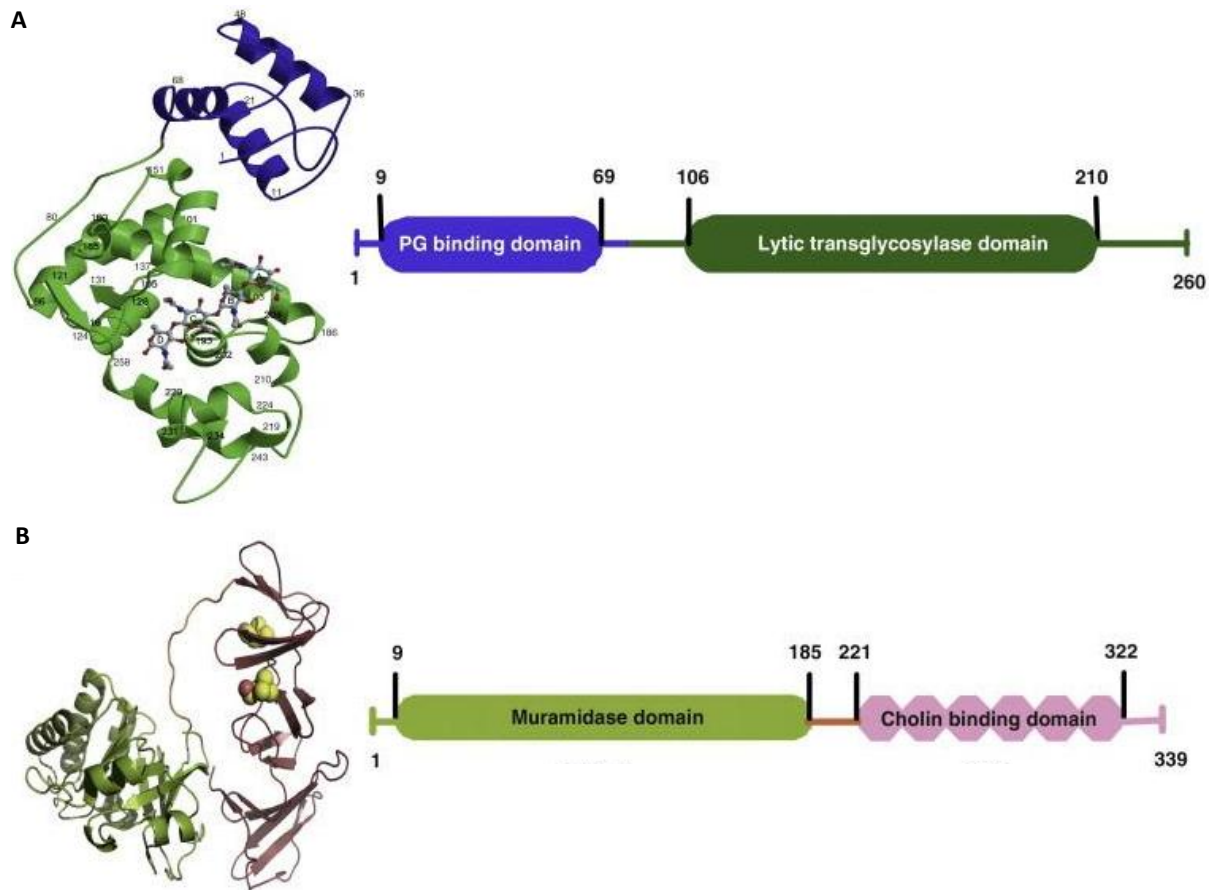


Figure 1.4: Three-dimensional structures (left) and modular compositions (right) of phage endolysins ϕ KZgp144 (or KZ144) (A) and Cpl-1 (B). (A) KZ144 of *P. aeruginosa* phage ϕ KZ contains an N-terminal peptidoglycan binding domain (in blue) and a C-terminal lytic transglycosylase domain (dark green) with a bound N-acetyl glucosamine tetramer visualized in the active site (Fokine et al, 2008). (B) Cpl-1 of *S. pneumoniae* phage Cp-1 has an N-terminal muramidase domain (light green), a small linker (orange) and a cholin binding domain consisting of six repeating motifs at its C-terminal end (pink). The substrate choline moieties are indicated bound to the peptidoglycan binding domain of Cpl-1 as yellow spheres. Numbers on the figure represent amino acid positions (Perez-Dorado et al, 2007).

to have a modular domain structure composed of an N-terminal peptidoglycan binding domain and a C-terminal catalytic domain, like the endolysins of *P. aeruginosa* phages ϕ KZ (KZ144, Figure 1.4) and EL (EL188) (Briers et al, 2007b; Fokine et al, 2008), or an N-terminal catalytic domain and a C-terminal peptidoglycan binding domain, as the recently discovered endolysin of *P. aeruginosa* phage Lu11 (Lu11gp113) (Adriaenssens et al, 2012a). The C-terminal catalytic domain of KZ144 proved to be a lytic transglycosylase (Fokine et al, 2008; Paradis-Bleau et al, 2007). The presence of modular endolysins in phage biology suggests that during early phage evolution different domain-coding gene fragments or “modules” have been exchanged between phages and that proteins of contemporary phages were built

up by rearranging simple gene fragments into new combinations (Garcia et al, 1988). The possibility to create functional chimeric proteins from the domains of pneumococcal endolysins and these of other Gram-positives is in agreement with this evolutionary exchange hypothesis (Lopez et al, 1997).

1.2.3.2 Catalytic activity

Catalytic domains of phage endolysins can display different enzymatic activities that target one of the bonds in the structure of the peptidoglycan (Figure 1.5). Table 1.1 gives an overview of the different groups of catalytic activity or specificity described in the literature.

Table 1.1: Catalytic activities present in bacteriophage endolysins.

Group	Specific activity		Phage lysin	Reference
Glycosidase	N-acetylglucosaminidase		λ Sa2 lysin	Pritchard et al, 2007
	N-acetylmuramidase (or lysozyme)		T4 lysozyme	Matthews & Remington, 1974
			P1 lysin	Xu et al, 2005
			Cp-1 lysin	Monterroso et al, 2002
			PlyBa04 lysin	Low et al, 2005
			Bcpl lysin	Porter et al, 2007
	Lytic transglycosylase		λ lysin	Evrard et al, 1998
			ϕ KZgp144	Fokine et al, 2007
Amidase	N-acetylmuramoyl-L-alanine amidase		LytA	Navarre et al, 1999
			LysK	Becker et al, 2009a
			Lyt2638A	Abaev et al, 2012
			CS74L	Mayer et al, 2012
			BPS13 endolysin	Park et al, 2012
Peptidase	Endopeptidase	D-alanyl-glycyl	LytA	Navarre et al, 1999
		L-alanoyl-D-glutamate	Ply500	Korndorfer et al, 2008
			Ply118	Loessner et al, 1995
			LysB4	Son et al, 2012

A first group of glycosidases cleaves the N-acetylglucosamine (GluNac or NAG) - N-acetylmuramic acid (MurNac or NAM) glycan backbone, and includes N-acetyl- β -D-glucosaminidases and N-acetyl- β -D-muramidases. N-acetyl- β -D-glucosaminidase activity, only found in the phage λ Sa2 endolysin (Pritchard et al, 2007), degrades the glycosidic bond at the reducing end of GluNac. N-acetyl- β -D-muramidases consist of lysozymes and transglycosylases, which both cleave the same glycosidic bond at the reducing end of MurNac, yet deliver different end products. Transglycosylases are no real hydrolases as no water is consumed in the cleavage of the glycoside bond, and a 1,6-anhydrobond is formed in the MurNac. Lysozyme activity was present in endolysins of coliphages T4 (Matthews & Remington, 1974) and P1 (Xu et al, 2005), in pneumococcal phage Cp-1 endolysin Cpl-1

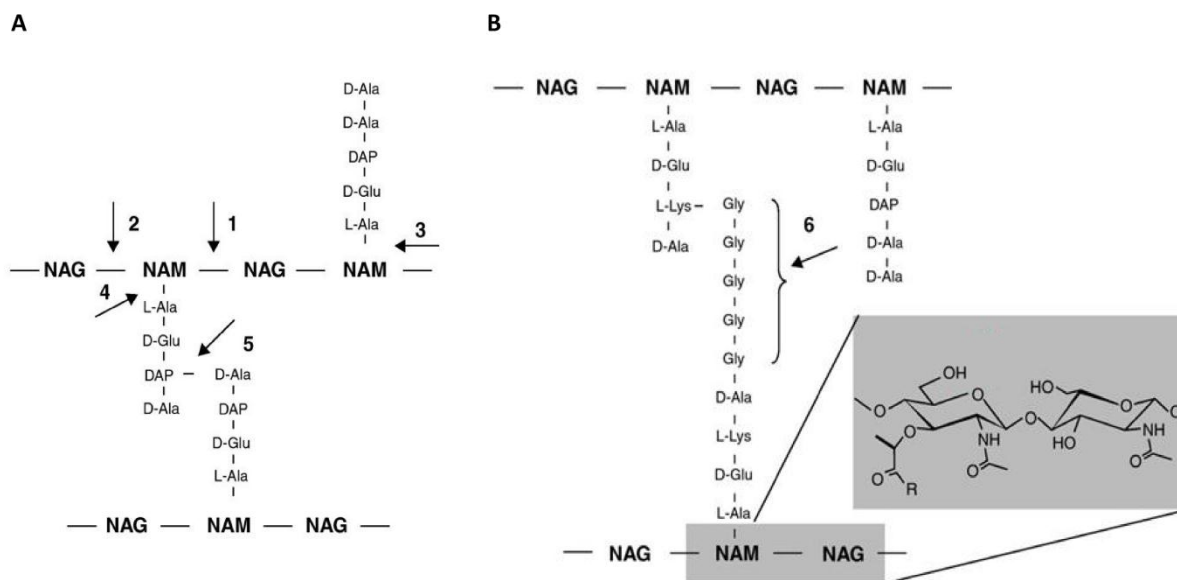


Figure 1.5: Enzymatic activities of phage endolysins on the peptidoglycan of *Escherichia coli* (A) and *Staphylococcus aureus* (B). The glycan backbone of peptidoglycan consists of β -1,4-linked sugar monomers of N-acetylglucosamine (NAG or GluNac) and N-acetylmuramic acid (NAM or MurNac). Side chains and cross-bridges between adjacent glycan chain molecules contain L- and D-forms of amino acids and in case of *E. coli* the unique amino acid meso-diaminopimelic acid (DAP) or m-DAP. Indicated here are the A1 γ chemotype of peptidoglycan for *E. coli*, which is conserved among all Gram-negative species, and the A3 α chemotype specific for *S. aureus* (Schleifer & Kandler, 1972). Arrows indicate bonds which are targeted by N-acetyl- β -D-muramidases, such as lysozymes and lytic transglycosylases (1), N-acetyl- β -D-glucosaminidases (2), N-acetylmuramyl-L-alanine amidases (3) and endopeptidases (L-alanoyl-D-glutamate endopeptidases (4) and interpeptide bridge endopeptidase (5) on *E. coli* peptidoglycan, D-alanyl-glycyl endopeptidase (6) on *S. aureus* peptidoglycan). The inset (grey box) in (B) shows the conformation of the NAM-NAG sugar backbone in *S. aureus* peptidoglycan. Activities 1, 2, 3 and 4 are also present on *S. aureus* peptidoglycan (not indicated).

(Monterroso et al, 2002) and in lysins of *B. anthracis* prophages PlyBa04 (Low et al, 2005) and Bcpl (Porter et al, 2007). Coliphage λ endolysin (Evrard et al, 1998) and *P. aeruginosa* phage ϕ KZ endolysin KZ144 (Fokine et al, 2007; Paradis-Bleau et al, 2007) were both shown to possess transglycosylase activity. A second group, the N-acetylmuramyl-L-alanine amidases, hydrolyze the amide bond between N-acetylmuramic acid and L-alanine, separating the peptide chain from the glycan strand. This kind of activity is more prevalent among endolysins of Gram-positive origin and is hypothesized to be more destabilizing for the peptidoglycan than other activities (Nelson et al, 2012). An N-acetylmuramyl-L-alanine amidase domain is present in the endolysins of the staphylococcal phage endolysins LytA (phage ϕ 11) (Navarre et al, 1999), LysK (phage K) (Becker et al, 2009a) and Lyt2638A (phage 2638A) (Abaev et al, 2012), the *Clostridium* phage ATCC 8074-B1 endolysin CS74L (Mayer et al, 2012) and the *Bacillus cereus* phage BPS13 endolysin (Park et al, 2012). A final group consists of distinct classes of endopeptidases and carboxypeptidases (both proteases) which cleave the bonds in the stem peptides and/or in the cross-bridges between adjacent peptidoglycan blocks (Vollmer et al, 2008b). The phage ϕ 11 endolysin LytA, besides its N-acetylmuramyl-L-alanine amidase domain, also possesses D-alanyl-glycyl endopeptidase activity to cut the interpeptide bridge in staphylococcal peptidoglycan (Navarre et al, 1999). listerial endolysins Ply500 and Ply118 (Korndorfer et al, 2008; Loessner et al, 1995) and *B. cereus* phage B4 endolysin LysB4 (Son et al, 2012) all target the bond between L-alanine and D-glutamate in the stem peptides (L-alanoyl-D-glutamate endopeptidases).

Several endolysins from Gram-positive infecting phages are found to have two or more catalytic domains with long flexible linkers in between. Examples are the endolysins of staphylococcal phages ϕ 11 (LytA), K (LysK) and ϕ WMY (all endopeptidase and amidase activity) and the phage B30 endolysin (endopeptidase-muramidase activity) (Donovan et al, 2006b; Navarre et al, 1999; Pritchard et al, 2007; Yokoi et al, 2005). However, in most of these endolysins one of the two activities turned out to be silenced at the biochemical level. In the case of staphylococcal endolysins LytA and LysK, the amidase domain showed no activity (Becker et al, 2009a; Sass & Bierbaum, 2007), whereas the λ SA2 endolysin contains an inactive glucosaminidase and an active amidase domain (Donovan & Foster-Frey, 2008). In contrast, PlyC was recently shown to possess two active and distinct catalytic domains displaying both amidase and glycosidase activity (McGowan et al, 2012).

1.2.3.3 Cell wall binding activity

Phage endolysins targeting Gram-positive bacteria typically contain cell wall binding domains that enhance the substrate affinity of the enzyme to levels comparable with affinity-matured antibodies (Medina et al, 1997). In this respect, Loessner (2005) demonstrated that *Listeria monocytogenes* phage endolysins Ply118 and Ply500 have a binding affinity ($3-6 \times 10^8 \text{ M}^{-1}$) that is comparable with the matured antibody-bacterial cell wall (ligand) affinity in a secondary immune response. Often, these domains are highly specific in recognizing and binding discrete epitopes inside the bacterial cell wall, mostly carbohydrates or teichoic acids, explaining their species- or even strain-specific activity. For example, the cell wall binding domains of the pneumococcal lysins Cpl-1 and Pal specifically bind certain choline moieties within the teichoic acids of pneumococcal peptidoglycan essential for bacterial survival (Perez-Dorado et al, 2007; Varea et al, 2004). Some endolysins from Gram-positive infecting phages, like PlyC have more than one cell wall binding domain (Nelson et al, 2006). In the case of PlyC, the total cell wall binding domain consists of 8 monomeric subunits which are able to specifically bind certain group A (*S. pyogenes*) and C (*S. equi*, *S. dysgalactiae*) streptococci with high affinity using an unknown cell wall epitope (McGowan et al, 2012). In contrast, cell wall binding domains or more specifically peptidoglycan binding domains are atypical for phage lysins from Gram-negative bacteria, but those that are found in giant *P. aeruginosa* phages like ϕ KZ and EL show a broad binding spectrum (Briers et al, 2007b). As such, they do not allow for bacterial differentiation, but when fused to the green fluorescent protein (GFP) they can be useful as biomarker to visualize or quantify outer membrane permeabilization in Gram-negative bacteria (Briers et al, 2009). The presence of these peptidoglycan binding domains is also speculated to explain the high muralytic activity of KZ144 and EL188 on peptidoglycan of *P. aeruginosa* by bringing substrate in close proximity to the active site of their catalytic domains (Briers et al, 2007b)

1.2.3.4 Domain shuffling

The relative independence of the catalytic domains and peptidoglycan binding domains of endolysins allows them to combine different domains (“domain shuffling”) into novel lytic enzymes with an increased activity and an extended lytic host spectrum, optimized for

various applications. Domain shuffling is therefore a powerful approach for rational design and optimization of desired properties of endolysins (Schmelcher et al, 2011). This domain exchange occurs regularly in nature as well (Donovan et al, 2006a). As already mentioned in a previous part, some streptococcal or staphylococcal phage lysins (e.g. PlyC, B30, LytA, LytK) contain multiple catalytic domains with different enzymatic activities. This modular recombination probably drives the environmental adaptation and evolution of these enzymes.

Recently, this “domain shuffling” idea was exploited to create two head-to-tail fusion proteins of mature lysostaphin, a staphylococcal bacteriocin, with endolysin LysK of staphylococcal phage K (Donovan et al, 2009) and with the tail-associated peptidoglycan hydrolase HydH5 of phage vB_SauS-philPL188 (Rodriguez-Rubio et al, 2012). As LysK possess a Cysteine-, Histidine-dependent Aminohydrolase/Peptidase (CHAP) and an amidase domain, HydH5 a CHAP and a lysozyme domain, and lysostaphin an endopeptidase domain, the resulting fusion proteins could target three unique bonds in the staphylococcal peptidoglycan. Separately, LysK and lysostaphin proved to act synergistically on different *S. aureus* strains, including Methicillin-Resistant *S. aureus* (MRSA) (Becker et al, 2008). Remarkably, the parental specificities of the separate peptidoglycan hydrolases were maintained in the LysK-lysostaphin fusion protein, since all three lytic domains in the fusion construct were still active (Donovan et al, 2009). Both the LysK-lysostaphin and the HydH5-lysostaphin fusion constructs showed a stronger *in vitro* antibacterial activity against a range of different clinical *S. aureus* isolates, than the separate hydrolases. In addition, LysK-lysostaphin was able to eradicate *S. aureus* infections in a rat nasal colonization model (Donovan, personal communication). Major advantage of the use of fusion proteins with more than one catalytic domain is the reduction of resistance development compared to the parental lysins, as was shown for the LysK-lysostaphin fusion protein (Donovan, personal communication). Fusion proteins consisting of different lysin domains are expected to be less prone to resistance development than the parental enzymes as the bacterial cell has to modify two or more different types of bonds to overcome lysin activities (Fischetti, 2005).

Other possibilities to exploit “domain shuffling” for lysin activity optimization comprise the change of the native cell wall binding domain by one with a higher binding affinity/specificity

for a certain peptidoglycan chemotype, as was done for the streptococcal prophage λ SA2 endolysin (Becker et al, 2009b) and the *Enterococcus faecalis* phage endolysins Lys168/Lys170 (Fernandes et al, 2012), or the addition of such a domain to hydrolases naturally lacking a binding domain, as for HydH5 (Rodriguez-Rubio et al, 2012). Replacing the native streptococcal-specific Cpl-7-like cell wall binding domains of the λ SA2 endolysin by the staphylococcal-specific SH3b binding domains of LysK or lysostaphin resulted in a 5-fold increase of the staphylolytic activity while the streptolytic activity was significantly maintained (Becker et al, 2009b). The fact that also the streptolytic activity is still maintained suggests that SH3b recognition is not staphylococcal-specific. Moreover, the λ SA2-SH3b fusion protein demonstrated efficient killing of penicillin-resistant *S. aureus* mastitis isolates *in vivo* (Schmelcher et al, 2012b). In case of *E. faecalis* phage Lys168/Lys170 endolysins, a fusion of their catalytic domains to the cell wall binding domain of a staphylococcal phage lysin (Lys87) even extended the lytic host spectrum of the native endolysins from targeting only *E. faecalis* strains to other enterococci, staphylococci and even group A streptococci (Fernandes et al, 2012). When the SH3b binding domain (of lysostaphin) was C-terminally fused to full-length HydH5, its lytic activity could be increased a 1.7-fold (Rodriguez-Rubio et al, 2012), suggesting the SH3b domain helped HydH5 to efficiently exert its muralytic activity.

Another suggestion for the fusion optimization of endolysins forms the binding to protein transduction domains (PTD) present in cell-penetrating peptides (Schwarze & Dowdy, 2000). A well-studied example of a cell-penetrating peptide is the TAT (Trans-Activator of Transcription) protein encoded by the HIV virus, that contains a PTD (amino acid sequence = YGRKKRRQRRR) with a nucleus localization signal (GRKKR) inside. When the green fluorescent protein (GFP) is fused to this TAT PTD, its uptake into mammalian cells is significantly enhanced (Ryu et al, 2003). Mostly, these protein transduction domains possess a high content of basic residues allowing translocation of the protein over the cytoplasmic membrane. The exact translocation mechanism, however, is poorly understood. Such a fusion is believed to enable the uptake of lytic enzymes in eukaryotic cells as well, potentially resulting in effective targeting of intracellular *S. aureus* infections (Borysowski & Gorski, 2010).

1.3 Gram-negative outer membrane as a natural barrier for external agents

Together with the thickness of the peptidoglycan, the presence of an outer membrane distinguishes the Gram-negative from the Gram-positive cell envelope. This layer is characteristically different from other biological membranes as it has an asymmetric form. The internal part of the outer membrane consists of phospholipids and embedded proteins, like many biological membranes, together with covalently bound lipoproteins. Outer membrane proteins and peptidoglycan-associated lipoproteins from the OmpA family serve as anchors between the outer membrane and peptidoglycan structures (Parsons et al, 2006). The highly diverse external side, composed of glycolipid lipopolysaccharides is called the lipopolysaccharide (LPS) layer and can be typically subdivided in three major regions: (1) the O-polysaccharide part as outermost layer, (2) the core polysaccharide as intermediate region and (3) the lipid A as the most inner part (Raetz & Whitfield, 2002) (Figure 1.6).

1.3.1 Structure and diversity of lipopolysaccharide

1.3.1.1 O-polysaccharide or O-antigen

The O-polysaccharide or O-antigen, a neutral polymer composed of repeating oligosaccharide units (between two and eight sugars) is the most heterogeneous part of LPS. This part confers serum resistance to a particular bacterium. In case of *Salmonella*, the length of the O-antigen defines if the serum complement system is activated (Murray et al, 2006). For the assembly of the O-antigen, extensive lateral transfer of genes took place among different bacterial strains, as assessed by sequence analysis. A huge amount of O-antigen variants or serotypes are observed among Gram-negative bacteria due to variations in O-antigenic sugars. For *P. aeruginosa*, *E. coli* and *Salmonella*, respectively 20, 181 and 67 different O-antigen serotypes have been described based on serological activity and structural diversity (Knirel et al, 2006; Liu et al, 2008). Despite their evolutionary relatedness, *Salmonella* and *E. coli* only share a few common O-serotypes (Samuel et al, 2004).

Typically, N-acyl derivatives of various, sometimes exotic, amino sugars, like 6-deoxyhexosamine, 2-amino-2-deoxyhexuronic acid, 2,3-diamino-2,3-dideoxyhexuronic

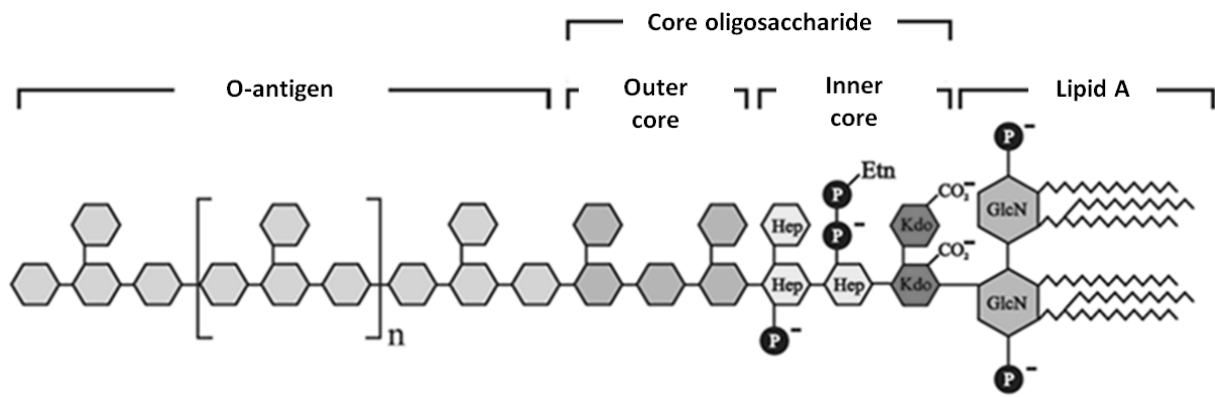


Figure 1.6: General structure of lipopolysaccharide layer (LPS) of Gram-negative bacteria. LPS is normally composed of three distinct parts: a highly variable outermost layer, the O-antigen or O-polysaccharide; a more conserved core oligosaccharide that can be divided in an inner and outer core; and the biological active lipid A, also called endotoxin. GlcN = N-acetylglucosamine, Kdo = 2-keto-3-deoxyoctanoate, Hep = heptose, P = phosphate, Etn = ethanolamine. Figure adapted from Lodowska et al (2007).

acid or 5,7-di-amino-3,5,7,9-tetradeoxynon-2-ulosonic acid are found in Gram-negative O-serotypes (Knirel et al, 2006). Modifications of O-antigenic sugars, like O-acetylation, epimerization, glycosylation and amidation, often appears in LPS synthesis, significantly extending the structural diversity of the O-antigen (Kaya et al, 1989; Liu et al, 2010; Vinogradov et al, 1987). Except for the serotype-specific O-antigens, also called “B-band” polysaccharides, *P. aeruginosa* is also able to synthesize “A-band” polysaccharide, a homopolymer of D-rhamnose sugars (Rocchetta et al, 1999). Some mucosal pathogens lack the O-polysaccharide part in their LPS, conferring immunity rescue (Raetz & Whitfield, 2002).

1.3.1.2 Core oligosaccharide

The non-repeating core oligosaccharide can conceptually be subdivided in inner (proximal to lipid A) and outer core. All sugars present in the core adopt a pyranose ring structure of 5 carbon residues with an α -stereo-isomeric configuration (Raetz & Whitfield, 2002). The structure of the inner core is often highly conserved within a Gram-negative genus or family, proving the importance of the inner core for LPS stability and integrity (Raetz & Whitfield, 2002). The inner core typically consists of two negatively charged 2-keto-3-deoxyoctanoate (Kdo^I and Kdo^{II}) and two L-glycero-D-mannoheptose (Hep^I and Hep^{II}) residues. Kdo is a unique molecule that is only found in Gram-negative LPS. A third heptose residue occurs in a few commensal *E. coli* strains. In some cases, the Kdo residues are substituted by a

derivative, D-glycero-D-talo-oct-ulosonic acid (Brade, 2000). Other sugars, like N-(acetyl)glucosamine (in some *E. coli* strains), and phosphate (P), (pyro)phosphoethanolamine ((P)PEtN), phosphorylcholine (PCho) and carbamoyl (typically on *P. aeruginosa* LPS) side groups are often found attached to these heptose residues. The *P. aeruginosa* core has a multiple phosphorylated inner core which, together with the 2 present Kdo residues, gives a average of 6.5 formal negative charges per LPS molecule (Nikaido, 2003). Phosphorylation can take place on three different sites in the *P. aeruginosa* inner core: on position 2 and 4 of Hep^I and on position 6 of Hep^{II} (Pier, 2007). Each phosphorylation site may be occupied by a phosphate, diphosphate or triphosphate group. This phosphorylation proved essential for *P. aeruginosa* viability and for intrinsic resistance against antibiotics (Knirel et al, 2006). Contrarily to *P. aeruginosa*, the *E. coli* core region only carries a phosphate on Hep^{II}, a PPEtN on Hep^I and a PEtN on Kdo^{II}, giving 5.5 formal negative charges per molecule which are more evenly distributed over the *E. coli* core compared to *P. aeruginosa* (Nikaido, 2003). Moreover, phosphorylation is not essential for viability of *E. coli* and *Salmonella* strains. Other Gram-negative bacteria, like *K. pneumoniae*, also show no phosphorylation of the heptoses in the inner core region, but the necessary negative charges are provided there by uronic acids, instead of phosphates (Raetz & Whitfield, 2002).

The outer core, which provides an attachment site for the O-antigen part, consists mainly of five to seven common hexoses (mainly D-glucose, D-galactose and L-rhamnose). It also shows a higher structural variability than the inner core, as the outer core comes in closer contact with the host immune system, bacteriophages and other external stress factors like antibiotics (Raetz & Whitfield, 2002). In case of *P. aeruginosa*, two structurally similar forms (glycoforms) of outer core occur: a glycoform 1 with 5 or 6 sugar residues and the L-rhamnose connected to the second most inner D-glucose and a glycoform 2 with 5 sugar residues and the L-rhamnose bound to the most inner D-glucose (Sadovskaya et al, 1998).

1.3.1.3 Lipid A

Lipid A is generally composed of a non-reducing β -1',6'-linked disaccharide backbone, acetylated on different positions (C₂, C₃, C_{2'} and C_{3'}) by primary hydroxy and non-hydroxy acyl groups with a variable length between 10 and 14 carbon atoms. Positions C₁ and C_{4'} of

the disaccharide backbone are normally phosphorylated. The primary fatty acids are on their turn further acetylated by secondary acyl groups, generating specific acyloxyacyl structures for tight anchoring of the LPS to the phosphomono layer of the outer membrane. Structural differences in lipid A mainly concern the amino-sugar type, the presence of phosphate, ethanolamine or other groups, the number of substitutions of the disaccharide backbone by primary acyl groups, and the type, number and distribution of secondary acyl groups (Lodowska et al, 2007; Raetz & Whitfield, 2002).

Lipid A is recognized by the Toll-like Receptor 4/MD-2/Cluster of Differentiation 14 (TLR4/MD-2/CD14) receptor complex, exposed on the surface of macrophages, mononuclear cells and epithelial cells in mammals. LPS-binding eventually leads to severe inflammatory responses, e.g. production of cytokines (IL-1 and 8, Tumor Necrosis Factor α) and chemokines (Hajjar et al, 2002). In *E. coli* lipid A, the two phosphate groups and secondary acyloxyacyl chains are responsible for immune triggering (Alexander & Rietschel, 2001).

Lipid A of environmental and laboratory *P. aeruginosa* strains is mainly penta-acylated (low acetylated lipid A) with fatty acids chains composed of 10 to 12 carbon atoms. In *E. coli* and *Salmonella* strains, no penta-acylated variant is present, only hexa- or hepta-acylations (high acetylated lipid A) occur, and fatty acid chains are minimal 14 carbon atoms long. The smaller penta-acyl chains present in *P. aeruginosa* lipid A are, for an unknown reason, less effective in activating the human TLR4/MD-2/CD14 receptor complex (Hajjar et al, 2002). This observation probably accounts for the lower cytotoxicity observed for *P. aeruginosa* lipid A compared to lipid A of other Gram-negative species, like *E. coli* or *Salmonella* (Knirel et al, 2006). The presence of a higher number of long fatty acid chains in lipid A of *E. coli* and *Salmonella* contributes to a stronger intermolecular hydrophobic stacking and consequently a more stabilized LPS structure. Furthermore, the fatty acid substituents in *P. aeruginosa* LPS are more equally distributed over the two sugars of the lipid A backbone than in *E. coli* or *Salmonella* LPS (Nikaido, 2003). The number of 2-hydroxylated secondary acyloxyacyl groups and thus the number of free hydroxyl groups for making hydrogen bonds is higher in *P. aeruginosa* LPS than in *E. coli* or *Salmonella*. *P. aeruginosa* seems to compensate the limited hydrophobic stacking due to smaller acyl chains by the higher number of free hydroxyl groups, resulting in increased hydrogen bonding between adjacent LPS molecules.

1.3.1.4 Physiological adaptations in LPS of *E. coli*, *S. Typhimurium* and *P. aeruginosa*

Structural adaptations in the lipid A of Gram-negative bacteria are mainly influenced by physiological factors like the presence of divalent ions or cationic AMPs in the environment and fluctuations in temperature. We give an overview here of the adaptations described in literature of the *E. coli*, *S. Typhimurium* and *P. aeruginosa* LPS.

- *E. coli* and *S. Typhimurium*

E. coli and *Salmonella* strains have developed several mechanisms to adapt their outer membrane, and specifically the lipid A moiety, to the destabilizing effect of low Ca^{2+} and Mg^{2+} concentrations or the presence of cationic AMPs. During infection, *Salmonella* specifically survives in phagosomes which only contain micromolar concentrations of divalent cations (Garcia-del Portillo et al, 1992). Both low $\text{Mg}^{2+}/\text{Ca}^{2+}$ concentrations (in micromolar range) and cationic AMPs present in the extracellular environment are shown to be sensed by the PhoQ sensor of the PhoPQ two component system, resulting in the phosphorylation of the PhoP regulator and the subsequent transcription of different genes encoding LPS modifying enzymes (Groisman, 2001; Guo et al, 1997).

Phosphorylated PhoP (PhoP-P) activates another two component system, the PmrAB system, that on its turn promotes the activation of enzymes necessary for addition of 4-amino-L-arabinose (l-Ara4N) or PEtn to the 1' or 4' phosphate groups on lipid A (Gunn et al, 1998; Trent et al, 2001b; Zhou et al, 2001) (Figure 1.7). Both modifications alter the net negative charge present at these positions of the LPS at neutral pH from -1.5 per phosphate group to 0, thereby reducing electrostatic repulsions and increasing lateral interactions between adjacent LPS molecules. In this way, the LPS structure becomes less dependent of the stabilizing $\text{Mg}^{2+}/\text{Ca}^{2+}$ divalent cations. Moreover, these modifications also lead to repulsion of positively charged AMPs and neutralization of toxicity. The *pmrAB* activating genes were originally discovered as being responsible for polymyxin-resistance (Vaara et al, 1979).

Furthermore, PhoP-P promotes the transcription of the *pagP* and *pagL* genes encoding for the PagP palmitoyl transferase and PagL palmitoyl deacylase, respectively (Figure 1.7). PagP

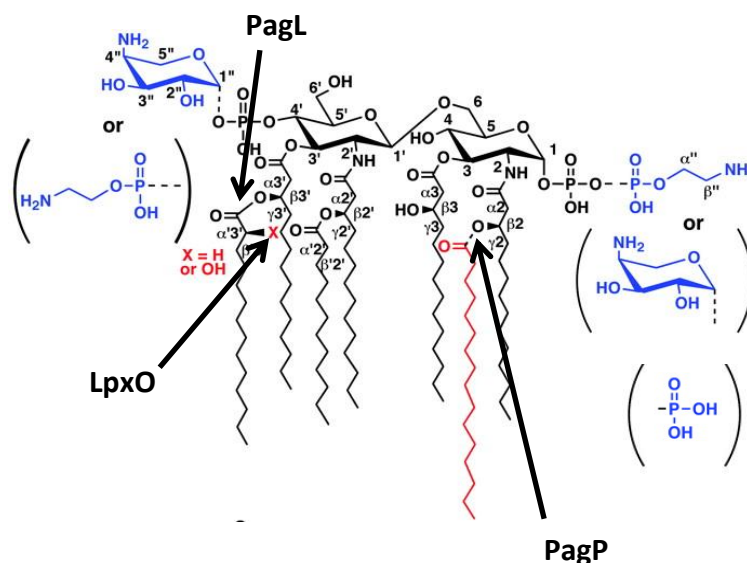


Figure 1.7: Adaptive modifications found in *E. coli* or *S. Typhimurium* lipid A structures in response to changing physiological parameters. The names of the modifying enzymes are marked in bold, and their action site is indicated by an arrow. Modifications under direct control of the PhoPQ system are in red, whereas PmrAB induced modifications are in blue. The connecting bonds of the different possible modifications at the C₁ and C₄ position (between brackets) are dashed. Adapted from Zhou et al (2001).

transfers a palmitate chain (C16:0) to the 3-OH group of the myristate (C14:0) present at position C₂ of the sugar backbone of lipid A (Guo et al, 1998). In this way, the amount of acyl groups bound to the sugar backbone is raised from six (hexa-acylated) to seven (hepta-acylated), a modification which is assumed to increase LPS stability due to a higher hydrophobic stacking between neighboring LPS molecules. This acylation is also believed to diminish AMP toxicity, as the decreased fluidity of the outer membrane prevents proper insertion of the AMP in the LPS layer (Anaya-Lopez et al, 2012). On the other hand, the outer membrane bound PagL enzyme removes the primary 3-OH myristate moiety by hydrolyzing the ester bond at the C_{3'} position of the sugar backbone (Trent et al, 2001a). Both PagP and PagL modifications help bacteria to evade the host immune system due to a reduced TLR4/MD-2/CD14 signaling of the deacetylated or palmitoylated lipid A (Kawasaki et al, 2004a; Kawasaki et al, 2004b).

In some cases, LpxO, an Fe²⁺ dependent dioxygenase activated by PhoP-P, catalyzes the 2-OH hydroxylation of the 3-OH myristate acyloxyacyl moiety at position C_{3'} (Gibbons et al, 2000) (Figure 1.7). This modification probably compensates for the loss of an OH-group by the PagP acyl transferase as the number of hydrogen bond donors is maintained in this way.

In *E. coli*, an additional gene named *lpxP* was found that is activated at a low temperature of 12°C. LpxP promotes the substitution of a laurate acid chain by an unusual palmitoleate and is therefore assumed to play a role in the adjustment of the outer membrane fluidity to colder environments (Carty et al, 1999).

- *P. aeruginosa*

Modifications of lipid A in environmental *P. aeruginosa* strains in response to magnesium-limiting growth conditions are, similar to *Salmonella* and *E. coli*, regulated by the two-component regulatory systems PhoPQ (PagP transferase/PagL deacylase) and PmrAB (palmitate/4-l-AraN addition). These modifications are reminiscent of the PhoPQ-induced modifications in *Salmonella* lipid A, except for the positions of the added palmitate (C_{3'} position instead of C₂) and the absence of phosphoethanolamine modifications at the C₁ position (McPhee et al, 2003; Nikaido, 2003). Laboratory strains (PAO1, PAK, PA14) grown in Mg²⁺-rich medium don't show these modifications and normally adopt the penta-acylated lipid A form (Moskowitz & Ernst, 2010).

The *P. aeruginosa* isolates from cystic fibrosis patients form a major exception. These strains show the PhoPQ/PmrAB induced type of lipid A modifications also under magnesium-rich conditions, conferring resistance to AMPs and increase proinflammatory signaling (Ernst et al, 2006; Moskowitz & Ernst, 2010). Clinical *P. aeruginosa* strains isolated from infected lungs in the early phase of the disease bear a modified lipid A structure with (I) a removed 3-OH decanoate moiety at the C₃ position by PagL deacylase action, (II) a palmitate (C16:0) acyloxyacyl group bound to the 3-OH residue of the decanoate (C10:0) at the 3' position of the backbone by PagP transferase and (III) an 4-amino-L-arabinose residue (l-4-AraN) attached to the phosphates at the C₁ and/or C_{4'} positions of the sugar backbone by action of enzymes PmrH, PmrF, PmrI, PmrJ, PmrK and PmrE (Ernst et al, 1999; Moskowitz & Ernst, 2010; Rutten et al, 2006) (Figure 1.8). In a later, more severe, stage of the disease, PagL becomes inactivated resulting in the presence of *P. aeruginosa* strains with a hepta-acylated lipid A structure, retaining the 3-OH decanoate group at C₃ position (Ernst et al, 2006; Ernst et al, 2007). Deciphering the role of this late adaptation may be important to understand the development and progression of cystic fibrosis.

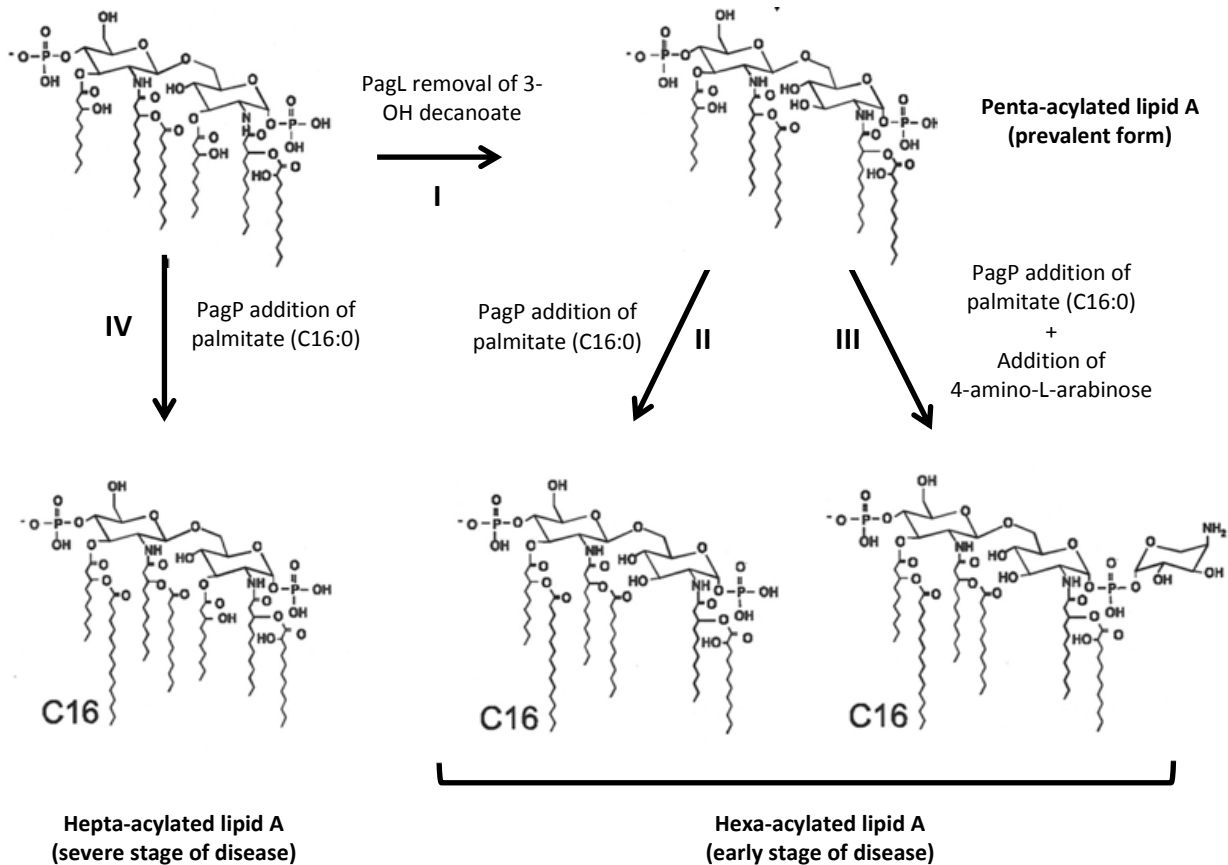


Figure 1.8: Adaptive modifications of lipid A structure found in different clinical *P. aeruginosa* strains isolated from cystic fibrosis patients. (I) In the early stage of disease, the 3-OH C10:0 decanoate moiety at the C₃ position of the sugar backbone is removed by the PagL deacylase to obtain the prevalent penta-acylated lipid A form. Further lipid A modifications appear by (II) addition of C16:0 palmitate acyl chain at the 3-OH group of the C₃ C10:0 decanoate (PagP transferase) and (III) 4-amino-L-arabinose residues at the phosphate groups at position C₁ or C₄ (PmrH, PmrF, PmrI, PmrJ, PmrK and PmrE). (IV) *P. aeruginosa* strains isolated from patients with a severe form of the disease mostly lack the PagL deacylase activity, retaining the 3-OH C10:0 decanoate acyl chain to obtain a hepta-acylated lipid A form. Adapted from Moskowitz & Ernst (2010).

1.3.2 Outer membrane-based resistance mechanisms

The Gram-negative outer membrane forms a tight and impermeable structure due to strong stabilizing forces and the presence of “slow” porins and multidrug efflux pumps embedded in the membrane. These characteristics greatly contribute to the resistance against hydrophilic and hydrophobic antibacterials. As already mentioned, the outer membrane is stabilized by two major forces: the presence of divalent cations cross-linking adjacent LPS

molecules and the dense hydrophobic stacking of acyl chains from the lipid A moiety in the inner phospholipid monolayer of the outer membrane.

As the inner phospholipid layer is not permeable for hydrophilic solutes, the outer membrane forms a selective barrier that prevents such molecules from entering the cell (Nikaido, 2003). Influx of hydrophilic nutrients happens through non-specific channel-forming proteins filled with water, called porins. The number and different variants of porins are essential for the outer membrane permeability of hydrophilic drugs. In *E. coli*, three major types of porins are assembled: OmpF (Outer membrane protein F) generally prefers the passage of larger, cationic compounds, OmpC smaller, cationic compounds and PhoE anionic compounds. Porin expression and formation in *E. coli* is tightly regulated by environmental conditions including nutrient level, osmotic strength, temperature, medium pH and presence of chemicals (Nikaido, 2003). Loss of OmpC in the *E. coli* outer membrane is related with decreased susceptibility to carbapenems and cefepime (Liu et al, 2012). In *P. aeruginosa*, the major porin OprF, also called “slow” porin, accounts for a much slower diffusion of hydrophilic nutrients than OmpF or OmpC, almost a 2 orders of magnitude lower rate. This property of the *P. aeruginosa* outer membrane is largely responsible for its lower permeability in comparison to the *E. coli* outer membrane. Furthermore, porins of *E. coli* structurally consist of three open β -barrel structures with a hydrophilic inner side and a hydrophobic outside. The OprF population, on the other hand, can fold in two different ways. The major fraction of OprF porins folds in a closed conformation, only a minority adopts the open β -barrel conformation, lowering the *P. aeruginosa* outer membrane permeability even further. Loss of OprD porins in *P. aeruginosa*, which specifically function in the uptake of positively charged amino acids, prevents the diffusion of imipenem through the outer membrane (Lambert, 2002). In *A. baumannii*, alterations in several porins, including the CarO porin that regulates the uptake of carbapenems, are assumed to contribute to emerging carbapenem resistance (Poirel & Nordmann, 2006).

The permeability of the outer membrane is further decreased by the action of multidrug efflux systems which actively remove antibiotics, dyes, detergents, fatty acids, organic solvents and homo-serine lactones from the cell interior. The RND- (Resistance-Nodulation-cell Division) type of efflux pumps present in *A. baumannii*, *E. coli*, *Salmonella* and

P. aeruginosa are associated with improved resistance against a broad spectrum of antibiotics (Alekshun & Levy, 2007) (Table 1.2). These type of efflux systems consist of three different modules (an inner membrane protein, a periplasm spanning protein and an outer membrane protein), all encoded in one operon, for direct connection of the cytoplasm with the extracellular environment. RND-type systems characteristically use the proton gradient present across the membrane to power efflux of unwanted compounds.

The most studied Gram-negative RND-type efflux system is the AcrAB-TolC system in *E. coli*, which renders the bacterium resistant against fluoroquinolones, chloramphenicol and tetracyclines (Alekshun & Levy, 2007). In *A. baumannii* and *P. aeruginosa*, respectively one (AdeABC) and seven (MexAB-OprM, MexCD-OprJ, MexEF-OprN, MexHI-OprD, MexJK-OprM, MexVW-OprM and MexXY-OprM) RND-type efflux systems have been described so far (Li et al, 2003; Poole, 2001). Upregulation of the efflux system encoding genes can eventually lead to an increased antibiotic resistance.

Table 1.2: The RND-type of efflux systems present in cell walls of *P. aeruginosa*, *A. baumannii* and *E. coli* and the antibiotic groups to which they confer resistance to. Adapted from Alekshun & Levy (2007).

Bacterial organism	Efflux system	Representative antibiotic resistance
<i>P. aeruginosa</i>	MExAB-OprM	β -lactams, fluoroquinolones
	MexCD-OprJ	fourth generation cephalosporins
	MexEF-OprN	fluoroquinolones, chloramphenicol
	MexHI-OprD	norfloxacin
	MexJK-OprM	ciprofloxacin, tetracycline, erythromycin
	MexVW-OprM	fluoroquinolones, chloramphenicol and tetracycline
	MexXY-OprM	aminoglycosides, tigecyclines
<i>A. baumannii</i>	AdeABC	aminoglycosides, fluoroquinolones, tetracycline, chloramphenicol and erythromycin
<i>E. coli</i>	AcrAB-TolC	β -lactams, fluoroquinolones, tetracycline, chloramphenicol

1.3.3 Possible strategies to overcome the outer membrane barrier

1.3.3.1 Chemical permeabilization using outer membrane permeabilizers

As mentioned previously, the interaction between the stabilizing divalent cations and the anionic LPS structure is essential for the outer membrane stability, especially in bacteria like *P. aeruginosa*. Based on their chemical characteristics, three different classes of chemical compounds or drugs are described in literature that are able to enhance outer membrane permeability by targeting these cation-LPS interactions, the so called “outer membrane permeabilizers” (Hancock & Wong, 1984). A first group comprises chelating agents that remove the stabilizing cross-bridging divalent cations (Ca^{2+} and Mg^{2+}) in the LPS structure by chelation, with ethylenediaminetetraacetic acid (EDTA) as type example (Hancock, 1984). Removal of Mg^{2+} and/or Ca^{2+} from the LPS increases the electrostatic repulsion between adjacent LPS molecules due to the presence of negatively charged phosphate and Kdo groups. This results in the substantial release of LPS in the extracellular environment (Leive et al, 1968). Nikaido and Vaara (1985) suggest that the resulting voids in the LPS structure are consequently filled with phospholipids that migrate from the inner leaflet of the outer membrane or cytoplasmic membrane to the outer leaflet. As a result, patches of glycerophospholipid bilayer are produced which allow facilitated transport of hydrophobic/lipophilic agents. The enhanced permeability of the outer membrane due to chelators is therefore a result of a change in outer membrane morphology. Weak organic acids like citrate, lactate, malate, sorbate and benzoate, in addition to their pH lowering antibacterial effect, also act as an outer membrane permeabilizer using the same chelating mechanism as EDTA, but in lesser extent (Alakomi et al, 2007; Alakomi et al, 2000; Guha et al, 2002; Helander & Mattila-Sandholm, 2000).

Large organic monovalent cations, like Tris(hydroxymethyl)aminomethane (Tris) and cetrимide, form the second group of permeabilizers. Tris, a bulky primary amine, contributes to outer membrane permeabilization by partially replacing the LPS bound cations (Nikaido & Vaara, 1985; Schindler & Teuber, 1978). Due to its low LPS binding affinity, Tris is only able to induce limited release of LPS at high concentrations (> 0.1 M) (Irvin et al, 1981). At lower concentrations, it only assists the permeabilizing action of EDTA (Hancock, 1984).

The third group of permeabilizers consists of polycationic compounds with polymyxin B and its derivatives, poly-L-lysine, polyethyleneimine and aminoglycosides (streptomycin and gentamycin) as major representatives. Their excess of positive charges competitively interferes with the stabilizing divalent cations for binding of the anionic LPS parts. This results in displacement of the divalent cations and destabilization and/or permeation of the outer membrane (Vaara & Vaara, 1981; Vaara et al, 1979). Polymyxin B, a cyclic peptide with net positive charge of 4 and a fatty acid tail, is the strongest outer membrane permeabilizer from this polycationic group due to the dual action of positive charges (competition with the divalent cations) and the fatty acid (detergent-like activity) on LPS/phospholipid bilayer (Wiese et al, 1998). The interaction between a polycationic compound and the anionic LPS is strongly dependent on the ionic strength of the environment and is lost when high NaCl concentrations are present (Nikaido, 1998).

1.3.3.2 Liposome delivery

Liposomes are spherical phospholipid bilayers of 0.02-10 μm in diameter, that can be filled with antibacterial compounds or vaccines for a safe and effective delivery across the outer and inner membrane to the particular action site (Drulis-Kawa & Dorotkiewicz-Jach, 2010). They are able to overcome the outer membrane impermeability by membrane fusion or endocytosis. Nowadays, liposomes are widely used as drug carriers in cosmetics and pharmaceutical industry. Two types of liposome formulations are described in literature: the “rigid” and the “fluid” liposome formulations (Beaulac et al, 1998). Fluid liposomes are mostly composed of dipalmitoylphosphatidylcholine (DPPC), distearylphosphatidylcholine (DSPC) or dimyristoylphosphatidylglycerol (DMPC), whereas rigid liposomes consists of natural phospholipids and cholesterol, which can be polymer-coated. Dependent on the charge of the targeted action site, fluid liposomes can be either prepared in a cationic form, by addition of cholesterol and dimethyloctadecylammonium bromide (DDAB) to DMPC/DPPC/DSPC, or in an anionic form by mixing of DMPC/DPPC/DSPC with phosphatidylinositol (PI) (Smith, 2005). As most eukaryotic or bacterial membranes are anionic surfaces, the cationic liposomes offer the strongest vesicle-cell interactions.

Liposomes for delivery of antimicrobial compounds can be engineered to obtain an optimal pharmacokinetics and bio-distribution of the encapsulated agent in the human body. Drug concentrations can be maintained longer in the blood stream due to a gradual and sustained release of the drug from the liposomal carrier (Bakker-Woudenberg et al, 1995; van Etten et al, 1995). Encapsulation also prevents the drug from being inactivated by hydrolytic enzymes or the immunological system (Schiffelers et al, 2001). Furthermore, liposomes offer a reduced toxicity, an enhanced antibacterial efficacy against intra- and extracellular pathogens and target selectivity (Drulis-Kawa & Dorotkiewicz-Jach, 2010). The latter is achieved by incorporation of specific immunoglobulins, proteins or oligosaccharide chains as ligands in the liposome surface (Willis & Forssen, 1998). In this way, liposome vesicles can be directed towards specific tissue types or defined bacterial cells. Liposome-encapsulated aminoglycosides have been successfully used to reduce multidrug-resistant *P. aeruginosa* (Mugabe et al, 2006) and *Burkholderia cepacia* (Halwani et al, 2007) strains *in vitro*, and to treat *Mycobacterium avium* infections in mice (Klemens et al, 1990) and *K. pneumonia* infections in rat lung tissue (Bakker-Woudenberg, 2002; Bakker-Woudenberg et al, 1995).

1.3.3.3 Outer membrane vesicle-delivery

In nature, all Gram-negative bacteria, pathogenic or non-pathogenic, constitutively release spherical lipid bilayer vesicles from the outer membrane, called outer membrane vesicles (OMV) (Mayrand & Grenier, 1989) (Figure 1.9). These OMVs range in size from approximately 20-200 nanometers. OMV production is triggered by environmental stress conditions, including pH or temperature fluctuations and availability of nutrients. It contributes to the bacterial survival by mediating bacterial envelope stress, biofilm formation, virulence/pathogenesis, horizontal gene transfer and eliminating niche-competitors (Collins, 2011). Various virulence factors (adhesins or hydrolytic enzymes like proteases and phospholipase C), pathogen-associated molecular patterns (LPS), periplasmic proteins (pro-elastase or alkaline phosphatase) and outer membrane components (lipids or membrane proteins) incorporated in OMVs activate the host immune response and mediate pro- and anti-inflammatory effects (Ellis & Kuehn, 2010; Kadurugamuwa & Beveridge, 1997). In this way, OMVs play an important part in the generation of pathogen-induced

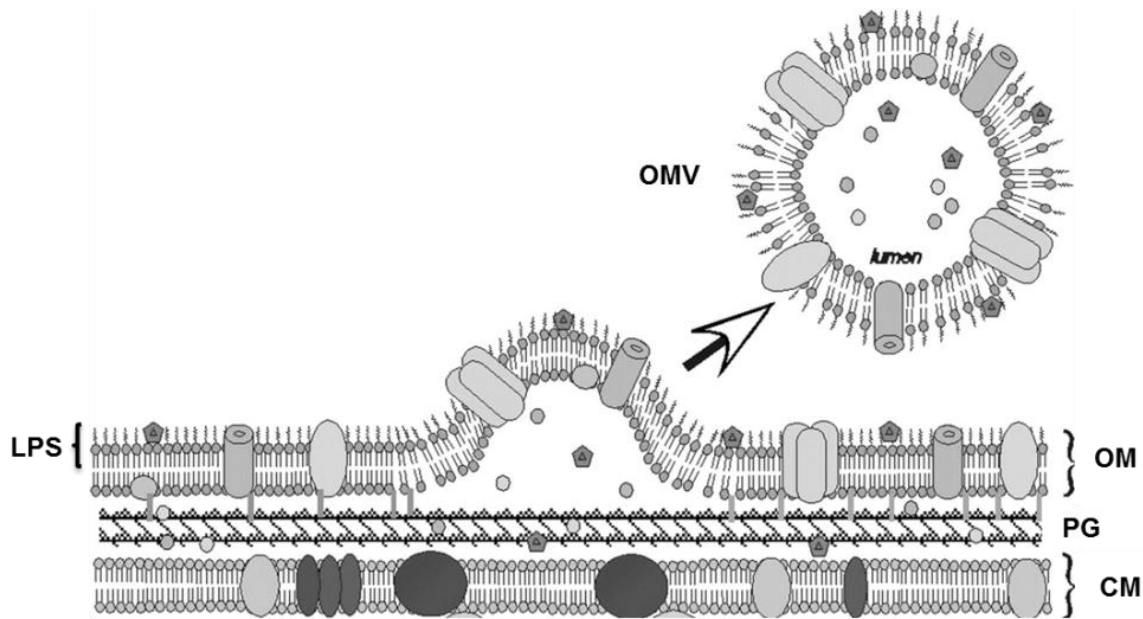


Figure 1.9: Outer membrane vesicle formation. OMVs consist of outer membrane phospholipids, LPS, outer membrane proteins and periplasmic proteins. Proteins and lipids of the cytoplasmic membrane are excluded from OMVs. Abbreviations: OM = outer membrane, CM = cytoplasmic membrane, PG = peptidoglycan, LPS = lipopolysaccharide, OMV = outer membrane vesicle. Adapted from Kuehn & Kesty (2005).

inflammation. Due to these immunogenic properties, OMVs are suitable candidates for vaccines or adjuvants development. Once liberated in the extracellular environment, the OMVs are able to adhere to another bacterial cell or a mammalian cell where they can then be internalized via a receptor-mediated endocytose pathway (engulfment), resulting in the release of their content in the cell cytoplasm and degradation of specific cellular parts (Ellis & Kuehn, 2010). Recent studies showed that different heterologous proteins can be packaged inside synthetic produced OMVs (s-OMVs) without losing their original activity by fusion with OMV-associated periplasmic or outer membrane proteins like the *E. coli* cytotoxin A (Kim et al, 2008). Heat labile enterotoxin of enterotoxigenic *E. coli* is a recent example of a virulence factor that could be successfully transported to mammalian host cells using the s-OMV-delivery pathway (Brown & Hardwidge, 2007). The same transport mechanism could possibly help cell wall targeting antibiotics or endolysins passing the outer membrane barrier for the implementation of their lytic function, as was successfully shown for an *P. aeruginosa* autolysin (Kadurugamuwa & Beveridge, 1996). Advantages of the use of this OMV-delivery pathway over other transport mechanisms are the target specificity determined by the OMV surface ligands interacting with certain cell receptors, the

protection of OMV content against extracellular proteases and the opportunity to deliver high concentrations of effector molecules to target cells in a stable way (Collins, 2011). A major disadvantage is the presence of LPS moieties at the OMV surface which is pyrogenic for mammalian cells.

1.3.3.4 Pressure-promoted outer membrane permeabilization

High hydrostatic pressure (HPP) treatment (100-500 MPa) is an emerging technique in food preservation that allows for an improved nutritional and sensorial quality of different food products by effective reduction of food-borne or spoilage organisms. HHP causes denaturation of key enzymes resulting in inactivation of vital cellular processes including transcription and/or translation (Aertsen et al, 2004; Erijman & Clegg, 1998), and structural disruption and permeabilization of the inner and outer cell membranes (pressure promoted permeabilization) (Ganzle & Vogel, 2001). Because of this, HHP can also be used to improve uptake of antimicrobial compounds through the outer membrane. For large antibacterial compounds like nisin or lysozyme, this pressure promoted permeabilization is transient meaning that bacteria are only susceptible during pressure application and that the outer membrane is reconstituted to its normal form after pressure relief (Hauben et al, 1996).

Masschalck and coworkers (2001) showed for the first time the synergistic action of two antibacterials, human lysozyme and lactoferrin, on Gram-negative bacteria at high pressure, without loss of enzymatic activity. Moreover, muralytic enzymes of diverse origin (phage, eukaryotic and mammalian lysozymes) greatly improve the bactericidal effect of HPP on different *Pseudomonas*, *Salmonella* and *Shigella* strains (Nakimbugwe et al, 2006). In addition, the bactericidal potency of HPP (175 MPa, 15 min, 20°C) on *P. aeruginosa* raised from 1 to 3.5 log units by application of 25 µg of the *P. aeruginosa* phage endolysins KZ144 and EL188 (Briers et al, 2008). Due to the observed synergistic action of HPP and muralytic enzymes, the pressure level required to obtain a certain antibacterial activity is reduced, which allows for a more cost-effective and sustainable food preservation.

1.4 Antimicrobial peptides

Antimicrobial peptides, abbreviated as AMPs, are a unique and diverse group of strong, broad-spectrum compounds, usually between 12 and 50 amino acids long. They are part of the innate immune system of many organisms, including humans. Their short length is in agreement with their production at low metabolic cost for rapid neutralization of microbes after infection. As factors of the innate immunity, AMPs are atypical as they function without high specificity (Boman, 1995). AMPs are able to physically disrupt bacterial, mycobacterial, fungal and mammalian cell membranes, eventually leading to cell lysis.

1.4.1 Structure of antimicrobial peptides

Based on three-dimensional conformation, sequence homologies and functional similarities, AMPs can be divided in five major groups: (a) anionic peptides, (b) cationic linear α -helical peptides without cysteines, (c) cationic linear peptides, without cysteines, but with a high proportion of specific amino acid residues, (d) anionic and cationic peptides with only one disulfide bridge in the C-terminal part and (e) anionic and cationic peptides with more than one disulfide bridge (Table 1.3) (Boman, 1995; Brogden, 2005). A first, rather small group of AMPs is formed by the anionic peptides. Members of this group, including maximin H5 or dermcidin, are typically enriched in negatively charged glutamic acid or aspartic acid residues, and normally require zinc as a cofactor for their antimicrobial activity (Brogden, 2005). The second group consists of cationic linear peptides with α -helical conformation. Peptides belonging to this group have two features in common: they possess (1) an excess of positive charges spread over the entire peptide chain due to presence of many basic residues, and (2) contain approximately 50 % of hydrophobic amino acids (Shai & Oren, 2001). Magainins, cecropins, dermaseptins and temporins are the best characterized examples from this group. The third group, the linear peptides enriched in certain amino acids, comprises proline-rich (Apidaecin Ia: GNNRPVYIPQPRPPHPRI), histidine-rich (Histatin 5: DSHAKRHHGYKRKFHEKHHSHRGY), tryptophan-rich (indolicidin: ILPWKWPW WPWRR) and arginine-rich (penetratin: RQIKIWFQNRRMKWKK) AMPs. Tryptophan and proline have preference for the interfacial region of lipid bilayers, while arginine and histidine provide the lipid layer with positive charges and hydrogen bonding options necessary for

Table 1.3: Overview of the major groups of AMPs based on their three-dimensional conformation, sequence homologies and functional similarities. For each group, the major representative peptides are given together with the peptide origin and the corresponding reference (Brogden, 2005).

Structure	Major representatives (origin)	Reference
Anionic peptides	Maximin H5 (amphibians) Dermcidin (human sweat glands)	Lai et al (2001) Schitteck (2012)
Cationic linear α -helical peptides	Cecropins (moth) Magainins (frog skin, human LL-37) Dermaseptins (frog skin, human LL-37)	Steiner (1982) Zasloff (1987) Mor et al (1994)
Cationic linear peptides enriched in specific amino acids	Apidaecins (honey bee lymph fluid) Indolicidin (bovine neutrophil) Histatin (human saliva) Penetratin (<i>Drosophila</i> fly)	Casteels et al (1989) Del Sal et al (1992) Brewer & Lajoie (2002) Bolton et al (2000)
Anionic and cationic peptides with one disulfide bond	Bactenecin (bovine neutrophils) Brevinin (frog skin) Esculentin (frog skin)	Radermacher et al (1993) Morikawa et al (1992) Simmaco et al (1994)
Anionic and cationic peptides with two or more disulfide bonds	Defensins (mammalian phagocytes) Tachyplesins (horseshoe crab hemocytes) Protegrins (porcine leukocytes)	Lehrer et al (1993) Nakamura et al (1988) Kokryakov et al (1993)

membrane interaction. The fourth group of peptides have one intra-molecular disulfide bond forming a loop structure in their C-terminus and a longer N-terminal tail. Bactenecin, brevenin and esculentin are the only members of this group identified so far. The final group consists of AMPs that are structurally constrained by more than one disulfide bond, like defensins (3 S-S bonds), tachyplesins (2 S-S bonds) and protegrins (2 S-S bonds). This group of AMPs predominantly form two or more β -sheets with antiparallel chains in a rigid structure.

1.4.2 Mode of action of antimicrobial peptides

AMPs have multiple modes of action on bacterial and eukaryotic membranes, which generally differ from conventional antibiotics. Apart from this membrane perturbing activity (Figure 1.10), some AMPs are also able to interact with periplasmic and intracellular targets affecting key cellular processes, including DNA, RNA, protein and cell wall synthesis.

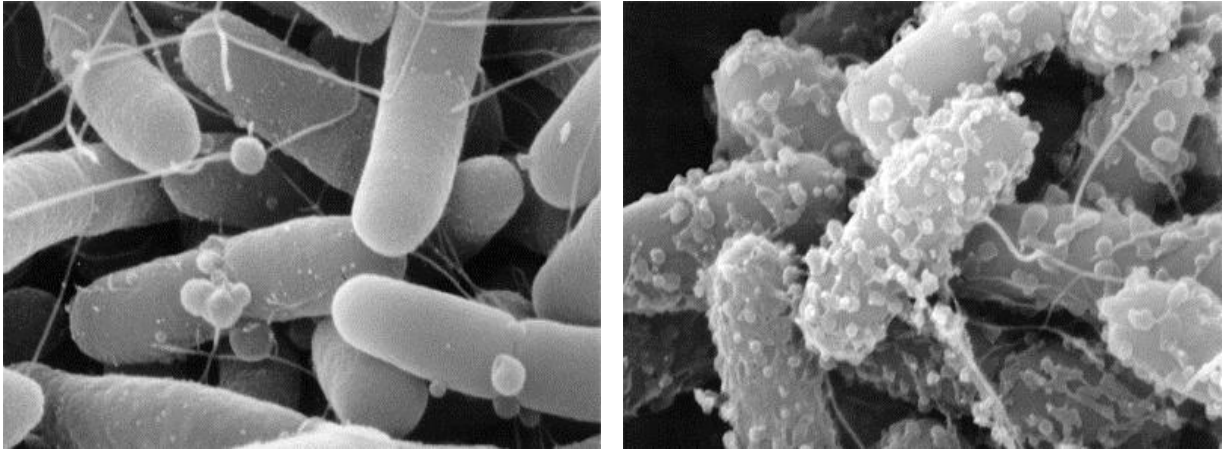


Figure 1.10: Transmission electron microscopy of AMP-treated *E. coli* cells. Left: cells after treatment with a low concentration of AMP. Right: cells after treatment with a high concentration of AMP. The formation of blebs or small spheres coming off from the bacterial outer membrane reveals permeabilizing activity (from <http://cmdr.ubc.ca/cool.html>, laboratory of R. E. W. Hancock, Department of Microbiology and Immunology, University of British Columbia, Canada). Photo: Copyright © - Susan Farmer

1.4.2.1 Membrane perturbing action

- Cytoplasmic membrane

Cytoplasmic membranes are recognized as main target for antibacterial activity of most AMPs. Studies on artificial phospholipid membranes or liposomes showed that AMPs act directly on these membranes, instead of using a receptor-mediated mechanism (Christensen et al, 1988; Kagan et al, 1990). However, the exact mechanism of membrane disruption is not completely understood and different competing models exist. These mechanisms are not mutually exclusive: one may represent an initial or intermediate step while another may be the consequence (Sato & Feix, 2006). With regard to the membrane permeability, AMPs could possibly induce complete cell lysis by membrane rupture (Bierbaum & Sahl, 1985) or cause local perturbation of the membrane layer allowing the leakage of intracellular components and electron gradient dissipation accompanied by the shutdown of vital cellular processes (Kragol et al, 2001). Three experimentally supported models suggested for membrane perturbation are the transmembrane pore formation by the “barrel-stave” and “toroidal-pore” mechanisms, and the detergent-like membrane solubilization by the “carpet-like” mechanism (Huang, 2000; Oren & Shai, 1998) (Figure 1.11).

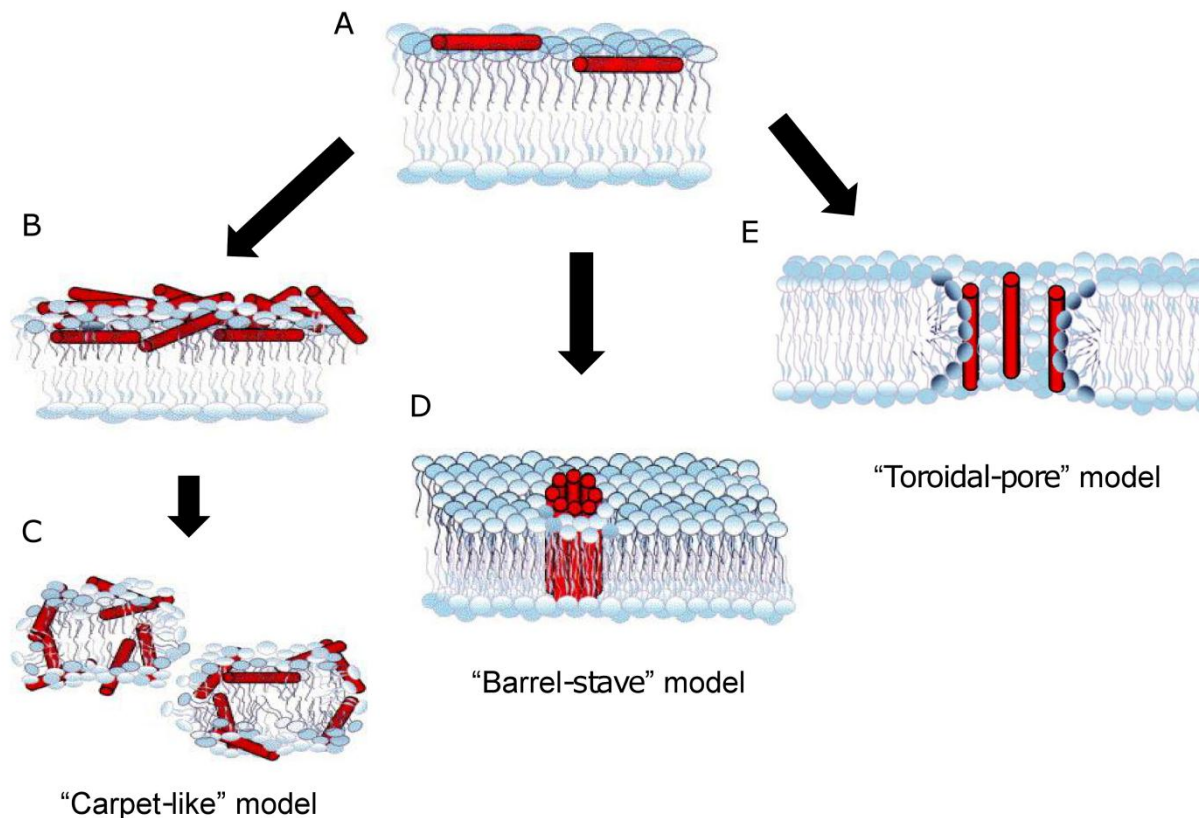


Figure 1.11: Representation of the “carpet-like” model (left pane), the “barrel-stave” model (intermediate pane) and the “toroidal-pore” model (right pane) suggested for membrane permeation by AMPs. (A) In a first common step, AMPs, appearing as dark grey cylinders, bind in parallel orientation to the membrane surface with their hydrophobic side to the phospholipid heads and their hydrophilic side pointed outwards. (B) In the “carpet-like” model, peptides accumulate and form a “carpet” layer of molecules on top of the membrane. (C) At a certain threshold concentration of bound peptide monomers, a reorientation of the hydrophobic peptide surface takes place towards the hydrophobic core of the membrane eventually leading to membrane disruption and micellization. (D) Peptides following the “barrel-stave” model are reoriented at a critical peptide concentration, with their hydrophobic part pointed inwards and the hydrophilic part outwards, leading to the formation of discrete pore channels that span the membrane. (E) In the “toroidal-pore” model, both AMPs and lipid head groups are part of the formed pored. Adapted from Sato and Feix (2006).

In the “barrel-stave” mechanism (Figure 1.11A,D), a two state model proposed by Huang and coworkers, peptides reorient themselves after a critical threshold of peptide concentration is reached to a position perpendicular to the cytoplasmic membrane with their hydrophobic part orientated outwards of the membrane and their hydrophilic part inwards (Huang, 2000). Reorientation will quickly lead to the formation of specific channels or pores spanning the membrane with a defined structure that dissipate the necessary ion gradients

(Ehrenstein & Lecar, 1977). This will cause a collapse of the transmembrane electrochemical gradients, uptake of water and ions, cell swelling and eventually osmolysis. Cecropin A and defensin were both proven to form voltage-dependent ion channels in lipid membranes which is in agreement with this hypothesized “barrel-stave” mechanism (Christensen et al, 1988; Kagan et al, 1990).

A second mechanism for pore formation is the “toroidal-pore” mechanism (Figure 1.11A,E). α -helices of AMPs, using this mechanism, insert into the membrane and force the lipid monolayers to bend through the pore. This action ends in a water core surrounded by both the inserted peptides and the lipid head groups, forming a toroidal pore. This mechanism of transmembrane pore formation is suggested for peptides that are too small to span a phospholipid bilayer in their α -helical conformation, and also require lipids to reach this goal. Examples of peptides for which the “toroidal-pore” mechanism is experimentally confirmed are magainins (Murzyn & Pasenkiewicz-Gierula, 2003), colicins (Sobko et al, 2006), melittins (Park et al, 2006) and bacteriocins (Yoneyama et al, 2009). The “toroidal-pore” model differs from the “barrel-stave” model as the inserted peptides always stay associated with the lipid head groups, even when inserted in the lipid bilayer (Yang et al, 2001).

Peptides using the “carpet-like” mechanism (Figure 1.11A-C), a third mechanism, are proposed to bind the membrane with their hydrophobic surfaces covering it like a “carpet” (Oren & Shai, 1998). At a certain threshold concentration of bounded peptide monomers, the peptide molecule will rotate leading to interaction of the hydrophobic peptide surface with the hydrophobic core of the membrane. By this rotation, the bilayer-form of the membrane is disrupted and micellization will take place in a detergent-like manner without formation of channels or pores (Gazit et al, 1995). Throughout the whole process, the peptide keeps associated with the phospholipid head groups of the membrane.

The efficiency of cytoplasmic membrane permeation depends on the binding affinity for the particular membrane. Highly positively charged peptides, like cecropins, magainins and dermaseptins, have a higher binding affinity for negatively charged acidic phospholipids than for zwitterionic phospholipids (Ehrenstein & Lecar, 1977; Gazit et al, 1995; Oren & Shai, 1998). Hence, these peptides are able to discriminate between bacterial cell membranes

which are negatively charged due to the presence of teichoic acids (Gram-positive cell wall) and LPS (Gram-negative cell wall), and mammalian cell membranes which are predominantly constituted of zwitterionic and sphingomyelin phospholipids (Verkleij et al, 1973). This difference in binding affinity probably explains why most AMPs are not toxic for normal mammalian cells, but do lyse bacterial cells efficiently.

- Gram-negative outer membrane

Before an AMP can reach the cytoplasmic membrane, the outer layers of the Gram-negative (outer membrane) and Gram-positive (thick peptidoglycan layer) bacterial cell wall should be crossed. Passage of cationic AMPs through the Gram-negative outer membrane is believed to happen by the self-promoted uptake mechanism described by Sawyer and coworkers (1988). A similar mechanism was proposed for the transfer of polycationic antibiotics, like polymyxins and aminoglycosides, across the outer membrane (Hancock et al, 1991). In this self-promoted uptake mechanism, AMPs initially interact with the surface LPS, competitively displacing the stabilizing divalent cations which form cross bridges between adjacent LPS molecules. Peptides then destabilize the outer membrane either by strongly binding to the lipopolysaccharide part or by neutralizing the negative charge over a smaller part of the outer membrane. Both actions results in the formation of local cracks in the outer membrane through which the cationic compound is translocated and able to reach and interact with the negatively charged cytoplasmic membrane (Hancock, 2001).

Until recently, the outer part of the LPS layer was believed to be the only binding site for many AMPs through electrostatic interaction with the Lipid A (endotoxin) part (Andersson et al, 1999). However, novel targets for α -helical cationic AMPs have been discovered in the form of the outer membrane proteins Lpp (Lipoprotein) and OprI (Outer membrane Protein I) of Enterobacteriaceae and *P. aeruginosa*, respectively (Chang et al, 2012a; Lin et al, 2010). Both proteins were found to interact with several cationic α -helical AMPs like CAP-18, SMAP-29 or LL-37 for Lpp and hRnase 7 for OprI, promoting the susceptibility for the antibacterial activity of these AMPs. The Lpp interaction seemed even insensitive for the inhibiting action of divalent cations, where normal AMPs are inactivated by them (Chang et al, 2012a). These

recent findings, together with the hypothesized peptide uptake or mode of actions, indicate that a large part in this field is yet to be revealed.

- Eukaryotic membrane

Some amphipathic, α -helical AMPs, like magainin-2, or the disulfide-containing NK-lysin, show potent anti-tumor activity in addition to their antibacterial activity (Andersson et al, 1996; Cruciani et al, 1991). NK-lysin is produced in the bone marrow and is an effector of cytotoxic T cells and natural killer (NK) cells in the mammalian immune system. More specific, the cationic core region (amino acids 39-65) of the NK-lysin, called NK-2, is responsible for its antibacterial and anti-tumor properties (Andra & Leippe, 1999; Schroder-Borm et al, 2003). Several studies showed that both magainin-2 and NK-2 peptide have a favorable activity towards certain types of cancer cells (Baker et al, 1993; Schroder-Borm et al, 2005). Magainin-2 was shown to form a ion-dependent channel in the hematopoietic tumor cell membrane causing it to lyse rapidly and irreversibly (Cruciani et al, 1991). In case of NK-2, cancer cells that possess an increased level of negatively charged phosphatidylserine components on their membrane surface were sensitive for the peptide action (Schroder-Borm et al, 2005). Normal mammalian cells, like human erythrocytes and keratinocytes, lack this phosphatidylserine (Andra & Leippe, 1999) and are therefore assumed to be protected against the toxic effects of the NK-2 peptide.

1.4.2.2 *Non-membrane perturbing actions of AMPs*

Apart from their membrane permeabilization or disruption properties, certain AMPs might also operate by entering the cell and interfering with critical cellular metabolic functions. Entrance to the cytoplasm usually happens by receptor-mediated endocytosis or with a receptor-independent, permease transport system (Nicolas, 2009). Examples of these periplasmic and intracellular actions include inhibition of cell wall synthesis, nucleic-acid synthesis and protein folding; alteration of the cytoplasmic membrane septum formation and inactivation of enzymes (Brogden et al, 2005). An overview of all the possible targets together with the corresponding AMPs for the model organism *E. coli* is given in Figure 1.12.

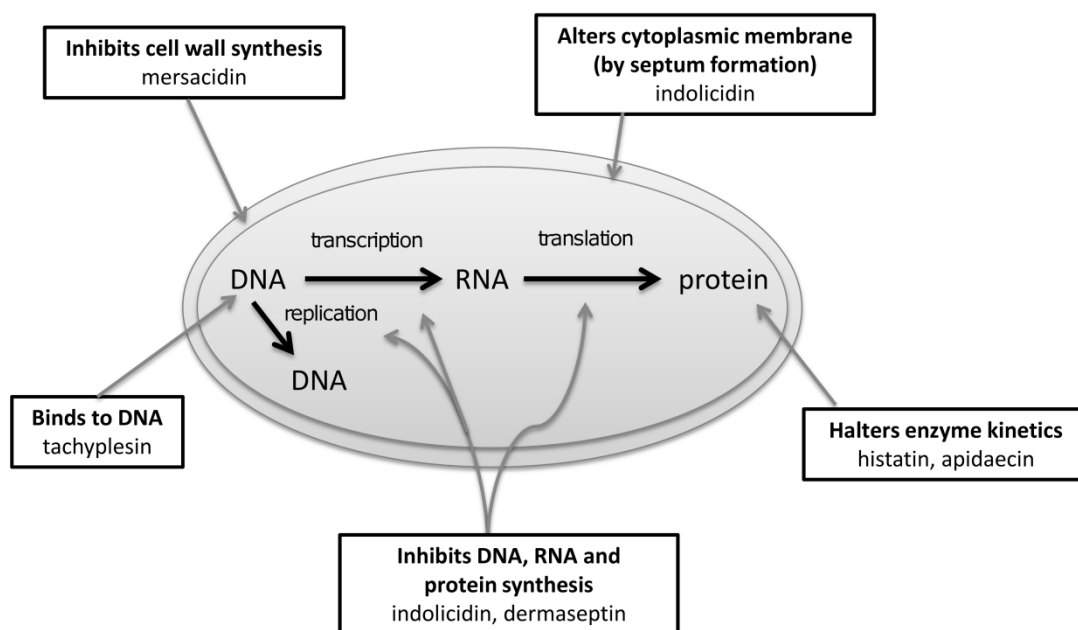


Figure 1.12: Non-membrane perturbing mode of actions of AMPs in *E. coli*. In addition to their membrane permeating potential, some AMPs are able to interact with key cellular processes in the bacterial cytoplasm or periplasm, including inhibition of cell wall synthesis, DNA replication, chaperone-based protein folding, enzyme kinetics and septum formation. Adapted from Brogden (2005).

Proline- and arginine-rich AMPs, like indolicidin and dermaseptins can inhibit DNA, RNA and protein synthesis via an unknown mechanism (Nan et al, 2009; Patrzykat et al, 2002; Subbalakshmi & Sitaram, 1998). Tachyplesin binds in the minor groove of the DNA helix, *in vitro*, and is thought to affect DNA replication (Yonezawa et al, 1992). The histidine-rich AMP, histatin 5, once inside the fungal or protozoal cell, accumulates in the mitochondrion where it causes a decrease in ATP synthesis by inhibition of a specific ATPase (Luque-Ortega et al, 2008). Short proline-rich AMPs, like apidaecins, are shown to specifically interact with the heat-shock protein DnaK and nonspecifically with the bacterial chaperone GroEL, thereby inhibiting correct protein folding (Otvos et al, 2000). Mersacidin, a lantibiotic produced by *Bacillus* species, binds the sugar phosphate head group of the lipid II precursor, thereby preventing the transglycosylation step during peptidoglycan biosynthesis (Sass et al, 2008). Addition of indolicidin to an *E. coli* culture results in cells with an extremely elongated morphology, which indicates the absence of cell division (Subbalakshmi & Sitaram, 1998). The exact mechanism causing this phenotype is unknown, but presumably membrane proteins involved in septum formation are inhibited by the peptides action.

1.4.3 Optimizing activity of antimicrobial peptides

Increasing the antibacterial efficacy of AMPs could be achieved either by optimizing their hydrophobicity and charge distribution or by fusion of the AMP with high-affinity membrane targeting modules. In both cases, specific modifications allow for a more efficient penetration of bacterial membranes. A first study on the optimization of AMP activity by changing hydrophobicity or charge distribution dates back to 1994, reporting the improvement of both the LPS-binding affinity and the outer membrane permeation of cecropin by C-terminal addition of two extra positively charged residues to the peptide (Piers et al, 1994). More recently, the C-terminal amidation of apidaecin-1b and the N-terminal addition of guanidine to higher the net positive charge of the peptide, increased its antibacterial activity on multidrug-resistant *E. coli* and *K. pneumonia* strains 4 to 32 times (Czihal et al, 2012). An alternative technique comprises the fusion of an AMP with a specific module that possesses a high affinity for certain membrane parts. In this respect, Arnush and coworkers (2012) were able to higher the antibacterial activity of a truncated magainin-2 analog against vancomycin-resistant enterococci by C-terminal conjugation with vancomycin. This agent efficiently targets the lipid II moiety in the cell membrane, a membrane-anchored precursor of cell wall synthesis (Breukink & de Kruijff, 2006).

The therapeutic use of hydrophobic AMPs is mostly hindered by their ability to destroy mammalian cell membranes leading to high hemolytic and cytotoxic side effects. Reduction of the hydrophobicity by introducing more polar residues in the α -helices of the AMP could significantly decrease the unwanted cytotoxic activity of the peptide while leaving the beneficial antimicrobial effect intact (Polyansky et al, 2009; Yin et al, 2012). Lysine-enriched variants of the cecropin-mellitin hybrid peptide CM15 showed a significantly lower hemolytic activity on cultured macrophages, while antimicrobial activities were similar (Sato & Feix, 2008). In case of the spider venom peptide latarcin, single-point mutations (isoleucine to lysine or glutamate) in the N-terminal end increased the half maximal effective concentration (EC_{50}) of the peptide on erythrocytes a 6-fold (Polyansky et al, 2009). By changing four leucine residues with alanine, Yin and coworkers (2012) reduced the hemolytic activity of designed cationic AMPs with 20 to 60 %. These examples prove the role of rational design in creating safe peptides with enhanced selectivity towards bacterial membranes.

Aims and study objectives

The main aims of this study consist of the characterization of a set of novel bacteriophage-encoded peptidoglycan hydrolases, also called endolysins, their engineering into effective antibacterial compounds against multidrug-resistant Gram-negative bacteria, and their evaluation in an *in vitro* human keratinocyte infection model and an *in vivo* nematode gut colonization model. The major challenge in the use of endolysins as enzyme-based antibacterials against Gram-negative bacteria is posed by the outer membrane barrier. The presence of this additional membrane hampers the passage of externally added phage endolysins to the peptidoglycan and protects Gram-negative bacteria from the lytic activity of these enzymes. By developing phage-encoded peptidoglycan hydrolases into compounds that are able to cross this barrier, the field of applications to target a wide range of Gram-negative pathogens with endolysins would become numerous. In this work, we specifically focus on endolysins encoded by Gram-negative infecting phages, a group of endolysins that still remain underexplored. This study builds further on research performed in the Laboratory of Gene Technology of the KU Leuven on three novel modular endolysins of *P. aeruginosa* infecting phages ϕ KZ, EL and ϕ KMV (Briers et al, 2007b; Lavigne et al, 2004).

To reach our aims, this project is subdivided in three major parts. In the first part, the pool of endolysins from Gram-negative phage origin is further expanded by characterization of 9 novel endolysins encoded by a wide range of Gram-negative infecting phages (Chapter 4- 6). From this first part, the most promising endolysins are selected for the further continuation of this study.

In the second part, an innovative approach to tackle the Gram-negative outer membrane and to enable access to the peptidoglycan layer is developed for the most promising endolysins from the first part, and extensively tested. This approach is based on the fusion of endolysins with antimicrobial peptides to provide these enzymes with intrinsic outer membrane destabilizing activity (Chapter 7). The impact of this fusion approach on the

biochemical and biological characteristics of endolysins is evaluated and the antibacterial strength of the fusion approach is further optimized (Chapter 8).

In a third and last part, we evaluate the cytotoxicity and antibacterial efficacy of the fusion approach on an *in vitro* human keratinocyte infection model (Chapter 9), on one hand, and tried to bridge the gap between *in vitro* and *in vivo* by evaluating the fusion approach on an *in vivo* *Caenorhabditis elegans* nematode gut colonization model (Chapter 10), on the other hand.

3.1 Bacterial strains and *Caenorhabditis elegans* SS104

Pseudomonas aeruginosa PAO1 (ATCC 15692) is a widely used laboratory strain fully sequenced by Stover et al (2000). The clinical *P. aeruginosa* strains Br667, a burn wound isolate collected in the intensive care unit in the Queen Astrid Military Hospital in Brussels (Belgium), PA14, a wound isolate from Boston (MA, USA) and Us447, a urine isolate from San Antonio (TX, USA) were all provided and characterized by Dr. Pirnay (Pirnay et al, 2009). *Pseudomonas putida* G1 was isolated from Russian soil in the neighborhood of Moscow (Prof V. Krylov, Laboratory of Bacteriophage Genetics). *Acinetobacter baumannii* 25 was an uncharacterized clinical isolate from the Queen Astrid Military hospital, donated by Maya Merabishvili (Lab MCT, Brussels, Belgium) and *Burkholderia pseudomallei* a clinical strain from the University Hospital of Gasthuisberg (Leuven, Belgium) isolated by Prof. dr. J. Verhaegen (Laboratory of Clinical Microbiology and Mycology, UZ Leuven). *Salmonella enterica* serovar Typhimurium LT2 (*S. Typhimurium* LT2), *Staphylococcus aureus* subsp. aureus Rosenbach ATCC 6538, *Micrococcus lysodeikticus* ATCC 4698, *Bacillus subtilis* PSB3 and *Lactococcus lactis* subsp. lactis were all provided by the Centre of Food and Microbial Technology (KU Leuven, Belgium). Different *Escherichia coli* strains were used in this study (Table 3.1): *E. coli* XL1-Blue MRF' (Agilent Technologies, Santa Clara, CA, USA) for antibacterial activity testing, *E. coli* TOP10 (Thermo Fischer Scientific, Waltham, MA, USA) for DNA cloning and cell stock storage, and *E. coli* BL21(DE3)pLysS, BL21-CodonPlus-(DE3)-RIL and BL21-CodonPlus-(DE3)-RP (Agilent Technologies) as host strains for protein expression. For proper selection, ampicillin (100 µg/ml, Roche Diagnostics, Mannheim, Germany) or chloramphenicol (50 µg/ml, Calbiochem®, Darmstadt, Germany) were used.

All mentioned strains were grown at 37°C, except for *P. putida* G1 at 30°C, in Lysogeny Broth (LB, 1 % (w/v) tryptone (Lab^M, Bury, UK), 1 % (w/v) NaCl (Acros Organics, Geel, Belgium) and 0.5 % (w/v) yeast extract (Lab^M)). For LB agar, an extra 1.5 % (w/v) Agar 1 (Lab^M) was added.

Table 3.1: Genotypes of *E. coli* strains used in this study.

Strains	Genotype
XL-1 Blue MRF ⁺	<i>(mcrA)183 Δ(mcrCB-hsdSMR-mmr)173 endA1 supE44 thi-1 recA1 gyrA96 relA1 lac [F'proAB lacI^qZΔM15 Tn10 (Tet^r)]</i>
TOP10	F ⁻ <i>mcrA Δ(mcrCB-hsdSMR-mrr) Φ80lacZΔM15 ΔlacX74 recA1 araD139 Δ(ara-leu)7697 galU galK rpsL(Str^r) endA1 λ⁻</i>
BL21(DE3)pLysS	F ⁻ <i>ompT hsdS_B(r_B⁻m_B⁻) gal dcm (λclts857 ind1 sam7 nin5 lacUV5-T7 gene 1) pLysS (Cam^r)</i>
BL21-CodonPlus-(DE3)-RIL	F ⁻ <i>ompT hsdS(r_B⁻m_B⁻) dcm⁺ Tet^r gal λ(DE3) endA Hte (argU ileY leuW Cam^r)</i>
BL21-CodonPlus-(DE3)-RP	F ⁻ <i>ompT hsdS(r_B⁻m_B⁻) dcm⁺ Tet^r gal λ(DE3) endA Hte ([argU proL Cam^r)</i>

Caenorhabditis elegans SS104 (genotype: *glp-4(bn2)*), provided by Prof. J-P. Hernalsteens (Institute of Molecular Biology and Biotechnology, VUB, Belgium), was maintained at 16°C on Nematode Growth Medium (NGM) agar plates, composed of 0.3 % (w/v) NaCl, 0.25 % (w/v) Bacto peptone (Difco Laboratories, Detroit, MI, USA), 1.7 % (w/v) Agar 1, 0.1 % (v/v) of 1 M MgSO₄ (Acros Organics), 0.1 % (v/v) of 1 M CaCl₂ (Sigma-Aldrich, St-Louis, MO, USA), 2.5 % (v/v) of 1 M potassium phosphate buffer (pH 6.0, VWR international, Poole, U.K.) and 0.1 % (v/v) of 5 mg/ml cholesterol (Sigma-Aldrich), covered with a lawn of *E. coli* OP50 as food source (Brenner, 1974). Nematode experiments were performed with synchronized L4 stage animals acquired by adult bleaching and hatching of the eggs at 16°C for 4 days.

3.2 Cloning, recombinant large scale expression and protein purification

An overview of all constructs ranked according to the different (sub-)chapters in this study is given in Table 3.2. The parameters for cloning, recombinant expression and protein purification are indicated for each construct.

Table 3.2: Overview of all expression constructs. The construct names, the corresponding primers used for PCR amplification (in 5' → 3' orientation), the cloning methodology, the expression (temperature/time/expression strain) and purification stringency are summarized. Expression of all constructs was induced at OD_{600nm} of 0.6 upon addition of 1 mM IPTG to the expression medium, unless indicated otherwise. All proteins were purified with Ni²⁺-NTA chromatography (HisTrap HP 1 ml columns, GE Healthcare) using the Aktä-FPLC system. The restriction endonuclease recognition sites used for cloning are marked in italics inside the primer sequences. Additional nucleotides necessary for in-frame cloning are indicated in bold. The nucleotides encoding the PK peptide are underlined and in bold.

Construct name	Primer sequences (5' -> 3')	Cloning methodology (template and vector)	Expression conditions	Purification stringency
Single-domain endolysins (Chapter 5)				
BcepC6Bgp22	ATGGGATCCGCGCGCATTGATATTGCA CGCCGTACCTACCGCCAGCCAA	BcepC6B genomic DNA T/A cloning in pEXP5CT/TOPO®	16°C-18h BL21(DE3)pLysS	60 mM imidazole
P2gp09	ATGGGATCCCCGGTAATTAACACGCATC AGCCGGTACGCCGCGCCAGCGGTACGC	P2 genomic DNA T/A cloning in pEXP5CT/TOPO®	37°C-4h BL21(DE3)pLysS	65 mM imidazole
PsP3gp10	ATGGGATCCCCGGTCATTAATACTACCAG TGCCATCACCCGCCAGCCGTG	PsP3 genomic DNA T/A cloning in pEXP5CT/TOPO®	37°C-4h BL21(DE3)pLysS	60 mM imidazole
K11gp3.5	ATGGATCCGCCAAGGTTCAATTCATAAG CCCACGGTCAGAAGTGACCAG	K11 genomic DNA T/A cloning in pEXP5CT/TOPO®	37°C-4h BL21(DE3)pLysS	50 mM imidazole
KP32gp15	ATGGCCAAGGTTCAATTCATC CCCATGGTCAGAAGTGACCAG	KP32 genomic DNA T/A cloning in pEXP5CT/TOPO®	37°C-4h BL21(DE3)pLysS	50 mM imidazole
CR8gp3.5	ATGGGATCCGGGAGTAATGTCATGT TCCTCGATCAGAAGTTACG	CR8 genomic DNA T/A cloning in pEXP5CT/TOPO®	16°C-18h BL21(DE3)pLysS	60 mM imidazole
Modular endolysins + domains (Chapter 6)				
OBPgp279	ATGAAAAATAGCGAGAAGAAT AACTATTCCGAGTGCTTTCTTTGT	OBP genomic DNA T/A cloning in pEXP5CT/TOPO®	37°C-4h BL21(DE3)pLysS	65 mM imidazole
PVP-SE1gp146	ATGGGATCCAATGCTGCAATTGCGGAGA CGAGGTTAGAACAGATTTTGCCT	PVP-SE1 genomic DNA T/A cloning in pEXP5CT/TOPO®	16°C-18h BL21(DE3)pLysS	70 mM imidazole
His ₆ -PVP-SE1gp146	AATGCTGCAATTGCGGA TTACGAGGTTAGAACAGATTTTGCC	PVP-SE1 genomic DNA T/A cloning in pEXP5NT/TOPO®	16°C-18h BL21(DE3)pLysS	65 mM imidazole
201φ2-1gp229	ATGGGATCCATCCTTAAAAACGGCTC CTTCCACCGAACTTTG	201φ2-1 genomic DNA T/A cloning in pEXP5CT/TOPO®	37°C-4h BL21(DE3)pLysS	65 mM imidazole
OBP ₁₂₇₋₃₂₇	ATGGGATCCCATATGTCTATTGAACAG TATTCCGAGTGCTTTCT	OBP genomic DNA T/A cloning in pEXP5CT/TOPO®	37°C-4h BL21(DE3)pLysS	60 mM imidazole
PVP ₈₂₋₂₃₅	ATGGGATCCGACCTGTTTAAAAAG TAGAACAGATTTTGCC	PVP-SE1 genomic DNA T/A cloning in pEXP5CT/TOPO®	37°C-4h BL21(DE3)pLysS	60 mM imidazole
201φ2-1 ₇₅₋₂₆₀	ATGGGATCCGATAAAGATTATCAATGGGCTG ACCGAACTTTGTATACGCGCT	201φ2-1 genomic DNA T/A cloning in pEXP5CT/TOPO®	37°C-4h BL21(DE3)pLysS	60 mM imidazole
OBP ₁₋₁₁₇ -EGFP	GGCCTGCAGTAAAAATAGCGAGAAG TTAGGATCCATCACAGTAGCAAGACCTAAT	OBP genomic DNA + pEGFP pEGFP- <i>PstI</i> / <i>Bam</i> HI + pEXP5CT/TOPO®	16°C-18h BL21(DE3)pLysS	65 mM imidazole

OBP ₇₋₅₄ -EGFP	GGCCCTGCAGTAATGCATCGATAAATTATGTC CGTGGATCCATGTTGGTGTGAAATTG	OBP genomic DNA + pEGFP pEGFP- <i>Pst</i> /BamHI + pEXP5CT/TOPO®	37°C-4h BL21(DE3)pLysS	60 mM imidazole
OBP ₅₇₋₁₁₇ -EGFP	GCGCTGCAGTCCGAGTAACACATATGA CGTGGATCCATCAACGTCGACCCAGC	OBP genomic DNA + pEGFP pEGFP- <i>Pst</i> /BamHI + pEXP5CT/TOPO®	37°C-4h BL21(DE3)pLysS	60 mM imidazole
PVP ₁₋₆₃ -EGFP	GGCCTGCAGTAATGCTGCAATTG TTAGGATCCATTTGTCCAGTTGTGC	PVP-SE1 genomic DNA + pEGFP pEGFP- <i>Pst</i> /BamHI + pEXP5CT/TOPO®	37°C-4h BL21(DE3)pLysS	60 mM imidazole
201φ2-1 ₁₋₆₃ -EGFP	GGCCTGCAGTATCCTAAAAACGGCTC GTCGGATCCATCAATACAGCCCATGTGTTATT	201φ2-1 genomic DNA + pEGFP pEGFP- <i>Pst</i> /BamHI + pEXP5CT/TOPO®	37°C-4h BL21(DE3)pLysS	60 mM imidazole
Direct N- and C-terminal fusion constructs (Chapter 7 and 8)				
PK -PVP-SE1gp146	ATG AAACGCAAGAAACGTAAGAAACGCAAA AATGCTGCAATTGCGGAG CGAGGTTAGAACAGATTTTGCCT	PVP-SE1 genomic DNA T/A cloning in pEXP5CT/TOPO®	16°C-18h BL21(DE3)pLysS	70 mM imidazole
PVP-SE1gp146- PK	ATGAATGCTGCAATTGCGGAGA TCA TTTGCCTTCTTACGTTTCTTGCCTTT ATGGTGATGGTGATGATGACCCCTCGAGGTTAGAACAGATTTTGCCT	PVP-SE1 genomic DNA T/A cloning in pEXP5CT/TOPO®	37°C-4h BL21(DE3)pLysS	50 mM imidazole
PP-PVP-SE1gp146	ATGGGATCCTTCTTCGTAGCACCGGGCTCCTCCAATGCTGCAAT CGAGGTTAGAACAGATTTTGCCT	PVP-SE1 genomic DNA T/A cloning in pEXP5CT/TOPO®	16°C-18h BL21-CodonPlus-(DE3)-RIL	70 mM imidazole
Ecl136II-PVP-SE1gp146	GGAATGGGGAGCTCCTCCAATGCTGCAATTGCGGAGAT CGAGGTTAGAACAGATTTTGCCT	PVP-SE1 genomic DNA T/A cloning in pEXP5CT/TOPO®		
α4-PVP-SE1gp146	TTGGAATGGGGAGCCGAACCGTGC AAAACGTGTAATCA CATTGGAGGAGCCGGTACGGAAGGTGGTGATTACCGTT	Ligation independent cloning in pEXP5CT/Ecl136II-PVP-SE1gp146	16°C-18h BL21-CodonPlus-(DE3)-RIL	60 mM imidazole
Lycotoxin1-PVP-SE1gp146	GGAATGGGGAGCATCTGGCTGACCGCACTGAAATTCCTCGGCAAAACAGCCGCAA CATTGGAGGAGCCAGTTTGATAATTGCTGTTTTGCCAGTTTCTTTCGCGCGTGT	Ligation independent cloning in pEXP5CT/Ecl136II-PVP-SE1gp146	16°C-18h BL21-CodonPlus-(DE3)-RIL	60 mM imidazole
Parasin1-PVP-SE1gp146	TTGGAATGGGGAGCAAAGGCCGTGGCAAGCAGGGAGGCAAAGTACGTG CATTGGAGGAGCCTGAGGAACGGGTCTTTGCTTTGCACGTACTTTGC	Ligation independent cloning in pEXP5CT/Ecl136II-PVP-SE1gp146	16°C-18h BL21-CodonPlus-(DE3)-RIL	60 mM imidazole
ArtMW1-PVP-SE1gp146	TTATGGGCTTCTTCATCCGGCAGTAATCCTGCCCTCCA CATTGGAGGAGCCGGTACGATCAGGAATGCGATGGAGGGCAGGATT	Ligation independent cloning in pEXP5CT/Ecl136II-PVP-SE1gp146	16°C-18h BL21-CodonPlus-(DE3)-RIL	65 mM imidazole
ArtMW2-PVP-SE1gp146	TTATGGGCAAACCGGGCTGGCTGATCAAAGTAGCACTGAAGTTCAAGA CATTGGAGGAGCCTGCCAGTCTCTCAGCGGACGACGGATCAGTTTCTTGAACCTCAG	Ligation independent cloning in pEXP5CT/Ecl136II-PVP-SE1gp146	16°C-18h BL21-CodonPlus-(DE3)-RIL	70 mM imidazole
PK -OBPgp279	ATG AAACGCAAGAAACGTAAGAAACGCAAA AAAAATAGCGAGAAGA AACTATTCCGAGTGCTTTCTTTGT	OBP genomic DNA T/A cloning in pEXP5CT/TOPO®	16°C-18h BL21(DE3)pLysS	60 mM imidazole
OBPgp279- PK	ATGAAAAATAGCGAGAAGAAT TCA TTTGCCTTCTTACGTTTCTTGCCTTT ATGGTGATGGTGATGATGACCCCTAACTATTCCGAGTGCTTTCTTTGT	OBP genomic DNA T/A cloning in pEXP5CT/TOPO®	16°C-18h/0.1 mM IPTG BL21-CodonPlus-(DE3)-RIL	50 mM imidazole
PP-OBPgp279	ATGGGATCCTTCTTCGTAGCACCGGGCTCCTCAAAAAATAGCGAGAAG AACTATTCCGAGTGCTTTCTTTGT	OBP genomic DNA T/A cloning in pEXP5CT/TOPO®	16°C-18h BL21-CodonPlus-(DE3)-RIL	65 mM imidazole

Ecl136II-OBPgp279	GGAATGGGGAGCTCCTCCAAAAATAGCGAGAAG AACTATTCCGAGTGCTTTCTTTGT	OBP genomic DNA T/A cloning in pEXP5CT/TOPO®		
α4-OBPgp279	TTGGAATGGGGAGCCGAACCGTGCAAACGTGTAATCA TATTTTTGGAGGAGCCCGTACGGAAGGTGGTGATTACACGTT	Ligation independent cloning in pEXP5CT/Ecl136II-OBPgp279	16°C-18h BL21-CodonPlus-(DE3)-RP	60 mM imidazole
Lycotoxin1-OBPgp279	GGAATGGGGAGCATCTGGCTGACCGCACTGAAATTCCTCGGCAAACACGCCGCAA TATTTTTGGAGGAGCCAGTTTGGATAATTGCTGTTTTGCCAGTTCTTTGCGGCGTGTT	Ligation independent cloning in pEXP5CT/Ecl136II-OBPgp279	16°C-18h BL21-CodonPlus-(DE3)-RIL	70 mM imidazole
Parasin1-OBPgp279	TTGGAATGGGGAGCAAAGGCCGTGGCAAGCAGGGAGGCAAAGTACGTG TATTTTTGGAGGAGCCTGAGGAACGGGTCTTTGCTTTGACAGTACTTTGC	Ligation independent cloning in pEXP5CT/Ecl136II-OBPgp279	16°C-18h BL21-CodonPlus-(DE3)-RIL	60 mM imidazole
ArtMW1-OBPgp279	TTATGGGCTTCTTCATCCCGGCAGTAATCTGCCTCCA TATTTTTGGATCTGCCGCCGGTACGATCAGGAATGCGATGGAGGGCAGGATT	Ligation independent cloning in pEXP5CT/Ecl136II-OBPgp279	16°C-18h BL21-CodonPlus-(DE3)-RIL	60 mM imidazole
ArtMW2-OBPgp279	TTATGGGCAAACCGGGCTGGCTGATCAAAGTAGCACTGAAGTTCAAGA TATTTTTGGATCTGCCCGCTGCCAGTCTTTCAGCGGACGACGGATCAGTTCTTGAACCTCAG	Ligation independent cloning in pEXP5CT/Ecl136II-OBPgp279	16°C-18h BL21-CodonPlus-(DE3)-RIL	60 mM imidazole
PK -201φ2-1gp229	ATGGGATCC AAACGCAAGAAACGTAAGAAACGCAAA ATCCTTAAAAACGGCTC CTTTCCACCGAACTTTG	201φ2-1 genomic DNA T/A cloning in pEXP5CT/TOPO®	16°C-18h BL21(DE3)pLysS	60 mM imidazole
PK -BcepC6Bgp22	ATGGGATCC AAACGCAAGAAACGTAAGAAACGCAAA AGCGCGCATTGATATTGCA CGCCGTACCTCACCGCCAGCCAA	BcepC6B genomic DNA T/A cloning in pEXP5CT/TOPO®	16°C-18h BL21(DE3)pLysS	60 mM imidazole
PK -P2gp09	ATGGGATCC AAACGCAAGAAACGTAAGAAACGCAAA CCGGTAATTAACACGCAT AGCCGGTACGCCGCCAGCGGTACGC	P2 genomic DNA T/A cloning in pEXP5CT/TOPO®	37°C-4h BL21(DE3)pLysS	80 mM imidazole
PK -PsP3gp10	ATGGGATCC AAACGCAAGAAACGTAAGAAACGCAAA CCGGTACCTAATACTCACCAG TGCCATCACCCGCCAGCCGTG	PsP3 genomic DNA T/A cloning in pEXP5CT/TOPO®	37°C-4h BL21(DE3)pLysS	60 mM imidazole
PK -CR8gp3.5	ATGGGATCC AAACGCAAGAAACGTAAGAAACGCAAA GGGAGTAAAGTCATGT TCCTCGATCAGAAGTTACG	CR8 genomic DNA T/A cloning in pEXP5CT/TOPO®	16°C-18h BL21(DE3)pLysS	60 mM imidazole
N-terminal double fusion constructs (Chapter 7)				
PK -PP-OBPgp279	ATGGGATCCAAACGCAAGAAACGTAAGAAACGCAAGCCTCCTCTTCTCGTAGCA AACTATTCCGAGTGCTTTCTTTGT	Tail PCR pEXP5CT/PP-OBPgp279	16°C-18h BL21-CodonPlus-(DE3)-RIL	60 mM imidazole
PP- PK -OBPgp279	ATGGGATCCTTCTCGTAGCACCGGGCTCCTCAAACGCAAGAAACGT AACTATTCCGAGTGCTTTCTTTGT	Tail PCR pEXP5CT/ PK -OBPgp279	16°C-18h BL21-CodonPlus-(DE3)-RIL	60 mM imidazole
PK -α4-OBPgp279	ATGGGATCCAAACGCAAGAAACGTAAGAAACGCAAGGCTCCTCCCGAACCCTGCA AACTATTCCGAGTGCTTTCTTTGT	Tail PCR pEXP5CT/α4-OBPgp279	16°C-18h BL21-CodonPlus-(DE3)-RIL	60 mM imidazole
Ecl136ii- PK -OBPgp279	GGAATGGGGAGCTCCTCC AAACGCAAGAAACGTAAGAAACGCAAA AAAAATAGCGAGAAG AACTATTCCGAGTGCTTTCTTTGT	OBP genomic DNA T/A cloning in pEXP5CT/TOPO®		
Ecl136ii- PK -PVP-SE1gp146	GGAATGGGGAGCTCCTCC AAACGCAAGAAACGTAAGAAACGCAAA AATGTGCAATTGCGGAGAT CGAGGTTAGAACAGATTTTGCCT	PVP-SE1 genomic DNA T/A cloning in pEXP5CT/TOPO®		

α 4- PK -PVP-SE1gp146	TTGGAATGGGGAGCCCGAACCGTGC AAAACGTGTAATCA GTTTGGAGGAGCCGGTACGGAAGGTGGTGATTACACGTT	Cassette ligation pEXP5CT/Ecl136II- PK -PVP-SE1gp146	16°C-18h BL21(DE3)pLysS	65 mM imidazole
α 4- PK -OBPgp279		Cassette ligation pEXP5CT/Ecl136II- PK -OBPgp279	16°C-18h BL21-CodonPlus-(DE3)-RIL	60 mM imidazole
Lycotoxin1- PK -PVP-SE1gp146	GGAATGGGGAGCATCTGGCTGACCGCACTGAAATTCCTCGGCAAACACGCCGCAA GTTTGGAGGAGCCAGTTTGGATAATTGCTGTTTTGCCAGTTTCTTTCGGCGGTGTT	Cassette ligation pEXP5CT/Ecl136II- PK -PVP-SE1gp146	16°C-18h BL21(DE3)pLysS	65 mM imidazole
Lycotoxin1- PK -OBPgp279		Cassette ligation pEXP5CT/Ecl136II- PK -OBPgp279	16°C-18h BL21-CodonPlus-(DE3)-RIL	60 mM imidazole
Parasin1- PK -PVP-SE1gp146	TTGGAATGGGGAGCAAAGGCCGTGGCAAGCAGGGAGGCAAAGTACGTG GTTTGGAGGAGCCTGAGGAACGGTCTTTGCTTTTGCACGTACTTTGC	Cassette ligation pEXP5CT/Ecl136II- PK -PVP-SE1gp146	16°C-18h BL21(DE3)pLysS	65 mM imidazole
Parasin1- PK -OBPgp279		Cassette ligation pEXP5CT/Ecl136II- PK -OBPgp279	16°C-18h BL21-CodonPlus-(DE3)-RIL	60 mM imidazole
ArtMW1- PK -PVP-SE1gp146	TTATGGGCTTCTTCATCCCGCAGTAATCTGCCTCCA GTTTGGAGGAGCCCGGTACGATCAGGAATGCGATGGAGGGCAGGAT	Cassette ligation pEXP5CT/Ecl136II- PK -PVP-SE1gp146	16°C-18h BL21(DE3)pLysS	65 mM imidazole
ArtMW1- PK -OBPgp279		Cassette ligation pEXP5CT/Ecl136II- PK -OBPgp279	16°C-18h BL21-CodonPlus-(DE3)-RIL	60 mM imidazole
ArtiMW2- PK -PVP-SE1gp146	TTATGGGCAAACCGGGCTGGCTGATCAAAGTAGCACTGAAGTTCAAGA GTTTGGAGGAGCCTGCCAGTCTTTCAGCGGACGACGGATCAGTTTCTTGAATACCA	Cassette ligation pEXP5CT/Ecl136II- PK -PVP-SE1gp146	16°C/18h BL21(DE3)pLysS	65 mM imidazole
ArtiMW2- PK -OBPgp279		Cassette ligation pEXP5CT/Ecl136II- PK -OBPgp279	16°C-18h BL21-CodonPlus-(DE3)-RIL	60 mM imidazole
N- and C-terminal linker extension constructs (Chapter 8)				
PK -L1-PVP-SE1gp146	ATG AAACGCAAGAAACGTAAGAAACGCAAA GCCGGCGCAGGAGCTAGCAATGCTGCAATTGCGGAG CGAGGTTAGAACAGATTTTGCCT	PVP-SE1 genomic DNA T/A cloning in pEXP5CT/TOPO®	37°C-4h BL21(DE3)pLysS	50 mM imidazole
PK -L1-OBPgp279	ATG AAACGCAAGAAACGTAAGAAACGCAAA GCCGGCGCAGGAGCTAGCAAAAATAGCGAGAAGA AACTATTCCGAGTGCTTTCTTTGT	OBP genomic DNA T/A cloning in pEXP5CT/TOPO®	16°C-18h BL21(DE3)pLysS	60 mM imidazole
PK -L2-PVP-SE1gp146	CCGGCGCAGGAGCTGGTGCAGGAG GATCGAGGACGTGGTCGAGGACGC	Cassette ligation in pEXP5CT/ PK -L1-PVP-SE1gp146	37°C-4h BL21(DE3)pLysS	50 mM imidazole
PK -L2-OBPgp279		Cassette ligation in pEXP5CT/ PK -L1-OBPgp279	16°C-18h BL21(DE3)pLysS	60 mM imidazole
PK -L3-PVP-SE1gp146	CCGGCGCAGGAGCTGGTGCAGGAGCTGGTGCAGGAG GATCGAGGACGTGGTCGAGGACGTGGTCGAGGACGC	Cassette ligation in pEXP5CT/ PK -L1-PVP-SE1gp146	37°C-4h BL21(DE3)pLysS	50 mM imidazole
PK -L3-OBPgp279		Cassette ligation in pEXP5CT/ PK -L1-OBPgp279	16°C-18h BL21(DE3)pLysS	60 mM imidazole

<u>PK</u> -L4-PVP-SE1gp146	CCGGCGCAGGAGCTGGTGCAGGAGCTGGTGCAGGAGCTGGTGCAGGAG GATCGAGGACGTGGTGCAGGACGTGGTGCAGGACGTGGTGCAGGACGC	Cassette ligation in pEXP5CT/ <u>PK</u> -L1-PVP-SE1gp146	37°C-4h BL21(DE3)pLysS	50 mM imidazole
<u>PK</u> -L4-OBPgp279		Cassette ligation in pEXP5CT/ <u>PK</u> -L1-OBPgp279	16°C-18h BL21(DE3)pLysS	60 mM imidazole
PVP-SE1gp146-L0- <u>PK</u>	ATGAATGCTGCAATTGCCGAGA TCATTTGCGTTTCTTACGTTTCTTGCGTTTCCCGCGCTAGCATGGTGTGGTGTGATGACCCCTTCGAGGTTAGAACAGATTTTACT	PVP-SE1 genomic DNA T/A cloning in pEXP5CT/TOPO®	16°C-18h BL21(DE3)pLysS	50 mM imidazole
OBPgp279-L0- <u>PK</u>	ATGAAAAATAGCGAGAAGAAT TCATTTGCGTTTCTTACGTTTCTTGCGTTTCCCGCGCTAGCATGGTGTGGTGTGATGACCCCTTAACCTATTCCGAGTGCTTTCTTTGT	OBP genomic DNA T/A cloning in pEXP5CT/TOPO®	16°C-18h/0.1 mM IPTG BL21-CodonPlus-(DE3)-RIL	50 mM imidazole
PVP-SE1gp146-L1- <u>PK</u>	CTAGCGGCGCAGGAG CCGGCTCCTGCGCCG	Cassette ligation in pEXP5CT/PVP-SE1gp146-L0- <u>PK</u>	16°C-18h BL21(DE3)pLysS	50 mM imidazole
OBPgp279-L1- <u>PK</u>		Cassette ligation in pEXP5CT/OBPgp279-L0- <u>PK</u>	16°C-18h/0.1 mM IPTG BL21-CodonPlus-(DE3)-RIL	50 mM imidazole
PVP-SE1gp146-L2- <u>PK</u>	CTAGCGGCGCAGGAGCTGGTGCAGGAG CCGGCTCCTGCACCAGCTCCTGCGCCG	Cassette ligation in pEXP5CT/PVP-SE1gp146-L0- <u>PK</u>	37°C-4h BL21(DE3)pLysS	50 mM imidazole
OBPgp279-L2- <u>PK</u>		Cassette ligation in pEXP5CT/OBPgp279-L0- <u>PK</u>	16°C-18h/0.1 mM IPTG BL21-CodonPlus-(DE3)-RIL	50 mM imidazole
PVP-SE1gp146-L3- <u>PK</u>	CTAGCGGCGCAGGAGCTGGTGCAGGAGCTGGTGCAGGAG CCGGCTCCTGCACCAGCTCCTGCACCAGCTCCTGCGCCG	Cassette ligation in pEXP5CT/PVP-SE1gp146-L0- <u>PK</u>	37°C-4h BL21(DE3)pLysS	50 mM imidazole
OBPgp279-L3- <u>PK</u>		Cassette ligation in pEXP5CT/OBPgp279-L0- <u>PK</u>	16°C/18h/0.1 mM IPTG BL21-CodonPlus-(DE3)-RIL	50 mM imidazole
PVP-SE1gp146-L4- <u>PK</u>	CTAGCGGCGCAGGAGCTGGTGCAGGAGCTGGTGCAGGAGCTGGTGCAGGAG CCGGCTCCTGCACCAGCTCCTGCACCAGCTCCTGCACCAGCTCCTGCGCCG	Cassette ligation in pEXP5CT/PVP-SE1gp146-L0- <u>PK</u>	37°C-4h BL21(DE3)pLysS	50 mM imidazole
OBPgp279-L4- <u>PK</u>		Cassette ligation in pEXP5CT/OBPgp279-L0- <u>PK</u>	16°C-18h/0.1 mM IPTG BL21-CodonPlus-(DE3)-RIL	50 mM imidazole

3.2.1 Cloning methodology

3.2.1.1 Standard cloning protocol

Open reading frames (ORFs) encoding the whole endolysins or separate catalytic domains were amplified (Pfu polymerase, 1.25 U, Thermo Fischer Scientific) with the primers listed in Table 3.2. Amplification took place on purified genomic DNA as template DNA, isolated from the respective phages. PCR samples were separated on a 1 % agarose (Eurogentec, Liège, Belgium) gel in TAE electrophoresis buffer (40 mM Tris (Acros Organics)-HCl pH 7.2, 500 mM sodium acetate (Acros Organics) and 50 mM EDTA (Acros Organics)), stained with ethidium bromide and visualized by UV illumination. For TA cloning into the commercially available pEXP5CT-TOPO®/pEXP5NT-TOPO® expression vectors, the protocol from the manufacturer's manual was applied (Life Technologies, Carlsbad, CA, USA). The pEXP5CT-TOPO® vector is a linearized expression vector that provides a C-terminal His₆-tag to cloned genes for downstream Ni²⁺-NTA purification, whereas the His₆-tag in pEXP5NT-TOPO® vector is situated at the N-terminal end of the cloned gene after ligation. All constructs were sequence-verified (Big Dye polymerase, ABI3130 Sequencher, Life Technologies) using vector-specific primers (Table 3.3). DNA purifications were carried out using the GeneJET™ PCR purification kit (Thermo Fischer Scientific).

Table 3.3: Overview of expression vectors used in this study with corresponding sequence primers (forward and reverse), resistance marker and function. Amp^r = ampicillin-resistant.

Expression vector	Vector-specific sequence primers	Resistance marker	Function
pEXP5CT/TOPO®	TAATACGACTCACTATAGGG ATCCGGATATAGTTCCTCCTTTC	Amp ^r	Recombinant expression
pEXP5NT/TOPO®	TAATACGACTCACTATAGGG TAGTTATTGCTCAGCGGTGG	Amp ^r	Recombinant expression
pEGFP	CCATGATTACGCCAAGCTTGC GACACCAGACAAGTTGGTAAT	Amp ^r	Fusion with EGFP

3.2.1.2 EGFP fusion constructs of peptidoglycan binding domains

To obtain fusion proteins of the peptidoglycan binding domains of endolysins OBPgp279, PVP-SE1gp146 and 201φ2-1gp229 to the “Enhanced Green Fluorescent Protein” (EGFP), the corresponding sequences (aa 1-117, aa 1-54 and aa 57-117 for OBPgp279; aa 1-63 for PVP-SE1gp146 and aa 1-63 for 201φ2-1gp229) encoding the different peptidoglycan binding moieties were amplified (Pfu polymerase, 1.25 U, primers: Table 3.2) and spliced to the 5' end of the EGFP encoding sequence on the pEGFP vector (kindly provided by Takara, Otsu, Japan, Table 3.3). For this splicing, the *Pst*I and *Bam*HI restriction sites situated in the 5' MCS of the pEGFP vector were used. The fusion fragments were then recloned (TA cloning) into the pEXP5CT-TOPO® expression vector for downstream protein expression and purification.

3.2.1.3 N- and C-terminal fusion of antibacterial peptides to endolysins

Single peptide fusions. The polycationic (PK) and the pentapeptide (PP) peptides were fused to endolysins by a standard tail PCR on purified genomic DNA of the respective phages using 5' (N-terminal fusion) or 3' (C-terminal fusion) primers that harbor the peptide-coding sequence (Pfu polymerase, primers: Table 3.2). PCR fragments were then cloned in a pEXP5CT/TOPO® expression vector. For N-terminal fusion of the α4, ArtMW1, ArtMW2, Lycotoxin1 and Parasin1 peptides, an adapted version of the Ligation Independent Cloning (LIC) technique (Haun et al, 1992) was used. Briefly, peptide-encoding cassettes, created by hybridization of specific primer pairs (20 μM each, Table 3.2), were treated with a mixture of dCTP (Promega) and T4 DNA polymerase (Fermentas) to introduce LIC-compatible 5' sticky ends. In parallel, the endolysin-encoding expression vectors were made LIC-compatible by introduction of a unique *Ecl*136II restriction endonuclease site upstream of the endolysin-encoding ORF using a standard tail PCR (Pfu polymerase, Table 3.2). The procedure was followed by linearization with *Ecl*136II endonuclease (New England Biolabs) and creation of complementary sticky ends by treatment with dGTP (Promega) and T4 DNA polymerase. A short incubation step of the hybridized peptide-encoding cassettes with the LIC-compatible vectors completed the cloning process.

Double peptide fusions. Two different types of double peptide fusions are constructed in this study: one type with the PK peptide situated N-terminal of the second peptide and the endolysin (type 1 conformation: PK - second peptide - endolysin) and another type with the PK peptide in between the second peptide and the endolysin (type 2 conformation: second peptide - PK - endolysin). For type 1, a standard tail PCR with a PK peptide-coding 5' primer (Pfu polymerase, primers: Table 3.2) was applied on purified pEXP5-CT/ α 4-endolysin and pEXP5-CT/PP-endolysin plasmid DNA, respectively. This was followed by TA cloning of the obtained double fusion fragments in a pEXP5CT/TOPO[®] vector. To obtain type 2 double fusion, the same adapted version of the LIC method as for the single fusion construction was used, except this time the pEXP5-CT/PK-endolysin vector was used as template.

3.2.1.4 Extending linker length between N- and C-terminal PK peptide and endolysins

To construct vectors with extended linkers between the PK-coding sequence and the endolysin-encoding open reading frame, a standard tail PCR (Pfu polymerase, primers: Table 3.2) was first used to introduce *NheI* and *NgoMIV* restriction endonuclease sites necessary for directional cloning. Upon double digestion of the obtained pEXP5CT/PK-*NheI*-*NgoMIV*-endolysin (for N-terminal end) and pEXP5CT/endolysin-*NgoMIV*-*NheI*-PK (for C-terminal end) vectors (*NgoMIV*: New England Biosciences; *NheI*: Fermentas), cassettes of variable length (L1 = GAGA, L2 = GAGAGAGA, L3 = GAGAGAGAGAGA, L4 = GAGAGAGAGAGAGAGA), constructed by hybridization of specific primer pairs (20 μ M each, Table 3.2), were inserted in the vectors with their 5' complementary sticky ends (T4 ligase, Fermentas).

3.2.2 Recombinant large scale expression and purification protocols

Recombinant expression of the different constructs was performed in an *E. coli*-based expression system upon induction of exponentially growing cells ($OD_{600nm} = 0.6$) with 1 mM isopropyl-beta-D-thiogalactopyranoside (IPTG, Fermentas). Expression parameters (temperature, time and expression strain) varied dependent on the protein to optimize the soluble expression levels for each construct (Table 3.2). Expression was stopped by centrifugation (3900g, 30', 4°C) and the obtained cell pellet was resuspended in 1/25 volumes of lysis buffer (20 mM NaH_2PO_4 (Merck, Darmstadt, Germany)/NaOH, 0.5 M NaCl,

pH 7.4). Dependent on the protein to purify, Pefabloc® SC protease inhibitor (40 mM final concentration, Merck) and Hen Egg White Lysozyme (HEWL) (1 mg/ml final concentration, Sigma-Aldrich) were added to the lysate to reduce protein degradation and to support cell lysis for non-muralytic enzymes, respectively. This cell lysate was then subjected to three freeze-thaw cycles (-80°C/22°C) prior to sonication (8 cycles of 30 s pulse and 30 s rest, amplitude of 40 %, Vibra Cell™ Sonics, Dandurry, CT, USA). The protein lysate was then filtered through 0.45 and 0.22 µm Durapore membrane filters (Millipore, Billerica, MA, USA).

Purification of the His₆-tagged fusion proteins was performed on an Aktä FPLC-system (GE Healthcare, Buckinghamshire, UK) driven by UNICORN™ 5.1 software with Ni²⁺-NTA columns (HisTrap HP 1 ml, GE Healthcare). Specifically for the C-terminal extended linker constructs, the His₆-tag between the PK-coding sequence and the endolysin gene, introduced by tail PCR, was used for purification instead of the His₆-tag of the expression vector itself. Ni²⁺ affinity chromatography is performed in 4 subsequent steps, all conducted at room temperature:

1. Equilibration of the Histrap HP 1 ml column with 10 column volumes of washing buffer (protein dependent imidazole concentration, 0.5 mM NaCl and 20 mM NaH₂PO₄-NaOH, pH 7.4) at a flow rate of 0.5 ml/min.
2. Loading of the total lysate on the Histrap HP 1 ml column at a flow rate of 0.5 ml/min.
3. Washing of the column with 15 column volumes of washing buffer at a flow rate of 1 ml/min.
4. Elution of bounded endolysin from the column with 10 column volumes of elution buffer (500 mM imidazole (Acros Organics), 5 mM NaCl, 20 mM NaH₂PO₄-NaOH, pH 7.4) at a flow rate of 0.5 ml/min

The wash buffer during purification contains a low protein-dependent imidazole concentration (50-80 mM) for higher purification stringency (Table 3.2). Purity of proteins was assessed visually on standard SDS-PAGE (sodium dodecyl sulfate polyacrylamide gel electrophoresis) gels containing 12 % acrylamide (Bio-Rad, CA, USA) with a LMW ("Low Molecular Weight", GE Healthcare) reference marker for comparison of protein band sizes and expression yields. The dialysis of proteins to certain buffers was done with Slide-A-Lyzer MINI Dialysis units (Pierce Biotechnology, Rockford, IL, USA). The protein concentration was

determined spectrophotometrically in silica cuvettes at a wavelength of 280 nm (Ultraspec III spectrophotometer, GE Healthcare). The extinction coefficient, necessary to quantify the protein concentration, was determined from the amino acid sequence of a specific protein with the ExPASy-Protparam tool (<http://www.expasy.org/protparam>) (Gasteiger et al, 2005).

3.3 Biochemical and biophysical assays

3.3.1 Peptidoglycan degrading or muralytic assay

For a muralytic assay, outer membrane-permeabilized cells were used as substrate, prepared according to Lavigne et al (2004). Briefly summarized, mid-exponentially growing *P. aeruginosa* PAO1, *S. Typhimurium* LT2 cells or *E. coli* XL1-Blue MRF' (OD_{600nm} = 0.6) were spun down (3900 g, 30', 4°C) and subsequently incubated by gently shaking for exactly 45 min in chloroform-saturated 0.05 M Tris/HCl (pH 7.7) at room temperature. Cells were then washed in a KH₂PO₄ (Boehringer, Mannheim, Germany)/K₂HPO₄ (VWR International) buffer (ionic strength = 80 mM, pH 7.2) to remove residual chloroform, and concentrated to an OD_{600nm} of 1.5. Efficiency of outer membrane permeabilization was tested by addition of 30 µg of HEWL to the freshly prepared substrate. To determine sensitivity of Gram-positive cell substrate, exponentially growing Gram-positive cells were autoclaved, spun down and resuspended in the same KH₂PO₄/K₂HPO₄ buffer to OD_{600nm} of 1.5. Addition of 30 µl of muralytic enzymes (at different concentrations ranging from 10 to 2000 nM) to 270 µl of outer membrane-permeabilized cells results in a decrease of the optical density over time, as measured spectrophotometrically at 655 nm (OD_{655nm}) using a Microplate Reader 680 (Bio-Rad). This drop in optical density is caused by degradation of the peptidoglycan layer through the lytic action of a muralytic enzyme and subsequent cell lysis. A standardized calculation method to quantify the muralytic activities of lytic enzymes using this assay was optimized and extensively described before (Briers et al, 2007a). Enzymatic activity is expressed in units per µM enzyme. Analogously to Briers and coworkers (2007a), a muralytic activity of 1 unit is defined here as the concentration of enzyme (in µM) necessary to create a drop in OD_{655nm} of 0.001 per minute:

$$Activity \left(\frac{units}{\mu M} \right) = \frac{\frac{slope \left(\frac{OD_{655nm}}{min} \right)}{\mu M}}{0.001}$$

Obtained activity values for the negative control (30 μ l of PBS pH 7.4) were subtracted from the sample values. The influence of pH on the muralytic activity was assessed using OM permeabilized cells resuspended in a universal pH buffer, composed of 150 mM KCl (Janssen Chimica, Belgium), 10 mM KH_2PO_4 , 10 mM Na-citrate (Acros Organics) and 10 mM H_3BO_4 (Acros Organics), adjusted to different pH's ranging from 3 to 10.

To investigate the thermal or heat stability, each endolysin was incubated at 42°C and 50°C for different time-intervals (1, 2, 3, 4, 8 and 24 hour) in a Biometra T3000 Thermocycler (Göttingen, Germany) followed by a cooling step to room temperature. Proteins showing full activity at 50°C were heated up to 60, 70, 80, 90 and 100°C during 20, 40 and 60 min time-intervals and cooled down again. The residual muralytic activity of each sample relative to the activity of unheated reference sample at time 0 (= 100 % activity) was quantified.

3.3.2 Fluorescence binding assay

The binding capacity of the peptidoglycan binding domains inside the modular endolysins was experimentally verified using a EGFP-based fluorescence assay specifically modified for Gram-negative cell walls (Briers et al, 2007b; Loessner et al, 2002). Purified EGFP-fusion proteins and recombinant EGFP (negative control) were incubated at a concentration of 2 μ M with 100 μ l of outer membrane-permeabilized *P. aeruginosa* PAO1 and *S. Typhimurium* LT2 cells for 5 min at room temperature. Unbound fusion proteins were removed with two consecutive washing steps in 5 mM HEPES (4-(2-hydroxyethyl)-1-piperazineethanesulfonic acid, Boehringer)/NaOH buffer (pH 7.4). Cells were visualized using epifluorescence microscopy (Leica type DMLB DS 0.6.23./100 S/F, McBain instruments, Chatsworth, NJ, USA, equipped with a LED light source Fluo LED 4000, McBain Instruments and a GFP filter). At conditions where no binding occurred, epifluorescence was overlaid by phase contrast to visualize uncolored cells.

To quantify binding, cell suspensions (100 μ l) were incubated with 2 μ M fusion protein in 200 μ l total volume. Subsequently, the labeled cells were washed twice with 5 mM HEPES/NaOH buffer (pH 7.4), transferred to microplate wells and placed in the Fluoroskan Ascent FL fluorescence reader (Thermo Fischer Scientific). Fluorescence was measured at 520 nm, using an excitation wavelength of 480 nm. in parallel, the OD_{600nm} was measured and fluorescence was expressed per OD_{600nm} to take differences in density into account.

3.3.3 Surface Plasmon Resonance

Surface plasmon resonance (Biacore X, Biacore AB, Uppsala, Sweden) was used to obtain sensorgrams for binding of PVP₁₋₆₃-EGFP to a surface of immobilized *S. Typhimurium* LT2 cells that are stripped of their outer membrane by autoclaving (Briers et al, 2009). In a first step, the carboxymethylated surface of a BIAcore Pioneer C1 chip was coated with 0.5 mg/ml PVP₁₋₆₃-EGFP (flow rate = 5 μ l/min; 10 mM sodium acetate pH 5.0), using the amine coupling technique (Fischer, 2010). Ethanolamine was added to block unbound positions on the chip. Secondly, autoclaved *S. Typhimurium* LT2 cells (3×10^{10} CFU/ml) resuspended in HBS-T buffer (10 mM HEPES, 150 mM NaCl, 3.4 mM EDTA, 0.005 % Tween 20, pH 7.8) were applied to the chip surface containing covalently bound PVP₁₋₆₃-EGFP (total volume = 30 μ l, flow rate = 3 μ l/min). The obtained double layer served as a basis for binding affinity measurements, performed at 25°C with 2 different concentrations (5 and 10 μ M) of PVP₁₋₆₃-EGFP for 3 min (association phase) and 12 min (dissociation phase) (flow rate = 10 μ l/min). Each concentration was measured in three-fold. Regeneration of the coated chip in between different measurements took place by several washing steps with increasing NaCl concentrations (2 M, 3 M, 4 M; 50 μ l; 10 μ l/min). Kinetic data were calculated based on the measurements using the BIAevaluation software (version 3.0; Biacore).

3.4 *In vitro* assays

3.4.1 *In vitro* antibacterial assay

Mid-exponentially growing intact Gram-negative cells (OD_{600nm} = 0.6, LB medium) were 100-fold diluted in 5 mM HEPES/NaOH (pH 7.4) to a final density of 10^6 colony forming units/ml.

Each cell culture (100 μ l) was incubated for 30 min at room temperature with 50 μ l muralytic enzyme dialyzed against PBS buffer (170 mM NaCl, 3 mM KCl, 12.7 mM Na₂HPO₄ and 2.2 mM KH₂PO₄, pH 7.4) together with 50 μ l of 5 mM HEPES/NaOH (pH 7.4) buffer or 50 μ l of EDTA-Na₂ (abbreviated as EDTA, disodium salt of EDTA, final concentration of 0.5 mM) dissolved in the same buffer. As negative control, 100 μ l of cells were added to 50 μ l of 5 mM HEPES/NaOH (pH 7.4) and 50 μ l of a PBS buffer (pH 7.4). After incubation, cell suspensions were diluted in three-fold to 10⁵, 10⁴ and 10³ cells/ml and 100 μ l of each dilution was plated out on LB agar plates. Colonies were counted after an overnight incubation at 37°C. The antibacterial activity was quantified as the relative inactivation in logarithmic units ($= \log_{10}(N_0/N_i)$ with N_0 = number of untreated cells (in the negative control) and N_i = number of cells for treated condition i).

3.4.2 *In vitro* biofilm assay

Biofilm formation takes place in a particular device, the Calgary biofilm device, composed of a lid of 96 polystyrene pegs that fits on a normal microtiter plate so that each peg is hanging in a microtiter plate well (Nunc-Immuno TSP, ThermoFischer Scientific) (Ceri et al, 1999). Overnight cultures of *P. aeruginosa* PAO1 were diluted 200 times in Mueller Hinton (MH) medium (0.2 % (w/v) BD bacto beef extract (Difco Laboratories), 1.75 % (w/v) acid hydrolyzed casein (Sigma-Aldrich) and 0.15 % (w/v) soluble starch (Difco Laboratories), pH 7.3) and each well of the microtiter plate was filled with 200 μ l of this diluted cell suspension. The microtiter plate was covered with the pegs-containing lid, submerging each peg in the medium. Then, the biofilm was allowed to form on the pegs by incubation at 37°C without shaking. After 24 hours of biofilm growth, the peg-containing lid was transferred to a new microtiter plate of which the wells contained 75 μ l of purified protein dialyzed in PBS buffer (pH 7.4), 75 μ l of 2 mM EDTA-Na₂ (EDTA) in PBS buffer (pH 7.4) and 50 μ l of 4xMH medium. Pure MH medium, PBS buffer (pH 7.4) and EDTA formed the negative controls of this experiment. To assess planktonic cell viability, the optical density at 600 nm wavelength of 135 μ l from each well of the old microtiter plate was measured and the OD_{600nm} for the pure MH control was subtracted. To quantify the biofilm growth/degradation for each condition, the pegs were washed in MH medium after 4 hours of incubation. The peg-attached bacteria were then stained with 0.1 % (w/v) crystal violet (Merck) in an

isopropanol-methanol-PBS mixture [1:1:18 (v/v)] for 30 min, washed with fresh medium and air-dried for another 30 min. The remaining crystal violet was extracted from the pegs in 30 % acetic acid and the intensity of the dye in each well was measured at 600 nm wavelength with the Multiskan RC (Thermo LabSystems, Finland). Dye intensity values measured for the pure MH medium were subtracted from these obtained for the different conditions. In this assay, four different overnight cultures of PAO1 were used and each condition was repeated four times to increase significance of the experimental outcome.

3.4.3 *In vitro* human keratinocyte assays

3.4.3.1 Cytotoxic effects of compounds on growing human keratinocytes

Cytotoxicity of endolysins and EDTA was evaluated on human epidermal keratinocytes derived from neonatal foreskin, provided by the Lab MCT of the Queen Astrid Military Hospital (Brussels, Belgium). Keratinocytes were seeded at 2500 cells/cm² and cultured in 25 cm vented culture flasks for 5 days (in EpiLife medium, 37°C, 5 % CO₂ and 95 % relative humidity) without medium change, in the presence of the endolysins (2 μM final concentration) and/or EDTA-Na₂ (EDTA, at 0.5-5-50-500 μM final concentrations). At day 5, the remaining keratinocytes were trypsinized with TrypLe Select recombinant trypsin (Life Technologies) for 5' at 37°C and washed in complete EpiLife medium. Viability counting of the keratinocytes proceeded microscopically using a Burker Cell Count chamber (VWR International) after Trypan Blue live/dead staining (VWR International). Living keratinocytes appeared as colorless cells under the microscope, whereas dead ones were stained blue.

3.4.3.2 Human epidermal keratinocyte infection and survival assay

Human epidermal keratinocytes from neonatal foreskin were seeded at 5000 cells/cm³ and cultured in 25 cm vented culture flasks till more than 90 % confluence has been reached (EpiLife medium, 6 days, 37°C, 5 % CO₂, 95 % RH). Confluent grown keratinocytes were infected with clinical *P. aeruginosa* strains PA14 and Br667 at an infectivity dose of 10⁵ (or 10⁷) colony forming units/ml. One hour after infection, both the unmodified and PK-modified endolysins (2 μM final concentration) were added together with EDTA-Na₂ (EDTA,

at 5 μM final concentration) to the keratinocyte cultures. Uninfected keratinocytes and infected, but untreated keratinocytes were included as negative controls. After an additional three hours of incubation, the infection process was stopped by trypsinization of the residual keratinocytes (TrypLE Select trypsin). Keratinocyte viability was microscopically evaluated (Burker Cell Count chamber) using Trypan Blue live/dead staining, as described above. For evaluation of the antibacterial activity of the *P. aeruginosa* strains, ten-fold dilutions of the keratinocyte culture were plated out on LB agar plates and the residual bacterial colony forming units for each condition were quantified after 18h incubation of the plates at 37°C. This time, the antibacterial activity for each condition is expressed in percentage reduction relative to the untreated negative control. Each tested condition was done in three-fold.

3.5 *In vivo* *Caenorhabditis elegans* assays

3.5.1 Cytotoxic effects of compounds on *C. elegans*

Synchronized L4 stage *C. elegans* SS104 nematodes grown on NGM agar were transferred to 96-well plates (+/- 10 nematodes per well), each well containing 100 μl of a mixture composed of 20 % NGM medium adjusted with 80 % M9 buffer (0.6 % (w/v) Na_2HPO_4 , 0.3 % (w/v) KH_2PO_4 , 0.5 % (w/v) NaCl and 0.025 % (w/v) MgSO_4). Unmodified and PK-modified endolysins (2 and 10 μM final concentration) and EDTA- Na_2 (EDTA; 0.05, 0.5 and 5 mM final concentrations) were added separately to determine their individual effect on the nematode survival, and in combination to the nematode-containing wells. Each individual enzyme or EDTA concentration and each combination was tested in three-fold. Nematode survival was scored 24 and 48 h after treatment by appearance of touch-provoked movement: dead nematodes appear as long, immobile rods, living ones move in a sinusoidal shape (Moy et al, 2006; Stiernagle, 2006).

3.5.2 *C. elegans* infection and survival assays

Bacterial lawns of *P. aeruginosa* cells for *C. elegans* infection were prepared by spreading 100 μl of a stationary growing culture on top of NGM agar plates. Plates were incubated at

37°C for 18h before seeding of +/- 50 synchronized L4 stage SS104 nematodes on the bacterial lawns. The infection itself took place for 24 h at 26°C. Nematode survival after infection was evaluated by the liquid assay (Stiernagle, 2006). Infected nematodes were washed three times with M9 buffer to remove attached bacteria and transferred to 96 well plates (\pm 10 nematodes per well). Wells contained 100 μ l of 20 % NGM/80 % M9 buffer mixture, 50 μ l of (PK-fused) endolysin dialyzed to PBS pH 7.4 and 50 μ l of EDTA- Na_2 (EDTA, at 0.5 mM final concentration) in PBS pH 7.4. In addition, PBS buffer (pH 7.4) and EDTA form the negative controls, ciprofloxacin (at a concentration of 5xMIC, Sigma-Aldrich) the positive control. Each condition was tested in ten-fold. Survival of *C. elegans* SS104 was determined by monitoring the presence/absence of touch-provoked movement for each nematodes at different time points during 72 h.

Selection of most promising Gram-negative phage endolysins

To extend the pool of endolysins of Gram-negative infecting phages, this dissertation started with a preliminary bio-informatics search for interesting candidate Gram-negative phage endolysins. These endolysins were chosen from the available Gram-negative infecting phage genomes in the online NCBI database and should meet all following criteria: (1) endolysins from different double-stranded DNA phages, (2) endolysins from phages infecting a range of, preferably pathogenic, Gram-negative species, including *Pseudomonas*, *E. coli*, *Salmonella*, *Klebsiella* and *Citrobacter*, (3) endolysins with different predicted catalytic specificities, (4) endolysins with a different predicted structure (a single-domain structure or a modular structure with more than one domain), and (5) endolysins without an N-terminal secretion signal peptide. The last criterium is chosen for expression reasons only. During expression, endolysins with a secretion signal would be translocated over the inner membrane to the periplasm by the bacterial secretion system, leading to early lysis of the peptidoglycan. This would be detrimental for the bacterial host and hinder successful expression.

A list of the selected phage endolysins based on the mentioned criteria is depicted in Table 4.1. The endolysin name, length of endolysin (in amino acids), bacterial host strain of the phage encoding the endolysin, the predicted structure and the catalytic specificity of the enzymatic domain are all indicated in this table. As predicted structure, endolysins can have either a single-domain structure or a modular, more than one domain structure (*see 1.2.3 Structural composition of phage endolysins*). The goal of this preliminary search is to obtain a set of interesting candidate endolysins that reflects the origin and structural diversity present among endolysins from Gram-negative infecting phages.

A phylogram constructed after multiple alignment of all selected endolysin amino acid sequences gives an overview of the relatedness of the selected endolysins (Figure 4.1). All

Table 4.1: List of endolysin candidates for this study. The protein name (with NCBI reference code), length of protein (in amino acids), bacterial host strain, predicted structure and catalytic specificity are indicated. The name of the phage source is underlined in the protein name. *Salmonella* Enteritidis = *Salmonella enterica* serovar Enteritidis, *Salmonella* Typhimurium = *Salmonella enterica* serovar Typhimurium. Structure and catalytic specificity were predicted by Blastp, Pfam and HHpred bio-informatic tools.

Protein (NCBI code)	Amino acids	Bacterial host	Predicted structure	Predicted catalytic specificity
<u>OBPgp279</u> (YP_004958186.1)	328	<i>Pseudomonas fluorescens</i>	modular	Lysozyme-like domain
<u>PVP-SE1gp146</u> (YP_004893953.1)	236	<i>Salmonella</i> Enteritidis	modular	Lysozyme-like domain
<u>201φ2-1gp229</u> (YP_001956952.1)	262	<i>Pseudomonas chlororaphis</i>	modular	Goose-like lysozyme
<u>CR8gp3.5</u> (unpublished)	152	<i>Citrobacter rodentii</i>	single-domain	N-acetylmuramoyl-L-alanine amidase
<u>BcepC6Bgp22</u> (YP_024942.1)	164	<i>Burkholderia cenocepacia</i>	single-domain	Lytic transglycosylase
<u>P2gp09</u> (NP_046765.1)	165	<i>Escherichia coli</i>	single-domain	Lytic transglycosylase
<u>PsP3gp10</u> (NP_958065.1)	165	<i>Salmonella</i> Typhimurium	single-domain	Lytic transglycosylase
<u>K11gp3.5</u> (YP_002003804.1)	151	<i>Klebsiella pneumoniae</i>	single-domain	N-acetylmuramoyl-L-alanine amidase
<u>KP32gp15</u> (YP_003347533.1)	151	<i>Klebsiella pneumoniae</i>	single-domain	N-acetylmuramoyl-L-alanine amidase
<u>Bcep1gp28</u> (NP_944336.1)	255	<i>Burkholderia cenocepacia</i>	modular	Goose-like lysozyme
<u>EcoDS1gp3.5</u> (ACF15800.1)	152	<i>Escherichia coli</i>	single-domain	N-acetylmuramoyl-L-alanine amidase
<u>A13gp3.5</u> (YP_002003950.1)	151	<i>Escherichia coli</i>	single-domain	N-acetylmuramoyl-L-alanine amidase
<u>T3gp18</u> (NP_523313.1)	151	<i>Escherichia coli</i>	single-domain	N-acetylmuramoyl-L-alanine amidase
<u>Luz24gp67</u> (YP_001671940.1)	132	<i>Pseudomonas aeruginosa</i>	single-domain	Lysozyme
<u>BA14gp3.5</u> (YP_002003466.1)	151	<i>Escherichia coli</i>	single-domain	N-acetylmuramoyl-L-alanine amidase

endolysins are clustered according to their predicted catalytic specificity and structure (single-domain or modular structure).

A second selection of endolysins out of these 15 candidates was made based on their maximal muralytic activity under physiological conditions (PBS buffer, pH 7.4) on outer membrane-permeabilized *P. aeruginosa* PAO1 cells (Figure 4.2). The drop in optical density of the cells upon addition of an excess (10 µg) of endolysin was monitored in function of

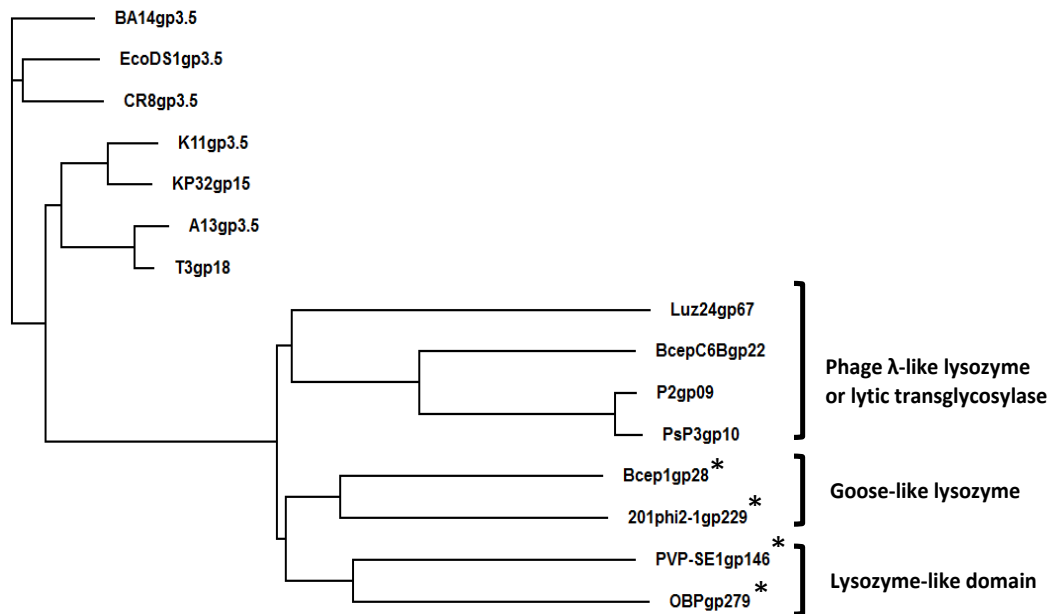


Figure 4.1: Phylogram of the selected endolysins in this study. This tree was composed by Treeview software (Page, 2002), after multiple alignment of the amino acid sequences of all selected endolysins with Clustal X2 (Larkin et al, 2007). Alignment parameters used: gap length = 10, gap extension = 2. Predicted catalytic specificities are indicated. The predicted modular structured endolysins are marked with an asterisk (*).

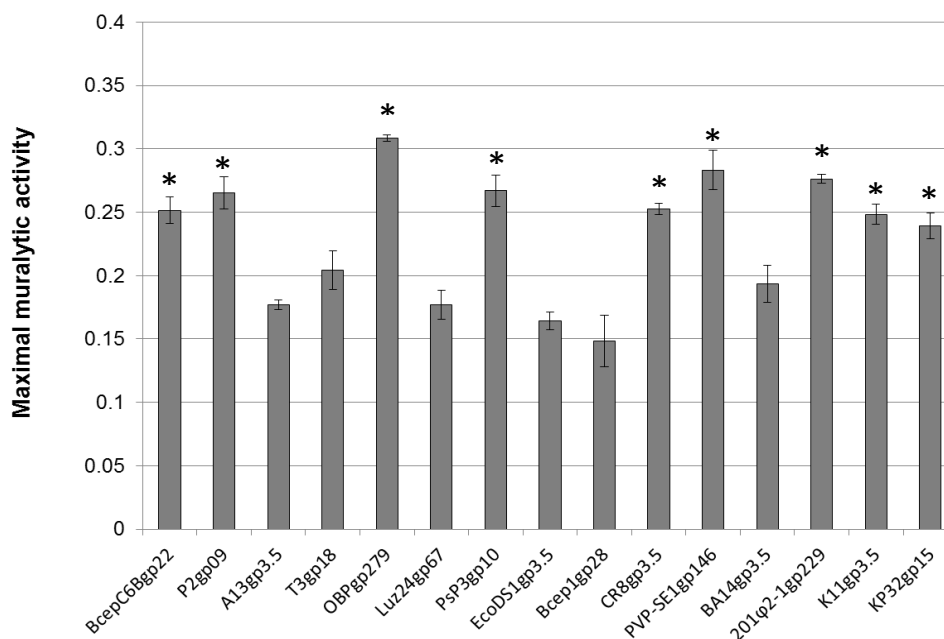


Figure 4.2: Overview of the maximal muralytic activity upon addition of an excess of different phage endolysins to outer membrane-permeabilized *P. aeruginosa* PAO1 cells. For each endolysin, 10 μ g was added to 270 μ l of cell substrate and the optical density was followed over time. The slope of the declining part of the OD_{655nm}/time curve was taken as a quantitative measure for the maximal muralytic activity of each endolysin (Y-axis). All endolysins with a cut-off slope value of 0.25 are marked with an asterisk (*). Endolysins were tested under physiological conditions (in PBS buffer, pH 7.4). Average values and standard deviations were depicted.

time. An arbitrary cut-off value for the maximal muralytic activity of 0.25 (= slope of the $OD_{655nm}/time$ curve for 10 μg of endolysin) was used to select the most active endolysins (Figure 4.2, indicated by an asterisk *). These nine selected endolysins can be subdivided in two groups based on their predicted structure: the modular endolysins OBPgp279, PVP-SE1gp146 and 201 ϕ 2-1gp146 and the single-domain endolysins P2gp09, PsP3gp10, BcepC6Bgp22, K11gp3.5 and KP32gp15. An extensive structural, biochemical and antibacterial characterization of these selected endolysins is described in Chapter 5, for the single-domain endolysins, and Chapter 6, for the modular endolysins, together with a thorough, application-focused comparison and discussion between both groups of endolysins.

Characterization of six novel, single-domain endolysins from Gram-negative infecting bacteriophages¹

The application of externally added endolysins from phages infecting Gram-positive bacteria as antibacterial compounds has proven successful in various fields (Callewaert et al, 2011). However, the use of endolysins from Gram-negative infecting phages against Gram-negative pathogens is an unexploited research area as these bacteria possess an outer membrane which prevents efficient peptidoglycan lysis. The majority of these type of endolysins adopt a single-domain structure, consisting of a catalytically active, muralytic domain. This single-domain feature is not found in endolysins from Gram-positive infecting phages. To date, the pool of characterized single-domain endolysins from Gram-negative infecting phages remains rather limited with phage T4 lysozyme (Matthews, 1995), phage λ lysozyme (actually a transglycosylase) (Taylor et al, 1975) and phage T7 lysozyme (actually an amidase) (Cheng et al, 1994) as major representatives. To extend this pool of single-domain endolysins, we focus in this chapter on the biochemical and antibacterial characterization of six novel, single-domain endolysins with a Gram-negative background. *In silico* genomic analysis of the *Burkholderia cenocepacia* phage BcepC6B (“Bpp-1 like viruses”, *Podoviridae*) (Summer et al, 2006), *E. coli* phage P2 (“P2-like viruses”, *Myoviridae*) (Christie et al, unpublished), *Salmonella* phage PsP3 (“P2-like viruses”, *Myoviridae*) (Bullas et al, 1991), *Citrobacter rodentii* phage CR8 (“T7-like viruses”, *Podoviridae*) and *Klebsiella pneumoniae* phages K11 (“T7-like viruses”, *Podoviridae*) (Savalia et al, unpublished) and KP32 (“T7-like viruses”, *Podoviridae*) (Drulis-Kawa et al, unpublished) revealed the presence of endolysins BcepC6Bgp22, P2gp09 (also known as P2gpK), PsP3gp10, CR8gp3.5, K11gp3.5 and KP32gp15, respectively. In this chapter, we tried to experimentally confirm their biological function and elucidated their fundamental properties. In addition, we verified their possible applicability as antibacterial compounds for treatment of Gram-negative infections.

¹This chapter is adapted from:

Walmagh M, Boczkowska B, Grymonprez B, Briens Y, Drulis-Kawa Z, Lavigne R. (2012) Characterization of five novel endolysins from Gram-negative infecting bacteriophages. *Appl Microbiol Biotechnol*. PMID:22832988.

5.1 *In silico* structural analysis of six novel, single-domain endolysins

Using the primary structure prediction tool Blastp (Altschul et al, 1997), a “phage λ -like lysozyme” domain is predicted in BcepC6Bgp22, PsP3gp10 and P2gp09. The “lysozyme” of phage λ is actually a lytic transglycosylase that hydrolyzes the β -1,4-glycosidic bond between GluNAc and MurNac in the bacterial peptidoglycan layer, followed by the formation of a 1,6-anhydromuramic acid terminal residue (Bienkowska-Szewczyk & Taylor, 1980) (Figure 5.1). PsP3gp10 and P2gp09, both originating from P2-like viruses, are almost 94 % identical with each other on the protein level, BcepC6Bgp22 and P2gp09 only 46 %. The catalytic residue Glu19 in phage λ lysozyme is assumed to play a crucial role in the interaction of the enzyme with the GluNAc moiety of the peptidoglycan backbone (Leung et al, 2001). This important residue seems conserved within PsP3gp10 and P2gp10 (both residue Glu21) and BcepC6Bgp22 (residue Glu25), but site-directed mutagenesis of these particular residues will be necessary to prove their role.

Phages K11 and KP32 encode endolysins that are highly conserved with 88 % similarity in amino acid sequence, mainly differing in their C-terminus. CR8gp3.5 is 71 and 69 % identical on the protein level to K11gp3.5 and KP32gp15, respectively. *In silico*, CR8gp3.5, K11gp3.5 and KP32gp15 possess a predicted Zn^{2+} -dependent N-acetylmuramoyl-L-alanine amidase activity (Figure 5.1). This activity is widely conserved among phages infecting Enterobacteriaceae. An N-acetylmuramoyl-L-alanine amidase hydrolyzes the amide bond that anchors the L-alanine moiety of the pentapeptide chain to the D-lactyl group of the MurNac sugar in the glycan backbone (Figure 5.1). CR8gp3.5, K11gp3.5 and KP32gp15 showed 72, 75 and 80 % similarity with T7 amidase, respectively. Three Zn^{2+} binding residues and two catalytic residues, conserved in the active sites of both T7 amidase (Cheng et al, 1994) and *B. anthracis* prophage PlyL amidase (Low et al, 2005), were also present in CR8gp3.5, K11gp3.5 and KP32gp15. The particular Zn^{2+} binding residues are His18, His123 and Cys131, the catalytic residues Tyr47 and Lys128. In T7 amidase, these specific residues are shown to play a major role in the catalytic amidase activity (Cheng et al, 1994). The fact that these amino acid residues are highly conserved, suggest a similar functional role of these endolysins in the replication cycle of the bacteriophage.

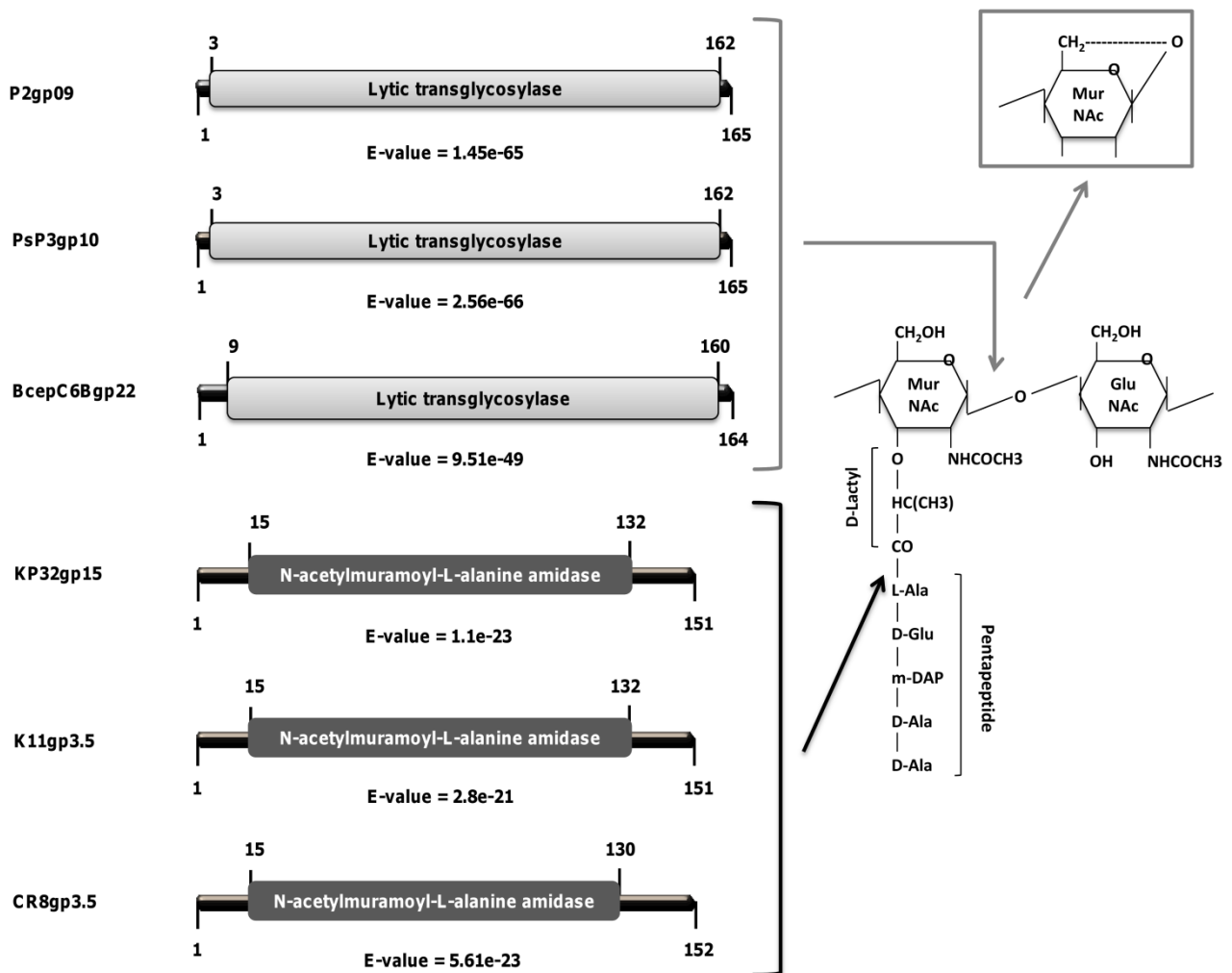


Figure 5.1: Predicted secondary domains and catalytic specificity of PsP3gp10, P2gp09, BcepC6Bgp22, K11gp3.5, KP32gp15 and CR8gp3.5. The e-values, which measure the significance of the predicted catalytic specificity, are determined for each catalytic domain by Blastp (Altschul et al, 1997) and added under the respective endolysin structures. The expected site of action of the endolysins on the Gram-negative peptidoglycan structure is indicated with light grey (transglycosylase) and dark grey (amidase) arrows. P2gp09, PsP3gp10 and BcepC6Bgp22 (“phage λ -like lysozyme” or transglycosylase, light grey) are expected to attack the β -1,4-glycosidic bond between N-acetylmuramic acid (MurNAc) and N-acetylglucosamine (GluNAc) in the peptidoglycan backbone, resulting in the formation of a 1,6-anhydromuramic acid terminal residue (see inset). CR8gp3.5, KP32gp15 and K11gp3.5 (N-acetylmuramoyl-L-alanine amidases, dark grey) are all assumed to target the amide bond between the D-lactyl group of the N-acetylmuramic acid and the L-alanine (L-Ala) of the pentapeptide chain. D-Glu = D-glutamate, m-DAP = meso-diaminopimelinic acid, D-Ala = D-alanine.

5.2 Biochemical properties of the six novel, single-domain endolysins

The biochemical characterization of endolysins BcepC6Bgp22, P2gp09, PsP3gp10, CR8gp3.5, K11gp3.5 and KP32gp15 was performed on Gram-negative bacterial cell substrate (of which the outer membrane was permeabilized by a chloroform/Tris-HCl treatment). The chloroform dissolves the lipid layer of the outer membrane, whereas the Tris compound will permeabilize the LPS layer. Endolysins added to this cell substrate easily gain access to the peptidoglycan layer, effectively exerting their muralytic activity.

5.2.1 pH-dependency

To determine the pH-dependency of the muralytic activity, each endolysin (2 μ M) was incubated with an excess of outer membrane-permeabilized *P. aeruginosa* PAO1 cell substrate, resuspended in an universal buffer with different pH-values ranging from 3 to 10. For each endolysin, an optimal activity was reached around a pH of 7 (Figure 5.2).

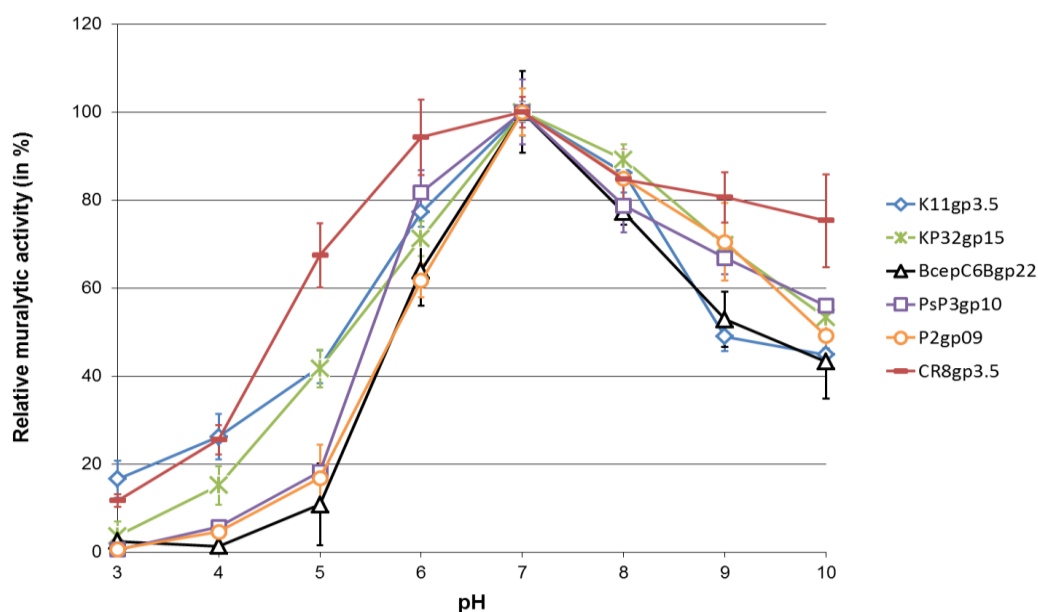


Figure 5.2: pH-dependency of muralytic activity for the single-domain endolysins P2gp09 (orange, circles), PsP3gp10 (purple, boxes), BcepC6Bgp22 (black, triangles), K11gp3.5 (blue, diamonds), KP32gp15 (green, X) and CR8gp3.5 (red, —). For each endolysin (2 μ M final concentration), the muralytic activity (= slope of Δ OD_{655nm}/min curve) was determined for pH-values between 3 and 10 relative to the pH with the highest observed muralytic activity for that endolysin (= 100 % relative activity). All endolysins were dialyzed against PBS buffer (pH 7.4). Averages and standard deviations over three independent experiments are depicted. Values are connected by trendlines.

A sharp decline in enzymatic activity was observed for PsP3gp10, P2gp09 and BcepC6Bgp22 below pH 6, whereas a higher remaining activity at these pH-values was observed especially for CR8gp3.5, but also for K11gp3.5 and KP32gp15. CR8gp3.5 was atypical as it also retained more than 50 % activity at more basic pH-values (pH 9-10). The optimal pH-value for muralytic activity of the six endolysins corresponds with the periplasmatic pH of Gram-negative bacteria, typically between pH 6.5 and pH 7.5 (Wilks & Slonczewski, 2007).

5.2.2 Quantification of muralytic activity

Lysis of outer membrane-permeabilized *P. aeruginosa* PAO1, *S. Typhimurium* LT2 and *E. coli* XL1-Blue MRF' was followed over time by monitoring the drop in optical density directly after addition of the six single-domain endolysins at their optimal pH for activity of 7. The muralytic activity of each endolysin increased linearly with higher concentrations in an enzyme dependent manner, until a saturation in enzyme activity was reached (Figure 5.3). At this level, the muralytic activity adopted a constant value independent of the concentration. Based on the linear relationship between lysis activity and enzyme concentration, the specific muralytic activity was calculated and expressed in enzymatic units per μM of added endolysin (Briers et al, 2007a) (Table 4.1). PsP3gp10 possessed the highest specific muralytic activity of the tested endolysins with a 1.7, 1.8, 4.4, 10.3 and 11.8 times higher value on outer membrane-permeabilized *P. aeruginosa* PAO1 than P2gp09, BcepC6Bgp22, CR8gp3.5, K11gp3.5 and KP32gp15, respectively. In general, the lytic transglycosylases P2gp09, PsP3gp10 and BcepC6Bgp22 showed a higher muralytic activity than the amidases CR8gp3.5, K11gp3.5 and KP32gp15. The specific muralytic activity values determined on outer membrane-permeabilized *S. Typhimurium* LT2 and *E. coli* XL1-Blue MRF' were consistent with those obtained for *P. aeruginosa* PAO1, due to a common chemotype of peptidoglycan (A1 γ) which is conserved among all Gram-negative bacterial species (Schleifer & Kandler, 1972). A mixture of 50 % PsP3gp10 and 50 % K11gp3.5, two endolysins with different catalytic specificity (transglycosylase and amidase), gave a specific muralytic activity value (576 units/ μM , dashed line, Figure 5.3) intermediate between the values for the single endolysins, suggesting an antagonistic effect (Table 5.1, Figure 5.3). If synergy in muralytic activity was present, this value would be higher than 50 % of the sum of both activity values for the single endolysins.

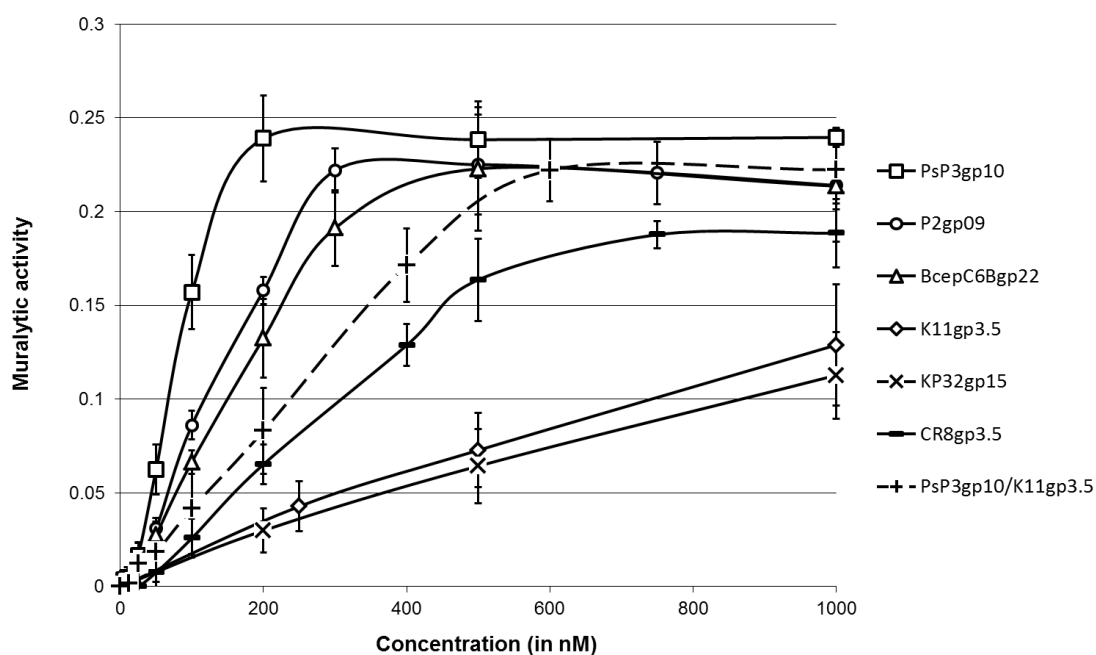


Figure 5.3: Saturation curves of muralytic activity for P2gp09 (circles), PsP3gp10 (squares), BcepC6Bgp22 (triangles), K11gp3.5 (diamonds), KP32gp15 (X), CR8gp3.5 (—) and the PsP3gp10/K11gp3.5 combination (+, dashed curve) on outer membrane-permeabilized *P. aeruginosa* PAO1 substrate at pH 7.2. The graph shows the muralytic activity values, measured as the slope of the corresponding $\Delta OD_{655nm}/min$ curve, for different endolysin concentrations. Averages and standard deviations of three independent measurements are depicted.

Table 5.1: Specific muralytic activities (in units/ μM enzyme) of the six single-domain endolysins and the PsP3gp10/K11gp3.5 combination. The specific muralytic activities of the endolysins were calculated from the slope of the best linear regression to the corresponding saturation curves, according to the definition for enzyme unit adapted from Briers and coworkers (Briers et al, 2007a). Outer membrane-permeabilized *P. aeruginosa* PAO1, *S. Typhimurium* LT2 and *E. coli* XL1-Blue MRF' cells, resuspended in a KH_2PO_4/K_2HPO_4 buffer (80 mM ionic strength, pH 7.2), were used to test enzymatic activities. Endolysins were dialyzed against PBS buffer (pH 7.4). The corresponding R-square values of the best linear regression to the linear part of the saturation curves are indicated between brackets. ND = not determined.

	Specific muralytic activity (in units/ μM)		
	<i>P. aeruginosa</i> PAO1	<i>S. Typhimurium</i> LT2	<i>E. coli</i> XL1-Blue MRF'
PsP3gp10	1,380 (0.976)	1,390 (0.954)	1,285 (0.988)
P2gp09	829 (0.992)	865 (0.943)	830 (0.943)
BcepC6Bgp22	786 (0.937)	767 (0.902)	765 (0.983)
CR8gp3.5	315 (0.961)	372 (0.921)	299 (0.961)
K11gp3.5	134 (0.983)	120 (0.992)	123 (0.973)
KP32gp15	117 (0.987)	110 (0.993)	117 (0.999)
PsP3gp10 + K11gp3.5	576 (0.990)	ND	ND

5.2.3 Stability at 4°C and 50°C

The stability of the six single-domain endolysins was assessed in solution (PBS buffer pH 7.4) by monitoring the residual muralytic activity (in %) after a prolonged incubation at 4°C (Figure 5.4A) and a short incubation at 50°C (Figure 5.4B). All endolysins could be preserved for more than one month on 4°C and remained stable for at least one hour at 50°C.

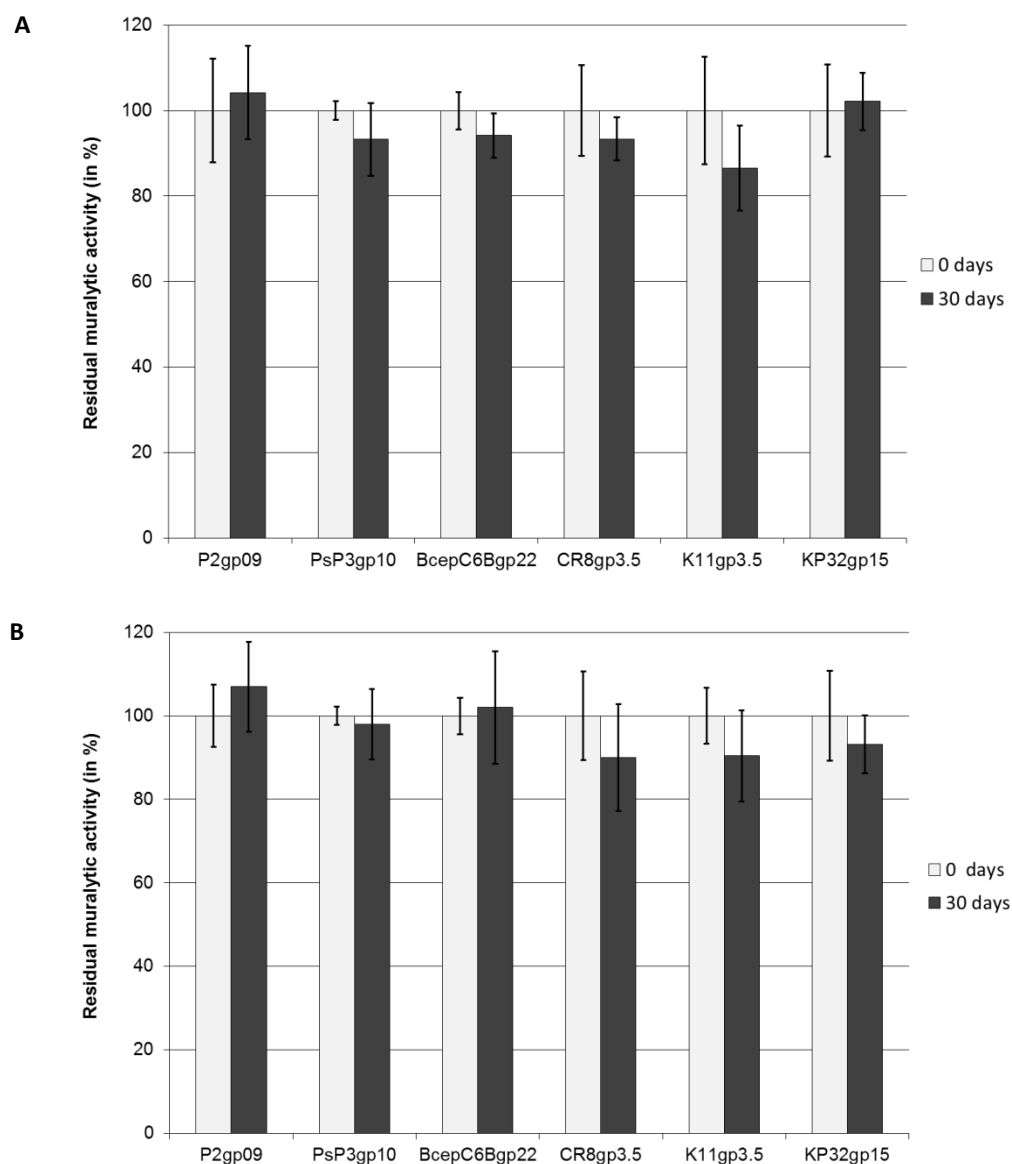


Figure 5.4: Enzymatic stability of P2gp09, PsP3gp10, BcepC6Bgp22, K11gp3.5, KP32gp15 and CR8gp3.5 after 30 days of incubation at 4°C (A) and 1 hour at 50°C (B). (A) The residual muralytic activity (1.5 μ M) was determined on outer membrane-permeabilized *P. aeruginosa* PAO1 after 30 days (black bars) of incubation in PBS buffer (pH 7.4) compared to initial activity (light grey bars). (B) In a similar way, the residual muralytic activity was assessed after 1 hour (black bars) of incubation at 50°C (initial activity = light grey bars). For each graph, averages and standard deviations of three independent measurements are depicted.

5.3 *In vitro* antibacterial activity

The *in vitro* antibacterial activity of PsP3gp10, P2gp09, BcepC6Bgp22, CR8gp3.5, K11gp3.5 and KP32gp15 was evaluated on four exponentially growing Gram-negative species: *P. aeruginosa* PAO1 (non-drug-resistant lab strain), *P. aeruginosa* Br667 (multidrug-resistant burn wound isolate) (Pirnay et al, 2003), *S. Typhimurium* LT2 (food isolate) and *E. coli* XL1-Blue MRF'. A concentration of 1.5 μM (at the saturation level of enzymatic activity) of all six endolysins was unable to effectively inactivate the four tested Gram-negative species, with log reduction values below 0.5 (Table 5.2A). This is due to the impermeable Gram-negative outer membrane, that protects the underlying peptidoglycan layer from enzymatic hydrolysis of exogenously added endolysins.

Secondly, the antibacterial activities of the single-domain endolysins (1.5 μM final concentration) were analyzed in combination with EDTA (0.5 mM final concentration). By permeabilization of the outer membrane, the added EDTA induced a significant rise in antibacterial activity of the six endolysins on *P. aeruginosa* PAO1 (Table 5.2B). Dependent on the endolysin used, the lethal effect on *P. aeruginosa* PAO1 varied between 1.87 ± 0.05 (for KP12gp15) and 3.38 ± 0.23 (for PsP3gp10) log units reduction. Contrarily, the other three strains showed no significant sensitivity for the endolysin/EDTA combination.

Next, we also tested the antibacterial effect of a combination of two endolysins with a different catalytic specificity, PsP3gp10 and K11gp3.5, in the presence of EDTA against intact *P. aeruginosa* PAO1 (Table 5.2B). We used the same sub-MIC concentration (750 nM final concentration) for both endolysins. Regardless of the EDTA addition, the obtained log reduction values for the PsP3gp10/K11gp3.5 combination (0.31 ± 0.03 log units without EDTA, 2.62 ± 0.11 log units with EDTA) were intermediate between the values obtained for the separate endolysins PsP3gp10 (0.38 ± 0.02 log units without EDTA, 3.08 ± 0.17 log units with EDTA) and K11gp3.5 (0.15 ± 0.10 log units without EDTA, 2.08 ± 0.16 log units with EDTA), both in a final concentration of 1500 nM.

Table 5.2: *In vitro* antibacterial activity of the six single-domain endolysins and the PsP3gp10/K11gp3.5 combination in the absence (A) and presence of EDTA (B) against *P. aeruginosa* PAO1, *P. aeruginosa* Br667, *S. Typhimurium* LT2 and *E. coli* XL-1 Blue MRF'. Cell suspensions ($\pm 10^6$ CFU/ml) in 5 mM HEPES buffer (pH 7.4) were incubated with an endolysin concentration at the saturation level of enzymatic activity (1.5 μ M) or with the PsP3gp10/K11gp3.5 combination (750 nM for each endolysin) without (A) or with (B) EDTA (0.5 mM). Endolysins were dialyzed against PBS buffer (pH 7.4). Antibacterial activity is indicated in logarithmic units ($= \log_{10}(N_0/N_i)$ with N_0 = number of untreated cells and N_i = number of treated cells, both counted after incubation). Averages and standard deviations of three repeated and independent experiments are shown here. Reduction values above one log unit are shaded in grey. ND = not determined.

Antibacterial activity (in log ₁₀ units)				
A	<i>P. aeruginosa</i> PAO1	<i>P. aeruginosa</i> Br667	<i>S. Typhimurium</i> LT2	<i>E. coli</i> XL1-Blue MRF'
PsP3gp10	0.38 ± 0.02	0.38 ± 0.06	0.28 ± 0.04	0.21 ± 0.03
P2gp09	0.37 ± 0.08	0.25 ± 0.04	0.08 ± 0.09	0.19 ± 0.05
BcepC6Bgp22	0.41 ± 0.30	0.18 ± 0.08	0.09 ± 0.06	0.17 ± 0.04
CR8gp3.5	0.21 ± 0.07	0.05 ± 0.03	0.03 ± 0.03	0.09 ± 0.04
K11gp3.5	0.15 ± 0.10	0.08 ± 0.08	0.08 ± 0.02	0.12 ± 0.10
KP32gp15	0.14 ± 0.07	0.01 ± 0.04	0.14 ± 0.05	0.04 ± 0.05
PsP3gp10 K11gp3.5	0.31 ± 0.03	ND	ND	ND
B	<i>P. aeruginosa</i> PAO1	<i>P. aeruginosa</i> Br667	<i>S. Typhimurium</i> LT2	<i>E. coli</i> XL1-Blue MRF'
EDTA	0.33 ± 0.15	0.01 ± 0.05	0.05 ± 0.03	0.15 ± 0.05
PsP3gp10	3.38 ± 0.23	0.67 ± 0.04	0.69 ± 0.04	0.39 ± 0.01
P2gp09	2.84 ± 0.08	0.58 ± 0.07	0.34 ± 0.11	0.29 ± 0.07
BcepC6Bgp22	3.08 ± 0.15	0.31 ± 0.05	0.32 ± 0.12	0.31 ± 0.12
CR8gp3.5	2.05 ± 0.08	0.06 ± 0.10	0.22 ± 0.07	0.23 ± 0.11
K11gp3.5	2.14 ± 0.30	0.08 ± 0.04	0.29 ± 0.10	0.16 ± 0.13
KP32gp15	1.87 ± 0.05	0.09 ± 0.03	0.20 ± 0.01	0.13 ± 0.09
PsP3gp10 K11gp3.5	2.81 ± 0.18	ND	ND	ND

5.4 Discussion

Bacteriophage endolysins exert an important function in the release of the phage progeny by lysis of the bacterial host cell wall at the end of the phage replication cycle (Borysowski et al, 2006). Bacteriophages infecting Gram-negatives evolved a diverse set of endolysins with different structural composition, catalytic specificity and peptidoglycan lytic potential (Callewaert et al, 2011). A majority of endolysins with Gram-negative background are assumed to adopt a single-domain structure, but only few of them have been fully characterized. This emphasizes that we are only at the beginning of unraveling the diversity of these proteins with a common lytic function.

We experimentally demonstrated the peptidoglycan lytic activity of six novel, single-domain endolysins (BcepC6Bgp22, P2gp09, PsP3gp10, CR8gp3.5, K11gp3.5 and KP32gp15) of phages infecting different Gram-negative host cells. As shown *in silico*, these endolysins all adopt a similar secondary structure composed of a single catalytic domain. Based on their predicted catalytic specificity, these endolysins can be divided in two different families (Figure 5.1). As potential “phage λ -like lysozymes” or transglycosylases, BcepC6Bgp22, P2gp09 and PsP3gp10 are predicted to target the glycoside bond between the MurNAc and the GluNAc components of the glycan backbone in the peptidoglycan. In contrast, the predicted amidases CR8gp3.5, K11gp3.5 and KP32gp15 are expected to hydrolyze the amide bond between the pentapeptide chains and the D-lactyl group of the MurNAc moiety (Figure 5.1). Besides its muralytic activity, K11gp3.5 was recently shown to inhibit transcriptional activity of the phage K11 RNA polymerase, analogous to the T7 lysozyme/amidase (Junn et al, 2005). Construction of chimeric proteins consisting of N- and C-terminal domains of K11gp3.5 and T7 lysozyme/amidase indicated the N-terminal region as being responsible for this RNA polymerase inhibition (Alcantara et al, 2007). By chromatographic and mass spectrometry analysis of the peptidoglycan cleavage products upon endolysin addition, the predicted catalytic specificities of these endolysins could be verified. Similar analyses were done for *P. aeruginosa* phage ϕ KMV endolysin KZ144 (a transglycosylase) and *Bacillus cereus* phage B4 endolysin LysB4 (an endopeptidase) (Paradis-Bleau et al, 2007; Son et al, 2012).

BcepC6Bgp22, P2gp09, PsP3gp10, CR8gp3.5, K11gp3.5 and KP32gp15 clearly differ in their efficiency to hydrolyze the peptidoglycan layer. The muralytic potential of the predicted lytic transglycosylases PsP3gp10, P2gp09 and BcepC6Bgp22 is 4.4 to 11.8 times higher than these of the predicted amidases CR8gp3.5, K11gp3.5 and KP32gp15, an observation which was consistent for three different Gram-negative species. The differences in muralytic activity between the lytic transglycosylases and amidases are also clearly reflected in their *in vitro* antibacterial activity on *P. aeruginosa* PAO1 in combination with the outer membrane permeabilizer EDTA: PsP3gp10, P2gp09 and BcepC6Bgp22 induce 3 to 3.5 log units reduction of PAO1 in the presence of EDTA, whereas reduction values for CR8gp3.5, K11gp3.5 and KP32gp15 are situated around 2 log units. The absence of Zn^{2+} in the test buffer could explain the lower enzymatic and antibacterial activity observed for the predicted Zn^{2+} -dependent amidases in comparison to the predicted transglycosylases or muramidase. Addition of small amounts of Zn^{2+} may improve enzymatic activity of CR8gp3.5, K11gp3.5 and KP32gp15 substantially, but is, on the other hand, expected to lower the outer membrane destabilizing capacity of EDTA by competitive inhibition with the stabilizing divalent Mg^{2+} and Ca^{2+} ions. This would lead to a less efficient antibacterial activity of these endolysins in the presence of EDTA. Based on these data, we may conclude for all six single-domain endolysins that a higher muralytic activity correlates with a higher antibacterial activity. Despite the fact that the amino acid sequences of PsP3gp10 and P2gp09 are almost identical (94 % similarity), both endolysins do show differences in muralytic (P2gp09 is 40 % less active than PsP3gp10) and antibacterial activity (3.38 log units for PsP3gp10 compared to 2.84 log units for P2gp09). The same is true, in lesser extent, for CR8gp3.5 and K11gp3.5/KP32gp15 who are 71/69 % identical. Subtle changes in the primary structure of an endolysin seem to have impact on its activity.

Previously, Loeffler and Fischetti (2003) successfully demonstrated the synergistic lethal effect of a combination of two modular endolysins with different catalytic specificity (lysozyme Cpl-1 and amidase Pal) on different resistant Gram-positive *S. pneumonia* strains. We were not able to show such a synergy between an amidase, K11gp3.5, and a lytic transglycosylase, PsP3gp10, on *P. aeruginosa* PAO1. Further investigation on combinations of single-domain endolysins with other catalytic specificities including lysozymes and endopeptidases, might possibly reveal similar synergistic effects.

To facilitate the passage of endolysins through the outer membrane, a combinatorial approach consisting of a single-domain endolysin with an outer membrane permeabilizer was used. Briers and coworkers recently demonstrated the efficacy of a combination of an endolysin with Gram-negative background (e.g. endolysin EL188 of *P. aeruginosa* infecting phage EL) and the outer membrane permeabilizer EDTA for reduction of the Gram-negative pathogen *P. aeruginosa* (Briers et al, 2011b). The positive effect of EDTA on antibacterial activity is caused by the powerful outer membrane permeabilization capacity of EDTA through binding and withdrawal of the stabilizing divalent Mg^{2+} and Ca^{2+} cations present in the lipopolysaccharide layer of the Gram-negative outer membrane (Leive et al, 1968). As a result, the bacterial peptidoglycan becomes more prone to the muralytic activity of the externally added endolysins. The combination of a single-domain endolysin with EDTA was able to efficiently reduce the non-drug-resistant lab strain *P. aeruginosa* PAO1 with 1.87 ± 0.05 (for KP22gp15) to 3.38 ± 0.26 (for PsP3gp10) log units reduction, dependent on the endolysin used. The multidrug-resistant *P. aeruginosa* Br667 was less sensitive for the single-domain endolysin/EDTA action with a maximal reduction of 0.67 log units (or 58 %) in case of the most active single-domain endolysin, PsP3gp10. Specific variations in outer membrane structure of *P. aeruginosa* clinical isolates, including O-acetylation, phosphorylation and (de)acetylation which improve membrane stability, could explain the difference in inactivation between PAO1 and Br667 (Ernst et al, 2007). However, due to the low amount of phosphate groups per lipopolysaccharide molecule and the corresponding amount of stabilizing divalent cations in the outer membrane of Enterobacteriaceae compared to that of *Pseudomonas* species (Knirel et al, 2006), the sensitivity of *E. coli* XL1-Blue MRF' and *S. Typhimurium* LT2 strains for the outer membrane destabilizing action of EDTA is less pronounced, resulting in lower inactivation levels beneath 0.7 log units. A similar observation was made for endolysin EL188 combined with EDTA (Briers et al, 2011b). Consequently, the type and structure of the outer membrane seems of crucial importance for the antibacterial efficiency of the endolysin/EDTA combinatorial approach. However, the biochemical and antibacterial characterization of six novel, single-domain endolysins allowed us to gain a better insight in the structure-activity relationship of these endolysins, which is crucial for their development into potential anti-Gram-negative compounds.

Characterization of modular bacteriophage endolysins from *Myoviridae* phages OBP, 201φ2-1 and PVP-SE1¹

The previous chapter described the biochemical and antibacterial characterization of six novel, single-domain endolysins. This single-domain structure is found in almost all endolysins from Gram-negative origin. *P. aeruginosa* phage endolysins KZ144 (from giant phage φKZ) and EL188 (giant phage EL), however, were the first endolysins of Gram-negative origin found to have a modular instead of a single-domain structure (Briers et al, 2007b). Apart from a catalytic domain at their C-terminus, KZ144 and EL188 also contain an N-terminal cell wall binding part. This chimeric composition is rather rare among endolysins from Gram-negative origin (Fischetti, 2010). Furthermore, the authors prove the link between the presence of a cell wall binding domain in KZ144 and EL188 and their high muralytic activity on peptidoglycan of *P. aeruginosa*, justifying the search for other modular endolysins with Gram-negative background. The recent genome analyses of the giant *Myoviridae* bacteriophages *Pseudomonas fluorescens* OBP (Cornelissen et al, 2012) and *Pseudomonas chlororaphis* 201φ2-1 (Thomas et al, 2008), both member of the recently discovered “phiKZ-like viruses” (Krylov et al, 2007), and the *Salmonella enterica* serovar Enteritidis (abbreviated as *S. Enteritidis*) PVP-SE1 (Santos et al, 2011), an “rV5-like virus”, revealed the presence of the predicted endolysins OBPgp279, 201φ2-1gp229 and PVP-SE1gp146, respectively. *In silico*, these proteins were predicted to have a modular structure, similar to KZ144 and EL188. In this chapter, we expand the pool of characterized modular endolysins from giant Gram-negative infecting *Myoviridae* phages by an extensive description of OBPgp279, 201φ2-1gp229 and PVP-SE1gp146 at the biochemical and antibacterial level. In addition, we comment on the differences between these modular endolysins and the single-domain endolysins from the previous chapter in regard to their applicability as enzyme-based antibacterials in future antibacterial treatments.

¹This chapter is adapted from:

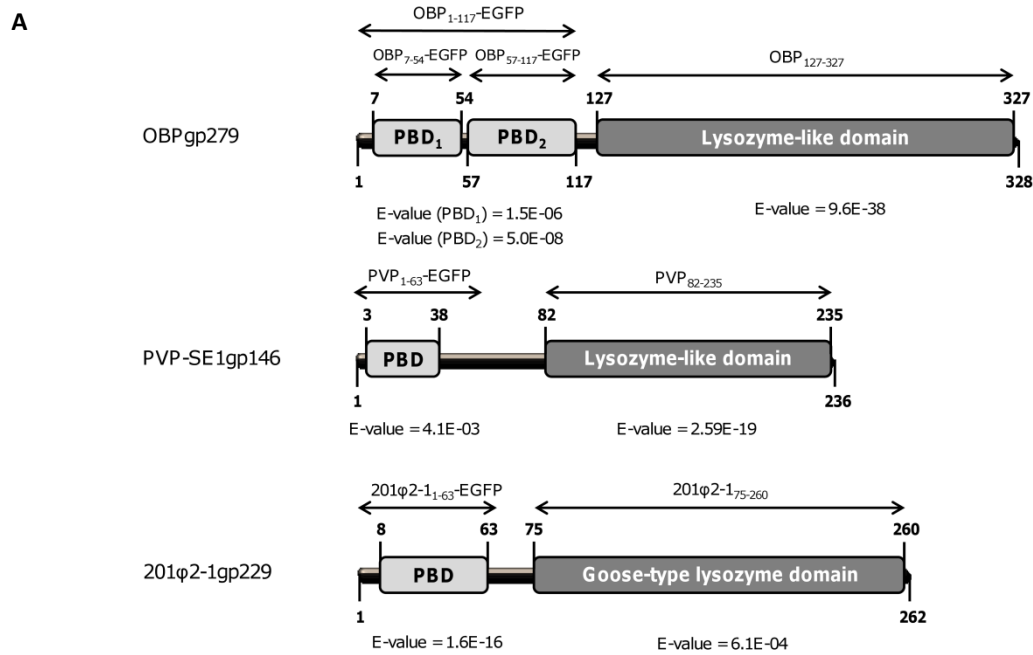
Walmagh M, Briers Y, Santos SB, Azeredo J, Lavigne R (2012). Characterization of modular bacteriophage endolysins from *Myoviridae* phages OBP, 201φ2-1 and PVP-SE1. PLoS One 7(5):e36991. doi:10.1371/journal.pone.0036991

6.1 Modularity feature in OBPgp279, 201φ2-1gp229 and PVP-SE1gp146

6.1.1 *In silico* domain prediction in OBPgp279, 201φ2-1gp229 and PVP-SE1gp146

Using Blastp (Altschul et al, 1997), Pfam (Finn et al, 2010) and HHpred (Soding et al, 2005) prediction tools, endolysins OBPgp279 (from *P. fluorescens* infecting phage OBP), 201φ2-1gp229 (from *P. chlororaphis* infecting phage 201φ2-1) and PVP-SE1gp146 (from *S. Enteritidis* infecting phage PVP-SE1) were predicted to adopt a modular structure with an N-terminal peptidoglycan binding domain and a C-terminal catalytic domain (Figure 6.1). The catalytic domain of 201φ2-1gp229 shows similarity with a goose-type lysozyme domain, known for its three-dimensional structural similarity with bacteriophage T4 lysozyme and HEWL (Weaver et al, 1985) (Figure 6.1A). The catalytic domains of OBPgp279 and PVP-SE1gp146 both contain a conserved sequence motif (Figure 6.1B), typically found in members of the glycoside hydrolase 19 (GH19) family (general sequence motif= F/H/Y-GR-G-A/P-X-Q-I/L-S/T-F/H/Y/W-H/N-F/Y-N/Y, X = hydrophilic amino acid) (Udaya Prakash et al, 2010). Other recently characterized endolysins like the *A. baumannii* phage φAB2 lysin (LysAB2) (Lai et al, 2011) or the *S. enterica* phage ε15 lysin (Kropinski et al, 2007) also belong to this GH19 family. Both the goose-type lysozyme and the GH19 family are members of the lysozyme-like superfamily which contains a broad range of lytic domains involved in hydrolysis of the β-1,4 linkages between the GluNAc and MurNAc sugars of the peptidoglycan backbone (Wohlkonig et al, 2010).

The N-terminal domains of OBPgp279, 201φ2-1gp229 and PVP-SE1gp146 possess specific repeated motifs that are conserved in the confirmed peptidoglycan binding domains of the modular endolysins KZ144 and EL188 (Briers et al, 2007b). These repeated motifs largely match the consensus sequence (D-G-(Pho)₂-G-X(X)-T/C, Pho = hydrophobic amino acid, X = hydrophilic amino acid) proposed previously. Two such motifs (D-G-L-F-G-E-K-C and D-G-K-W-G-G-T) were present in the N-terminal domain of OBPgp279 (one in each predicted subdomain) and one in 201φ2-1gp229 (D-G-V-F-G-D-N-T) and PVP-SE1gp146 (D-G-L-Y-G-P-A-T) (Figure 6.1B). This conserved feature is present in many proteins that interact with repeated structures such as peptidoglycan (Wren, 1991).



B

OBPgp279

MKNSEKNASIIMSIQRTLASLSLYGGR**IDGLFGEKCR**GAIILMLNKVYPNFSTNKLPSNTYQ
 AESVFTFLQ~~TALAGVGLY~~TITIDGKWGGTSQGAIDALVKS~~YRQITEAERAGSTLPLGLATV~~
 MSKHMSIEQLRAMLP~~TDRQGYAEVYIDPLNETMDIFEINTPLRIAHFMAQILHETACFKYT~~
 EELASGKAYEGRADLGNTRPGDGLF**KGRGLLOITGR**LNYVKCQVYLREKLKDP~~TFDITS~~
 SVTCAQQLSESP~~LLAALASGYFWRFIKPKLNETADKDDIYVVS~~VYVNGYAKQANPPY~~PN~~
 RDKEPNHMKERVQMLAVTKKALGIV

PVP-SE1gp146

MNA~~AI~~AEIQRM~~LI~~EGGFSV~~GK~~SGA**DGLYGPAT**KAALQK~~CIAQATS~~GN~~NKGGT~~LKLTQAQL
 DKIFPVGASSGRNAKFLKPLN~~DLFEKTEINTVNRVAGF~~LSQIGVESAEFR~~YVRELGNDA~~YF~~~~
 DKYDTGPIAERLGNTPQKDG~~GAKYKGRGLIQVTGL~~ANYKACGKALGLDLVNHPELLEQ
 PEYAVASAGWYWDTRNINAACDADDIVK~~ITKLVN~~GGTNHLAERTAYYKKA~~KS~~SVLTS

201φ2-1gp229

MILKNGSKGDDVIRLQ~~RKLIGL~~GYSVK**DDGVFGDNTE**KAVKAVQLRFNLKDDGIVGNNT
 WAVLDTPTTTRPALTDKDYQWAADYLQVDLPAVKAVKEVEAPAGGFLPDGRVTILYERH
 VMFKRLRVNGINPEPFAANPSIVNKSTGGYLGKSAEYTRLEQAEKID~~EVSALESC~~SWGGA
 YQIMGYHWKLLGF~~SVHDFLAKM~~KESERGQLECFVKFIKADAALLKNLRAKDWAKFAAG
 YNGPNYRQNNYDVKLASAYTKFGGK

Figure 6.1: Schematic diagram of the predicted domain organization (A) and amino acid sequences (B) of OBPgp279, 201φ2-1gp229 and PVP-SE1gp146. The predicted N-terminal peptidoglycan binding domains (PBD) are marked in light grey, the C-terminal catalytic domains (lysozyme-like or goose-like lysozyme domains) in dark grey. (A) E-values for OBP₁₂₇₋₃₂₇ (predicted by HHpred), PBD₁ and PBD₂ of OBPgp279 (both HHpred), PVP₈₂₋₂₃₅ (Blastp), PBD of PVP-SE1gp146 (Pfam), 201φ2-1₇₅₋₂₁₀ (HHpred) and PBD of 201φ2-1gp229 (Pfam) are all indicated below the respective domains. The names of the different constructs used are also marked above each predicted structure. (B) The PBD motifs which show some similarity with consensus sequence D-G-(Pho)₂-G-X(X)-T/C (Pho = hydrophobic amino acid, X = hydrophilic acid) of the PBDs in KZ144 and EL188 (Briers et al, 2007b) are underlined and marked in bold. A seven amino acid motif L-A-X-Pho-X-L-Y (X = the same hydrophilic amino acid, Pho = hydrophobic amino acid, boxed) is present in front of both repeated PBD motifs of OBPgp279, each with four amino acids in between. Inside the catalytic domains of OBPgp279 and PVP-SE1gp146, motifs matching the consensus sequence for GH19 family members (F/H/Y-G-R-G-A/P-X-Q-I/L-S/T-F/H/Y/W-H/N-F/Y-N/Y, X = hydrophilic amino acid) (Udaya Prakash et al, 2010) are underlined and italicized.

In case of OBPgp279, seven conserved amino acids (L-A-X-Pho-X-L-Y, X = same hydrophilic amino acid, Pho = hydrophobic amino acid) were detected preceding both repeated motifs with four amino acids in between. This observation strengthens the hypothesis that the peptidoglycan binding domain of OBPgp279 was duplicated throughout evolution. The presence of these peptidoglycan binding motifs inside the N-terminal domains strongly supports the predicted peptidoglycan binding function. Furthermore, the observation of these conserved repeated motifs suggests the presence of a general consensus sequence among peptidoglycan binding domains of modular endolysins from Gram-negative origin.

6.1.2 The predicted peptidoglycan binding domains in OBPgp279, 201φ2-1gp229 and PVP-SE1gp146

6.1.2.1 Peptidoglycan binding capacity

To evaluate peptidoglycan binding capacity, we recombinantly produced the fusion proteins OBP₁₋₁₁₇-EGFP, PVP₁₋₆₃-EGFP and 201φ2-1₁₋₆₃-EGFP, comprising the predicted binding domains of OBPgp279 (amino acids 1-117), PVP-SE1gp146 (amino acids 1-63) and 201φ2-1gp229 (amino acids 1-63) N-terminally fused to the Enhanced Green Fluorescent Protein (EGFP). Outer membrane-permeabilized *P. aeruginosa* PAO1 and *S. Typhimurium* LT2 cells were incubated with 2 μM fusion protein for 5 min and were washed to remove unbound protein. The retained fluorescence of peptidoglycan bound protein was then quantified and visualized (Figure 6.2). A negative control, unbound EGFP, and a positive control, KZ₁₋₈₃-EGFP, were included for comparison. KZ₁₋₈₃-EGFP is the fusion protein of the peptidoglycan binding domain of KZ144 (amino acids 1 to 83) with EGFP, previously shown to possess peptidoglycan binding capacity (Briers et al, 2009).

Figure 6.2A shows that the N-terminal parts of OBPgp279, 201φ2-1gp229 and PVP-SE1gp146 possess peptidoglycan binding activity, as the measured fluorescence levels under saturating concentrations were comparable with KZ₁₋₈₃-EGFP. This observation also implies that the same number of binding sites was occupied by an excess of the different fusion proteins. The cell wall binding capacity of OBP₁₋₁₁₇-EGFP, 201φ2-1₁₋₆₃-EGFP and PVP₁₋₆₁-EGFP was visually confirmed using epifluorescence microscopy (Figure 6.2B). The cell wall of the targeted

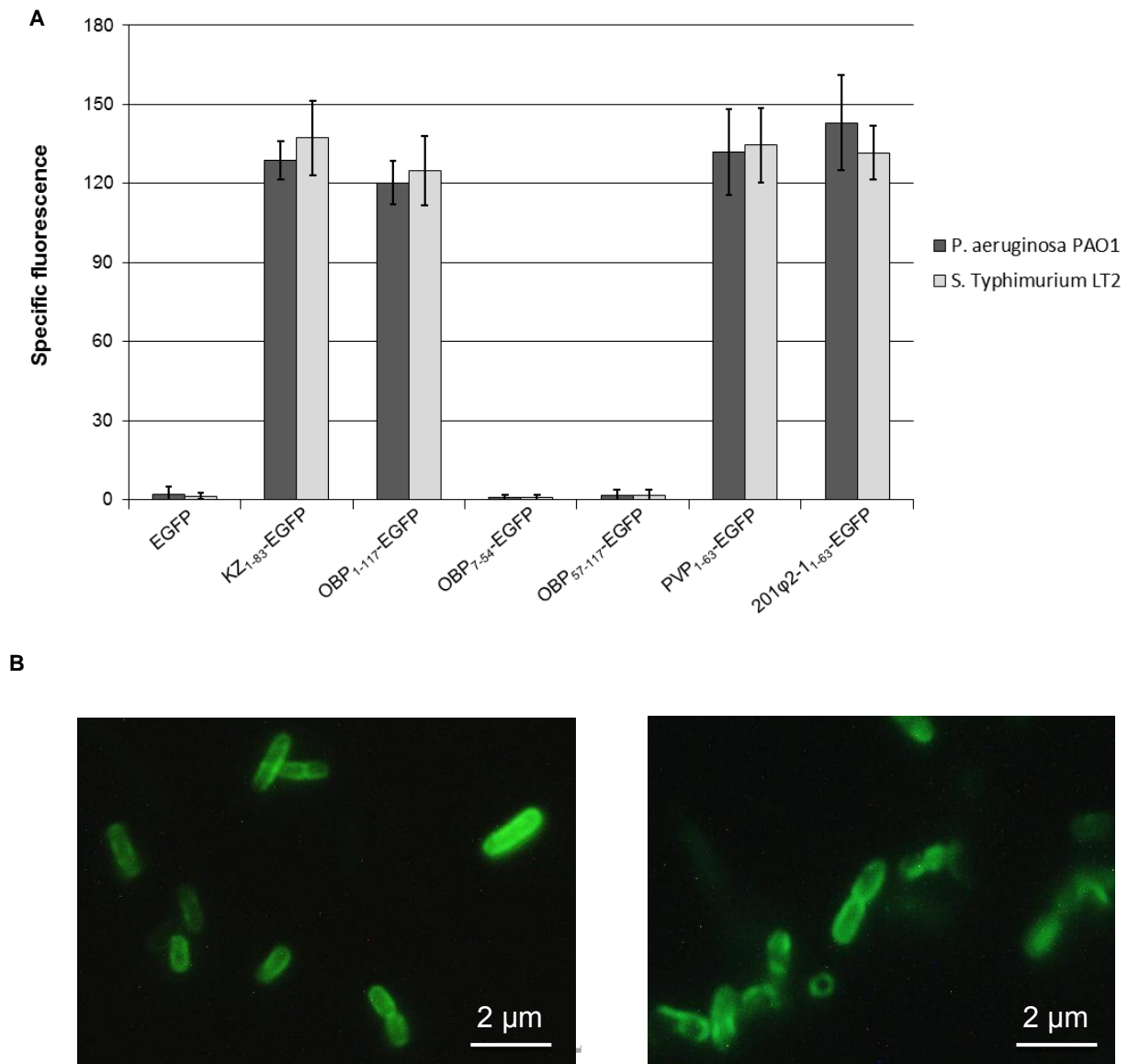


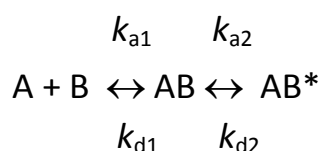
Figure 6.2: Peptidoglycan binding capacity of fusion proteins OBP_{1-117} -EGFP, OBP_{7-54} -EGFP, OBP_{57-117} -EGFP, PVP_{1-63} -EGFP and $201\phi 2-1_{1-63}$ -EGFP. (A) The relative fluorescence (e.g. the fluorescence of the treated cells subtracted by the fluorescence of untreated cells and cell buffer) of 2 μ M of each fusion protein measured after incubation with outer membrane-permeabilized *P. aeruginosa* PAO1 (dark grey bars) or *S. Typhimurium* LT2 cells (light grey bars) is shown here for the different EGFP fusion constructs. Obtained values were compared with the specific fluorescence of the unbound wild-type EGFP (negative control). 2 μ M of KZ-EGFP, the fusion protein of the peptidoglycan binding domain of KZ144 and EGFP, was used as positive control. Average and standard deviation values of three independent experiments are shown. (B) Epifluorescence microscopy of outer membrane-permeabilized *P. aeruginosa* PAO1 cells treated with OBP_{1-117} -EGFP (left) and PVP_{1-63} -EGFP (right). Cells were incubated with 2 μ M of each fusion protein for 5 min. Cell pellets were washed twice and visualized using epifluorescence microscopy (with 500x magnification, size bar is indicated). Both fusion proteins are visualized in green targeted to the bacterial cell wall.

P. aeruginosa PAO1 and *S. Typhimurium* LT2 cells became fluorescent in the shortest handling time possible upon incubation with the three fusion constructs. However, a single subdomain (either OBP₇₋₅₄ or OBP₅₇₋₁₁₇) of OBPgp279 was not sufficient for cell wall binding since no fluorescence was retained with any of both fusion proteins (Figure 6.2A). Possible explanations are the improper folding of the single subdomains in the absence of the other subdomain, or the need for both subdomains for effective cell wall binding.

6.1.2.2 Peptidoglycan binding affinity

The binding affinity of PVP₁₋₆₃-EGFP for peptidoglycan of *Salmonella* was analyzed on outer membrane-permeabilized *S. Typhimurium* LT2 cells (= ligand), using surface plasmon resonance analysis (Briers et al, 2009). This technique allows us to follow the interaction between the fusion protein and immobilized Gram-negative cells in real time and to determine the binding affinity constant for each interaction. Therefore, autoclaved *S. Typhimurium* LT2 cells were immobilized on a sensor chip which was coupled with PVP₁₋₆₃-EGFP. This double layer was then exposed to free PVP₁₋₆₃-EGFP proteins in a triple-layer sandwich set-up, allowing us to quantify the interaction between the fusion proteins and the immobilized cells.

To calculate the apparent affinity constant K_{aff} for binding of the PVP₁₋₆₃-EGFP fusion protein to the *Salmonella* cell wall, we used an indicative two-state model which assumes that a 1:1 binding (AB) between fusion protein (A) and ligand (B) occurs followed by a conformational change in the complex (AB*):



This proposed model fitted the data in the best way, enabling us to calculate the association (k_{a1}), dissociation (k_{d1}), forward (k_{a2}) and backward (k_{d2}) rate constants. Using the formula $K_{aff} = (k_{a1}/k_{d1}) * (k_{a2}/k_{d2})$, a K_{aff} constant of $1.26 \times 10^6 \text{ M}^{-1}$ (or a dissociation constant (= $1/K_{aff}$) of $7.93 \times 10^{-7} \text{ M}$) was determined for fusion protein PVP₁₋₆₃-EGFP (Table 6.1). This means that in equilibrium only one in a million PVP₁₋₆₃-EGFP molecules is in the unbound state.

Table 6.1: Apparent association and dissociation kinetic data for the binding of PVP₁₋₆₃-EGFP to immobilized *S. Typhimurium* LT2 cells. Two different analyte concentrations (5 and 10 μ M) were measured in three-fold and the corresponding averages are represented. The association rate (k_{a1}), dissociation rate (k_{d1}), forward rate (k_{a2}) and backward rate (k_{d2}) constants are calculated according to a two-state model that describes a 1:1 binding (AB) of the fusion protein analyte (A) to the immobilized ligand (B), followed by a conformational change in the complex ($AB \leftrightarrow AB^*$).

Analyte concentration (M)	A+B \leftrightarrow AB		AB \leftrightarrow AB*		Apparent affinity constant (k_{a1}/k_{d1}) * (k_{a2}/k_{d2}) (M^{-1})
	Association rate constant k_{a1} ($M^{-1} s^{-1}$)	Dissociation rate constant k_{d1} (s^{-1})	Forward rate constant k_{a2} (s^{-1})	Backward rate constant k_{d2} (s^{-1})	
5.00×10^{-6}	6.78×10^3	3.34×10^{-2}	9.64×10^{-2}	2.25×10^{-3}	1.09×10^6
10.0×10^{-6}	1.14×10^3	5.94×10^{-2}	3.94×10^{-3}	6.07×10^{-4}	1.43×10^6
Average					1.26×10^6

6.2 Biochemical properties of OBPgp279, 201 ϕ 2-1gp229 and PVP-SE1gp146

6.2.1 Substrate specificity

To confirm the predicted catalytic activity and to determine the activity spectrum, each endolysin (1 μ M final concentration) was incubated with three different outer membrane-permeabilized Gram-negative cell substrates (*P. aeruginosa* PAO1, *S. Typhimurium* LT2 and *E. coli* XL1-Blue MRF') and four intact Gram-positive bacteria with different chemotypes of peptidoglycan (*S. aureus* subsp. *aureus* Rosenbach ATCC 6538 = A3 α chemotype, *M. lysodeikticus* ATCC 4698 = A2 α chemotype, *L. lactis* subsp. *lactis* = A4 α chemotype and *B. subtilis* PSB3 = A1 γ chemotype) (Figure 6.3). All three outer membrane-permeabilized Gram-negative cell substrates were efficiently lysed by the tested endolysins as shown by the decrease in optical density, demonstrating their muralytic properties. In contrast, all tested Gram-positive bacteria were almost insensitive for the lytic action upon addition of an excess of OBPgp279, PVP-SE1gp146 and 201 ϕ 2-1gp229 (Figure 6.3). A minor activity, around 5 % of their activity on Gram-negative bacteria, could be observed for endolysins OBPgp279 and PVP-SE1gp146 on *M. lysodeikticus* ATCC 4698 and *B. subtilis* PSB3.

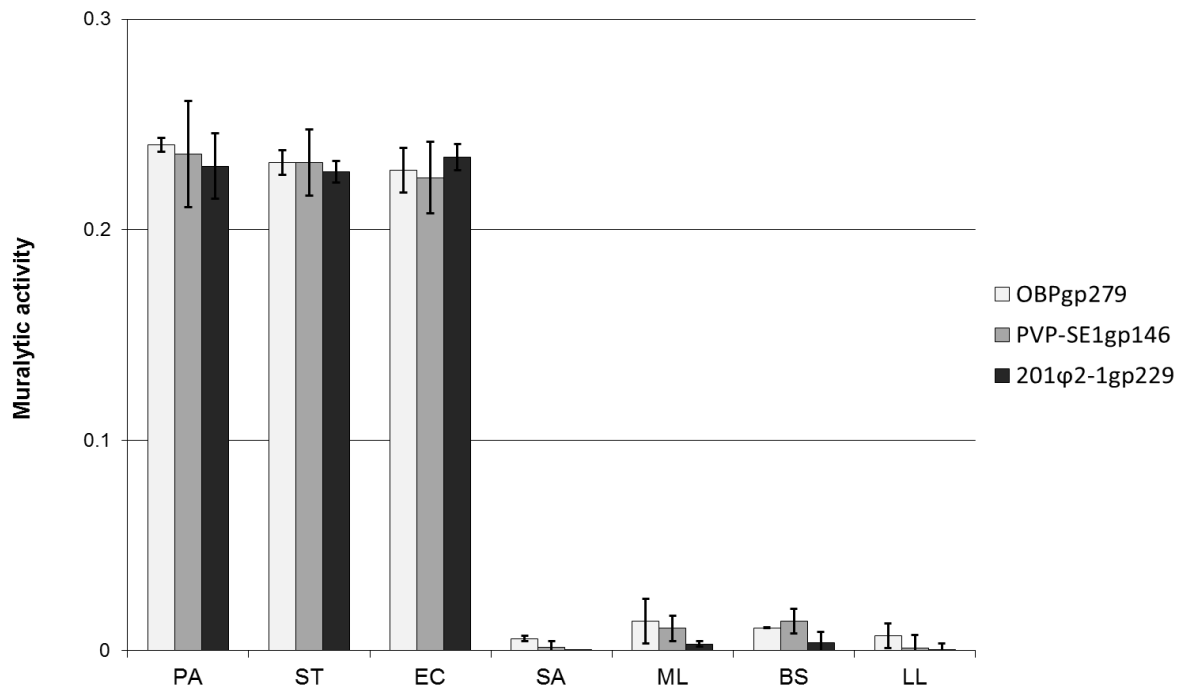


Figure 6.3: Bacterial host spectrum of OBPgp279 (white bars), PVP-SE1gp146 (grey bars) and 201φ2-1gp229 (black bars). Each endolysin (1 μM) is added to outer membrane-permeabilized *P. aeruginosa* PAO1 (PA), *S. Typhimurium* LT2 (ST), *E. coli* XL1-Blue MRF' (EC) and intact *S. aureus* subsp. *aureus* Rosenbach ATCC 6538 (SA), *M. lysodeikticus* ATCC 4698 (ML), *B. subtilis* PSB3 (BS) and *L. lactis* subsp. *lactis* (LL). The muralytic activity, represented as the slope of the resulting decrease of OD_{655nm} in function of time after endolysin addition, is depicted here. Averages and standard deviations of three independent experiments are shown.

6.2.2 Quantification of muralytic activity

Similar to the single-domain endolysins of Chapter 5, the muralytic activities of OBPgp279, 201φ2-1gp229 and PVP-SE1gp146 were first quantified on outer membrane-permeabilized *P. aeruginosa* PAO1 (Briers et al, 2007a). All endolysins reach their maximal activity around pH 7, corresponding to the pH of bacterial cytoplasm, a pH between 6.5 and 7.5 (Wilks & Slonczewski, 2007) (Figure 6.4). An identical observation was made for single-domain endolysins from Gram-negative infecting phages (see 5.2.1 pH-dependency). Furthermore, PVP-SEgp146 shows a reduced activity under more acid conditions. At pH 5, PVP-SE1gp146 still possesses more than 50 % of its maximal enzymatic activity, whereas OBPgp279 and 201φ2-1gp229 only have 40 and 20 % left of their activity at this pH-value, respectively. At pH 7.2, lysis of *P. aeruginosa* PAO1 was detected upon addition of 10 to 20 nM of endolysin. Enzymatic activity further increased linearly dependent on the endolysin concentration. A

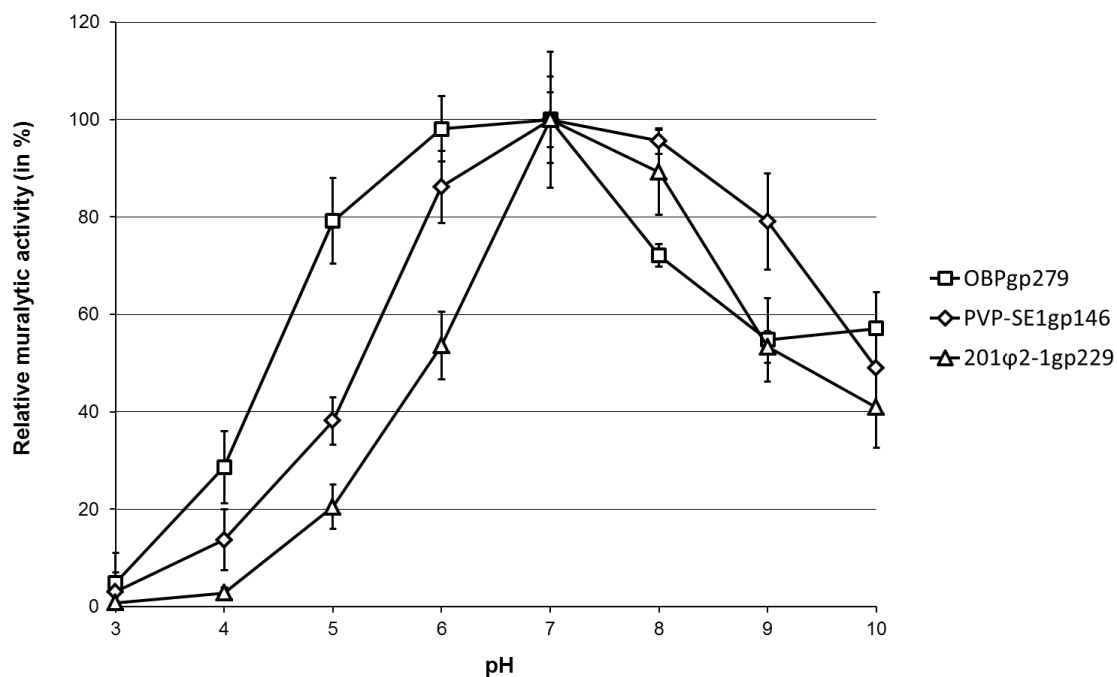


Figure 6.4: pH-dependency of enzymatic activity for OBPgp279 (diamonds), PVP-SE1gp146 (squares) and 201φ2-1gp229 (triangles) on outer membrane-permeabilized *P. aeruginosa* PAO1 cells. Muralytic activity for each endolysin is measured as the slope of the $\Delta OD_{655nm}/min$ curve (Y-axis) for a pH range between 3 and 10 (X-axis) and is shown here relative to the pH with the highest observed muralytic activity for that endolysin. Final concentrations used here are 1 μM OBPgp279, 5 μM PVP-SE1gp146 and 3 μM 201φ2-1gp229, each dialyzed against PBS buffer (pH 7.4). Averages and standard deviations of three repeated experiments are depicted. Each value is connected with the other by use of trendlines.

saturated enzymatic activity was reached at concentrations of 50, 200 and 100 nM for OBPgp279, 201φ2-1gp229 and PVP-SE1gp146, respectively (data not shown). Based on the linear relation between lysis and concentration, the specific muralytic activity for each endolysin was quantified in units per μM of enzyme (Table 6.2) (Briers et al, 2007a). OBPgp279 possessed a 1.5 to 6 times higher muralytic activity value than PVP-SE1gp146 and 201φ2-1gp229, respectively, and a 5 to 10 times higher value compared to the previously reported modular endolysins EL188 and KZ144 (Briers et al, 2007b). As expected, the specific muralytic activity values determined on outer membrane-permeabilized *S. Typhimurium* LT2 and *E. coli* XL1-Blue MRF' were consistent with those obtained for *P. aeruginosa* PAO1 (Table 6.2). The orientation of the His₆-tag, N- or C-terminal, did not significantly influence the enzymatic activity of the endolysin, as assessed for PVP-SE1gp146 (Table 6.2). Nonetheless, the lower expression yield (C-His₆: 38.1 mg/liter culture; N-His₆: 0.54 mg/liter culture), probably due to folding difficulties, made us choose for the C-terminal His₆-tag variants.

Table 6.2: Comparison of specific muralytic activities (in units/ μ M enzyme) of OBPgp279, PVP-SE1gp146 with N- or C-terminal His₆-tag, 201 ϕ 2-1gp229, the catalytic domains of OBPgp279 (OBP₁₂₇₋₃₂₇) and 201 ϕ 2-1 (201 ϕ 2-1₇₅₋₂₆₀) with published data for phage endolysins KZ144 and EL188 on three outer membrane-permeabilized Gram-negative cell substrates. The specific muralytic activities of the endolysins were calculated from the slope of the best linear regression of the corresponding saturation curves, according to the definition for enzyme unit adapted from Briers and coworkers (Briers et al, 2007a). Outer membrane-permeabilized *P. aeruginosa* PAO1, *S. Typhimurium* LT2 and *E. coli* XL1-Blue MRF' cells resuspended in the optimal KH₂PO₄/K₂HPO₄ buffer (pH 7.2), was used as substrate to test enzymatic activities. The endolysins were dialyzed against PBS buffer (pH 7.4). Activity values of KZ144 and EL188 on *P. aeruginosa* PAO1, published previously (Briers et al, 2007b), are marked with an asterisk (*). R-square values for each slope are indicated between brackets. Constructs are listed from the highest to the lowest muralytic activity on *P. aeruginosa* PAO1. ND = not determined.

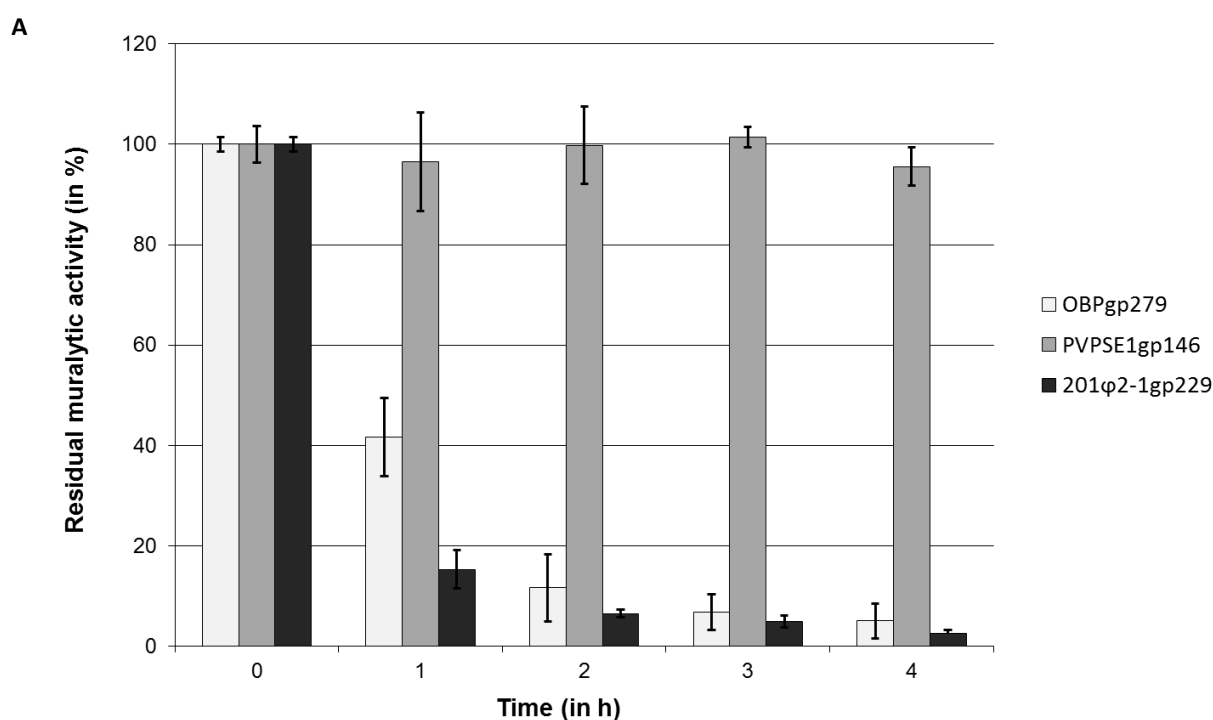
	Specific muralytic activity (in units/ μ M)		
	<i>P. aeruginosa</i> PAO1	<i>S. Typhimurium</i> LT2	<i>E. coli</i> XL1-Blue MRF'
OBPgp279	19,979 (0.983)	18,276 (0.996)	18,078 (0.995)
His₆-PVP-SE1gp146	14,109 (0.931)	ND	ND
PVP-SE1gp146-His₆	13,614 (0.905)	12,273 (0.981)	12,536 (0.994)
OBP₁₂₇₋₃₂₇	12,362 (0.981)	ND	ND
EL188	*4,735 (0.983)	ND	ND
201ϕ2-1gp229	4,469 (0.995)	3,500 (0.942)	3,427 (0.938)
KZ144	*2,058 (0.992)	2,177 (0.986)	1,906 (0.906)
201ϕ2-1₇₅₋₂₆₀	1,951 (0.970)	ND	ND

In addition, we tested the necessity of the peptidoglycan binding domain for proper muralytic activity. Therefore, the individual C-terminal catalytic domains of OBPgp279 (OBP₁₂₇₋₃₂₇), PVP-SE1gp146 (PVP₈₂₋₂₃₅) and 201 ϕ 2-1gp229 (201 ϕ 2-1₇₅₋₂₆₀) were cloned and purified to compare their activity with the obtained value for the full length endolysin. In case of PVP₈₂₋₂₃₅, no soluble protein could be obtained despite changes in expression parameters. Expression of both OBP₁₂₇₋₃₂₇ and 201 ϕ 2-1₇₅₋₂₆₀ yielded pure protein in large amounts for activity testing (Table 6.2). In the absence of the peptidoglycan binding domain, the individual catalytic domains of OBPgp279 and 201 ϕ 2-1gp229 were still active, retaining 62 and 44 % of the muralytic activity of the full length endolysins on outer membrane-permeabilized *P. aeruginosa* PAO1, respectively (Table 6.2). For OBP₁₂₇₋₃₂₇, the residual value

was significantly higher than the full length modular endolysins 201 ϕ 2-1gp229, KZ144 and EL188. These results indicate that both catalytic domains work independently from the peptidoglycan binding domain and emphasize that this domain also has an important contribution to the total enzymatic activity of the full length modular endolysin.

6.2.3 Activity after heat treatment

All three endolysins could be stored at 4°C in the elution buffer, containing 20 mM Na₂HPO₄-NaOH, 0.5 M NaCl and 0.5 M imidazole (pH 7.4), for several weeks and months without loss of activity. The capacity of the enzyme to remain active after heat treatment, is determined by measuring the residual muralytic activity (in %) on outer membrane-permeabilized *P. aeruginosa* PAO1 after heating at 42 and 50°C. No reduction of enzymatic activity was observed after prolonged incubation of the enzymes at 42°C (data not shown). When heated at 50°C, the muralytic activity of OBPgp279 and 201 ϕ 2-1gp229 dropped below 20 % of the initial activity after 2 and 1 h incubation, respectively (Figure 6.5A). In contrast, PVP-SE1gp146 remained fully active, even after 24 h of incubation. At higher temperatures, PVP-SE1gp146 retained its maximal activity at 80°C for 1 h, only to be totally inactivated after 40 min at 100°C (Figure 6.5B).



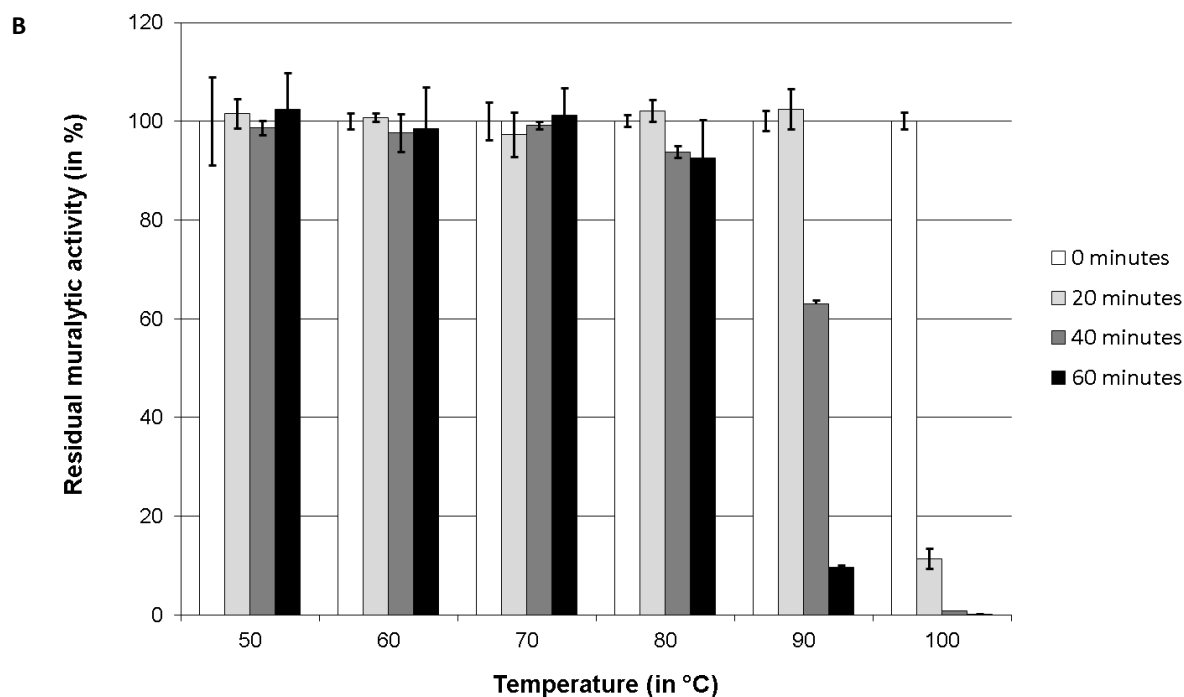


Figure 6.5: Activity after heat treatment of OBPgp279, PVP-SE1gp146 and 201 ϕ 2-1gp229. (A) The residual muralytic activity of OBPgp279 (1 μ M, white bars), PVP-SE1gp146 (5 μ M, grey bars) and 201 ϕ 2-1gp229 (3 μ M, black bars) on outer membrane-permeabilized *P. aeruginosa* PAO1 cell substrate after 1, 2, 3 and 4 h of heat treatment at 50°C is shown. (B) For PVP-SE1gp146 (5 μ M), the residual activity on outer membrane-permeabilized *P. aeruginosa* PAO1 after incubation for 0 (white bars), 20 (light grey bars), 40 (dark grey bars) and 60 (black bars) min on different temperatures between 50 and 100°C was determined. For each curve, averages and standard deviations of three repeated and independent experiments are shown

6.3 *In vitro* antibacterial activity

The antibacterial activity of OBPgp279, 201 ϕ 2-1gp229 and PVP-SE1gp146 was investigated on the Gram-negative bacteria *P. aeruginosa* PAO1, *P. aeruginosa* Br667, *E. coli* XL1-Blue MRF' and *S. Typhimurium* LT2 in the absence and presence of outer membrane permeabilizer EDTA, and compared with the antibacterial activity of endolysins KZ144 and EL188 (Table 6.3A). Remarkably, OBPgp279 reduced *P. aeruginosa* PAO1 and the multidrug-resistant *P. aeruginosa* Br667 with 1.10 ± 0.07 and 1.08 ± 0.08 log units, respectively, in the absence of EDTA. Contrarily, *E. coli* XL1-Blue MRF' and *S. Typhimurium* LT2 showed no sensitivity to the endolysins action. Both PVP-SE1gp146 or 201 ϕ 2-1gp229 did not affect the two *P. aeruginosa* strains in the absence of EDTA, neither did KZ144 or EL188 (Table 6.3A).

Table 6.3: Antibacterial activity of OBPgp279, PVP-SE1gp146 and 201φ2-1gp229 in combination with EDTA against different Gram-negative species compared to KZ144 and EL188. Cell suspensions ($\pm 10^6$ CFU/ml) in 5 mM HEPES buffer (pH 7.4) were incubated for 30 min with OBPgp279 (1.5 μ M), PVP-SE1gp146 (5 μ M), 201φ2-1gp229 (3 μ M), EL188 (3 μ M) and KZ144 (3 μ M) dialyzed against PBS (pH 7.4) in the absence (A) and the presence of 0.5 mM EDTA (B). Bacterial reduction is determined in logarithmic units ($= \log_{10}(N_0/N_i)$ with N_0 = number of untreated cells; N_i = number of treated cells after incubation). Averages \pm standard deviations of three repeated, independent experiments are shown. Reduction values above 1 log unit are shaded in grey.

Antibacterial activity (in \log_{10} units)						
A		OBPgp279	201φ2-1gp229	PVP-SE1gp146	KZ144	EL188
<i>P. aeruginosa</i> PAO1		1.10 \pm 0.07	0.17 \pm 0.10	0.19 \pm 0.01	0.55 \pm 0.14	0.32 \pm 0.06
<i>P. aeruginosa</i> Br667		1.08 \pm 0.08	0.08 \pm 0.03	0.10 \pm 0.03	0.34 \pm 0.07	0.11 \pm 0.04
<i>E. coli</i> XL1-Blue MRF'		0.38 \pm 0.03	0.04 \pm 0.04	0.14 \pm 0.01	0.14 \pm 0.03	0.21 \pm 0.12
<i>S. Typhimurium</i> LT2		0.08 \pm 0.01	0.07 \pm 0.04	0.13 \pm 0.02	0.12 \pm 0.04	0.09 \pm 0.02
B		OBPgp279	201φ2-1gp229	PVP-SE1gp146	KZ144	EL188
	EDTA	EDTA	EDTA	EDTA	EDTA	EDTA
<i>P. aeruginosa</i> PAO1	0.58 \pm 0.02	4.36 \pm 0.29	3.25 \pm 0.10	3.68 \pm 0.13	3.05 \pm 0.11	3.30 \pm 0.12
<i>P. aeruginosa</i> Br667	0.03 \pm 0.02	3.14 \pm 0.22	0.17 \pm 0.20	0.12 \pm 0.02	0.88 \pm 0.04	0.75 \pm 0.12
<i>E. coli</i> XL1-Blue MRF'	0.29 \pm 0.11	1.18 \pm 0.20	0.58 \pm 0.25	0.34 \pm 0.02	0.45 \pm 0.13	0.59 \pm 0.17
<i>S. Typhimurium</i> LT2	0.05 \pm 0.05	0.77 \pm 0.05	0.26 \pm 0.02	0.14 \pm 0.21	0.33 \pm 0.14	0.24 \pm 0.15

To overcome the outer membrane barrier and increase the enzymatic efficiency of the endolysins, 0.5 mM EDTA was added (Table 6.3B). The addition of EDTA caused a significant increase of antibacterial activity for OBPgp279 on all four strains. This observation was more pronounced for *P. aeruginosa* PAO1 (3 additional log units) and *P. aeruginosa* Br667 (2 additional log units) than for *E. coli* XL1-Blue MRF' and *S. Typhimurium* LT2 (both 0.70 additional log units). Remarkably, only OBPgp279 was able to effectively reduce Br667 in presence of EDTA (3.14 log units), an observation which might correlate with the intrinsic antibacterial activity of OBPgp279 in the absence of EDTA. Both PVP-SE1gp146 and 201φ2-1gp229 could only efficiently reduce *P. aeruginosa* PAO1 when 0.5 mM EDTA was added.

6.4 Discussion

Modular endolysins of Gram-negative origin

Based on their structural and biochemical characteristics, OBPgp279, PVP-SE1gp146 and 201φ2-1gp229 are assumed to play an important role in the host lysis at the end of the phage replication cycle. *In silico*, these three endolysins share a modular structure with a peptidoglycan binding domain at the N-terminal side of the protein and a catalytic domain at the C-terminal side. The presence of the peptidoglycan binding domain was experimentally confirmed for all three endolysins. Even though they share the same general function and modular composition, OBPgp279, PVP-SE1gp146 and 201φ2-1gp229 are rather unrelated at the sequence level, except for a common repeated motif in their peptidoglycan binding domains. The unrelatedness of these endolysins emphasizes the relevance of the biochemical and antibacterial characterization of these enzymes in order to discover new and desirable traits for use as biocontrol tools.

We may question why some endolysins of Gram-negative infecting phages have a peptidoglycan binding domain contained within their structure. For Gram-positive infecting phages, the presence of a peptidoglycan binding domain is speculated to be necessary to keep the enzyme bound to the cell wall debris. In this way, surrounding bacteria (which are potential candidates for a new infection) remain protected from the hydrolyzing activity of newly released endolysin (Fischetti, 2010). In this respect, Loessner and coworkers (Loessner et al, 2002) demonstrated that the cell wall binding domains of *Listeria monocytogenes* phage endolysins Ply118 and Ply500 have a binding affinity ($3 - 6 \times 10^8 \text{ M}^{-1}$) for carbohydrate moieties in the cell wall comparable with the affinity of antibodies for bacterial cell surface antigens, during the secondary humoral immune response (Medina et al, 1997). Contrarily, Gram-negative bacteria possess an outer membrane surrounding their peptidoglycan layer, which eliminates the risk of premature lysis before a new infection can occur. Therefore; there is no need for a cell wall binding domain. Despite the fact that the binding affinities of the peptidoglycan binding domains of the Gram-negative phage endolysins KZ144 ($2.95 \times 10^7 \text{ M}^{-1}$) (Briers et al, 2009) and PVP-SE1gp146 ($1.26 \times 10^6 \text{ M}^{-1}$) are 10 to 100 times lower than these for the cell wall binding domains of Ply118 and Ply500, their affinity

constants are still relatively high and fall within the range of SH2 (Src Homology 2) domains and typical cell adhesion molecules (Larose et al, 1995).

Not only endolysins of phiKZ-related phages feature a modular composition (Briers et al, 2007b), but also members of other unrelated and smaller myoviruses as shown here for *S. Enteritidis* phage PVP-SE1 (“rV5-like virus”) and as described in literature for *P. aeruginosa* phage ϕ CTX (“P2-like virus”) (Nakayama et al, 1999) and *Burkholderia cepacia* phages Bcep781 and Bcep1 (“Bcep789-like viruses”) (Summer et al, 2006). The endolysins from phages ϕ CTX (gp12, two motifs = D-G-H-F-G-A-A-T and D-G-I-A-G-P-K-T), Bcep781 (gp27, motif = D-G-V-Y-G-S-Q-T) and Bcep1 (gp28, motif = D-G-V-Y-G-S-Q-T) also bear repeated motifs in their predicted peptidoglycan binding domains that match the consensus motif (D-G-(Pho)₂-G-X-X-T/C) proposed for the modular endolysins in this chapter. This conserved consensus motif could also help to predict peptidoglycan binding domains in other endolysins from Gram-negative origin.

Biochemical activity of modular endolysins

Based on their biochemical activity, OBPgp279 and PVP-SE1gp146 degrade the peptidoglycan layer of the tested Gram-negative species with the highest efficiencies compared to 201 ϕ 2-1gp229, EL188 and KZ144. In contrast to the catalytic transglycosylase specificity of KZ144 and EL188 (Briers et al, 2007b; Paradis-Bleau et al, 2007), OBPgp279, PVP-SE1gp146 and 201 ϕ 2-1gp229 presumably all have lysozyme-like activity. Despite the similar catalytic function, a large variation in muralytic activity values is observed for the individual catalytic domains of OBPgp279 and 201 ϕ 2-1gp229, due to differences in the primary protein structure. This variation only partially explains the large differences in muralytic activity values of the full length endolysins, since the peptidoglycan part also affects the muralytic activity in a protein specific manner.

Previously, Briers and co-workers revealed the insensitivity of Gram-positive bacteria for the muralytic action of modular endolysins KZ144 and EL188 (Briers et al, 2007b). This was conferred for OBPgp279, PVP-SE1gp146 and 201 ϕ 2-1gp229 which leave the Gram-positive bacteria *S. aureus* subsp. *aureus* Rosenbach ATCC 6538, *M. lysodeikticus* ATCC 4698, *L. lactis* subsp. *lactis* and *B. subtilis* PSB3 unharmed. An explanation must be found in the structure

of their peptidoglycan layer. Sensitive Gram-negative species share a common A1 γ chemotype of peptidoglycan with a direct peptide bond between adjacent muropeptides, whereas insensitive *S. aureus*, *M. lysodeikticus* and *L. lactis* have a peptidoglycan of the A3 α , A2 α and A4 α chemotype, respectively (Courtin et al, 2006; Schleifer & Kandler, 1972). These last 3 chemotypes show resistance to other muralytic enzymes due to the absence of a direct inter-peptide cross-link (Archibald et al, 1993). *B. subtilis*, however, possesses the A1 γ chemotype of its Gram-negative counterparts but 17.3 % of the glucosamine sugars in its peptidoglycan are N-deacetylated (Atrih et al, 1999). This species-specific modification explains for the resistance against peptidoglycan lytic enzymes, as was previously shown for HEWL (Archibald et al, 1993). Therefore, a direct cross-linked A1 γ chemotype of peptidoglycan without substantial N-deacetylation is an essential prerequisite for efficient hydrolysis by endolysins from Gram-negative infecting phages.

Activity of PVP-SE1gp146 after heat treatment

An unexpected result is the capacity of endolysin PVP-SE1gp146 to remain active after treatment at temperatures up to 100°C, as most endolysins are not known to be stable at such high temperatures. Either an unusual high unfolding temperature (thermostability) or a low rate of irreversible denaturation of the unfolded state (thermoresistance) could explain the observed stability. To discriminate between a thermostable or thermo-resistant enzyme, both the unfolding temperature and the secondary structure after refolding, should be investigated by differential scanning calorimetry (DSC) and by circular dichroism (CD), respectively. The presence of stabilizing intramolecular disulfide bridges between two of the three cysteines in PVP-SE1gp146 might explain the remarkable activity upon heating. To our knowledge, PVP-SE1gp146 is the first Gram-negative phage derived endolysin described so far to be active after being heated to such high temperatures. The C-terminal catalytic domain of the structural lysin gp36 of *P. aeruginosa* phage ϕ KMV (KMV36C) was previously shown to be thermo-resistant (Briers et al, 2006; Lavigne et al, 2004). Heat-inactivated, unfolded KMV36C has the capacity to refold into its (partially) active form after cooling and therefore retains part of its enzymatic activity. Recently, the thermo-resistance mechanism was suggested by Schmelcher and coworkers to explain the high kinetic stability of Gram-positive *Listeria monocytogenes* phage endolysins HPL118 and HPL511 (Schmelcher et al, 2012c). In their study, HPL118 and HPL511 retained 35 % of activity after 30 min incubation

at 90°C. The authors prove that the unfolding of HPL118 and HPL511 at higher temperatures is followed by a rapid refolding upon cooling. This proposed refolding mechanism may preserve the enzyme activity and could also explain the observed data for PVP-SE1gp146. From this perspective, PVP-SE1gp146 could be an interesting candidate as antibacterial component in a hurdle approach for food preservation, in addition to other antibacterial additives like bacteriocin and nisin (Galvez et al, 2007). Because of the retained activity of PVP-SE1gp146 upon heating, the use of chemical preservatives and the intensity of heat treatments could be reduced in such a way that quality foods of higher nutritional value are obtained.

Potential use of OBPgp279 as an enzybiotic

Despite the presence of an outer membrane which shields the peptidoglycan layer from the externally added endolysin, OBPgp279 is capable to reduce both *P. aeruginosa* PAO1 and the multidrug-resistant *P. aeruginosa* Br667, in contrast to PVP-SE1gp146, 201φ2-1gp229, KZ144 and EL188. Therefore, OBPgp279 is a potential candidate for the use as enzybiotic to control multidrug-resistant opportunistic *Pseudomonas* infections in human and animals. In addition to its high muralytic activity, we suggest that OBPgp279 intrinsically destabilizes the outer membrane in the *Pseudomonas* cell wall. This intrinsic activity helps the endolysin in reaching its enzymatic target which could explain the observed reductions. A similar characteristic was suggested for the *Bacillus amyloliquefaciens* phage IAM1521 endolysin *Lys1521* (Morita et al, 2001). In the case of this endolysin, the presence of positively charged amino acids in the C-terminal cell wall binding part that interact with the outer membrane, determined the antibacterial property of the endolysin (Orito et al, 2004). For OBPgp279, a similar mechanism is unlikely to induce the proposed outer membrane destabilization since its C-terminal end does not contain more positively charged amino acids than the inactive PVP-SE1gp146 and 201φ2-1gp229 endolysins. Furthermore, no obvious amphipathic helices which may intercalate into the outer membrane structure resulting in permeabilization (Sato & Feix, 2006) were detected at the N- and C-terminal ends of OBPgp279. Further structural analysis of the interaction between OBPgp279 and the *Pseudomonas* cell wall will be necessary to reveal the mechanism and determinants responsible for the observed *Pseudomonas* sensitivity.

Single-domain versus modular

Unlike the single-domain endolysins from a Gram-negative background, characterized in the previous chapter, the modular endolysins tested here possess a cell wall binding domain, more specifically a peptidoglycan binding domain, in their secondary structure. Modular endolysins are assumed to exert a higher enzymatic activity than non-modular or single-domain ones due to the presence of this additional peptidoglycan binding domain. This domain probably diminishes the distance between the active site and the targeted bond keeping the enzyme in close proximity of the peptidoglycan substrate. The assumption that modular endolysins are more active than single-domain ones is illustrated here: the specific muralytic activity of the modular endolysins OBPgp279, PVP-SE1gp146 and 201φ2-1gp229 is 18, 10 and 3 times higher compared to the value for PsP3gp10, the single-domain endolysin with the highest specific muralytic activity in Chapter 5. The presence of a peptidoglycan binding domain at least partly explains this significant difference as this domain was shown to increase the total enzymatic activity of OBPgp279 and 201φ2-1gp229 with 38 and 56 %, respectively. For an unknown reason, some Gram-negative infecting phages possess strong and fast-acting modular endolysins instead of less active, single-domain ones.

The impact of a N-terminal cell wall binding domain on muralytic activity also seems to be translated to the antibacterial potential of OBPgp279. The antibacterial activity of this endolysin on *P. aeruginosa* PAO1 and *E. coli* XL1-Blue MRF' in the presence of EDTA is 1 and 0.8 log units higher than the single-domain endolysin PsP3gp10. Unlike the single-domain endolysins, OBPgp279 also possess a strong antibacterial activity on the multidrug-resistant *P. aeruginosa* Br667 strain, inactivating this strain in the presence of EDTA with more than 3 log units reduction. This result hints at the applicability of this combination towards multidrug-resistant *P. aeruginosa* strains as alternative for antibiotic treatment. Activity towards this multidrug-resistant strain was also reported for modular endolysin EL188 (Briers et al, 2011b), but could not be demonstrated here.

Through biochemical and antibacterial characterization of six novel, single-domain endolysins (Chapter 5) and three novel, modular endolysins (Chapter 6), we were able to make a broad comparison between single-domain and modular endolysins towards applicability as anti-Gram-negative compounds. The different results in activity between

these single-domain and modular endolysins emphasize that, besides the catalytic specificity (transglycosylase - amidase - lysozyme), also the structural composition (one domain – more than one domain) is a main determinant in the overall muralytic strength and anti-Gram-negative capacity of an endolysin. Because of their stronger enzymatic/antibacterial capacity and their broader host spectrum, modular endolyins with transglycosylase activity should be favored over single-domain ones for development into potential antibacterial compounds against Gram-negative pathogens. In this respect, the elucidation of the unique biochemical and antibacterial characteristics of the modular endolysins OBPgp279, PVP-SE1gp146 and 201φ2-1gp229 (modularity, active upon heat treatment, outer membrane-destabilizing activity) is a crucial first step in development of future antibacterial therapies based on modular Gram-negative endolysins.

N-terminal single and double fusion modifications of OBPgp279 and PVP-SE1gp146

7.1 Introduction

In general, endolysins are not capable of passing the Gram-negative outer membrane by themselves. In the past, the fusion of peptidoglycan hydrolytic enzymes, including HEWL and human lysozyme, to hydrophobic peptides or chemical moieties has proven to be a successful approach to help them passing this barrier (Arima et al, 1998; Ito et al, 1997). In this chapter, this fusion approach was applied on the endolysins with the highest antibacterial potential, OBPgp279 and PVP-SE1gp146. Both enzymes were N-terminally fused with a set of seven selected outer membrane-interacting peptides. The goal is to provide PVP-SE1gp146 with an intrinsic outer membrane destabilizing or permeabilizing activity and to strengthen the predicted outer membrane destabilizing activity of OBPgp279, enabling them to efficiently penetrate the outer membrane of diverse Gram-negative species and subsequently degrade the peptidoglycan layer. For this purpose, four antibacterial peptides (α_4 -helix, PP, Parasin1 and Lycotoxin1) were selected from the available literature fulfilling the following three criteria: (1) peptide efficiently reduces Gram-negative bacteria, (2) length of the peptide should be limited between 5 and 30 aa for practical reasons, and (3) peptide should have hydrophobic, polycationic or amphipathic properties to provide OBPgp279 and PVP-SE1gp146 with permeabilizing activity towards this goal (Table 7.1). Three other peptides were randomly designed to contain an excess of polycationic (PK) or hydrophobic residues (ArtiMW1), or to adopt an amphipathic α -helix conformation at the C-terminal end (ArtiMW2), as assessed by a helical wheel projection (Figure 7.1).

7.1.1 Hydrophobic peptides: pentapeptide and ArtiMW1 peptide

Hydrophobic compounds are able to intercalate into the lipid A acyl chain-phospholipid moieties of the outer membrane, leading to a reduced hydrophobic stacking and subsequent outer membrane destabilization (Nikaido, 2003). The Phe-Phe-Val-Ala-Pro pentapeptide (PP) and the self-designed peptide ArtiMW1 both contain a majority of hydrophobic amino acids.

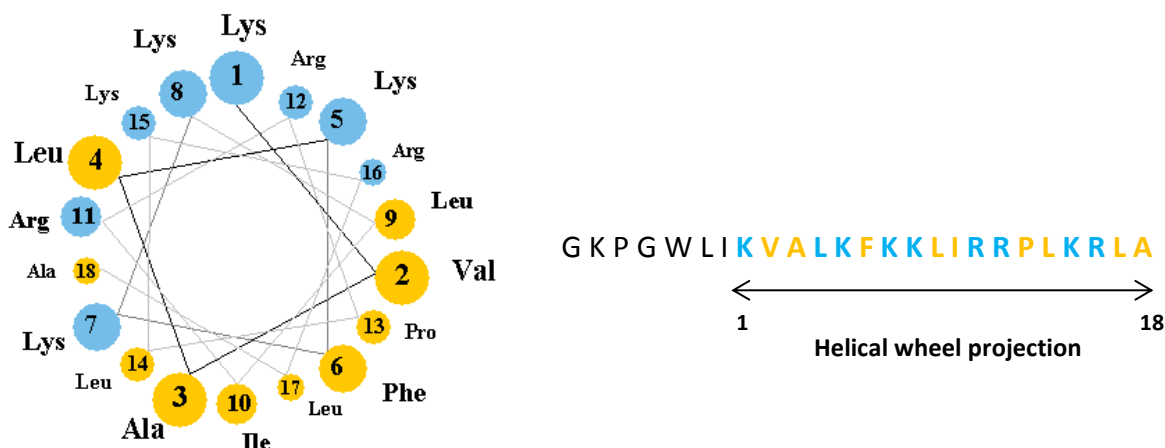


Figure 7.1: Helical wheel projection of C-terminal end of randomly designed ArtiMW2 peptide. yellow = hydrophobic, non-polar residues and blue = basic residues. Construction of helical wheel made with online tool (<http://cti.itc.virginia.edu/~cmg/Demo/wheel/wheelApp.html>).

Therefore, they are thought to increase hydrophobicity of endolysins OBPgp279 and PVP-SE1gp146 upon N-terminal fusion. Ibrahim and coworkers (1994) showed the ability of the Phe-Phe-Val-Ala-Pro pentapeptide to adopt a protruding β -strand conformation, that interacts with bacterial outer membranes. Furthermore, when this pentapeptide was C-terminally fused to HEWL, the number of viable *E. coli* cells was reduced with 85 %. The 18 amino acids long ArtiMW1 peptide (GGFIPAVILPSIAFLIVP, hydrophobic residues are underlined) is designed to be highly hydrophobic (88 %).

Table 7.1: List of selected or developed antibacterial peptides used for fusion modifications of OBPgp279 and PVP-SE1gp146. For each peptide, the amino acid sequence, literature reference and physicochemical properties are depicted here. Peptides marked with an asterisk (*) are randomly designed. Hydrophobic residues are underlined in the amino acid sequences, whereas cationic residues are in bold.

Peptide	Physicochemical property	Amino acid sequence	Reference
PK*	Polycationic	KRKKRKKRK	Patent WO/2010/149792
α_4 -helix of T4 lysozyme	Amphipathic	<u>P</u> N <u>R</u> A <u>K</u> <u>R</u> <u>V</u> <u>I</u> <u>T</u> <u>T</u> <u>F</u> <u>R</u> <u>T</u>	Matthews & Remington (1974)
Pentapeptide (PP)	Hydrophobic	<u>FFVAP</u>	Ibrahim et al (1994)
ArtiMW1*	Hydrophobic	<u>GGFIPAVILPSIAFLIVP</u>	Walmagh, unpublished
ArtiMW2*	Amphipathic	G K <u>P</u> <u>G</u> <u>W</u> <u>L</u> <u>I</u> K <u>V</u> <u>A</u> <u>L</u> <u>K</u> <u>F</u> <u>K</u> <u>K</u> <u>L</u> <u>I</u> <u>R</u> <u>R</u> <u>P</u> <u>L</u> <u>K</u> <u>R</u> <u>L</u> <u>A</u>	Walmagh, unpublished
Parasin1	Amphipathic	K <u>G</u> <u>R</u> <u>G</u> <u>K</u> <u>Q</u> <u>G</u> <u>G</u> <u>K</u> <u>V</u> <u>R</u> <u>A</u> <u>K</u> <u>A</u> <u>K</u> <u>T</u> <u>R</u> <u>S</u> <u>S</u>	Park et al (1998)
Lycotoxin1	Amphipathic	<u>I</u> <u>W</u> <u>L</u> <u>T</u> <u>A</u> <u>L</u> <u>K</u> <u>F</u> <u>L</u> <u>G</u> <u>K</u> <u>H</u> <u>A</u> <u>A</u> <u>K</u> <u>K</u> <u>L</u> <u>A</u> <u>K</u> <u>Q</u> <u>Q</u> <u>L</u> <u>S</u> <u>K</u> <u>L</u>	Yan & Adams (1998)

7.1.2 Polycationic peptide: PK peptide

Polycationic agents (like polymyxin B or poly-L-lysine) induce outer membrane permeabilization by displacement of the stabilizing divalent Ca^{2+} and Mg^{2+} cations and subsequent formation of local cracks in the outer membrane through which the polycationic agent is taken up (“self-promoted uptake mechanism”) (see 1.4.2.1 *Membrane perturbing action*) (Hancock et al, 1991; Vaara & Vaara, 1981). To simulate their action, we opted to design a 9-mer polycationic peptide, abbreviated as PK peptide, composed of alternating arginine (CGC/CGT) and lysine (AAG/AAA) residues (Lys-Arg-Lys-Lys-Arg-Lys-Lys-Arg-Lys). The choice for an alternating composition was based on the possible risk for tRNA depletion and frameshifts (in case of AAG, CGC and CGT) during transcription/translation of the PK-fused enzymes, when only lysine or arginine residues were used.

7.1.3 Combining the best of both: amphipathic peptides

Amphipathic peptides are known to rapidly permeabilize both the Gram-negative outer membrane and the cytoplasmic membrane (see 1.4.2.1 *Membrane perturbing action*) (Oren & Shai, 1998). The α_4 , ArtiMW2, Parasin1 and Lycotoxin1 peptides are all linear, amphipathic peptides adopting an α -helical structure with one side of the helix covered by positively charged residues and the opposite side by hydrophobic residues. The synthetic 13-mer α_4 -peptide that corresponds with the α_4 -helix of T4 lysozyme (aa 143-155) is highly active on different biological membranes, including bacterial, fungal and plant cell membranes (During et al, 1999). Based on its helical wheel projection (Figure 7.1), ArtiMW2, a designed amphipathic peptide, forms an α -helix with amino acids 5 to 25. Lycotoxin1, an antibacterial peptide isolated from the venom of the wolf spider *Lycosa carolinensis*, was shown to reduce the ion and voltage gradients across liposomal membranes, indicating a pore-forming activity (Yan & Adams, 1998). In addition to its bactericidal activity, Lycotoxin1 also demonstrates a strong hemolytic activity. A shortened Lycotoxin1-analogue (aa 1 to 15) was revealed to lack the hemolytic activity of the full length peptide (Adao et al, 2008). Parasin1 is secreted by the catfish *Parasilurus asotus* in response to epidermal injury (Park et al, 1998). It shows strong activity towards bacterial outer and inner membranes, but lacks toxicity on mammalian membranes as assessed by a hemolytic assay. The α -helical part in

Parasin1 is located between residues 9 and 17, flanked by two random coil regions (residues 1-8 and 18-19) in helix-promoting environments. The basic lysine residue at the N-terminal end of Parasin1 appears to be essential for its membrane binding activity: deletion of this residue resulted in poor membrane-binding and permeabilizing activities (Koo et al, 2008).

7.2 Cloning, expression and purification of N-terminally fused OBPgp279 and PVP-SE1gp146 variants

Two different cloning techniques were selected for recombinant fusion engineering of OBPgp279 (ORF279) and PVP-SE1gp146 (ORF146):

1. A variant of the Ligation Independent Cloning technique (LIC) (Haun et al, 1992), optimized for usage with the commercial available pEXP5CT-TOPO[®] vector, was used for N-terminal fusion of the α_4 -, ArtMW1-, ArtMW2-, Lycotoxin1- and Parasin1-encoding cassettes to ORF279 and ORF146 (Figure 7.2). The blunt end-cutting Ecl136II restriction enzyme and the flanking glycine (G) and serine (S) residues were chosen for compatibility reasons.
2. PP and PK peptides were introduced N-terminally of ORF279 and ORF146 by a tail PCR with extended 5' primers to which a fragment encoding five (Phe-Phe-Val-Ala-Pro), in case of PP, or nine (Lys-Arg-Lys-Lys-Arg-Lys-Lys-Arg-Lys), in case of PK, residues is added.

All fusion variants of OBPgp279 and PVP-SE1gp146 were expressed in a *E. coli* cell-based expression system and purified by Ni²⁺-NTA chromatography using the C-terminal His₆-tag. This tag was fused to each ORF upon ligation in pEXP5CT-TOPO[®] expression vector. The soluble expression level of each fusion protein was optimized by changing temperature (16°C or 37°C), inducer concentration (0.1 mM or 1 mM) or expression strain (BL21(DE3)pLysS, BL21-CodonPlus-(DE3)-RP or BL21-CodonPlus-(DE3)-RIL (Table 3.2). Purification stringency was optimized to assure maximal protein purity by varying the imidazole concentration (50-80 mM). Optimal expression yields, in mg of recombinant protein per liter expression culture, for all fusion proteins are summarized in Table 7.2. Remarkably, the production of both PK-OBPgp279 and PK-PVP-SE1gp146 resulted in a much

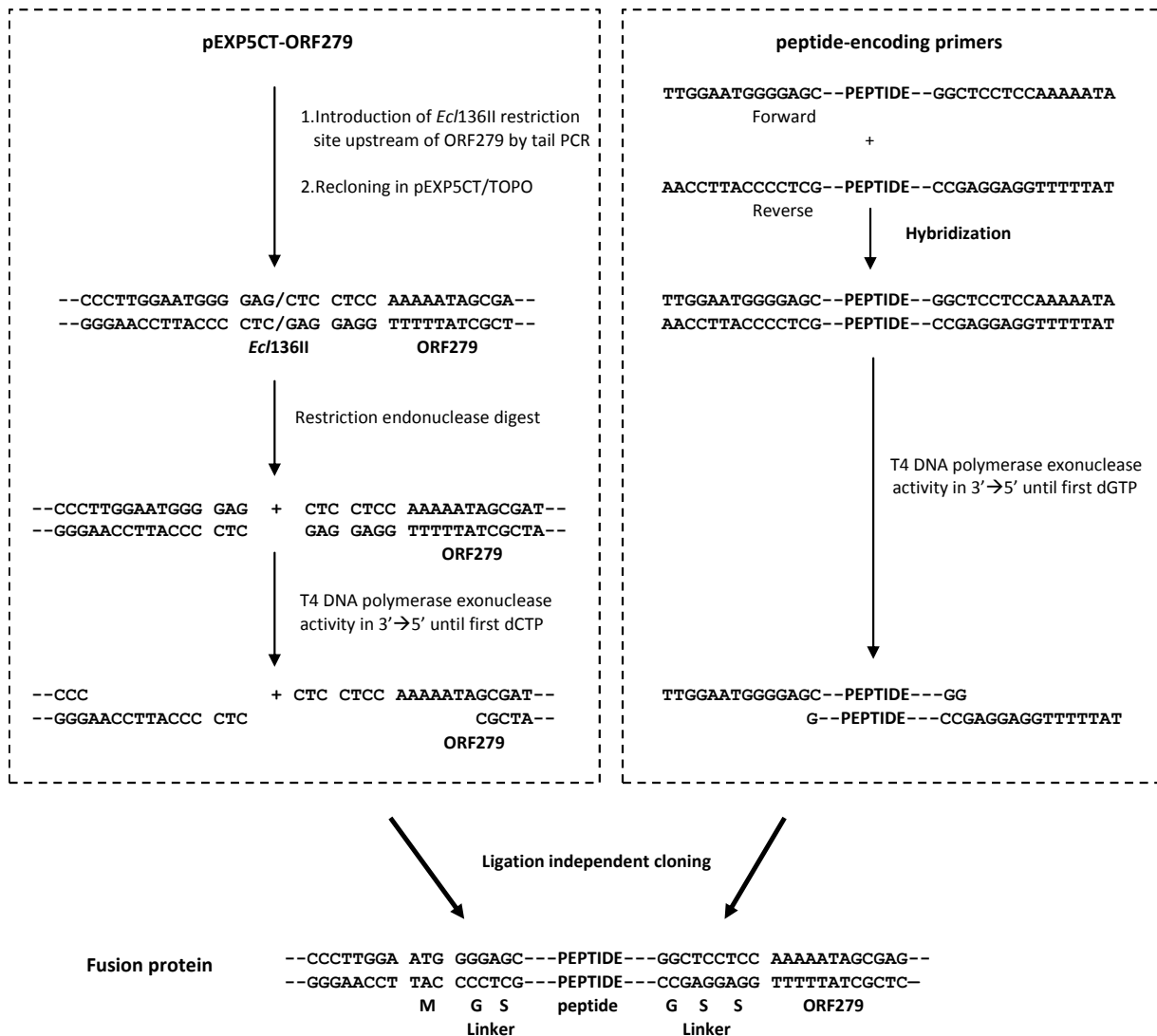


Figure 7.2: Variant of ligation independent cloning (LIC) technique for construction of fusion modified OBPgp279 variants. First, a 6-nucleotide *Ecl136II* restriction site was introduced downstream of ORF279 by a tail PCR (with a *Ecl136II* restriction site in the 5' tail primer). This tail PCR fragment was ligated (TA-ligation) into a pEXP5CT-TOPO® vector and the obtained pEXP5CT-*Ecl136II*-OBPgp279 plasmid was linearized with *Ecl136II* restriction enzyme. To create 3' LIC compatible overhanging ends, nucleotides in 3'→5' direction of the linearized plasmid are removed by incubation with T4 polymerase and dCTP. The exonuclease activity of the T4 polymerase stops at the first dCTP present in the sequence. Two complementary oligonucleotides encoding the fusion peptide with extra 5' and 3' LIC-compatible regions are hybridized. LIC-compatible overhanging ends are introduced at the 3' sides of the obtained peptide cassette in a similar way as for the linearized vector, by incubation with T4 polymerase (3'→5' exonuclease activity) and dGTP. Incubation of these vector and peptide cassette fragments for 20 min at room temperature closes the vector without the necessity of ligase.

larger protein yield than the corresponding unmodified endolysins with almost a double amount of recombinant protein. The PK peptide fusion seems to enhance the cellular transcription/translation processes of both endolysins, resulting in higher proteins yields.

Table 7.2: Protein expression yields for N-terminal OBPgp279 and PVP-SE1gp146 fusion proteins. The total yield for each fusion protein is shown as the amount of purified recombinant protein, in mg, per liter *E. coli* expression culture. This yield value is quantified spectrophotometrically at 260 nm wavelength. Arrows indicate the increase (↑) or decrease (↓) in yield compared to the unmodified endolysin.

	Yield (in mg/l)	
	OBPgp279	PVP-SE1gp146
Unmodified	3.7	38.2
PK	7.7 ↑	65.2 ↑
α₄	1.3 ↓	1.5 ↓
PP	2.5 ↓	4.3 ↓
ArtiMW1	0.3 ↓	5.1 ↓
ArtiMW2	2.9 ↓	3.2 ↓
Parasin1	0.4 ↓	2.4 ↓
Lycotoxin1	1.7 ↓	1.7 ↓

Recombinant expression of all other fusion proteins resulted in significant lower protein yields, possibly due to the toxic interaction of the hydrophobic/amphipathic peptide with the cytoplasmic membrane of the *E. coli* strain during expression. If this is the case, the fusion of a protecting group to the enzyme that prevents the fused peptide from interacting with the *E. coli* membrane might offer a solution. Variation in expression time, temperature and strain did not improve the yield. Remarkably, all fusion variants of PVP-SE1gp146 form multimers (di- and trimerization), similar to unmodified PVP-SE1gp146. This multimerization was caused by formation of disulfide bonds in the protein, as these multimers disappear after reduction with β-mercapto-ethanol.

7.3 *In vitro* antibacterial activity of N-terminal OBPgp279 and PVP-SE1gp146 fusion variants

To assess antibacterial activity and activity spectrum of the purified fusion variants, exponential growing *P. aeruginosa* PAO1, *S. Typhimurium* LT2 and *E. coli* XL1-Blue MRF' were incubated at a cell density of 10⁶ CFU/ml with unmodified OBPgp279/PVP-SE1gp146 and their fusion variants at room temperature for 30 min. Concentrations of 1.5 and 5 μM were used for OBPgp279 and PVP-SE1gp146 variants, respectively. Residual colonies were counted after an overnight incubation at 37°C (Table 7.3).

Table 7.3: Antibacterial activity of the N-terminal fusion variants of OBPgp279 and PVP-SE1gp146 without (A and B) and with (C and D) outer membrane permeabilizer EDTA (0.5 mM) on Gram-negative bacteria compared to the unmodified endolysins. Exponential growing cells (10^6 CFU/ml) were incubated with 1.5 μ M (OBPgp279 variants) and 5 μ M (PVP-SE1gp146 variants) of undialyzed proteins. Antibacterial activity was quantified as the relative inactivation in logarithmic units ($= \log_{10}(N_0/N_i)$) with N_0 = number of untreated cells and N_i = number of treated cells counted after incubation). All samples were replicated in threefold. Averages +/- standard deviations are given. Significant higher values than unmodified endolysin = \uparrow , significantly lower = \downarrow , no difference = --- (two-tailed t-test, $P < 0.05$).

A OBPgp279				B PVP-SE1gp146			
Fusion	<i>P. aeruginosa</i> PAO1	<i>E. coli</i> XL1-Blue MRF'	<i>S. Typhimurium</i> LT2	Fusion	<i>P. aeruginosa</i> PAO1	<i>E. coli</i> XL1-Blue MRF'	<i>S. Typhimurium</i> LT2
Unmodified	1.10 ± 0.07	0.38 ± 0.03	0.08 ± 0.04	Unmodified	0.19 ± 0.01	0.14 ± 0.04	0.13 ± 0.02
PK	2.61 ± 0.09 \uparrow	0.63 ± 0.02 \uparrow	0.23 ± 0.03 \uparrow	PK	1.56 ± 0.10 \uparrow	0.69 ± 0.09 \uparrow	0.30 ± 0.10 \uparrow
α_4	0.92 ± 0.09 ---	0.07 ± 0.14 \downarrow	0.17 ± 0.08 ---	α_4	1.26 ± 0.12 \uparrow	0.42 ± 0.21 ---	0.14 ± 0.12 ---
PP	0.64 ± 0.05 \downarrow	0.06 ± 0.17 \downarrow	0.09 ± 0.01 ---	PP	1.16 ± 0.17 \uparrow	0.26 ± 0.09 ---	0.24 ± 0.16 ---
ArtiMW1	0.42 ± 0.12 \downarrow	0.33 ± 0.08 ---	0.15 ± 0.07 ---	ArtiMW1	1.26 ± 0.07 \uparrow	0.20 ± 0.05 ---	0.10 ± 0.07 ---
ArtiMW2	0.45 ± 0.01 \downarrow	0.16 ± 0.12 \downarrow	0.12 ± 0.06 ---	ArtiMW2	0.63 ± 0.11 \uparrow	0.10 ± 0.09 ---	0.12 ± 0.12 ---
Lycotoxin1	0.60 ± 0.24 \downarrow	0.01 ± 0.08 \downarrow	0.01 ± 0.11 ---	Lycotoxin1	1.00 ± 0.24 \uparrow	0.59 ± 0.39 ---	0.20 ± 0.22 ---
Parasin1	0.59 ± 0.08 \downarrow	0.05 ± 0.15 \downarrow	0.20 ± 0.14 ---	Parasin1	0.52 ± 0.12 \uparrow	0.49 ± 0.15 \uparrow	0.04 ± 0.03 \downarrow

C OBPgp279/EDTA				D PVP-SE1gp146/EDTA			
Fusion	<i>P. aeruginosa</i> PAO1	<i>E. coli</i> XL1-Blue MRF'	<i>S. Typhimurium</i> LT2	Fusion	<i>P. aeruginosa</i> PAO1	<i>E. coli</i> XL1-Blue MRF'	<i>S. Typhimurium</i> LT2
EDTA	0.58 ± 0.02	0.29 ± 0.11	0.05 ± 0.05	EDTA	0.58 ± 0.02	0.29 ± 0.11	0.05 ± 0.05
Unmodified	4.36 ± 0.28	1.18 ± 0.20	0.77 ± 0.05	Unmodified	3.68 ± 0.13	0.34 ± 0.02	0.14 ± 0.21
PK	5.38 ± 0.19 \uparrow	1.70 ± 0.05 \uparrow	0.91 ± 0.04 \uparrow	PK	4.92 ± 0.23 \uparrow	0.85 ± 0.17 \uparrow	0.73 ± 0.30 \uparrow
α_4	2.28 ± 0.50 \downarrow	0.93 ± 0.15 ---	0.43 ± 0.09 \downarrow	α_4	4.22 ± 0.30 \uparrow	0.85 ± 0.17 \uparrow	0.47 ± 0.24 ---
PP	2.83 ± 0.36 \downarrow	1.34 ± 0.04 ---	0.52 ± 0.04 \downarrow	PP	3.69 ± 0.11 ---	0.54 ± 0.10 \uparrow	0.47 ± 0.07 \uparrow
ArtiMW1	2.15 ± 0.21 \downarrow	0.55 ± 0.07 \downarrow	0.41 ± 0.08 \downarrow	ArtiMW1	3.95 ± 0.09 \uparrow	0.36 ± 0.11 ---	0.27 ± 0.15 ---
ArtiMW2	2.38 ± 0.09 \downarrow	1.20 ± 0.17 ---	0.36 ± 0.07 \downarrow	ArtiMW2	3.99 ± 0.17 ---	0.16 ± 0.10 \downarrow	0.41 ± 0.25 ---
Lycotoxin1	2.71 ± 0.13 \downarrow	1.37 ± 0.14 ---	0.51 ± 0.04 \downarrow	Lycotoxin1	3.79 ± 0.07 ---	0.34 ± 0.15 ---	0.87 ± 0.28 \uparrow
Parasin1	1.95 ± 0.19 \downarrow	1.12 ± 0.13 ---	0.60 ± 0.05 \downarrow	Parasin1	3.85 ± 0.08 ---	0.69 ± 0.24 ---	0.59 ± 0.38 ---

As already observed in Chapter 6, *P. aeruginosa* PAO1 showed sensitivity for the unmodified OBPgp279 (1.10 ± 0.07 log units reduction) (Table 7.3A). On the other tested strains and in case of unmodified PVP-SE1gp146 (Table 7.3B) no significant reduction was present due to the impermeability of the outer membrane structure for unmodified endolysins. Of all fusions, the strongest antibacterial activity was achieved with the PK peptide. Especially for *P. aeruginosa* PAO1, the fusion of this peptide to both OBPgp279 and PVP-SE1gp146 significantly (two-tailed *t*-test, $P < 0.05$) increased their antibacterial activities with 1.51 and 1.07 log units reduction, respectively, compared to the unmodified endolysins. On *S. Typhimurium* LT2 and *E. coli* XL1-Blue MRF', this positive effect of the PK peptide fusion on the inactivation level was less pronounced, as compared to the unmodified endolysin. The PK-OBPgp279 fusion protein tended to be more antibacterially active against *P. aeruginosa* PAO1 than the PK-PVP-SE1gp146 fusion peptide. This observation is probably related to the intrinsic activity of the unmodified OBPgp279. Similar to the PK peptide, but in lesser extent, also all other PVP-SE1gp146 fusion variants were able to inactivate *P. aeruginosa* PAO1 with a peptide-dependent significant increase of minimal 0.33 (for Parasin1 peptide) to maximal 1.07 (for α_4 and ArtMW1 peptides) log units. This was not the case for the OBPgp279 fusion variants: all other fusions than the PK peptide significantly reduced, or equalized the antibacterial activity of the original, unmodified endolysin on all three strains. Except for the PK peptide, N-terminal fusion of these peptides seem to inhibit the intrinsic antibacterial activity of OBPgp279, possibly by steric hindrance or blocking of the N-terminal end. This observation suggests that the intrinsic activity might be located in the N-terminal end of the endolysin. In case of the PK peptide, this possible blocking effect could be overcome by the stronger activity of this peptide on the negatively charged outer membrane of *P. aeruginosa*.

To boost the antibacterial potential of the above fusion proteins, small amounts of the outer membrane permeabilizer EDTA (0.5 mM final concentration) were added to the buffer conditions. In a similar way as without EDTA, the antibacterial activity caused by these fusion proteins/EDTA mixtures were determined on three Gram-negative strains (Table 7.3C-D). In all cases, the reduction with EDTA was higher than without. Depending on the peptide fusion, endolysin or bacterial strain used, synergistic, additive or antagonistic effects were observed in antibacterial activity between the fusion protein and EDTA. The same conclusions as without EDTA could be made for the fusion peptides/EDTA combination.

Again, the fusion with the PK peptide was by far the strongest antibacterial fusion on all three Gram-negative strains, with a rise of 1.02 and 1.24 log units in reduction level for PK-OBPgp279 (to a maximal reduction of 5.38 ± 0.19 log units) and PK-PVP-SE1gp146 (to a maximal reduction of 4.92 ± 0.23 log units), respectively, compared to the unmodified endolysin/EDTA combination. Also in the presence of EDTA, the OBPgp279 fusion variants other than the PK peptide were less active than the unmodified OBPgp279. Some other peptide fusions to PVP-SE1gp146 significantly improve activity of unmodified PVP-SE1gp146 on *E. coli* and *Salmonella* in the presence of EDTA, but in lesser extent than the PK peptide.

Since the most promising results were obtained for the PK peptide fusion, we choose this fusion for further optimization screens. In a second part of this chapter, we tried to engineer an endolysin with a double N-terminal fusion comprising the PK peptide fusion and a second antibacterial peptide selected from the six other peptides (α_4 , PP, ArtiMW1, ArtiMW2, Lycotoxin1 and Parasin1).

7.4 Cloning, expression and purification of N-terminal double fusion variants of OBPgp279 and PVP-SE1gp146

The same two cloning methodologies as for the engineering of the single fusion variants (*see 7.2 Cloning, expression and purification of N-terminally fused OBPgp279 and PVP-SE1gp146 variants*), were used to construct the double fusions variants of OBPgp279 and PVP-SE1gp146. Two possibilities for the orientation of the two peptides in the N-terminal double fusion variant are tested: a double fusion consisting of an N-terminal PK peptide, followed by a second peptide; or a double fusion composed of the peptides in the reverse order. All double fusion variants of OBPgp279 and PVP-SE1gp146 created in this study are depicted in Table 7.4.

All double fusion variants of OBPgp279 and PVP-SE1gp146 were expressed in *E. coli* BL21-CodonPlus-(DE3)-RIL cells upon induction with 1 mM IPTG. Their C-terminal His₆ tag was used for downstream purification using Ni²⁺-NTA chromatography. The obtained expression yields of all constructs in mg recombinant purified protein per liter expression culture are listed in Table 7.5.

Table 7.4: Overview of all N-terminal double fusion variants of OBPgp279 and PVP-SE1gp146 constructed in this study with corresponding cloning methodology. To construct a double fusion with the PK peptide in front of the second antibacterial peptide (AP), a tail PCR with extended 5' primer encoding the PK peptide cassette was performed on the available pEXP5CT-AP-OBPgp279 vector. To obtain the reverse peptide orientation, with the AP in front, the LIC method described previously was applied on the pEXP5CT/PK-OBPgp279 and pEXP5CT/PK-PVP-SE1gp146 vectors. AP = antibacterial peptide, PK = PK peptide.

Orientation	Cloning methodology	Constructs
	Tail PCR	PK-PP-OBPgp279 PK- α_4 -OBPgp279
	LIC method on pEXP5CT/PK-OBPgp279 and pEXP5CT/PK-PVP-SE1gp146 vectors	α_4 -PK-OBPgp279 α_4 -PK-PVP-SE1gp146 PP-PK-OBPgp279 ArtiMW1-PK-OBPgp279 ArtiMW1-PK-PVP-SE1gp146 ArtiMW2-PK-OBPgp279 ArtiMW2-PK-PVP-SE1gp146 Lycotoxin1-PK-OBPgp279 Lycotoxin1-Pk-PVP-SE1gp146 Parasin1-PK-OBPgp279 Parasin1-PK-PVP-SE1gp146

Table 7.5: Protein expression yields for N-terminal double fusion variants of OBPgp279 and PVP-SE1gp146. The total yield for each fusion protein is shown as the amount of purified recombinant protein, in mg, per liter *E. coli* expression culture. This yield value is quantified spectrophotometrically at 280 nm wavelength. ND = not determined. Arrows indicate the increase (\uparrow) or decrease (\downarrow) in yield compared to the single PK-modified endolysin.

	Yield (in mg/l)	
	OBPgp279	PVP-SE1gp146
PK	7.7	65.2
α_4 -PK	0.6 \downarrow	0.3 \downarrow
PK- α_4	7.6 =	ND
PP-PK	2.8 \downarrow	ND
PK-PP	45.1 \uparrow	ND
ArtiMW1-PK	0.8 \downarrow	1.3 \downarrow
ArtiMW2-PK	1.8 \downarrow	0.3 \downarrow
Parasin1-PK	0.2 \downarrow	4.9 \downarrow
Lycotoxin1-PK	8.1 =	1.2 \downarrow

Only in case of PK-PP-OBPgp279, the double fusion could further improve the expression yield of the single PK peptide fusion protein. For all other constructs, the obtained yield was similar (for PK- α_4 -OBPgp279 and Lycotoxin1-PK-OBPgp279) or substantially lower. To improve protein yield of both OBPgp279 and PVP-SE1gp146, an N-terminal single PK peptide fusion remains the best option. In conclusion for both single and double fusion constructs, the impact on the protein yield of an N-terminal fusion seems to be very peptide-specific.

7.5 *In vitro* antibacterial activity of N-terminal double fusion variants of OBPgp279 and PVP-SE1gp146

Exponential growing (10^6 CFU/ml) *P. aeruginosa* PAO1, *S. Typhimurium* LT2 and *E. coli* XL1-Blue MRF' were incubated with the purified N-terminal double fusion variants of OBPgp279 (1.5 μ M) and PVP-SE1gp146 (5 μ M) in the absence or in the presence of EDTA (0.5 mM) for 30 min at room temperature. The obtained reduction values are summarized in Table 7.6. Interestingly, an N-terminal fusion of the PP, ArtiMW1 and ArtiMW2 peptides to the single PK peptide fusion variant of OBPgp279 significantly (two-tailed *t*-test, $P < 0.05$) increased the inactivation of *E. coli* XL1-Blue MRF', compared to PK-OBPgp279, with 0.91, 1.03 and 1.25 log units reduction, respectively (Table 7.6A). This significant increase was also detected in the presence of EDTA, but less pronounced with maximal 0.5 log units reduction extra for the PP peptide (Table 7.6C). This result is remarkable, as the single fusion of these three peptides to OBPgp279 had no enhanced effect on antibacterial activity (Table 7.3). The fusion of a combination of the polycationic PK peptide with a second hydrophobic/amphipathic peptide to endolysin OBPgp279 seems a prerequisite for inactivation of *E. coli* XL1-Blue MRF'. Independent of EDTA addition, fusion of the same peptides to PK-PVP-SE1gp146 almost completely inactivated its antibacterial capacity on the *E. coli* strain, reflecting the endolysin dependency of the fusion strength (Table 7.6B). On *P. aeruginosa* PAO1 and *S. Typhimurium* LT2, the N-terminal fusion of a second antibacterial peptide to PK-OBPgp279 and PK-PVP-SE1gp146 could not improve their antibacterial activity. In case of *P. aeruginosa* PAO1, this extra fusion significantly inhibited the activity of both PK-OBPgp279 and PK-PVP-SE1gp146, with almost a complete inactivation by fusion with ArtiMW1 and Lycotoxin1, in case of PK-OBPgp279, and ArtiMW2, in case of PK-PVP-SE1gp146. With EDTA, this inactivation is still present, except for the α_4 -PK and PK- α_4 double peptide fusions to PK-OBPgp279. Possibly,

Table 7.6: Antibacterial activity of the N-terminal double fusion variants of OBPgp279 and PVP-SE1gp146 without (A and B) and with (C and D) EDTA on Gram-negative bacteria compared to the single PK-modified endolysins. Exponential growing cells (10^6 CFU/ml) were incubated with 1.5 μ M (OBPgp279 double variants) and 5 μ M (PVP-SE1gp146 double variants) of undialyzed proteins, with or without 0.5 mM EDTA. The antibacterial activity was quantified in logarithmic units reduction ($= \log_{10}(N_0/N_i)$ with N_0 = number of untreated cells and N_i = number of treated cells counted after incubation). All samples were replicated in threefold. Averages \pm standard deviations are given. Significant higher values than PK-modified endolysin = \uparrow , significantly lower = \downarrow , no difference = -- (two-tailed t-test, $P < 0.05$).

A				C			
OBPgp279				OBPgp279/EDTA			
Fusion	<i>P. aeruginosa</i> PAO1	<i>E. coli</i> XL1-Blue MRF'	<i>S. Typhimurium</i> LT2	Fusion	<i>P. aeruginosa</i> PAO1	<i>E. coli</i> XL1-Blue MRF'	<i>S. Typhimurium</i> LT2
PK	2.61 \pm 0.09	0.63 \pm 0.02	0.23 \pm 0.03	EDTA	0.58 \pm 0.02	0.29 \pm 0.11	0.05 \pm 0.05
α_4 -PK	0.59 \pm 0.02 \downarrow	0.55 \pm 0.06 ---	0.22 \pm 0.03 ---	PK	5.38 \pm 0.19	1.70 \pm 0.05	0.91 \pm 0.04
PK- α_4	1.10 \pm 0.05 \downarrow	0.54 \pm 0.17 ---	0.23 \pm 0.04 ---	α_4 -PK	5.07 \pm 0.03 \downarrow	0.98 \pm 0.13 \downarrow	0.35 \pm 0.11 \downarrow
PP-PK	0.94 \pm 0.04 \downarrow	1.34 \pm 0.12 \uparrow	0.11 \pm 0.02 \downarrow	PK- α_4	5.23 \pm 0.21 ---	0.86 \pm 0.12 \downarrow	0.29 \pm 0.06 \downarrow
PK-PP	0.95 \pm 0.08 \downarrow	1.69 \pm 0.17 \uparrow	0.22 \pm 0.06 ---	PP-PK	4.29 \pm 0.04 \downarrow	2.22 \pm 0.09 \uparrow	0.32 \pm 0.04 \downarrow
ArtiMW1-PK	0.20 \pm 0.09 \downarrow	1.46 \pm 0.08 \uparrow	0.12 \pm 0.03 \downarrow	PK-PP	4.00 \pm 0.06 \downarrow	2.12 \pm 0.13 \uparrow	0.42 \pm 0.05 \downarrow
ArtiMW2-PK	0.57 \pm 0.10 \downarrow	1.68 \pm 0.12 \uparrow	0.17 \pm 0.02 ---	ArtiMW1-PK	3.66 \pm 0.12 \downarrow	1.94 \pm 0.07 \uparrow	0.17 \pm 0.07 \downarrow
Lycotoxin1-PK	0.08 \pm 0.05 \downarrow	0.41 \pm 0.04 \downarrow	0.17 \pm 0.07 ---	ArtiMW2-PK	3.91 \pm 0.09 \downarrow	1.96 \pm 0.10 \uparrow	0.25 \pm 0.04 \downarrow
Parasin1-PK	0.75 \pm 0.03 \downarrow	0.70 \pm 0.09 ---	0.27 \pm 0.11 ---	Lycotoxin1-PK	3.73 \pm 0.27 \downarrow	0.90 \pm 0.24 \downarrow	0.29 \pm 0.06 \downarrow
B				D			
PVP-SE1gp146				PVP-SE1gp146/EDTA			
Fusion	<i>P. aeruginosa</i> PAO1	<i>E. coli</i> XL1-Blue MRF'	<i>S. Typhimurium</i> LT2	Fusion	<i>P. aeruginosa</i> PAO1	<i>E. coli</i> XL1-Blue MRF'	<i>S. Typhimurium</i> LT2
PK	1.56 \pm 0.10	0.69 \pm 0.09	0.30 \pm 0.10	EDTA	0.58 \pm 0.02	0.29 \pm 0.11	0.05 \pm 0.05
α_4 -PK	0.24 \pm 0.12 \downarrow	0.34 \pm 0.02 \downarrow	0.26 \pm 0.08 ---	PK	4.92 \pm 0.23	0.85 \pm 0.17	0.73 \pm 0.30
ArtiMW1-PK	0.17 \pm 0.04 \downarrow	0.11 \pm 0.03 \downarrow	0.12 \pm 0.10 ---	α_4 -PK	2.88 \pm 0.50 \downarrow	0.48 \pm 0.12 \downarrow	0.43 \pm 0.15 ---
ArtiMW2-PK	0.03 \pm 0.06 \downarrow	0.07 \pm 0.04 \downarrow	0.01 \pm 0.08 \downarrow	ArtiMW1-PK	2.26 \pm 0.16 \downarrow	0.52 \pm 0.09 \downarrow	0.49 \pm 0.24 ---
Lycotoxin1-PK	0.24 \pm 0.08 \downarrow	0.02 \pm 0.05 \downarrow	0.09 \pm 0.08 \downarrow	ArtiMW2-PK	2.04 \pm 0.36 \downarrow	0.90 \pm 0.11 ---	0.48 \pm 0.14 ---
Parasin1-PK	0.31 \pm 0.04 \downarrow	0.04 \pm 0.06 \downarrow	0.13 \pm 0.02 \downarrow	Lycotoxin1-PK	2.82 \pm 0.44 \downarrow	0.16 \pm 0.04 \downarrow	0.27 \pm 0.18 ---
				Parasin1-PK	3.00 \pm 0.45 \downarrow	0.19 \pm 0.09 \downarrow	0.47 \pm 0.24 ---

the second fusion prevents the fused PK peptide from efficiently interacting with the negatively charged phosphate moieties of the *P. aeruginosa* outer membrane.

To analyze the potential influence of the double fusion orientation on the antibacterial activity of the OBPgp279 fusion proteins, we compared the obtained reduction values in both possible orientations. This was specifically done for the PP and PK peptides, on one hand, and α_4 and PK peptides, on the other hand. Independent of the EDTA addition, no significant difference in antibacterial activity was observed between both orientations, except for the α_4 and PK double peptide fusion without EDTA on *P. aeruginosa* (Table 7.6A). In this case, the impact of a second α_4 peptide in between the PK peptide and OBPgp279 on activity appeared to be less negative than when the α_4 peptide is located in front, with a 0.51 log units difference in activity. Nonetheless, in both orientations, the antibacterial potential was significantly lower than the single PK peptide fusion variant.

7.6 Discussion

This chapter focuses on the possibility of enhancing the anti-Gram-negative activity of an externally added endolysin by N-terminal fusion with outer membrane permeabilizing peptides. In literature, there are many studies on the fusion of peptidoglycan hydrolytic enzymes, like HEWL or human lysozyme, with hydrophobic peptides or chemical moieties with the goal to alter membrane permeability (Arima et al, 1997; Ito et al, 1997). These studies specifically focus on non-phage peptidoglycan hydrolases. Here, we prove that this peptide fusion approach is also amenable to phage endolysins. In general, the success of this fusion approach to ameliorate the antibacterial capacity of endolysins is protein- and peptide-specific. The addition of 9 polycationic amino acids (KRKKRKKRK) to the N-terminal end of both OBPgp279 and PVP-SE1gp146, significantly improves their antibacterial potential against *P. aeruginosa* PAO1 (+ 1.3 to 1.5 log units), and in lesser extent against *E. coli* XL1-Blue MRF' (+ 0.25 to 0.45 log units) and *S. Typhimurium* LT2 (+ 0.15 to 0.17 log units). We hypothesize that these bacteria are inactivated by a combined action of local crack formation in the outer membrane by the PK peptide action, and subsequent peptidoglycan lysis after passage of the fusion protein through these (temporary) cracks in the outer

membrane. This hypothesis is in accordance with the self-promoted uptake mechanism proposed for polycationic agents by Hancock and coworkers (1993).

The fusion of other antibacterial peptides than the PK peptide turned out to be less successful to improve anti-Gram-negative activity. The specific outer membrane structure of each Gram-negative organism plays an important role in the effectiveness by which the peptide fusion approach is able to inactivate this organism. *P. aeruginosa* is known to have a stronger negatively charged LPS structure than *E. coli* and *Salmonella*, due to a higher phosphate content per LPS molecule (see 1.3.1.3 Lipid A) (Knirel et al, 2006; Nikaido, 2003). Disturbance of the divalent cation stabilization, the Achilles' heel of the outer membrane, through interaction with the PK-modified endolysin, is therefore more critical for *P. aeruginosa* LPS integrity, leading to a more effective inactivation (higher reduction values) compared to the *E. coli* and *Salmonella* outer membranes. In contrast to *P. aeruginosa*, the outer membranes of *E. coli* and *Salmonella* are more stabilized by the hydrophobic stacking of the multiple fatty acid chains in the lipid A moiety of the LPS (see 1.3.1.3 Lipid A). Therefore, we expected that by addition of amphipathic and hydrophobic components to both endolysins, the outer membrane integrity of *E. coli* and *Salmonella* could be efficiently tackled. In case of the single fusion of amphipathic/hydrophobic peptides, no improved activity against *E. coli* and *Salmonella* could be detected. However, the double fusion of the hydrophobic/amphipathic PP, ArtiMW1 and ArtiMW2 peptides to PK-modified OBPgp279 were able to reduce *E. coli* XL1-Blue MRF' with 1.34 ± 0.22 to 1.69 ± 0.17 log units, an effect which could be improved by EDTA addition to maximal 2.22 ± 0.09 log units (for PP-PK double fusion). Remarkably, this anti-*E. coli* activity is only present for the double fusions with the self-designed peptides, reflecting the importance of rational design in improving endolysin activity. Despite this promising result, we must be careful in our interpretation as this particular *E. coli* strain lacks part of the O-antigenic region in its LPS rendering it more sensitive for cell penetrating compounds. Therefore, other *E. coli* strains with intact LPS layer, including clinical strains, should be tested in the future on their sensitivity for these compounds.

None of the double fusions could enhance the antibacterial activity of OBPgp279 and PVP-SE1gp146 against *S. Typhimurium* LT2. These observations reflect the importance of a

species-specific fusion approach for efficient targeting and killing of certain Gram-negative bacteria. A more species-specific approach will be necessary to overcome the *Salmonella* outer membrane. Possible optimizing strategies comprise using higher amounts of fusion proteins and EDTA, applying repeated dosages and increasing the incubation time.

Independent of endolysin or peptide used, the outer membrane permabilizer EDTA is the ideal enhancer of the antibacterial potential of the fusion proteins. Recently, Briers and coworkers (2010) came to the same conclusion for the unmodified endolysin EL188. Here, this observation can be explained by the fact that both the EDTA and the antibacterial peptide differ in mode or site of action in the outer membrane. In case of the PK peptide, the same site of action is targeted as EDTA, e.g. the stabilizing divalent cations in the outer membrane, but a different mode of action is used. As polycationic compound, the PK peptide is believed to go in competition with the divalent cations for binding of the phosphate groups present in the LPS, as described for polymyxin or poly-L-lysine (Hancock & Wong, 1984; Vaara, 1992). Instead of phosphate binding, EDTA chelates the divalent cations and pulls them out of the outer membrane structure, leaving the phosphate groups behind (Matsushita et al, 1978). In case of the hydrophobic/amphipathic peptides, the increased hydrophobicity of the fusion protein improves the interaction with the hydrophobic lipid A part, a totally different site of action than EDTA. Due to this different mode or site of action, the peptide and the EDTA are able to act complementary on the outer membrane and improve the antibacterial potential significantly.

Of all single or double fusions tested in this chapter, the PK peptide fusion to both OBPgp279 and PVP-SE1gp146 in combination with EDTA was the most promising approach to tackle the Gram-negative outer membrane with maximal reduction values of 5.38 ± 0.19 , 2.22 ± 0.09 , 0.91 ± 0.04 log units for *P. aeruginosa*, *E. coli* and *S. Typhimurium*, respectively. Therefore, the next chapter of this dissertation will focus on this promising PK peptide fusion approach.

Evaluation and optimization of PK peptide fusion approach

8.1 Introduction

In the previous chapter, the self-designed PK peptide was shown to be the most promising peptide out of a set of seven antibacterial peptides to enhance the antibacterial activity of the two modular endolysins, OBPgp279 and PVP-SE1gp146, by N-terminal fusion. This chapter focuses more in depth on the characteristics of this remarkable peptide when used in a fusion approach. First, we try to evaluate the influence of the PK peptide fusion on some characteristics (the expression yield, protein stability, optimal pH, thermo-stability, muralytic activity and antibacterial activity) of the single-domain endolysins PsP3gp10, P2gp09, BcepC6Bgp22 and CR8gp3.5 (Chapter 5), and the modular endolysins OBPgp279, PVP-SE1gp146 and 201φ2-1gp229 (Chapter 6), introduced earlier in this dissertation study. In a second part, the biofilm degradation potential of this PK peptide fused protein will be addressed. The third and last part focuses on the optimization of the N-terminal PK peptide fusion approach by switching the PK peptide to the C-terminal end of the enzyme, on one hand, and increasing the linker length and flexibility between the N- or C-terminal PK peptide and the endolysin, on the other hand.

8.2 Influence of N-terminal PK peptide fusion on endolysin characteristics

8.2.1 Influence on expression yield

All endolysin-encoding ORFs were fused at their 5' terminus with the PK peptide-encoding cassette by tail PCR using specifically designed 5' primers that contain the PK peptide encoding sequence. After TA-ligation in the commercially available pEXP5CT-TOPO® expression vector, all PK peptide modified endolysins were expressed at large scale in an *E. coli* BL21(DE3)pLysS expression system upon induction with 1 mM IPTG. Purification was achieved with Ni²⁺-NTA affinity chromatography, using the C-terminal His₆-tag. The obtained

yields for the PK-fused endolysins are listed in Figure 8.1 together with the yields of the corresponding unmodified endolysins. Protein purity was more than 90 % for all PK-fused endolysins as checked by SDS-PAGE. Some of the PK-fused endolysins showed multimerization when this was also shown for the corresponding unmodified endolysin.

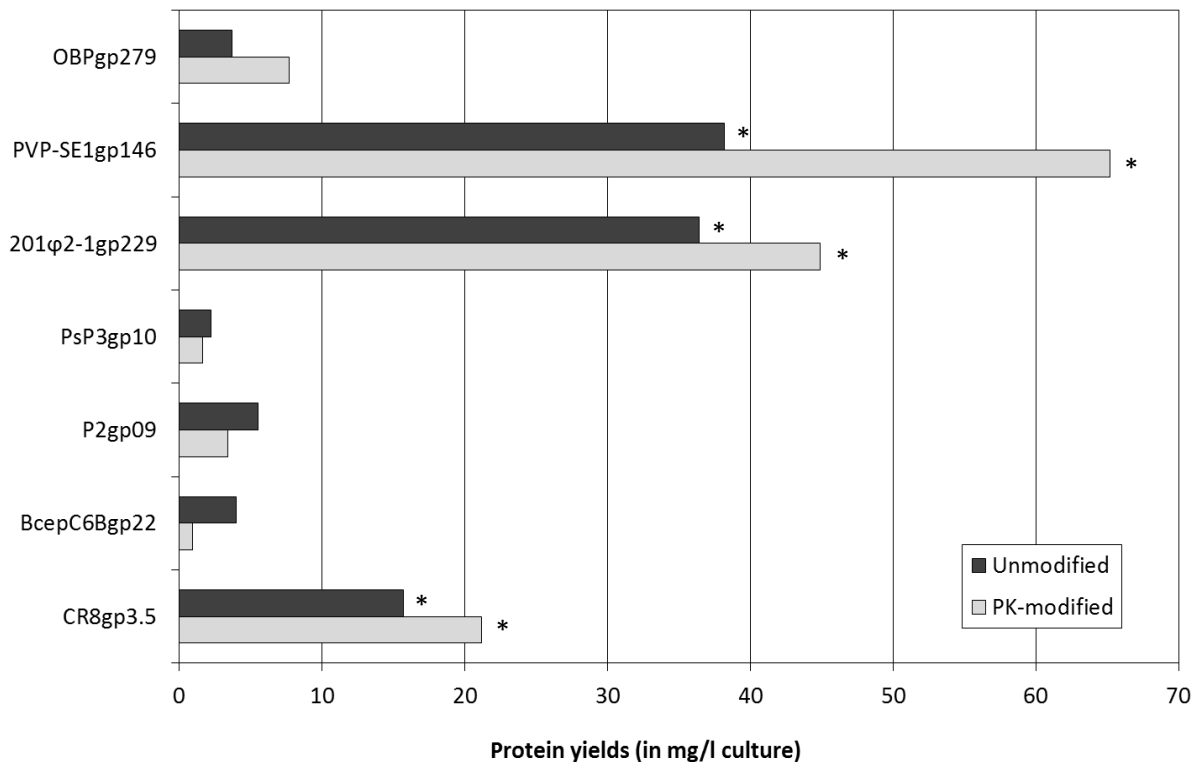


Figure 8.1: Yields of recombinant purification for PK-modified variants (grey bars) of selected endolysins compared with the unmodified, wild-type endolysins (black bars). The total yield for each protein is indicated in amount of purified protein (in mg) per liter of *E. coli* expression culture. Proteins showing multimerization are marked with an asterisk (*).

From this figure, we may envisage that the influence on the expression yield and multimerization is endolysin-specific. For the modular endolysins OBPgp279, PVP-SE1gp146 and 201φ2-1gp229, and the single-domain endolysin CR8gp3.5, the PK peptide fusion positively influences expression, improving the yield with 52, 41, 23 and 26 %, respectively. The single-domain endolysins PsP3gp10, P2gp09 and BcepC6Bgp22, on the other hand, undergo a less effective protein folding/expression when N-terminally fused with the PK peptide, resulting in a decrease in expression yield with 27, 38 and 78 %, respectively.

8.2.2 Influence on muralytic activity

To determine the influence of the N-terminal PK peptide fusion on the muralytic activity of the seven endolysins, the specific muralytic activities of the fusion variants were quantified on chloroform/Tris-HCl permeabilized *P. aeruginosa* cells (see 3.3.1 Peptidoglycan degrading or muralytic assay) and compared to the specific activities of the corresponding unmodified endolysins (Table 8.1). All PK-fused endolysins showed a reduced muralytic activity on *P. aeruginosa* substrate, but still remained active. Reductions in specific activities of the seven PK-modified endolysins ranged from 52 % for 201φ2-1gp229 to 94 % for PVP-SE1gp146. Possible steric hindrance of endolysin domains or influence on protein folding by the fused PK peptide are plausible reasons for the observed reduction in enzymatic activity. However, at saturated concentrations of the different PK-modified endolysins, the muralytic activity reaches the same value as the corresponding unmodified endolysins (data not shown). Therefore, further experiments in this chapter made use of saturated enzyme concentrations to allow a more reliable comparison.

Table 8.1: Influence of the N-terminal PK peptide fusion on specific muralytic activity of the selected modular and single-domain endolysins. The specific muralytic activities (in units/ μM) of the PK-modified and unmodified endolysins were listed together with the reduction percentage relative to the specific activity of the unmodified endolysin (= 100 % activity), tested simultaneously. R-square values corresponding with activity values are indicated between brackets. All enzymes were dialyzed to PBS pH 7.4, prior to the measurements.

Endolysin	Specific muralytic activity (in units/ μM)		Reduction percentage
	Unmodified	PK-modified	
OBPgp279	19,979 (0.983)	4,195 (0.990)	79 %
PVP-SE1gp146	13,614 (0.905)	828 (0.992)	94 %
201φ2-1gp229	4,469 (0.995)	2,205 (0.993)	52 %
PsP3gp10	1,380 (0.976)	538 (0.995)	61 %
P2gp09	829 (0.992)	232 (0.994)	72 %
BcepC6Bgp22	786 (0.983)	204 (0.987)	74 %
CR8gp3.5	315 (0.961)	72 (0.964)	77 %

8.2.3 Influence on pH-dependency

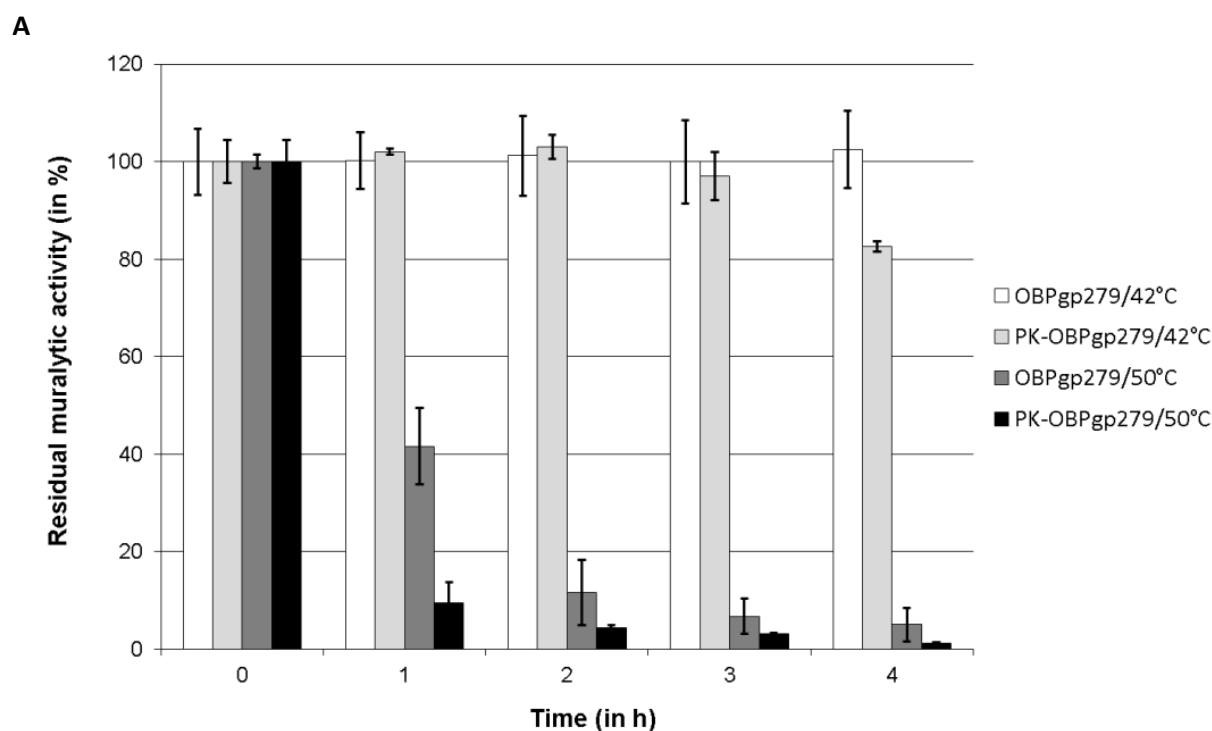
One of the crucial parameters that influences stability and activity of an enzyme is the pH. In this part, we assess the influence of the PK peptide fusion on the pH spectrum of the selected endolysins. To reach this goal, the muralytic activity of a saturated concentration of unmodified and PK-modified endolysin was quantified in an universal pH buffer with pH values ranging from 3 to 10 (Table 8.2). Between pH values of 4 to 6, the activity of all four tested endolysins significantly decreased upon N-terminal fusion with the PK peptide. At pH 9, the unmodified endolysins OBPgp279 and CR8gp3.5 also significantly differ from their PK-modified variants. The increase in iso-electric point (pI) value, from 8.93, 8.96, 9.16 and 9.15 to 9.53, 9.60, 9.64 and 9.88 upon N-terminal fusion of the PK peptide to OBPgp279, PVP-SE1gp146, 201φ2-1gp22 and CR8gp3.5, respectively, might explain the observed differences.

Table 8.2: pH-dependency of PK-modified endolysins. Muralytic activities of each PK-modified and unmodified endolysins (1500 nM final concentration, dialyzed against PBS buffer pH 7.4) on outer membrane-permeabilized *P. aeruginosa* PAO1 were expressed for pH-values between 4 and 9, relatively to the pH with the highest activity value for that (modified) endolysin (= 100 %). Averages and standard deviations of two independent experiments were depicted here. Significant differences between PK-modified and unmodified endolysins for a specific pH value are shaded in grey.

Endolysins		pH					
		4	5	6	7	8	9
OBPgp279	Unmodified	13.7 ± 6.2	38.2 ± 4.9	86.2 ± 7.4	100.0 ± 8.9	95.6 ± 2.7	79.1 ± 9.9
	PK-modified	0.4 ± 0.2	9.2 ± 4.2	52.7 ± 9.2	100.0 ± 16.9	87.5 ± 10.9	48.1 ± 4.5
PVP-SE1gp146	Unmodified	28.7 ± 7.4	79.2 ± 8.8	98.1 ± 6.7	100.0 ± 5.6	72.1 ± 2.3	54.8 ± 8.5
	PK-modified	10.7 ± 1.6	50.0 ± 5.1	92.7 ± 0.0	100 ± 6.6	78.7 ± 6.3	78.1 ± 11.0
201φ2-1gp229	Unmodified	2.9 ± 1.1	20.5 ± 4.6	53.6 ± 6.9	100.0 ± 13.9	89.1 ± 8.7	53.3 ± 3.2
	PK-modified	2.7 ± 2.3	8.3 ± 1.7	35.4 ± 4.0	100.0 ± 5.9	99.5 ± 11.4	55.3 ± 5.8
CR8gp3.5	Unmodified	25.5 ± 3.3	67.4 ± 7.3	94.3 ± 8.6	100.0 ± 3.5	84.7 ± 6.7	80.6 ± 5.8
	PK-modified	21.1 ± 8.8	33.1 ± 3.6	55.6 ± 9.8	100.0 ± 10.4	64.3 ± 3.3	40.4 ± 3.9

8.2.4 Influence on activity of OBPgp279 and PVP-SE1gp146 after heat treatment

Earlier in this study, the exceptional nature of PVP-SE1gp146 to stay active to temperatures of 100°C has been discussed (see 6.2.3 Activity after heat treatment). In this part, we determine the influence of the PK peptide fusion on activity of PVP-SE1gp146 (5 µM) and OBPgp279 (1 µM) upon heating. Activity of both PK-modified endolysins was measured on chloroform/Tris-HCl permeabilized *P. aeruginosa* PAO1 after heat treatment at 42°C and 50°C and compared with the unmodified endolysin (Figure 8.2A). Similar to unmodified PVP-SE1gp146, no significant reduction in muralytic activity of PK-PVP-SE1gp146 was observed after 4 h of incubation at 42 and 50°C (data not shown). In contrast, PK-OBPgp279 differed from unmodified OBPgp279: after four hours of incubation at 42°C and one hour at 50°C, the fusion variant became 20 and 30 % less active than the unmodified OBPgp279, respectively. At higher temperatures, the negative effect of the PK peptide fusion on the activity of PVP-SE1gp146 becomes more pronounced (Figure 8.2B). Whereas the unmodified PVP-SE1gp146 remained fully active up to temperatures of 90°C for at least 20 min, PK-PVP-SE1gp146 retained only 55 % of its activity at 80°C and became completely inactivated at 90°C after the same incubation time. To explain the lower activity upon heating due to the fusion, the unfolding temperatures (by DSC) and the secondary structure upon refolding (by CD) of



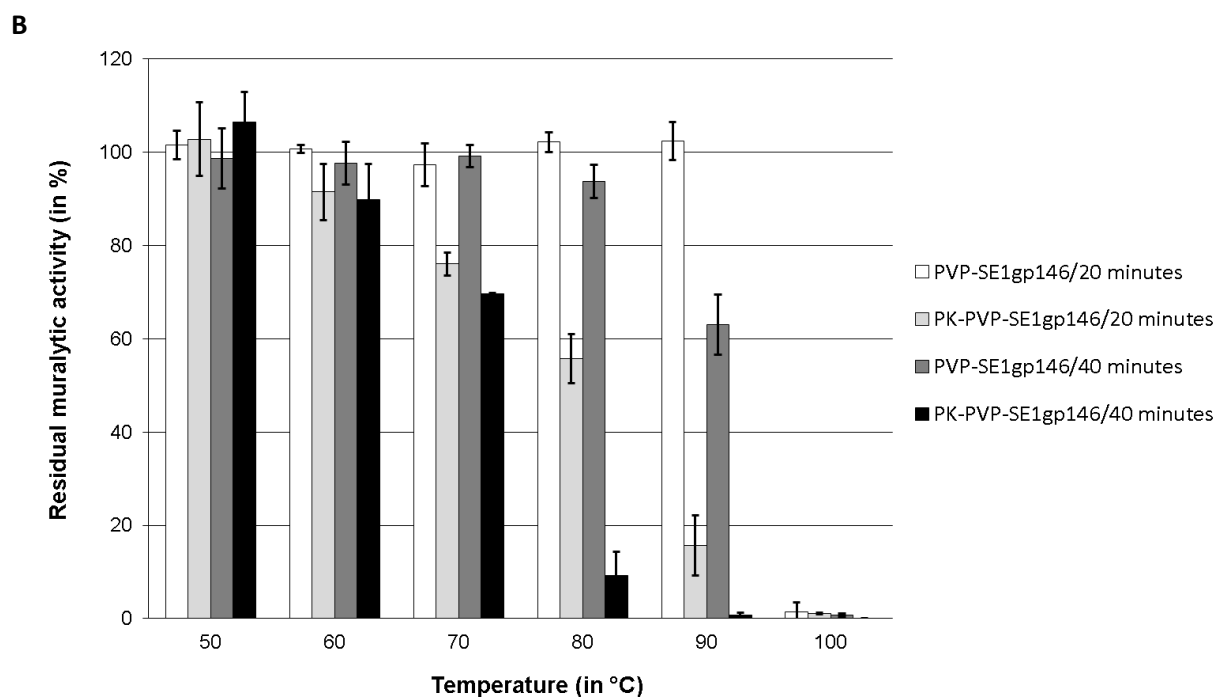


Figure 8.2: Impact of PK peptide fusion on stability at high temperatures of OBPgp279 (A) and PVP-SE1gp146 (B). (A) The residual muralytic activities on *P. aeruginosa* PAO1 of OBPgp279 after 1, 2, 3 and 4 hours of incubation at 42°C (white bars) and 50°C (dark grey bars) were compared with the values obtained for PK-OBPgp279 (42°C = light grey bars and 50°C = black bars). (B) For PVP-SE1gp146 and PK-PVP-SE1gp146, the residual muralytic activities were determined after 20 (PVP-SE1gp146: white bars; PK-PVP-SE1gp146: light grey bars) and 40 min (PVP-SE1gp146: dark grey bars; PK-PVP-SE1gp146: black bars) of incubation at different temperatures ranging from 50 to 90°C. For both curves, the averages and standard deviations of two repeated experiments are depicted.

modified and unmodified endolysins should be compared. We hypothesize that the N-terminally fused PK peptide either lowers the melting temperature or promotes the irreversible denaturation process of the enzyme, both leading to lower activity upon heating.

8.2.5 Influence on *in vitro* antibacterial activity

In addition to OBPgp279 and PVP-SE1gp146 (see 7.3 *In vitro* antibacterial activity of N-terminal OBPgp279 and PVP-SE1gp146 fusion variants), we also evaluated the influence of the N-terminal PK peptide fusion modification on the *in vitro* antibacterial activity of 201φ2-1gp229, P2gp09, PsP3gp10 and CR8gp3.5 in the absence and presence of EDTA (parameters: 10^6 CFU/ml of exponentially growing cells, 5 μM endolysin, 0.5 mM EDTA, 30 min incubation) (Table 8.3). Due to the promising results obtained with the PK peptide fusion, the set of

Table 8.3: Antibacterial activity of PK-fusion variants of six endolysins without (A) and with (B) EDTA (0.5 mM) compared to unmodified endolysins. Cell suspensions (10^6 CFU/ml, 5 mM HEPES pH 7.4) were incubated with enzymes dialyzed against PBS buffer (pH 7.4). The antibacterial activity is shown in logarithmic units ($= \log_{10}(N_0/N_i)$) with N_0 = number of untreated cells and N_i = number of residual, treated cells). Averages and standard deviations of three independent experiments are shown. Significant increase in reduction values between unmodified and PK-modified endolysins = \uparrow , no significant difference = --- (two-tailed t test, $P < 0.05$).

		Antibacterial activity (in \log_{10} units)					
A		<i>P. aeruginosa</i> PAO1	<i>P. aeruginosa</i> Br667	<i>P. putida</i> G1	<i>B. pseudomallei</i>	<i>E. coli</i> XL1-Blue MRF'	<i>S. Typhimurium</i> LT2
OBPgp279 (1.5 μ M)	Unmodified	1.10 \pm 0.07	1.08 \pm 0.08	0.94 \pm 0.13	0.99 \pm 0.13	0.38 \pm 0.03	0.08 \pm 0.01
	PK-modified	2.61 \pm 0.09 \uparrow	1.56 \pm 0.06 \uparrow	1.91 \pm 0.08 \uparrow	1.81 \pm 0.29 \uparrow	0.43 \pm 0.02 ---	0.23 \pm 0.01 \uparrow
PVP-SE1gp146 (5 μ M)	Unmodified	0.19 \pm 0.01	0.10 \pm 0.03	0.34 \pm 0.01	ND	0.14 \pm 0.01	0.13 \pm 0.02
	PK-modified	1.56 \pm 0.10 \uparrow	1.09 \pm 0.03 \uparrow	0.76 \pm 0.20 \uparrow	ND	0.29 \pm 0.09 \uparrow	0.30 \pm 0.10 \uparrow
201 ϕ 2-1gp229 (3 μ M)	Unmodified	0.17 \pm 0.10	0.08 \pm 0.03	0.09 \pm 0.01	0.04 \pm 0.05	0.04 \pm 0.04	0.07 \pm 0.04
	PK-modified	0.73 \pm 0.08 \uparrow	0.66 \pm 0.05 \uparrow	0.78 \pm 0.11 \uparrow	0.02 \pm 0.03 ---	0.19 \pm 0.01 \uparrow	0.06 \pm 0.03 ---
PsP3gp10 (1.5 μ M)	Unmodified	0.38 \pm 0.02	0.38 \pm 0.06	ND	0.41 \pm 0.03	0.21 \pm 0.03	0.28 \pm 0.04
	PK-modified	0.44 \pm 0.16 ---	0.45 \pm 0.09 ---	ND	0.51 \pm 0.09 ---	0.21 \pm 0.09 ---	0.33 \pm 0.06 ---
P2gp09 (1.5 μ M)	Unmodified	0.37 \pm 0.08	0.25 \pm 0.04	ND	ND	0.19 \pm 0.05	0.08 \pm 0.09
	PK-modified	0.43 \pm 0.07 ---	0.35 \pm 0.06 ---	ND	ND	0.21 \pm 0.04 ---	0.18 \pm 0.10 ---
CR8gp3.5 (2.5 μ M)	Unmodified	0.21 \pm 0.07	0.05 \pm 0.03	ND	ND	0.09 \pm 0.04	0.03 \pm 0.03
	PK-modified	0.38 \pm 0.09 ---	0.37 \pm 0.06 \uparrow	ND	ND	0.14 \pm 0.06 ---	0.08 \pm 0.05 ---
B		<i>P. aeruginosa</i> PAO1	<i>P. aeruginosa</i> Br667	<i>P. putida</i> G1	<i>B. pseudomallei</i>	<i>E. coli</i> XL1-Blue MRF'	<i>S. Typhimurium</i> LT2
EDTA		0.58 \pm 0.02	0.03 \pm 0.02	0.41 \pm 0.06	0.22 \pm 0.08	0.29 \pm 0.11	0.05 \pm 0.05
OBPgp279 (1.5 μ M)	Unmodified	4.36 \pm 0.28	3.14 \pm 0.22	3.89 \pm 0.11	4.08 \pm 0.10	1.18 \pm 0.20	0.77 \pm 0.05
	PK-modified	5.38 \pm 0.19 \uparrow	4.27 \pm 0.15 \uparrow	4.89 \pm 0.02 \uparrow	4.81 \pm 0.05 \uparrow	1.70 \pm 0.01 \uparrow	0.91 \pm 0.04 \uparrow
PVP-SE1gp146 (5 μ M)	Unmodified	3.68 \pm 0.13	0.12 \pm 0.02	0.34 \pm 0.02	ND	0.34 \pm 0.02	0.14 \pm 0.21
	PK-modified	4.92 \pm 0.23 \uparrow	1.12 \pm 0.03 \uparrow	1.36 \pm 0.01 \uparrow	ND	0.85 \pm 0.17 \uparrow	0.73 \pm 0.30 \uparrow
201 ϕ 2-1gp229 (3 μ M)	Unmodified	3.25 \pm 0.10	0.17 \pm 0.20	1.80 \pm 0.03	0.42 \pm 0.04	0.58 \pm 0.25	0.26 \pm 0.02
	PK-modified	4.30 \pm 0.20 \uparrow	1.31 \pm 0.04 \uparrow	4.36 \pm 0.07 \uparrow	0.90 \pm 0.07 \uparrow	1.17 \pm 0.03 \uparrow	0.77 \pm 0.09 \uparrow
PsP3gp10 (1.5 μ M)	Unmodified	3.38 \pm 0.23	0.67 \pm 0.04	ND	1.47 \pm 0.06	0.39 \pm 0.01	0.69 \pm 0.04
	PK-modified	4.15 \pm 0.12 \uparrow	0.89 \pm 0.12 \uparrow	ND	2.56 \pm 0.02 \uparrow	0.58 \pm 0.02 \uparrow	0.75 \pm 0.03 ---
P2gp09 (1.5 μ M)	Unmodified	2.84 \pm 0.08	0.58 \pm 0.07	ND	ND	0.29 \pm 0.07	0.34 \pm 0.11
	PK-modified	3.47 \pm 0.05 \uparrow	0.95 \pm 0.21 \uparrow	ND	ND	0.58 \pm 0.03 \uparrow	0.28 \pm 0.13 ---
CR8gp3.5 (2.5 μ M)	Unmodified	2.05 \pm 0.08	0.06 \pm 0.10	ND	ND	0.23 \pm 0.11	0.22 \pm 0.07
	PK-modified	2.92 \pm 0.08 \uparrow	0.08 \pm 0.02 ---	ND	ND	0.43 \pm 0.09 ---	0.39 \pm 0.12 ---

tested strains is expanded with three other relevant strains: *P. aeruginosa* Br667, *P. putida* G1, also from the *Pseudomonas* genus, and the multidrug-resistant clinical isolate *B. pseudomallei*, a member from the *Burkholderia* genus. *P. putida* occasionally causes catheter-related bloodstream infections (Yoshino et al, 2011), whereas *B. pseudomallei* provokes systemic infections in humans with a high mortality rate (melioidosis) (Wuthiekanun & Peacock, 2006).

Interestingly, the PK peptide fusion significantly improved the antibacterial activity of the three modular endolysins, and in lesser extent the single-domain endolysins, on most of the tested strains (Table 8.3A). The difference between unmodified and PK-modified endolysins became more pronounced, especially for the single-domain endolysins, upon addition of EDTA. This observation indicates the presence of possible synergistic effects between EDTA and the PK-modified endolysins (Table 8.3B). Considering the reduced muralytic activity of the PK-modified endolysins (see 8.2.2 Influence on the muralytic activity of endolysins), the increase in antibacterial activity is even more outspoken. The observed drop in muralytic activity is completely antagonized by the outer membrane permeabilizing capacity of the PK moiety, resulting in a net improvement of the antibacterial activity. For all tested strains in this experiment, the highest antibacterial activity was achieved for a combination of PK-OBPgp279 with EDTA, resulting in 5.38, 4.27, 4.89, 4.81, 1.70 and 0.91 log units reduction on *P. aeruginosa* PAO1, *P. aeruginosa* Br667, *P. putida* G1, *B. pseudomallei*, *E. coli* XL1-Blue MRF' and *S. Typhimurium* LT2, respectively.

From our data, we conclude that the positive impact of the PK peptide on the antibacterial activity of endolysins is family-, strain- and protein-dependent. The increase in antibacterial activity is higher for the tested species of the Pseudomonads (*P. aeruginosa* PAO1, *P. aeruginosa* Br667, *P. putida* G1) and Burkholderiaceae (*B. pseudomallei*) families than for the members of the Enterobacteriaceae (*S. Typhimurium* LT2 and *E. coli* XL1-Blue MRF'). Activities on Pseudomonads and Burkholderiaceae members are enhanced with values in between 0.6 to 1.5 log units reduction, whereas the maximal increase in reduction for the Enterobacteriaceae is 0.5 log units. A similar trend is observed for the intrinsic activity of OBPgp279 (± 1 log unit reduction) for the tested Pseudomonads and Burkholderiaceae members. This family dependency was observed for OBPgp279 and PVP-SE1gp146 (see 7.5

Discussion), but could now be extended for 201 ϕ 2-1gp229 and the single-domain endolysins as well. An explanation for this phenomenon should be found in the fundamental structural differences in outer membrane stabilization between *Pseudomonads* and *Burkholderiaceae* (more stabilized by cationic interactions), on one hand, and *Enterobacteriaceae* (less stabilized by cationic interactions), on the other hand (see 1.3.1.3 Lipid A).

In addition to the inter-family differences, the impact of the PK peptide on antibacterial activity also seems strain-dependent. Especially for the modular endolysins, the difference between *P. aeruginosa* PAO1 and Br667 was significant, with a maximal increase in activity of 1.5 log units for PAO1 (OBPgp279), and only 1 log unit for Br667 (PVP-SE1gp146). This trend became even more pronounced upon addition of EDTA. As discussed earlier, the main difference between those two strains is their varying degree of antibiotic resistance (Pirnay et al, 2003). In clinical isolates of *P. aeruginosa*, antibiotic resistance is related to an improved impermeability of the outer membrane, caused by specific modifications (O-acetylation, hydroxylation, secondary substitutions of phosphate and amino-arabinose groups) in the LPS moiety (Ernst et al, 2007; Hajjar et al, 2002). Presumably, similar modifications in the outer membrane of Br667 are responsible for the diminished sensibility for the PK-modified endolysins and for the chelating agents EDTA. Nonetheless, these data show that also multidrug-resistant *P. aeruginosa* strains could be effectively inactivated with the PK peptide fusion approach, which is promising from a therapeutic point of view.

The effectiveness of the PK fusion is also protein-dependent. PK-OBPgp279 is the only PK-modified endolysin that is able to significantly inactivate *Pseudomonas* and *Burkholderia* strains without the necessity of EDTA. In contrast, the PK-modification only significantly improves the activity of the three single-domain endolysins when EDTA is added.

8.3 Biofilm-degrading potential of PK peptide fusion approach

In natural environments, most Gram-negative bacteria, including *P. aeruginosa* and *A. baumannii*, are generally recognized to live predominantly in biofilms (Kim & Wei, 2007). Biofilm formation is one of the major mechanisms bacteria employ to protect themselves against antibiotics, including the β -lactam antibiotic ampicillin (Stewart & Costerton, 2001)

or vancomycin (Monzon et al, 2002). Bacteria living in biofilms are surrounded by a dense extracellular matrix composed of exopolysaccharide, protein, nucleic acid and lipid material. This matrix provides bacteria with a thousand fold stronger protection against antibiotics compared to free-living or planktonic cells (Mah, 2012). In regard to potential therapeutic application, it is important to evaluate whether bacterial cells within a biofilm are also susceptible for the antibacterial action of the PK peptide fusion approach. In this section, we therefore analyze the antibacterial activity and the biofilm degrading potential of a (PK-)PVP-SE1gp146/EDTA mixture after 4 hours of treatment on a 24-hour old *P. aeruginosa* PAO1 biofilm (Figure 8.3). The biofilm degradation is quantified by spectrophotometrical assessment (OD_{600nm}) of the proportion of crystal violet taken up by the residual biofilm.

Treatment of the PAO1 biofilm with EDTA (0.5 mM) for 4 hours reduced the biofilm with 20 %, as compared with the PBS buffer control, whereas the number of planktonic bacteria did not differ significantly from the control. EDTA, at high concentrations, has been described in literature as a potential inhibitor of biofilm formation by *Listeria monocytogenes* (Chang et al, 2012b) and *Enterococcus faecalis* (Soares et al, 2010) and might also be able to degrade an established biofilm by a putative mechanism independent from cell reduction, as shown by our data.

In the presence of EDTA, PVP-SE1gp146 could only significantly improve the biofilm degradation and the planktonic cell reduction from a concentration of 25 μ M, compared to the EDTA control (two-tailed *t* test, $P < 0.05$). PK-PVP-SE1gp146, on the other hand, was able to further improve the biofilm degradation induced by EDTA with 27 % and reduce planktonic cell count together with EDTA with 89 %, at the highest tested concentration of 25 μ M. This inactivation rate of planktonic cells was already observed at the lowest concentration of PK-PVP-SE1gp146 tested (5 μ M). However, no significant difference could be observed in biofilm degradation at this concentration, compared to the EDTA control. To obtain a similar elimination rate of the bacterial cells in a biofilm than for free-living planktonic cells seems to require a concentration higher than 25 μ M. This observation is in agreement with other antibacterial compounds, including antibiotics or bile salts, where even a hundred to thousand times stronger concentration is required to obtain a similar antibacterial activity for the biofilm and planktonic cells (Stewart & Costerton, 2001).

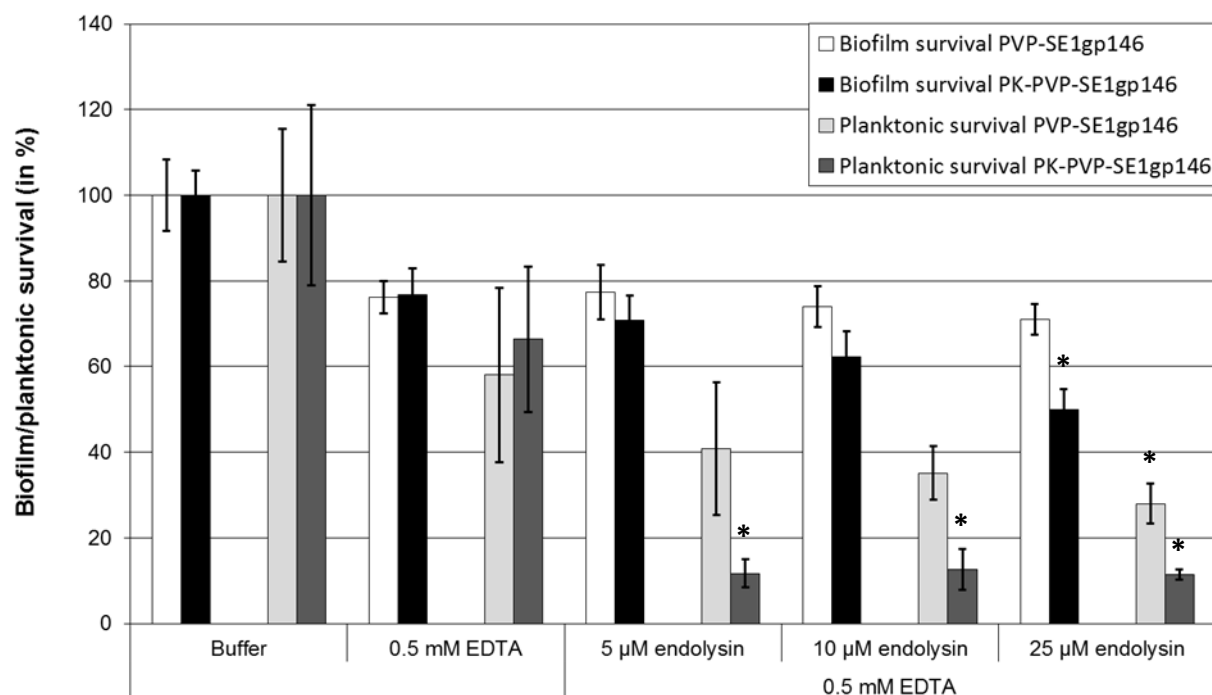


Figure 8.3: Biofilm degradation capacity of the PK peptide fusion approach on a 24-hour old biofilm of *P. aeruginosa* PAO1 mediated by (PK-)PVP-SE1gp146/EDTA combination. Pre-formed biofilms were incubated with 0.5 mM EDTA and three different concentrations of PVP-SE1gp146 and PK-PVP-SE1gp146. After 4 hours of treatment, the residual biofilm (PVP-SE1gp146: white bars; PK-PVP-SE1gp146: black bars) and planktonic survival (PVP-SE1gp146: light grey bars; PK-PVP-SE1gp146: dark grey bars) were scored in percentages relative to the untreated control samples (100 %). Four independent experiments were performed with four repeats for each parameter combination. Averages and standard deviations are depicted here. Significant differences in values compared with the 0.5 mM EDTA control are marked by an asterisk (*) (two-tailed *t* test, $P < 0.05$).

8.4 Strategies to optimize the PK peptide fusion approach

8.4.1 By switching the PK peptide to the C-terminal end of OBPgp279 and PVP-SE1gp146

8.4.1.1 Construction, expression and purification of the C-terminal PK peptide fusion variants

Similar as for the construction of the N-terminal fusion variants, the PK peptide is fused to the C-terminal side of the endolysin by use of a tail PCR, except that the PK-encoding cassette is now incorporated in a reverse orientation in the 3' reverse primer, instead of in the 5' forward one (Figure 8.4). Adjacent to the PK-encoding cassette, the 3' primer also contains a His₆-encoding sequence for insertion of a His₆-tag in between the endolysin and

the PK peptide, necessary for purification. Finally, downstream of the PK encoding cassette, a stop codon sequence is introduced to exclude the His₆-tag encoded by the pEXP5CT-TOPO[®] vector, from the translation product. In this way, the PK peptide is C-terminally fused to the ORFs of the endolysins with the highest enzymatic activity: OBPgp279 and PVP-SE1gp146. Highest soluble yields of PVP-SE1gp146-PK were obtained by expression in *E. coli* BL21(DE3)pLysS upon induction with 1 mM IPTG on 37°C, whereas for OBPgp279-PK an *E. coli* BL21-CodonPlus-(DE3)-RIL culture (AT-rich gene translation), 0.1 mM IPTG and 16°C came out as optimal expression parameters.

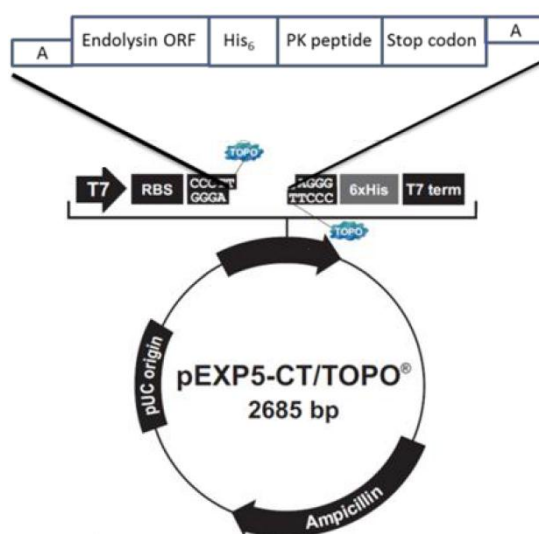


Figure 8.4: Schematic diagram for construction of the C-terminal PK peptide fusion variant of an endolysin. Upon addition of a stop codon (TGA) downstream of the PK peptide coding sequence, the vector specific His₆-tag is not incorporated by transcription/translation of the protein.

The obtained yields for the C-terminal PK fusion variants of OBPgp279 (OBPgp279-PK) and PVP-SE1gp146 (PVP-SE1gp146-PK) were compared with those for the N-terminal PK variants and the unmodified endolysins (Figure 8.5). For both endolysins, the C-terminal PK fusion variants showed a lower optimized expression yield than the corresponding unmodified endolysins. Unlike the N-terminal PK peptide fusion which was beneficial for protein expression of both endolysins, a C-terminal fusion of the same peptide seems to diminish the protein yield. A possible negative impact of the intermediate position of the His₆-tag and the highly charged PK peptide on the Ni²⁺-His₆ interaction could be excluded as almost no protein was present in the flow through fractions for both endolysins. Therefore, the effect of a C-terminal PK fusion is mainly on expression level. Similar to PVP-SE1gp146 and PK-PVP-SE1gp146, multimerization was also present in the elution fractions of PVP-SE1gp146-PK.

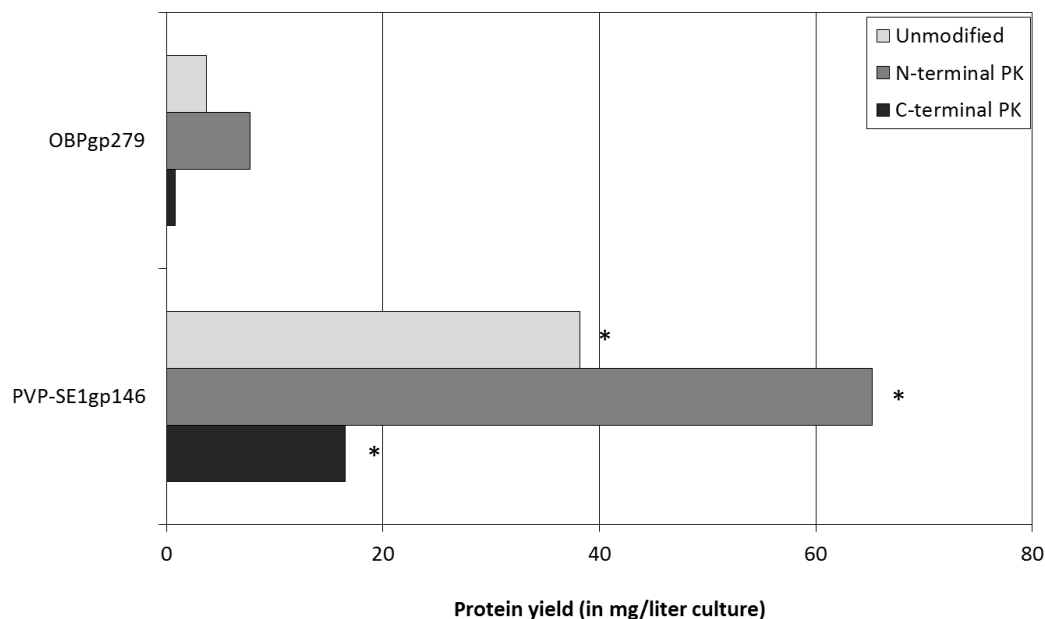


Figure 8.5: Comparison of protein expression yields for N- and C-terminal PK-fusion variants of OBPgp279 and PVP-SE1gp146. Unmodified = light grey bars, N-terminal PK fusion = dark grey bars and C-terminal PK-fusion = black bars. The obtained protein yield is expressed as amount of protein (in mg) per liter expression culture. Proteins with multimerization are marked with an asterisk (*).

8.4.1.2 Impact of C-terminal PK peptide fusion on muralytic activity

To determine the influence of the C-terminal PK peptide fusion on the muralytic activity of the OBPgp279 and PVP-SE1gp146, the specific muralytic activities of these fusion variants were quantified on chloroform/Tris-HCl permeabilized *P. aeruginosa* PAO1 cells (see 3.3.1 Peptidoglycan degrading or muralytic assay) and compared relatively to the specific activities of the corresponding unmodified endolysins and N-terminal PK fusion variants (Figure 8.6). Similar to the N-terminal fusion variants, the fusion of a PK peptide to the C-terminal end of the OBPgp279 and PVP-SE1gp146, close to their C-terminal catalytic domains, substantially decreases their muralytic activities, with 97 and 95 %, respectively. In case of PVP-SE1gp146, this reduction in muralytic activity by the N- or C-terminal PK peptide fusion is comparable. Contrarily, a fusion to the C-terminal end of OBPgp279 is significantly more detrimental for its muralytic activity than a N-terminal fusion. As the C-terminal catalytic domain comprises the major part of the total muralytic activity of OBPgp279 (67 %), a possible interference of the PK peptide with this domain could have a higher impact on enzyme inactivation than a fusion in close proximity to the N-terminal peptidoglycan binding domain.

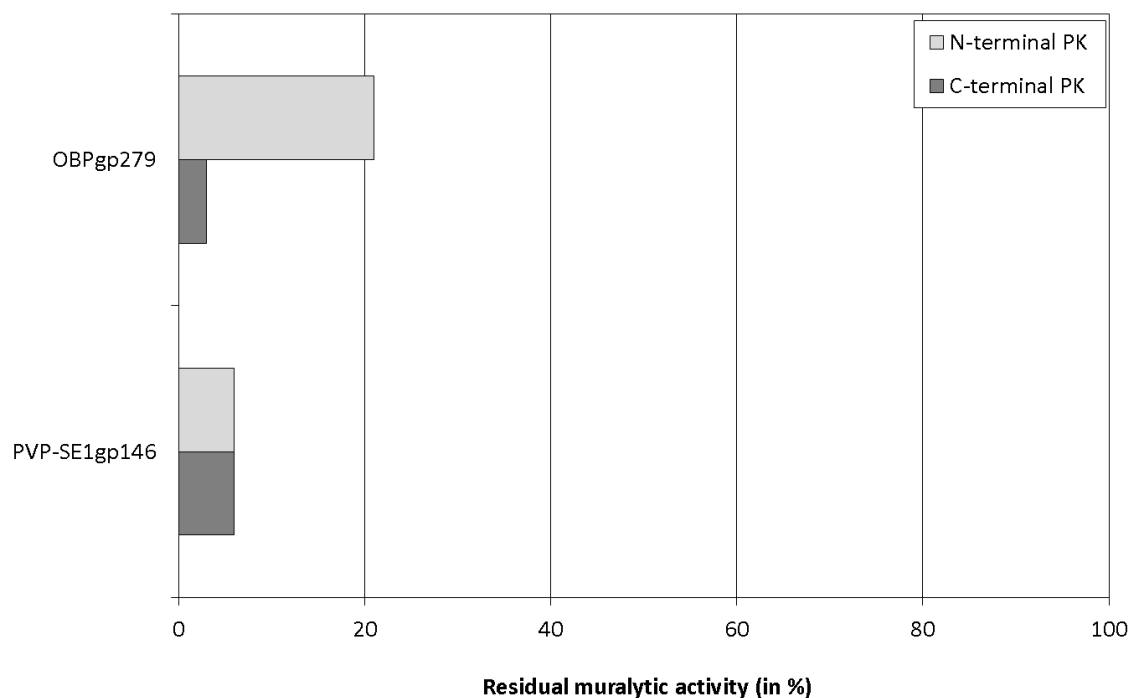


Figure 8.6: Comparison of the influence of the N- and C-terminal PK peptide fusions on murelytic activity of OBPgp279 and PVP-SE1gp146 against outer membrane-permeabilized *P. aeruginosa* PAO1. N-terminal = light grey bars, C-terminal = dark grey bars. The specific murelytic activities of the modified and unmodified endolysins were expressed in percentages relative to the specific activity of the unmodified endolysin (= 100 % activity), tested simultaneously. All enzymes were dialyzed to PBS buffer (pH 7.4), prior to the measurements.

8.4.1.3 Impact of C-terminal PK peptide fusion on *in vitro* antibacterial activity

The influence of the fusion of a C-terminal PK peptide to endolysins OBPgp279 and PVP-SE1gp146 on their antibacterial activity was analyzed for *P. aeruginosa* PAO1, *S. Typhimurium* LT2 and a multidrug-resistant clinical *A. baumannii* 25 isolate, according to the standard protocol (parameters = 10^6 CFU/ml of exponential growing cells, application of 5 μ M of endolysins, 0.5 mM EDTA, 30 min incubation at room temperature) (Table 8.4). The *Acinetobacter* genus is also a member of the Pseudomonadales order and thus related to the *Pseudomonas* genus. As the PK peptide fusion approach is doing excellent on bacterial species from the Pseudomonadales, an *A. baumannii* strain was selected to evaluate the C-terminal fusion approach.

In the absence of EDTA, the fusion of the PK peptide to the C-terminus of both endolysins results in a lower antibacterial activity against *P. aeruginosa* PAO1 compared to the corresponding N-terminal variants. With *S. Typhimurium* LT2, no significant differences were observed between N- and C-terminal PK-fusion variants. In the presence of EDTA, both *P. aeruginosa* PAO1 and *A. baumannii* 25 become inactivated with 5 log units reduction or more, irrelevant of the N- and C-terminal PK peptide constructs used. In case of *S. Typhimurium* LT2, the N-terminal PK fusion was again more successful than the C-terminal one.

Table 8.4: Antibacterial activity of C-terminal PK fusion variants of OBPgp279 (1.5 μ M) and PVP-SE1gp146 (5 μ M) without (A) and with (B) 0.5 mM EDTA on *P. aeruginosa* PAO1, *A. baumannii* 25 and *S. Typhimurium* LT2. Exponentially growing cells (10^6 CFU/ml) were incubated with undialyzed endolysins without or with EDTA. Antibacterial activity is indicated in logarithmic units ($= \log_{10}(N_0/N_i)$) with N_0 = number of untreated cells and N_i = number of treated cells, both counted after incubation). Averages and standard deviations of three repeated and independent experiments are shown. Significant differences in activity between N- and C-terminal fusion variants are indicated. ↓ = significantly lower, --- = no significant difference (two-tailed *t* test, $P < 0.05$). ND = not determined.

		Antibacterial activity (in \log_{10} units)		
A		<i>P. aeruginosa</i> PAO1	<i>S. Typhimurium</i> LT2	<i>A. baumannii</i> 25
OBPgp279	N-terminal PK	2.61 \pm 0.09	0.23 \pm 0.01	ND
	C-terminal PK	2.18 \pm 0.11 ↓	0.25 \pm 0.11 ---	1.46 \pm 0.02
PVP-SE1gp146	N-terminal PK	1.20 \pm 0.11	0.30 \pm 0.10	ND
	C-terminal PK	0.81 \pm 0.03 ↓	0.14 \pm 0.04 ---	0.12 \pm 0.04
B		<i>P. aeruginosa</i> PAO1	<i>S. Typhimurium</i> LT2	<i>A. baumannii</i> 25
EDTA		0.58 \pm 0.02	0.11 \pm 0.15	0.18 \pm 0.11
OBPgp279 + EDTA	N-terminal PK	5.38 \pm 0.19	0.91 \pm 0.04	ND
	C-terminal PK	4.94 \pm 0.24 ---	0.28 \pm 0.15 ↓	4.96 \pm 0.28
PVP-SE1gp146 + EDTA	N-terminal PK	4.92 \pm 0.23	0.73 \pm 0.30	ND
	C-terminal PK	4.99 \pm 0.41 ---	0.15 \pm 0.04 ↓	5.33 \pm 0.20

8.4.2 By extension of linker length between N- or C-terminal PK peptide and endolysin

8.4.2.1 Construction, expression and purification of extended linker variants

To increase flexibility and outer membrane interaction of the N- or C-terminally fused PK peptide, the linker length between the PK peptide and the endolysin was extended with four (Link 1), eight (Link 2), twelve (Link 3) and sixteen (Link 4) glycine (G) or alanine (A) amino acids. Glycine and alanine were chosen because of their small size (less steric hindrance) and high flexibility, conferred by the presence of a sp³-hybridized carbon atom in their centre. A schematic overview for the construction of these extended linker constructs is shown in Figure 8.7. Linker cassettes of different lengths, encoding for alternating glycine and alanine residues (one to four GAGA building blocks), are introduced in between the N- or C-terminal PK peptide encoding cassette and the endolysin ORF. In case of the N-terminal linkers, the undigested vector with NgoMIV/NheI restriction sites corresponds with the Link 1 construct.

Expression of the extended linker variants of OBPgp279 and PVP-SE1gp146 was performed in *E. coli* BL21-CodonPlus-(DE3)-RIL (AT-rich gene expression) and *E. coli* BL21(DE3)pLysS, respectively, upon induction with 0.1 (OBPgp279 variants) and 1 mM (PVP-SE1gp146) IPTG. The obtained expression yields for all N- and C-terminal extended linker constructs were summarized in Table 8.5. Dependent on the endolysin used, the extension of the linker length between the N- or C-terminal PK peptide and the endolysin was beneficial or disadvantageous for the protein yield. For OBPgp279, the N-terminal extended linkers further improved the yield with 85 (Link 3) to 115 (Link 1) % as compared with the direct N-terminal PK peptide fusion variant. In case of PVP-SE1gp146, the highest improvement of the yield was obtained for the C-terminal Link 4 variant with an increase of 134 % on the yield of the direct C-terminal PK peptide fusion variant. In both cases, significant difference in yield was observed between the N- and C-terminal extended linker.

8.4.2.2 Influence of N- or C-terminal extended linkers on muralytic activity of endolysin

The specific muralytic activities for the N- and C-terminal extended linker variants of OBPgp279 and PVP-SE1gp146 were shown in relative percentages compared to the value for

Table 8.5: Comparison of expression yields for N-and C-terminal PK-fused OBPgp279 and PVP-SE1gp146 variants with extended linkers The obtained yield is expressed as amount of protein (in mg) per liter expression culture. Proteins with multimerization are marked with an asterisk (*).

	Protein yields (in mg/l culture)		
	Linker length	N-terminal PK	C-terminal PK
OBPgp279	No linker	7.7	0.8
	Link 1	17.7	0.7
	Link 2	15.9	0.2
	Link 3	13.1	0.2
	Link 4	13.7	0.4
PVP-SE1gp146	No linker	65.2*	16.5*
	Link 1	11.7	24.3
	Link 2	14.4	17.8
	Link 3	24.5	20.7
	Link 4	7.2	44.1

Table 8.6: Influence of linker extension for the N- and C-terminal PK peptide fusion variants on muralytic activity of OBPgp279 and PVP-SE1gp146. The specific muralytic activities of the extended linker variants of both endolysins were expressed in percentages relative to the specific activity of the unmodified, wild-type endolysin (= 100 % activity), tested simultaneously. All enzymes were dialyzed to PBS pH 7.4, prior to the measurements.

	Relative muralytic activity (in %)		
	Linker length	N-terminal PK	C-terminal PK
OBPgp279	No linker	21	3
	Link 1	23	16
	Link 2	26	15
	Link 3	32	18
	Link 4	34	24
PVP-SE1gp146	No linker	6	6
	Link 1	ND	6
	Link 2	ND	8
	Link 3	ND	13
	Link 4	ND	12

the unmodified endolysins (Table 8.6). Interestingly, extension of the linker length between PK peptide and the endolysin partly restored the reduced muralytic activity caused by the direct PK peptide fusion. This improvement was observed for both fusions at the N- (for OBPgp279) and C-terminal (for OBPgp279 and PVP-SE1gp146) ends. In general, the muralytic activity increased with a longer linker length. For C-terminal PK peptide fusion variants of OBPgp279, the positive effect of the extended linker on muralytic activity was most pronounced with a eight-fold higher value (Link 4) compared to the direct PK fusion variant. Extension of the linker length between the C-terminal PK peptide and PVP-SE1gp146, and the N-terminal PK peptide and OBPgp279, improved the enzymatic activity 2 and 1.6 times respectively. These observations demonstrate that insertion of a longer, more flexible linker is beneficial for the muralytic activity of a fusion protein. Probably, a longer spatial distance of the fused PK peptide to the N-terminal peptidoglycan binding or C-terminal catalytic domains allows for a less detrimental interaction with these domains, subsequently reducing the negative impact on the enzyme's activity. It is possible that the optimal linker length for muralytic activity has not been reached with the 16 extra amino acids and longer linkers are still able to further improve the muralytic activity.

8.4.2.3 Influence of N-or C-terminal extended linkers on *in vitro* antibacterial activity

The impact of a linker extension on the antibacterial activity was evaluated against *P. aeruginosa* PAO1, *S. Typhimurium* LT2, *E. coli* XL1-Blue MRF' (only for N-terminal extended linker constructs) and *A. baumannii* 25 (only for C-terminal extended linker constructs). A standard *in vitro* antibacterial activity assay was used here with the following parameters: 10^6 CFU/ml exponentially growing cells, application of 1.5 μ M for OBPgp279 variants and 5 μ M for PVP-SE1gp146 variants, 0.5 mM EDTA, 30 min incubation (Table 8.7).

Without EDTA, extension of the linker length increases or diminishes the antibacterial activity compared to the corresponding non-linker PK-fusion, dependent on the bacterial strain targeted or the endolysin used. Specifically for PK-OBPgp279, the observed antibacterial activity increases with the linker length. For the N-terminal extended linker variants, maximal improvements of 0.8 (OBPgp279, Link 4) and 0.42 (PVP-SE1gp146, Link 2) log units in reduction were observed, whereas for the C-terminal linker constructs the

Table 8.7: Antibacterial activity of N- and C-terminal extended linker variants of OBPgp279 (1.5 μ M) and PVP-SE1gp146 (5 μ M) without (A) and with (B) 0.5 mM EDTA on exponentially growing Gram-negative bacteria. Antibacterial activity indicated in logarithmic units. Averages \pm standard deviations of two repeated, independent experiments are shown. Significance classes for linker variants are indicated with A (class A = significant lower or equal to non-linker variant), B (class B = equal or significant higher than non-linker variant) or C (class C = significant higher than class B), according to two-tailed *t* test ($P < 0.05$). * = detection level of 10 CFU/ml is reached. ND = not determined.

		Antibacterial activity (in log ₁₀ units)					
A		<i>P. aeruginosa</i> PAO1		<i>S. Typhimurium</i> LT2		<i>E. coli</i> XL1-Blue MRF'	<i>A. baumannii</i> 25
	Linker length	N-terminal PK	C-terminal PK	N-terminal PK	C-terminal PK	N-terminal PK	C-terminal PK
PK-L _{1->4} -OBPgp279 OBPgp279-L _{1->4} -PK	No linker	2.61 \pm 0.09 ^A	2.18 \pm 0.11 ^B	0.23 \pm 0.01 ^A	0.25 \pm 0.11 ^A	0.43 \pm 0.02 ^A	1.46 \pm 0.02 ^A
	Link 1	3.02 \pm 0.01 ^B	2.54 \pm 0.09 ^C	0.36 \pm 0.03 ^B	0.31 \pm 0.07 ^A	0.45 \pm 0.01 ^A	1.54 \pm 0.07 ^A
	Link 2	3.10 \pm 0.04 ^B	2.18 \pm 0.15 ^B	0.34 \pm 0.03 ^B	0.39 \pm 0.05 ^A	0.46 \pm 0.05 ^A	1.50 \pm 0.05 ^A
	Link 3	3.36 \pm 0.12 ^C	2.14 \pm 0.17 ^B	0.35 \pm 0.03 ^B	0.41 \pm 0.23 ^A	0.49 \pm 0.04 ^A	1.53 \pm 0.02 ^B
	Link 4	3.41 \pm 0.18 ^C	1.69 \pm 0.10 ^A	0.33 \pm 0.02 ^B	0.13 \pm 0.08 ^A	0.50 \pm 0.06 ^A	1.57 \pm 0.08 ^A
PK-L _{1->4} -PVP-SE1gp146 PVP-SE1gp146-L _{1->4} -PK	No linker	1.20 \pm 0.11 ^A	0.81 \pm 0.03 ^B	0.30 \pm 0.10 ^B	0.14 \pm 0.04	0.29 \pm 0.09 ^A	0.12 \pm 0.04 ^B
	Link 1	1.50 \pm 0.13 ^B	1.00 \pm 0.18 ^B	0.39 \pm 0.05 ^B	ND	0.27 \pm 0.04 ^A	0.12 \pm 0.03 ^B
	Link 2	1.76 \pm 0.12 ^C	0.41 \pm 0.24 ^A	0.42 \pm 0.03 ^B	ND	0.28 \pm 0.01 ^A	0.09 \pm 0.06 ^B
	Link 3	1.62 \pm 0.08 ^B	0.68 \pm 0.28 ^B	0.44 \pm 0.11 ^B	ND	0.34 \pm 0.09 ^A	0.03 \pm 0.02 ^A
	Link 4	1.37 \pm 0.16 ^A	2.38 \pm 0.19 ^C	0.05 \pm 0.04 ^A	ND	0.28 \pm 0.01 ^A	0.05 \pm 0.02 ^A
B		<i>P. aeruginosa</i> PAO1		<i>S. Typhimurium</i> LT2		<i>E. coli</i> XL1-Blue MRF'	<i>A. baumannii</i> 25
	Linker length	N-terminal PK	C-terminal PK	N-terminal PK	C-terminal PK	N-terminal PK	C-terminal PK
PK-L _{1->4} -OBPgp279 + EDTA OBPgp279-L _{1->4} -PK + EDTA	EDTA	0.58 \pm 0.02		0.11 \pm 0.15		0.29 \pm 0.11	0.18 \pm 0.11
	No linker	5.38 \pm 0.19	4.94 \pm 0.24 ^A	0.91 \pm 0.04 ^A	0.28 \pm 0.15 ^A	1.70 \pm 0.01 ^A	4.96 \pm 0.28 ^A
	Link 1	>5.50*	4.96 \pm 0.10 ^A	1.37 \pm 0.09 ^B	0.60 \pm 0.30 ^A	1.96 \pm 0.02 ^B	5.18 \pm 0.17 ^A
	Link 2	>5.50*	4.84 \pm 0.07 ^A	1.39 \pm 0.13 ^B	0.54 \pm 0.32 ^A	2.04 \pm 0.08 ^B	4.69 \pm 0.11 ^A
	Link 3	>5.50*	5.04 \pm 0.12 ^A	1.46 \pm 0.11 ^B	0.18 \pm 0.05 ^A	2.04 \pm 0.14 ^B	5.08 \pm 0.25 ^A
PK-L _{1->4} -PVP-SE1gp146 + EDTA PVP-SE1gp146-L _{1->4} -PK + EDTA	No linker	4.92 \pm 0.23 ^A	4.99 \pm 0.41 ^B	0.73 \pm 0.30 ^A	0.15 \pm 0.04 ^A	0.85 \pm 0.17 ^A	5.33 \pm 0.20 ^C
	Link 1	5.07 \pm 0.13 ^A	4.99 \pm 0.21 ^B	0.74 \pm 0.08 ^A	0.17 \pm 0.09 ^A	0.89 \pm 0.01 ^A	4.30 \pm 0.29 ^B
	Link 2	5.30 \pm 0.18 ^B	4.69 \pm 0.15 ^B	0.83 \pm 0.08 ^A	0.19 \pm 0.06 ^A	0.95 \pm 0.08 ^A	3.80 \pm 0.16 ^A
	Link 3	5.47 \pm 0.08 ^B	4.77 \pm 0.52 ^B	0.85 \pm 0.09 ^A	0.10 \pm 0.03 ^A	0.95 \pm 0.02 ^A	4.07 \pm 0.20 ^A
	Link 4	4.89 \pm 0.10 ^A	3.94 \pm 0.41 ^A	0.89 \pm 0.12 ^A	0.12 \pm 0.07 ^A	0.89 \pm 0.05 ^A	3.89 \pm 0.14 ^A

maximal increases in reduction were 0.36 (OBPgp279, Link 1) and 1.57 (PVP-SE1gp146, Link 4) log units, respectively.

In presence of EDTA, bacterial reduction by the extended linker variants of PK-OBPgp279 is pushed under the detection limit of 10 CFU/ml (Table 7.7B). However, this is not significantly different from the corresponding construct without linker. Furthermore, the positive impact of the N-terminal extended linker variants of OBPgp279 was also observed on *S. Typhimurium* LT2 (+ 0.60 log units maximally, Link 4) and *E. coli* XL1-Blue MRF' (+ 0.71 log units maximally, Link 4). Except for the PK-Link 3-PVP-SE1gp146/EDTA combination on *P. aeruginosa* PAO1 (+ 0.55 log units), no significant added value in activity was present for the other linker constructs in the presence of EDTA. In case of *A. baumannii* 25, a longer C-terminal linker even significantly diminished the antibacterial activity of OBPgp279-PK and PVP-SE1gp146-PK. For the N-terminal extended linker variants of OBPgp279 with EDTA, the detection limit of 10 CFU per ml (= maximal measurable reduction with this experiment) was reached on *P. aeruginosa* PAO1.

In general, elongation of the linker length at the N- or C-terminal end of the endolysin seemed beneficial for its antibacterial activity, but this effect remains to be tested for every specific case. Dependent on the bacterial strain targeted, EDTA was necessary to observe the added value of the elongated linker constructs. This positive effect of the N-terminal extended linker on the antibacterial activity of the endolysin could be explained by the improvement of the muralytic activity, on one hand, and by the higher flexibility of the PK peptide, on the other hand. A flexible PK peptide probably interacts better with the outer membrane as it is able to penetrate deeper into this structure, resulting in a more efficient permeabilization and cell lysis.

8.5 Discussion

Impact of N-terminal PK peptide on enzyme characteristics

In this chapter, the impact of the PK peptide fusion approach, selected as most promising in the previous chapter, on protein expression, biochemical characteristics (including pH

dependence, muralytic activity and stability at higher temperatures) and *in vitro* antibacterial activity was evaluated in depth. A direct N-terminal fusion of the PK peptide significantly improved the enzyme yield during protein expression for four out of seven screened endolysins. Furthermore, the PK peptide fusion significantly improved the *in vitro* antibacterial potential of both modular, in presence and absence of EDTA, and single-domain endolysins, in presence of EDTA, especially on different *Pseudomonads*, including the multidrug-resistant *P. aeruginosa* Br667, and *Burkholderia*. In theory, this bacterial inactivation could be ascribed to the PK peptide alone. Indeed, polycationic peptides are thought to independently penetrate the Gram-negative outer membrane using the self-promoted uptake mechanism, showing bactericidal activity on its own (Hancock & Farmer, 1993). However, we think that a combination of the PK peptide action with the peptidoglycan lytic activity of the endolysin causes the observed bacterial inactivation. Whether the presence of the PK peptide is sufficient for the observed bactericidal effect or the catalytic and peptidoglycan binding properties of the endolysin are necessary, is not tested here. This could be investigated by inactivating both domains using site-specific mutagenesis of essential residues and monitoring the antibacterial strength of these mutants (Arima et al, 1997). One major disadvantage of the N-terminal PK fusion approach, the negative impact on enzymatic activity, is compensated by the outer membrane-permeabilizing capacity of the fused PK peptide. Another disadvantage of this approach is the negative impact on activity upon heat treatment, which specifically makes the PK-modified PVP-SE1gp146 variant less appropriate for usage in hurdle technology for food preservation than the unmodified endolysin. The Enterobacteriaceae *E. coli* XL1-Blue MRF' and *S. Typhimurium* LT2 are generally less sensitive for the PK peptide action due to structural differences in outer membrane stabilization. Despite the mentioned disadvantages, the data from this chapter surely prove the *in vitro* applicability of the PK peptide fusion approach against *Pseudomonads* and *A. baumannii*, which is a first major step in its development towards effective anti-Gram-negative compounds.

Biofilm degrading potential of PK-PVPgp146/EDTA approach

Improving the polycationicity of PVP-SE1gp146 seems to be beneficial for elimination of a 24-hour old *P. aeruginosa* PAO1 biofilm. This beneficial effect may be ascribed to the following two mechanisms: (1) the outer membrane permeabilizing potential of PK peptide

resulting in an efficient reduction or growth inhibition of bacteria within the biofilm, and (2) interaction of the positively charged residues of the PK peptide with the negatively charged stabilizing matrix components, including extracellular DNA, in a biofilm. Whitchurch and coworkers (2002) prove the essential role of this extracellular DNA in keeping the integrity of an existing *P. aeruginosa* biofilm. Furthermore, extracellular DNA serves as a structural component in all stages of biofilm formation by *Shewanella oneidensis* MR-1 under static and hydrodynamic conditions (Godeke et al, 2011). The interaction of the PK peptide with this stabilizing DNA may lead to the observed biofilm degradation, and subsequently to a better access of the PK-modified endolysin to the biofilm-forming cells.

Optimizing PK peptide fusion approach

In the last section of this chapter, we tried to optimize the direct PK fusion approach by switching the PK peptide from the N- terminal to the C-terminal end of the endolysin, on one hand, and by extension of the linker length between the N- or C-terminal fused PK peptide and the endolysin, on the other hand. The first optimization step, a C-terminal PK peptide fusion, was chosen to evaluate whether the observed enzyme-inhibiting effect could be abolished when the fused PK peptide is in close proximity to the catalytic domain, instead of the peptidoglycan binding domain. This switch turned out to be less effective for protein stability, enzymatic activity and antibacterial activity of OBPgp279 and PVP-SE1gp146, compared to the corresponding N-terminal PK peptide fusion. Both N- or C-terminal fusion modifications of endolysins decrease their enzymatic activity and the impact is protein-dependent. In literature, a limited amount of enzyme modifications to optimize characteristics of lytic enzymes have been described so far and the fusions described are all C-terminal fusions (Arima et al, 1997). The C-terminal fusion of HEWL with the pentapeptide Phe-Phe-Val-Ala-Pro diminished the enzymatic activity with 26 % compared to the unmodified HEWL (Ibrahim et al, 1994). The specific architecture of modular endolysins OBPgp279 and PVP-SE1gp146 demands for an N-terminal fusion instead of a C-terminal one, as the impact on the catalytic domain seems of higher importance for the original enzyme characteristics than the impact on the peptidoglycan binding domain. Based on these results, we suggest that future fusion modifications of Gram-negative modular endolysins should be targeting the peptidoglycan binding domain, whether it is located N-terminal, like

KZ144 or EL188, or C-terminal, like the putative endolysin (Lu11gp113) of the recently sequenced *P. aeruginosa* infecting phage Lu11 (Adriaenssens et al, 2012a).

Unlike the direct C-terminal fusion, the linker extension at both N- and C-termini, a second optimization step, is able to ameliorate the enzymatic activity (a 1.6 to 8-fold) and the *in vitro* antibacterial activity against *P. aeruginosa* PAO1 (with 0.4 to 1.57 log units reduction), dependent on the endolysin and linker length. In addition, this technique could significantly improve the antibacterial activity against the less sensitive Enterobacteriaceae *S. Typhimurium* LT2 and *E. coli* XL1-Blue MRF' with maximal reductions of 1.52 ± 0.07 and 2.41 ± 0.08 log units reduction, respectively, obtained with the PK-Link 4-OBPgp279/EDTA mixture (Table 7.8). We hypothesize that the higher flexibility of the PK peptide offers a less disturbing interaction with the enzyme and a more independent or autonomous action. This dual effect results in a more efficient outer membrane permeabilization and subsequent peptidoglycan lysis upon migration of the fusion protein through the bacterial outer membrane. In view of these preliminary results, the effect of constructs with longer extended linkers (> 16 amino acids) should be investigated in the future. The above results emphasize the important role for the optimization of the PK-fusion approach in improving its antibacterial activity and broaden its host range on Gram-negative bacterial pathogens.

Table 8.8: Optimal peptide-fused endolysin approach for each strain tested in this study. Reduction is expressed in logarithmic and procentual values.

Organism	Optimal approach	Bacterial reduction (in log ₁₀ units)
<i>P. aeruginosa</i> PAO1	PK-Link 4-OBPgp279/EDTA	> 5.50
<i>P. aeruginosa</i> Br667	PK-OBPgp279/EDTA	4.27 ± 0.15
<i>P. putida</i> G1	PK-OBPgp279/EDTA	4.89 ± 0.02
<i>B. pseudomallei</i>	PK-OBPgp279/EDTA	4.81 ± 0.05
<i>S. Typhimurium</i> LT2	PK-Link 4-OBPgp279/EDTA	1.52 ± 0.07
<i>E. coli</i> XL1-Blue MRF'	PK-Link 4-OBPgp279/EDTA	2.41 ± 0.08
<i>A. baumannii</i> 25	PVP-SE1gp146-PK/EDTA	5.33 ± 0.20

Antibacterial potential and cytotoxicity of PK-fused endolysin on an *in vitro* human keratinocyte infection model

9.1 A keratinocyte monolayer as alternative *in vitro* model

Since the first application of human keratinocytes for medical purposes (Green et al, 1979), improvements in the clinical use of cultured keratinocytes as skin grafts have been crucial for ameliorating treatments of patients with second or third degree burn wounds. On the other hand, these cultured keratinocytes also form an interesting *in vitro* alternative for the study of pathogen-skin interactions (de Breij et al, 2012; Sobral et al, 2007) and evaluation of new antibacterial compounds (Boyce et al, 1995) in a cost-effective and ethical-free way, instead of laborious *in vivo* models. As major part of the epidermis, keratinocytes form the outermost layer of the human skin functioning as a barrier against environmental damage, including ultra-violet radiation and bacterial infections. Barrier-disrupted human skin gets very easily infected by different Gram-negative bacteria, most importantly the opportunistic pathogens *P. aeruginosa* and *A. baumannii* (Taylor et al, 1990). In this chapter, we implement a human keratinocyte model, developed by Pirnay and coworkers in the Queen Astrid Military Hospital in Neder-Over-Heembeek (Brussels, Belgium), for evaluation of the cytotoxicity and antibacterial potential of the promising (PK-)OBPgp279/EDTA and (PK-)PVP-SE1gp146/EDTA mixtures upon infection with *P. aeruginosa*. The keratinocytes used in this model were specifically derived from neonatal foreskin from different human donors and cultured into monolayers according to clinical standards.

9.2 Cytotoxicity assessment on growing human keratinocytes

To assess possible cytotoxicity of the (PK-fused) endolysins ((PK-)OBPgp279 and (PK-)PVP-SE1gp146) and EDTA on a keratinocyte model, fresh keratinocytes are incubated for five days in the presence of different compound concentrations (EDTA: 0.5-5-50-500 μ M, endolysins: 2 μ M). In this way, the lethal concentrations of each compound can also be determined.

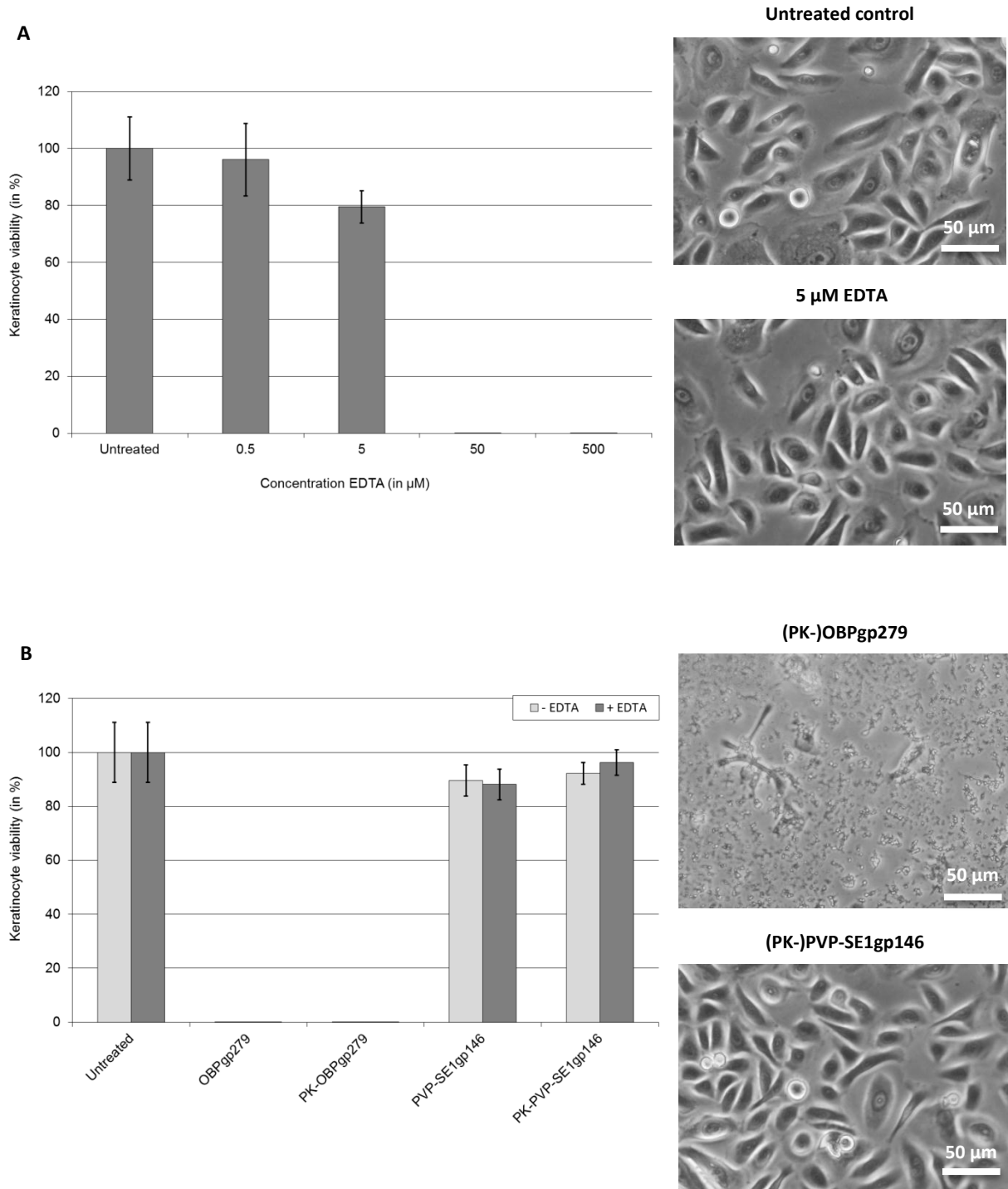


Figure 9.1: Assessment of cytotoxicity of EDTA, (PK-)OBPgp279, (PK-)PVP-SE1gp146 and a combination on fresh pre-cultured human keratinocytes. Keratinocytes were incubated with 0.5, 5, 50 and 500 μM of EDTA (A), 2 μM of each wild-type and PK-modified endolysin (B, light grey), and a combination of each endolysin with 5 μM of EDTA (B, dark grey bars) while growing into a confluent keratinocyte monolayer for five days. Components were supplied to the growth medium. After five days of incubation, viability of keratinocytes was determined in percentages relative to the untreated keratinocyte control (left graph). In addition, a corresponding microscopic visualization (100 x magnification) of the treated keratinocytes is depicted (right pictures) showing normal (for 5 μM EDTA and (PK-)PVP-SE1gp146) and toxic (for (PK-)OBPgp279) phenotypes.

At the end of the incubation period, the formed keratinocyte monolayer is trypsinized and keratinocyte viability is quantified microscopically by live/dead-staining with Trypan Blue. In Figure 9.1, percentages of keratinocyte viability relative to the untreated keratinocytes (= 100 %) are indicated together with microscopic evaluation of keratinocyte phenotypes.

In case of EDTA, 5 μM is the highest concentration that results in a normal adhesion/morphology of the keratinocyte monolayer (Figure 9.1A). Applying higher EDTA concentrations (50 and 500 μM) eventually leads to the release of the keratinocytes from the bottom of the culture flasks. This made the formation of a monolayer and the subsequent quantification of keratinocyte viability using Trypan Blue staining impossible. In the past, Watt and coworkers (Watt et al, 1984) showed that EDTA-induced monolayer dissociation (at concentrations of 600 μM EDTA or more) is due to complexation of the available Ca^{2+} -ions in the culture, which form a prerequisite for the connection of adjacent keratinocytes to obtain a stratified monolayer. For compatibility reasons, 5 μM of EDTA has been used to assess cytotoxicity of the combination of EDTA with the (PK-)endolysins.

Interestingly, when we look to the effect of the unmodified endolysins on the keratinocyte growth, a different outcome can be observed. The keratinocytes that were incubated with OBPgp279 were disintegrated or lysed, and appeared as patches of cell debris under the microscope (Figure 9.1B). The presence of lysed keratinocytes was already observed after one day of incubation with the protein. The exact reason for this effect induced by OBPgp279 awaits further investigation, but could possibly be linked to LPS impurities still present in the enzyme sample by potential LPS binding capacity of the protein. Keratinocytes treated with PVP-SE1gp146, on the other hand, formed a normal monolayer after 5 days of incubation (Figure 9.1B). For the PK-modified endolysins PK-OBPgp279 and PK-PVP-SE1gp146, the same effect on keratinocyte growth was observed as for the corresponding unmodified endolysins. Based on the result for PK-PVP-SE1gp146, we conclude that the N-terminal addition of a PK peptide to an endolysin does not have a negative impact on its cytotoxicity towards human keratinocytes. In addition, the combination of (PK-)PVP-SE1gp146 with 5 μM of EDTA induced no toxic effects on the keratinocytes either (data not shown). It is therefore justified to use this combination for assessment of the *in vitro* antibacterial efficacy on a human keratinocyte monolayer model.

9.3 Antibacterial efficacy on a keratinocyte infection model

In a next step, the antibacterial activity of the (PK-)PVP-SE1gp146/EDTA and (PK-)OBPgp279/EDTA combinations was evaluated on a 100 % confluent grown keratinocyte monolayer. Two clinical *P. aeruginosa* isolates, Br667 (a burn wound isolate) and PA14 (a urinary tract isolate), were selected for infection of this monolayer. Both strains differ in multidrug-resistance and keratinocyte cytotoxicity, representing the differences present among clinical *P. aeruginosa* strains (Pirnay et al, 2009). Br667 is resistant to 10 out of 11 commonly used antibiotics, but is only slightly cytotoxic for keratinocytes. Contrarily, PA14 is strong cytotoxic for keratinocytes due to its ability to secrete the virulence factor exoenzyme U, a bacterial toxin that is correlated with highly virulent and cytotoxic *P. aeruginosa* strains (Schulert et al, 2003). PA14, however, shows almost no antibiotic resistance.

In a first trial, the keratinocyte monolayer was infected with Br667 or PA14 at an initial cell density of 10^5 CFU per ml. One hour after infection, (PK-)PVP-SE1gp146 or (PK-)OBPgp279 (2 μ M) were added with EDTA (5 μ M) to the keratinocyte monolayer and incubated for an additional 3 hours. After 4 hours of infection, keratinocyte viability and bacterial reduction were quantified by Trypan Blue live/dead staining and plating, respectively. Results for both bacterial strains are depicted in Figure 9.2. Interestingly, unmodified or PK-modified PVP-SE1gp146 in combination with EDTA is able to protect the keratinocytes from the cytotoxic effects upon infection with PA14 (Figure 9.2B). The keratinocyte viability increases from 46 % for the untreated, PA14-infected keratinocytes to 91 and 97 % for the PVP-SE1gp146- and PK-PVP-SE1gp146-treated keratinocytes, respectively. This remarkable increase in viability obtained for both proteins is due to the bacterial reduction of PA14 with 89 % by PVP-SE1gp146 and 94 % by PK-PVP-SE1gp146, as concluded from the bacterial count data (Figure 9.2A). Despite the previous observation of disintegrated keratinocytes upon addition of OBPgp279 and PK-OBPgp279, both proteins are still active here, resulting in a reduction of PA14 with 91 and 95 % in the presence of EDTA, respectively (Figure 9.2A). In contrast to (PK-)PVP-SE1gp146/EDTA, however, the keratinocyte viability is not improved upon endolysin/EDTA treatment, but remains identical to the viability for the untreated, PA14-infected keratinocytes (43 %). The presence of LPS impurities in the (PK-)OBPgp279 samples due to potential LPS binding might explain the absence of keratinocyte recovery.

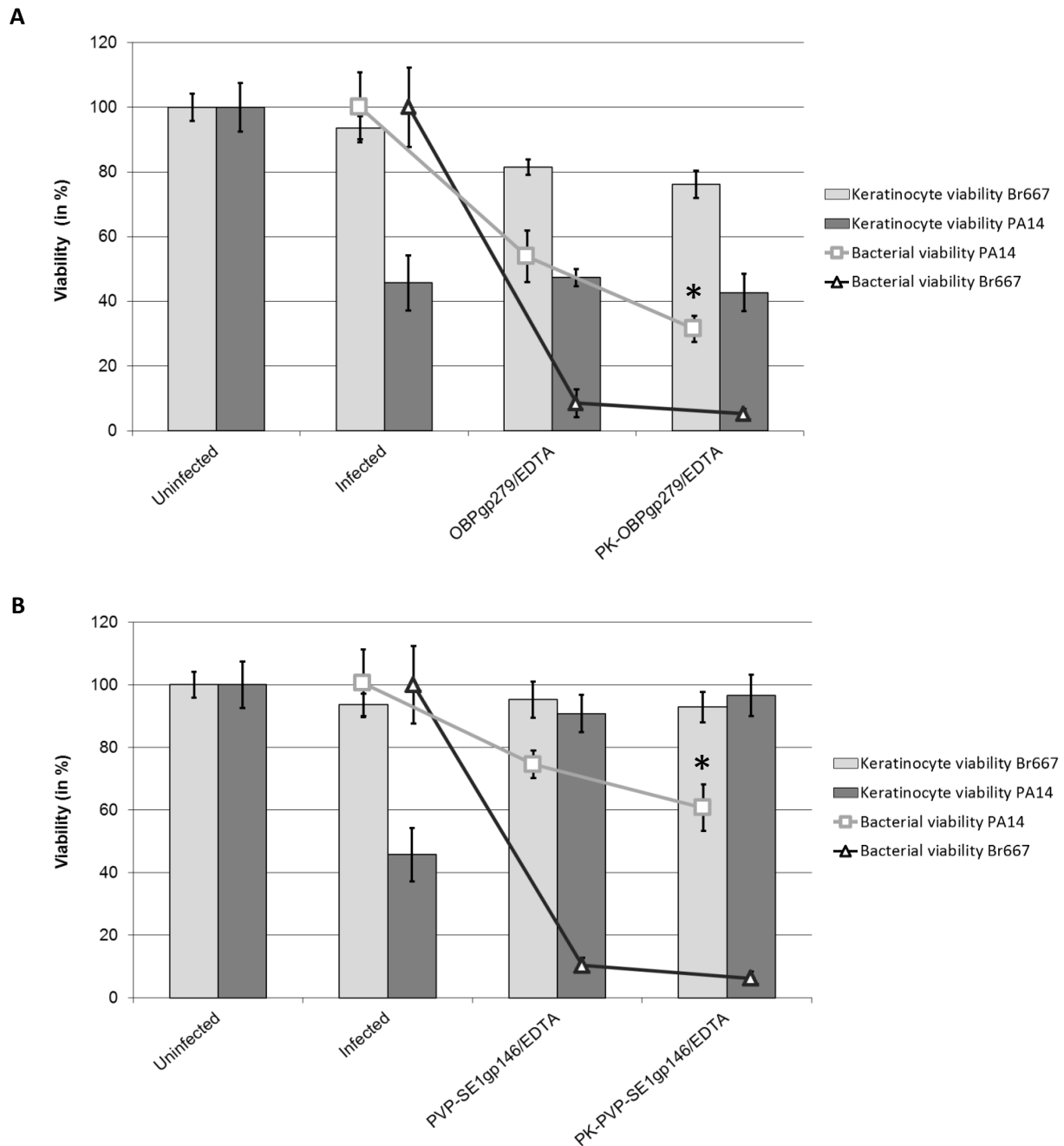


Figure 9.2: *In vitro* antibacterial efficacy of (PK-)OBPgp279/EDTA (A) and (PK-)PVP-SE1gp146/EDTA (B) combinations on human keratinocyte infected by *P. aeruginosa* Br667 and PA14. A 100 % confluent keratinocyte monolayer was infected with 10^5 CFU/ml of each strain. One hour after infection, 2 μ M of endolysin together with 5 μ M of EDTA were added. Bacterial viability (lines) and keratinocyte viability (bars) were quantified after four hours of infection by a plating/counting assay and a Trypan Blue live/dead staining assay, respectively. Bacterial viability is shown in percentages relatively to the untreated, infected control (= 100 %). Keratinocyte viability is determined as the proportion of living keratinocytes to the total amount of keratinocytes, and is shown in percentages relatively to the uninfected keratinocyte control (= 100 %). Averages and standard deviations of two independent experiments are depicted. Significant differences between unmodified and PK-modified endolysins are marked with an asterisk (*) (two-tailed *t* test, $P < 0.05$).

As a result, the apparent keratinocyte disintegration and the efficient bacterial reduction induced by the (PK-)OBPgp279/EDTA mixture, balance each other, leading to an almost unchanged keratinocyte viability.

In case of *P. aeruginosa* strain Br667, the bacterial reduction induced by PVP-SEgp146 (22 %) and PK-PVP-SE1gp146 (39 %) is more limited. Due to the low cytotoxicity of Br667 on human keratinocytes (only 6 % viability reduction), no significant increase in keratinocyte viability could be detected, compared to the untreated, infected control. Almost the same conclusion could be made for OBPgp279 and PK-OBPgp279, except for the lower keratinocyte viability (around 80 %) compared to the untreated, Br667-infected keratinocytes due to the observed cytotoxicity. In contrast to PA14, the PK peptide significantly increased the antibacterial activity of PVP-SE1gp146 and OBPgp279.

Due to the strong antibacterial effect of PVP-SE1gp146/EDTA under the tested conditions, we could not determine if the PK peptide had an added value on the *in vitro* antibacterial efficacy of PVP-SE1gp146 against *P. aeruginosa* PA14. Therefore, we repeated the experiment with a higher initial cell density of 10^7 CFU/ml for PA14 (Figure 9.3). At this cell density, the untreated, PA14-infected keratinocytes were almost completely eradicated with only 3 % of keratinocyte viability left after 4 hours of infection. The higher PA14 titer allowed for a stronger keratinocyte lysis due to the ExoU toxin and a less efficient, yet significant, bacterial reduction induced by PVP-SE1gp146/EDTA (31 % reduction) and PK-PVP-SE1gp146/EDTA (71 % reduction) compared to the 10^5 CFU/ml cell density. In this experiment, the PK peptide induced an significant increase both in bacterial reduction, from 31 to 71 % reduction, and in keratinocyte viability, from a 14 % viability for PVP-SE1gp146 to a 27 % viability for PK-PVP-SE1gp146. This observation definitely proves the added value of the PK peptide in improving the *in vitro* antibacterial efficacy of PVP-SE1gp146 on a human keratinocyte model.

9.4 Discussion

In this chapter, we selected a human keratinocyte monolayer for evaluation of the cytotoxicity and antibacterial efficacy of two endolysins, OBPgp279 and PVP-SE1gp146, and

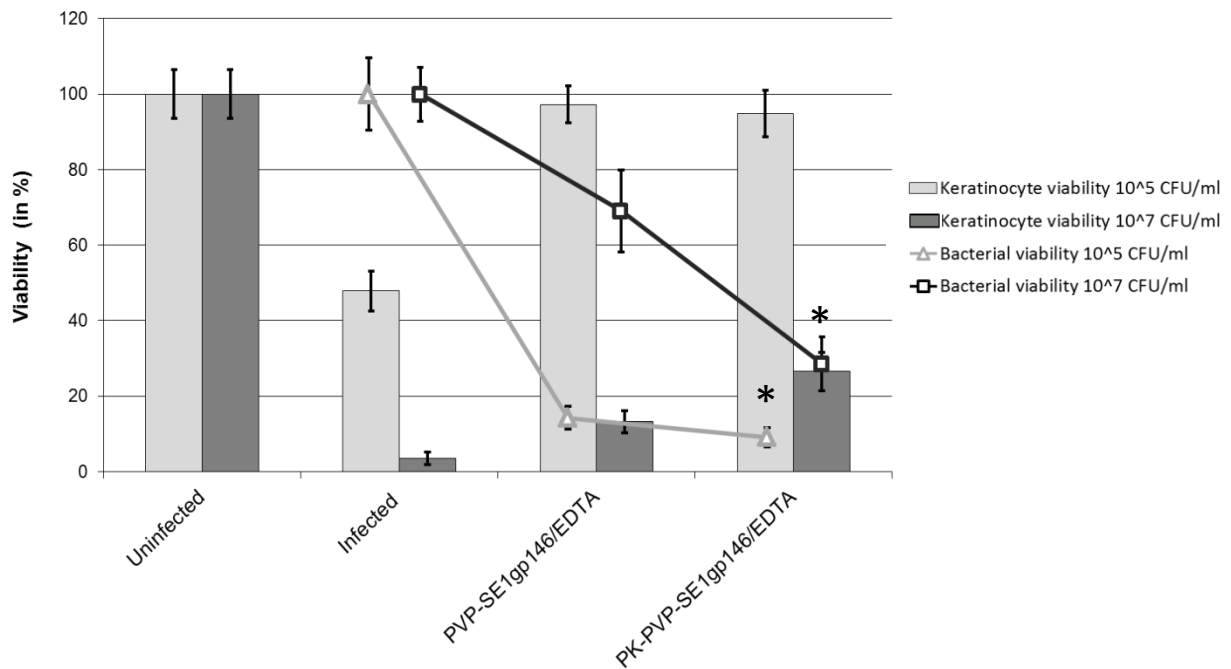


Figure 9.3: *In vitro* antibacterial efficacy of (PK-)PVP-SE1gp146/EDTA combination on human keratinocyte model infected by 10⁵ and 10⁷ CFU/ml of *P. aeruginosa* PA14. A five day old keratinocyte monolayer culture; grown to 100 % confluence, was infected. One hour after infection, 2 μ M of endolysin together with 5 μ M of EDTA were applied on the keratinocyte monolayer. Bacterial viability (lines) and keratinocyte viability (bars) were quantified after four hours of infection by a plating/counting assay and a Trypan Blue live/dead staining assay, respectively. Bacterial viability is shown in percentages relatively to the untreated, infected control (= 100 %). Keratinocyte viability is determined as the proportion of living keratinocytes to the total amount of keratinocytes, and is shown in percentages relatively to the uninfected keratinocyte control (= 100 %). For both graphs, averages and standard deviations of two independent experiments are depicted. Significant differences between unmodified and PK-modified endolysin are marked with asterisk (*) (two-tailed *t* test, $P < 0.05$).

their PK-modified variants (PK-OBPgp279 and PK-PVP-SE1gp146), upon infection with *P. aeruginosa* PA14 and Br667. A keratinocyte model forms an interesting alternative for cost-expensive and time-consuming *in vivo* assays circumventing ethical regulations and issues. Furthermore, the number of animal testing can be reduced significantly. This keratinocyte infection model mimics the upper layer of a *P. aeruginosa*-infected human skin, and therefore forms a logical bridging step between earlier *in vitro* assays (see Chapters 4 to 8) and further *in vivo* gut colonization in a *C. elegans* nematode model (see Chapter 10).

Remarkably, our data revealed the disintegration of growing keratinocytes upon addition of OBPgp279 and PK-OBPgp279, in contrast to (PK-)PVP-SE1gp146. One hypothesis is the potential presence of high amounts of LPS molecules that are copurified with the enzymes

during the single-step Ni²⁺-NTA purification process. Another hypothesis is the potential LPS-binding ability of OBPgp279, as described for other enzymes including lactoferrin, an iron-binding antimicrobial glycoprotein present in human secretory fluids (Drago-Serrano et al, 2012), or the bacterial and mammalian 20S proteasome, an enzyme complex necessary for proteolysis of damaged proteins (Qureshi et al, 2003). Both copurified and bound LPS could trigger a complex immunological pathway in human keratinocytes by activation of the TLR4/MD-2/CD14 receptor complex present on the keratinocyte cell membrane, resulting in a rapid intracellular Ca²⁺ response and the production and secretion of proinflammatory cytokines and chemokines (Song et al, 2002). The presence of LPS impurities in the OBPgp279 solution might be detected and quantified with the chromogenic “Limulus amoebocyte lysate” assay (Cooper et al, 1972). Bound LPS could be detected in a similar way after enzymatic digestion (proteinase K) (Petsch et al, 1998) or denaturation of (PK-)OBPgp279 and subsequent release of the bound LPS molecules. Using LPS-free expression systems (yeast or cell-free expression) with LPS-free medium might offer possibilities to reduce the amount of LPS in the OBPgp279 sample and test the proposed hypotheses. Based on these results, we can exclude the presence of cytotoxic effects under the tested conditions due to the fused PK peptide. The absence of cytotoxicity for the PK peptide could be linked with the lower affinity of cationic antimicrobial peptides for a keratinocyte membrane consisting of neutral, zwitterionic phospholipids, instead of anionic ones, like in bacterial membranes (see 1.4.2.1 Membrane perturbing action) (Oren & Shai, 1998).

Interestingly, both PVP-SE1gp146/EDTA and PK-PVP-SE1gp146/EDTA were able to protect the infected keratinocytes from the cytotoxic effects of *P. aeruginosa* PA14 (10⁵ CFU/ml) by efficiently reducing this pathogen with 89 and 95 %, respectively. The strong cytotoxicity of PA14 can be ascribed to the aggressive ExoU toxin, which is directly injected through a type III secretion system in the keratinocyte cytoplasm upon adhesion of PA14 to the keratinocyte cell wall. Once inside the cytoplasm, ExoU mediates rapid lysis or necrosis of the targeted cell by membrane-disruption using its phospholipase domain (Gendrin et al, 2012).

When the keratinocytes are infected with a higher initial PA14-titer (10⁷ CFU/ml), the added value of the PK peptide on keratinocyte viability and the bacterial reduction became more clear, but higher amounts are probably needed for full protection. This protection could not

be visualized for OBPgp279/EDTA and PK-OBPgp279/EDTA, although (PK-)OBPgp279/EDTA could efficiently reduce PA14 (90-95 % reduction) in the applied keratinocyte model. The positive evaluation of (PK-)PVP-SE1gp146/EDTA on the human keratinocyte model is an important boost for the future application of the PK-fused endolysin approach in the treatment of skin infections. However, the observed disintegration of growing keratinocytes upon (PK-)OBPgp279 addition emphasizes the importance of a careful evaluation of fusion proteins on human keratinocytes. To our knowledge, this study proves for the first time the antibacterial potential of a wild-type and a modified endolysin in combination with micromolar EDTA concentrations on a human keratinocyte infection model.

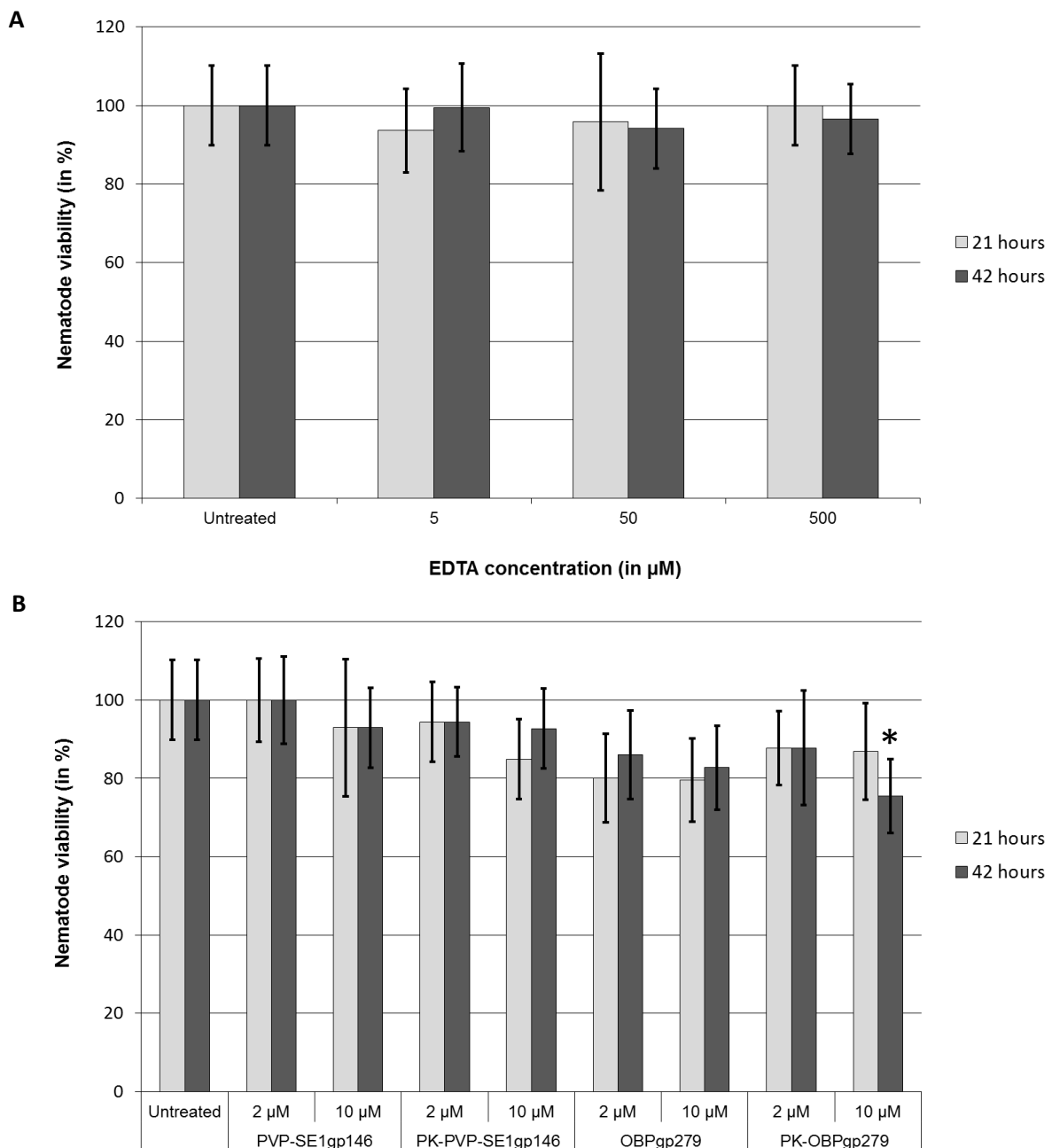
Antibacterial potential and cytotoxicity of PK fusion endolysins on *in vivo* *Caenorhabditis elegans* nematode model

10.1 *C. elegans* as model organism for bacterial pathogenesis

Since the discovery by Brenner in 1974 (Brenner, 1974), *C. elegans*, a soil-dwelling nematode, has been used extensively as a model organism in many fields of biological research, including cell development, aging and neurobiology. In the last two decades, scientists also started to use this small worm for the research of microbial pathogenesis, the innate immune system and drug development (Ewbank & Zugasti, 2011). Its simplicity (only 20,000 genes), short generation time, transparency, easy growth conditions and lack of ethical legislation/concerns make it the ideal animal model for rapid *in vivo* high-throughput experiments. Furthermore, *C. elegans* can be infected by a broad range of Gram-positive and Gram-negative bacterial pathogens (Powell & Ausubel, 2008; Sifri et al, 2005), including pathogenic *P. aeruginosa* (Tan et al, 1999), *A. baumannii* (Smith et al, 2004), *S. Typhimurium* (Aballay et al, 2000) and *E. coli* (Garsin et al, 2002). As a food source in laboratory conditions, the non-pathogenic *E. coli* OP50 strain is used which is taken up through the nematode's mouth and grinded for extraction of necessary nutrients by the terminal pharyngeal bulb. Pathogens, however, have developed a way to circumvent this grinding process as they are able to further invade and colonize the gut of the nematode, eventually leading to the nematode's death. All these characteristics define *C. elegans* as a useful *in vivo* model to assess the influence of antimicrobial compounds on bacterial pathogenesis. Recently, Uccelletti and coworkers (2010) could successfully increase the survival rate of *Pseudomonas*-infected *C. elegans* by treatment with the frog-derived antimicrobial peptide esculentin. Analogously, we implement the *C. elegans* nematode model as an *in vivo* setting to evaluate the potential cytotoxic effects, on one hand, and the antibacterial efficiency, on the other hand, of (PK-)OBPgp279/EDTA and (PK-)PVP-SE1gp146/EDTA mixtures. Both toxicity and *in vivo* antimicrobial activity are fundamental prerequisites that should be addressed for further successful development into potential therapeutic enzyme-based antibacterials.

10.2 Cytotoxicity assessment on *C. elegans*

Prior to the assessment of the *in vivo* antibacterial efficacy, a toxicity experiment of the different components (EDTA, (PK-)OBPgp279 and (PK-)PVP-SE1gp146) and the combination of these components was conducted on *C. elegans* SS104. This allows us to determine the *in vivo* lethal doses of the components against uninfected nematodes. Briefly, a total of ± 30 nematodes were incubated for 42 hours in liquid medium for each condition (single components and combination) to be tested. Nematode viability was manually assessed by pinching the nematodes 21 and 42 hours after addition (Figure 10.1).



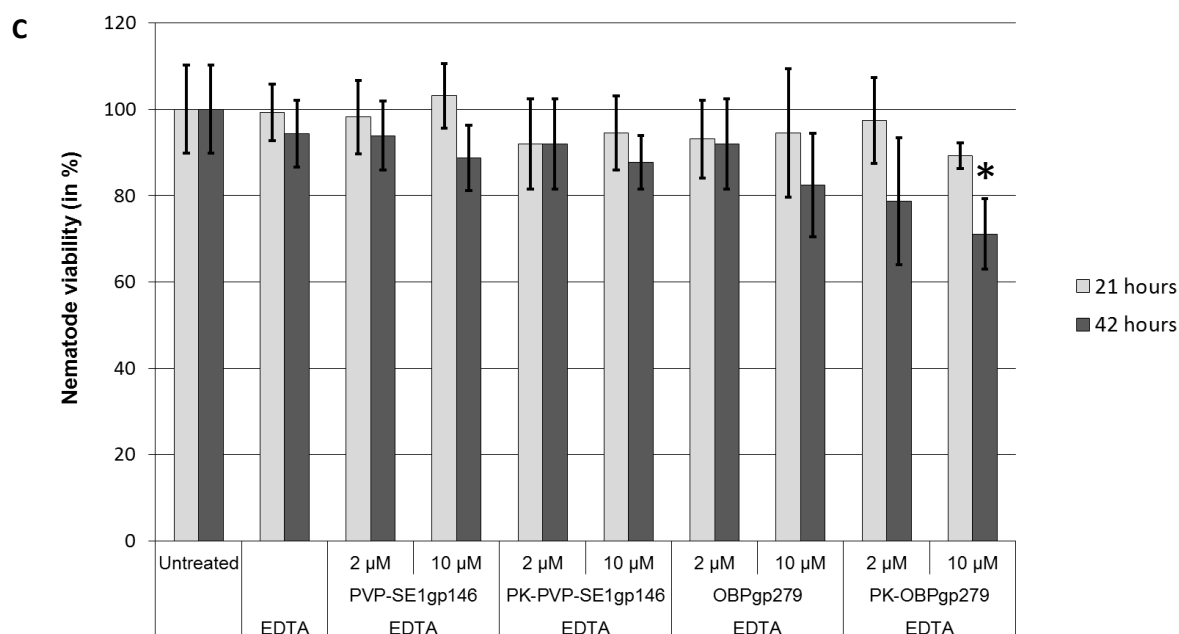


Figure 10.1: *In vivo* cytotoxicity of EDTA (A), (PK-)OBPgp279 and (PK-)PVP-SE1gp146 (B), and the combination of both (C) on *C. elegans* SS104 nematodes. Uninfected L4 stage synchronized nematodes were incubated together with the compounds and nematode survival was visually monitored by pinching them 21 (grey bars) and 42 (black bars) hours after infection. Survival was expressed as a percentage relative to the non-treated nematodes. Three different concentrations of EDTA (5, 50 and 500 μ M) and 2 different concentrations of (PK-)OBPgp279 and (PK-)PVP-SE1gp146 (2 and 10 μ M) were applied. For the combination, 500 μ M EDTA was used. Averages and standard deviations of two independent experiments are depicted here. Asterisks (*) mark the statistical significant values with the untreated control (two-tailed *t*-test, $P < 0.05$)

For PVP-SE1gp146, no significant toxicity was present at 2 and 10 μ M, whereas OBPgp279 reduces the nematodes with ± 20 % irrelevant of the tested concentration, but not significant compared to the control (Figure 10.1B). In case of PK-OBPgp279, a significant reduction in nematode viability (± 25 %) was observed at a concentration of 10 μ M, but only after 42 hours of incubation. As seen in Figure 10.1A, EDTA had no negative impact on *C. elegans* SS104 survival, at all tested concentrations. Therefore, we chose the highest concentration (500 μ M) of EDTA for cytotoxicity assessment of the (PK fusion) endolysin/EDTA combinations. For PK-OBPgp279, nematode reduction was also present in combination with 500 μ M EDTA after 42 h, at 2 (± 22 %) and 10 (± 30 %) μ M (Figure 10.1C). For PK-PVP-SE1gp146 in the presence of EDTA, such a slight toxicity was not observed, neither after 42 hours incubation and at the highest tested concentration of 10 μ M. The impact on *C. elegans* SS104 viability seems protein-dependent. Nonetheless, safety may become an issue in further stages and should therefore be extensively tested on higher-order animals, including mouse or rat infection models if further development is wanted.

10.3 *In vivo* antibacterial efficacy on *C. elegans*

10.3.1 Selection of appropriate *P. aeruginosa* strain for infection of *C. elegans* SS104

Based on a preliminary infection screen, *P. aeruginosa* PA14 was chosen as candidate from three different pathogenic *P. aeruginosa* strains (Br667, Us447 and PA14) to infect *C. elegans* SS104 for assessment of *in vivo* antibacterial efficacy of the (PK fusion) endolysins in presence of EDTA (Figure 10.2). More than 60 % of the PA14-infected *C. elegans* SS104 worms are killed 3 days after infection, whereas Br667 and Us447 don't influence *C. elegans* SS104 viability during the same period. Bacterial colonization can be followed microscopically by the appearing of small, black dots inside the nematode gut as a function of time, indicating the presence of proliferating bacterial cells. In this way, we observed that the infection by Br667 and Us447, both multidrug-resistant clinical isolates, developed slower than a PA14 infection. This observation was consistent with the lower killing rate of *C. elegans* observed for Br667 and Us447 in comparison to PA14.

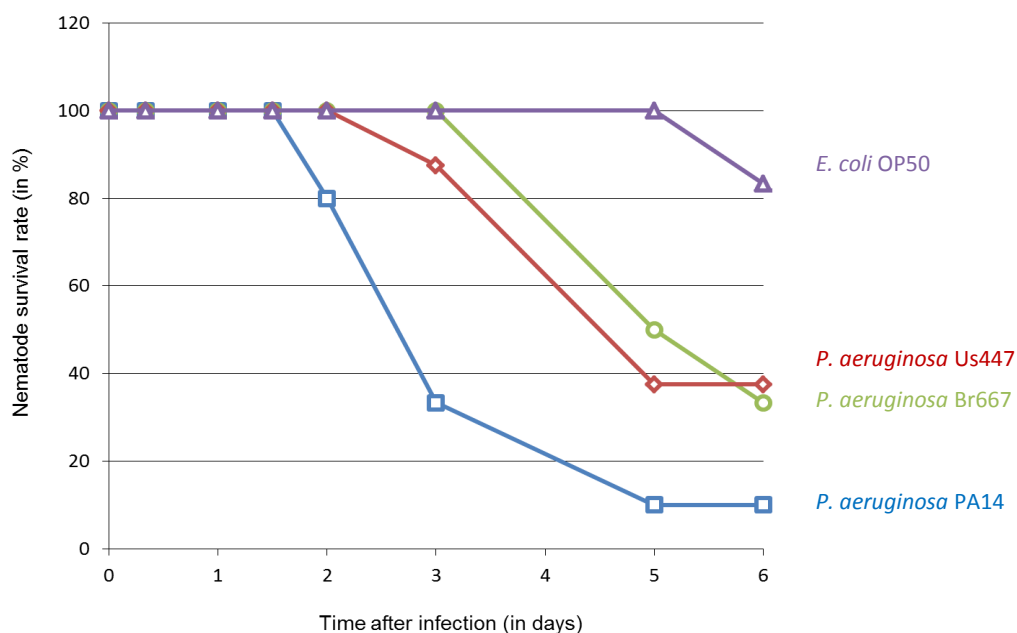


Figure 10.2: Killing rate of *C. elegans* SS104 by *P. aeruginosa* PA14 (blue squares), Us447 (red diamonds) and Br667 (green circles) in function of time. L4 stage synchronized *C. elegans* SS104 nematodes were infected by seeding them on NGM agar plates overgrown with the specific bacterial strain and subsequent incubation for 24 hour at 37°C. Nematode viability was assessed by pinching at different time points for 6 days after infection. Non-pathogenic, food source *E. coli* OP50 (purple triangles) was used as negative control.

10.3.2 Survival of *P. aeruginosa* PA14-infected *C. elegans* SS104 after endolysin treatment

Using the appropriate *P. aeruginosa* strain and the suitable conditions for infection, mixtures of (PK-)OBPgp279 or (PK-)PVP-SE1gp146 (both at concentrations of 2 and 10 μM) with EDTA (0.5 mM) were tested to assess the potential effect on the viability of the PA14-infected *C. elegans* SS104. As a positive control for effective antibacterial activity against PA14 in the nematode gut, the antibiotic ciprofloxacin was used at a concentration of 0.3125 $\mu\text{g}/\text{ml}$, which is 5 times the MIC value for this antibiotic. Ciprofloxacin does not induce toxic effects on the *C. elegans* model at this concentration (data not shown). Untreated nematodes grown on PA14 (negative control) and the non-pathogenic *E. coli* OP50 were added for correct interpretation of the experimental outcome. Before treatment, infected nematodes were washed to remove external bound bacterial cells that could interfere with the experimental outcome. A total of 50 washed nematodes were incubated at 25°C in the presence of each different test condition and their viability was assessed by nematode pinching 1 and 5 days after addition of the test compounds (Figure 10.3).

Interestingly, both combinations of OBPgp279 and PVP-SE1gp146 with EDTA increase the nematode survival with a 23 % and 21 % for 2 μM , and a 27 and 23 % for 10 μM , respectively, compared to the untreated control after 5 days of treatment. For both unmodified endolysins, nematode survival is not significantly enhanced by increasing the enzyme concentration in this time period. In case of PK-PVP-SE1gp146, the presence of the PK peptide is responsible for a significant increase (24 % for 2 μM and 33 % for 10 μM) in survival compared with unmodified PVP-SE1gp146. Such a promotive effect could not be detected for the other PK-modified endolysin, PK-OBPgp279, where the additional reduction is more limited (6 % for 2 μM and 8 % for 10 μM). The different impact of the PK peptide on nematode survival after 5 days of treatment between PK-OBPgp279 and PK-PVP-SE1gp146 might be due to the small toxic effects induced by PK-OBPgp279 (Figure 10.1), resulting in a lower nematode viability. Remarkably, more nematodes are rescued by a treatment with 2 and 10 μM PK-PVP-SE1gp146/EDTA (55 and 66 %, respectively) than with ciprofloxacin (39 %) after 5 days.

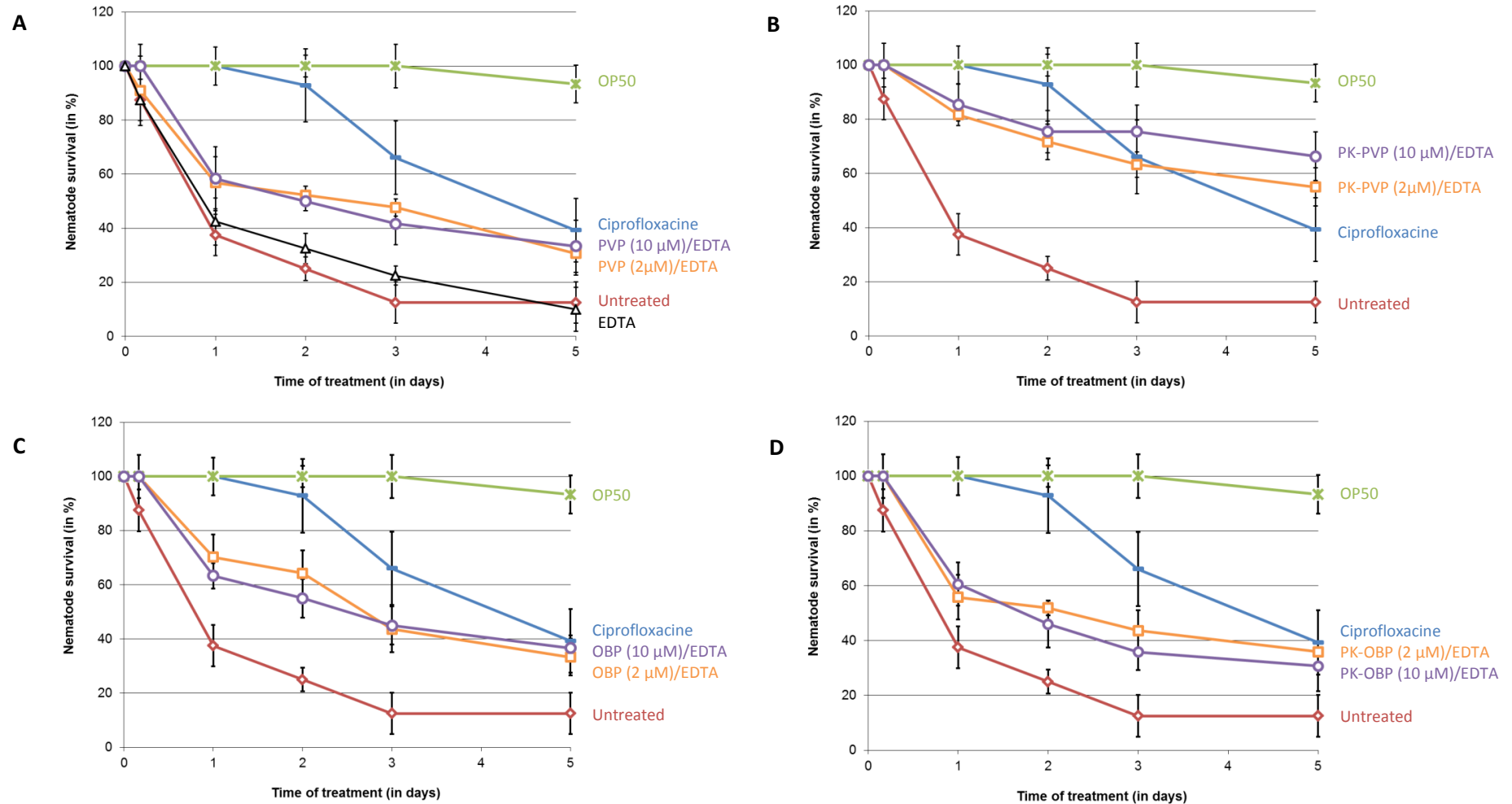


Figure 10.3: Survival of PA14-infected *C. elegans* SS104 nematodes treated with PVP-SE1gp146/EDTA (A), PK-PVP-SE1gp146/EDTA (B), OBPgp279/EDTA (C) and PK-OBPgp279/EDTA (D) mixtures. For each endolysin, 2 (orange, circles) and 10 (purple, squares) μM were added with 0.5 mM EDTA. Ciprofloxacin (0.3125 $\mu\text{g}/\text{ml}$) (blue) was used as positive control for antibacterial activity. Other controls included were EDTA-treated, PA14-infected nematodes (black, triangles, only shown in A), untreated, PA14-infected nematodes (red, diamonds) and untreated nematodes grown on *E. coli* OP50 (green, *). A total of thirty PA14-infected worms were used for each condition. Nematode viability was assessed at different time points after compound addition. Averages and standard deviations of two independent experiments are depicted.

10.4 Discussion

Key aspects in the development of a new antibacterial agent are the potential cytotoxicity and antibacterial efficacy in *in vivo* animal models. Here, we used a *C. elegans* nematode model to evaluate the potency of the (PK-)OBPgp279/EDTA and (PK-)PVP-SE1gp146/EDTA combinations to rescue nematodes infected with the cytotoxic *P. aeruginosa* strain PA14. This gastro-intestinal model forms the ideal stepping stone to future mice experiments.

Our experimental outcome pointed out that most of the different tested components, including (PK-)OBPgp279, (PK-)PVP-SE1gp146 and EDTA, lack strong toxicity on the *C. elegans* nematodes. Only for (PK-)OBPgp279 with and without EDTA, small reductions in viability were monitored. Similar as for the keratinocyte model, this observation might be due to LPS copurification, associated with the single-step purification process, or LPS binding. Addition of a second purification step (e.g. ion exchange chromatography) should higher purity of the enzyme solutions. In addition, assessing the biochemical (cell apoptosis, oxidative stress) and molecular-level (modifications in gene expression) responses upon administration of these compounds to the nematodes could clarify if toxic effects are present or not (Li et al, 2012). The fact that the nematodes in this study are hardly affected by these compounds does not immediately implicate that higher organisms are not sensitive for the compound's activities. *C. elegans* lacks the adaptive immune system present in mammals and only relies on an innate immunity system that partly resembles the systems in flies and mammals (Kurz & Ewbank, 2003). It is especially the adaptive immunity of humans that triggers an immune response on exposure with unknown proteins or peptides (like endolysins), leading to transcription of cytokines, chemokines and other potentially toxic, immune-related effector molecules. Evaluation of toxicity on another model organism that is evolutionary closer to humans, for example a mouse infection model, will still be necessary as alternative to approve safety for further therapeutic applications.

P. aeruginosa PA14 was selected from four different *P. aeruginosa* strains to infect *C. elegans*. This strain is known to mediate two types of infection, dependent on the growth media (Sifri et al, 2005). When grown on minimal medium, PA14 kills *C. elegans* relatively

slowly over the course of several days by colonization of the nematode digestive tract (“slow killing”). In contrast, PA14 is able to produce diffusible toxins from the phenazine/pyocyanin class when grown on rich medium that rapidly kill the nematodes in a 24 hour time frame without colonization (“fast toxin-mediated killing”) (Mahajan-Miklos et al, 1999). In our study, the slow killing mechanism was used as it took more than three days to eradicate the majority of nematodes. In addition, the presence of colonizing bacterial cells was detected microscopically as black dots in the nematode gut, typically for slow killing.

Both OBPgp279 and PVP-SE1gp146 in presence of EDTA were able to significantly promote the survival of PA14-infected *C. elegans* nematodes with 21 to 27 % in a five day time period. In case of PVP-SE1gp146, this increase in viability could be significantly improved by an N-terminal fusion of the anti-*Pseudomonas* PK peptide to the endolysin, which reduced lethality of the infected worms with an additional 30 %. A critical factor in the possible outcome for the *in vivo* antibacterial activity is the presence of proteases produced by the nematode which could degrade the endolysins during the five day incubation period. In the past, several aspartyl (Geier et al, 1999; Lochnit et al, 2006) and cysteine (Xue et al, 1996) proteases were detected in *C. elegans*. Addition of protease inhibitors, or administration of multiple compound dosages, for example each 24 hour, might exclude protease interference (Bhatia et al, 2011).

Despite the positive effect on the survival rate, we still need to investigate whether the increased survival is really due to the bacterial reduction in the nematode gut induced by the PK fusion endolysin/EDTA mixture. This could be achieved either by an invasive or a non-invasive procedure. In the invasive method, infected nematodes are first washed in gentamycin to remove external bound bacterial cells, broken with Triton X-100 or glass beads and the residual colony forming units present in the nematode gut are quantified (Uccelletti et al, 2010). The non-invasive method makes use of a fluorescent-labeled or bioluminescent *P. aeruginosa* strain, like the Lumi-PAK strain available from the Pasteur Institute (Debarbieux et al, 2010), for infection of the nematodes. Fluorescence-labeling could be achieved by transformation of a particular bacterial strain with a GFP-encoding plasmid under a constitutive promoter. In both ways, the achieved bacterial reduction can

be easily monitored and quantified by measurement of the emitted light throughout the incubation period.

Regardless of the remaining challenges and restrictions in using the *C. elegans* model, the above *in vivo* work is an important step in the further development of the PK fusion endolysin approach for therapeutic application. To our knowledge, this is the first report that shows the positive influence of a modified endolysin/EDTA mixture on the survival of *P. aeruginosa*-infected *C. elegans* nematodes.

General conclusions and future perspectives

In this last chapter, we give a short overview of the most important conclusions from this dissertation, together with a discussion on future perspectives and implications of this work. This final chapter is split up in three major parts. A first part focusses on more fundamental conclusions and perspectives of endolysins from Gram-negative infecting phages (11.1). Secondly, we give an application-focused description of the PK-fusion approach together with some potential issues towards the development into enzyme antibiotics (11.2). Finally, possible other phage-based or predator-based alternatives for endolysins are discussed to expand the antibacterial arsenal (11.3).

11.1 From fundamental conclusions and perspectives....

11.1.1 Modular versus single-domain endolysins of Gram-negative infecting phages

A huge diversity of bacteriophages is present in nature, an estimated 10^{31} phages (Serwer et al, 2007), constituting an inexhaustible source of peptidoglycan lytic enzymes. In the last decade, an exponential amount of studies concerning Gram-positive phage endolysins have been published, especially on endolysins of staphylococcal origin (Nelson et al, 2012). Surprisingly, research on endolysins from Gram-negative infecting phages remained underexplored. The limited number of experimentally characterized endolysins originating from Gram-negative infecting phages represent only the tip of the iceberg, fostering this study on these enzymes. We were able to expand this tiny pool of experimentally described phage-lytic enzymes by characterization of six single-domain endolysins (PsP3gp10, P2gp09, BcepC6Bgp22, CR8gp3.5, K11gp3.5 and KP32gp15, Chapter 5) and three modular endolysins (OBPgp279, PVP-SE1gp146 and 201φ2-1gp229, Chapter 6). The latter, all encoded by giant *Myoviridae* phages, were enzymatically more active than the single-domain endolysins, an observation that was translated into a higher anti-Gram-negative activity of these enzymes in presence of EDTA. In addition, our data shows that the modular endolysins OBPgp279 and PVP-SE1gp146 by far excels all other tested endolysins in enzymatic activity.

In conclusion, modular endolysins should be favored over single-domain ones for the development into future antibacterial compounds.

A major advantage of Gram-negative phage endolysins, single-domain or modular, is that each endolysin of Gram-negative origin has an equal enzymatic activity on the peptidoglycan of each Gram-negative bacterial species, due to a highly conserved A1 γ peptidoglycan (Schleifer & Kandler, 1972). Therefore, each endolysin can theoretically be developed towards an enzybiotic against all A1 γ peptidoglycan containing Gram-negative bacteria, provided that their outer membranes can be properly passed. In general, endolysins of Gram-positive origin are highly specific towards one Gram-positive bacterial species or strain, as a higher divergence in peptidoglycan chemotype exists among Gram-positives.

11.1.2 Extending the base of the endolysin pyramid

The fact that modular endolysins are superior over single-domain ones justifies the preference for modular lytic enzymes in future endolysin research. In this respect, exploration and expansion of (meta)genomic databases, created by laborious genome sequencing of environmental samples, for unidentified giant phages is of great importance. Extensive genome exploration with special interest for giant phages would deliver opportunities for expansion of the modular endolysin pool. Not only would this allow us to discover novel, modular candidate endolysins with atypical, yet interesting functionalities, but this would also provide more insight in the evolutionary relationship and origin of this modularity, by comparison of their sequences with other unexplored modular or single-domain endolysins. From an evolutionary point of view, this modularity which is only present in a limited number of endolysins from Gram-negative origin, is an interesting feature.

A continuous search for and a full characterization of novel endolysins is worthy as unexpected, yet interesting characteristics, like the high enzymatic activity of OBPgp279 and PVP-SE1gp146, the activity of PVP-SE1gp146 after heat treatment to 100°C, or the intrinsic antibacterial activity of OBPgp279, all disclosed in this dissertation, may be revealed. In addition, mixtures of endolysins with different functional characteristics, could largely expand the types of endolysin-based applications. The combination of Cpl-1 (muramidase)

and Pal (amidase) was shown to induce synergistic effects in anti-streptococcal activity (Loeffler & Fischetti, 2003). In parallel, the combination of a modular lysozyme-like domain (OBPgp279 or PVP-SE1gp146) with a single-domain amidase (e.g. CR8gp3.5) might work synergistic as well. Furthermore, resistance development against two different catalytic activities is also less likely to appear (Donovan et al, 2009).

11.1.3 Structural analysis of characterized endolysins and their interactions

In-depth structural analysis of OBPgp279 and PVP-SE1gp146 will be a starting point to gain insight in the underlying mechanism of the remarkable temperature tolerance of PVP-SE1gp146, and the intrinsic activity of OBPgp279. Single crystal X-ray diffraction to determine the crystalline conformation might offer structural information to elucidate the total three-dimensional structure of these endolysins and their structure-function relationship. Recently, attempts were made to crystallize PVP-SE1gp146 and OBPgp279 in cooperation with the Biomolecular Architecture Research group of the KU Leuven chemistry department of prof. L. Van Meervelt. Until now, we were only able to obtain crystals (trigonal-pyramid shaped) of the catalytic domain (amino acids 127 to 327) of OBPgp279, but with a high diffraction pattern to nearly atomic resolution (1.4 Å). Once their full three-dimensional structures are revealed, a comparison with the structure of the *P. aeruginosa* phage ϕ KZ endolysin KZ144, the only modular endolysin of Gram-negative origin with a known three-dimensional structure so far, might provide insight in the enzymology of modular endolysins. In addition, co-crystallization of OBPgp279 and PVP-SE1gp146 in the presence of sugar (NAM-NAG) or peptide moieties of the peptidoglycan, will deliver more information regarding enzyme-substrate interactions and possible conformational changes in enzyme structure upon substrate binding.

11.2 ...to application-oriented conclusions and perspectives

11.2.1 PK peptide fusion as ideal starting point to tackle the outer membrane *in vitro*

In 2001, Fischetti and coworkers added a novel antibacterial compound, specifically phage endolysins, to the list of possible alternatives for antibiotics by proving their therapeutic

potential in the biocontrol of Gram-positive bacteria (Fischetti, 2001). This article marked the onset of the use of phage endolysins in different biotechnological fields, including medicine and food technology (Callewaert et al, 2011). Unfortunately, the exogenous addition of phage endolysins is not applicable for inactivation of Gram-negative bacteria, without an effective method to overcome the outer membrane barrier, which prevents the passage of these enzymes to the peptidoglycan. To address this challenge, the most active endolysins OBPgp279 and PVP-SE1gp146 were selected to evaluate an approach for outer membrane penetration of different Gram-negative outer membrane types. This approach consists of the fusion of both endolysins to short antimicrobial peptides (5-25 amino acids long) to alter their hydrophobic, amphipathic or cationic character, providing them with specific membrane-destabilizing properties.

From all tested single and double fusion peptides, the addition of a 9-mer polycationic PK peptide solely consisting of lysine and arginine residues (KRKKRKKRK) to OBPgp279 and PVP-SE1gp146 was the most successful (Chapter 7). This PK peptide is believed to compete with the stabilizing divalent cations (Mg^{2+} and Ca^{2+}) for binding to the negative charged phosphate groups in the LPS layer. These cations constitute the Achilles' heel of the LPS layer and in extent of the Gram-negative outer membrane. In Table 11.1, we summarize the most important aspects for both PK-OBPgp279 and PK-PVP-SE1gp146 in presence of EDTA.

Table 11.1: Summary of *in vitro* and *in vivo* characteristics determined in this study for the most promising PK-OBPgp279/EDTA and PK-PVP-SE1gp146/EDTA combinations. ND = not determined.

	PK-OBPgp279/EDTA	PK-PVP-SE1gp146/EDTA
Influence of PK on enzymatic activity	79 % reduction	94 % reduction
Antibacterial activity on <i>P. aeruginosa</i> PAO1	5.38 ± 0.19 log units	4.92 ± 0.23 log units
Biofilm-degrading activity	ND	47 % reduction
Cytotoxicity on growing keratinocytes	Disintegrated cells	Normal cells
Protection of PA14-infected keratinocytes	No protection	Fully protection
Cytotoxicity on L4 stage <i>C. elegans</i> SS104	Slightly toxic at 10 µM	No toxicity
Rescue of PA14-infected <i>C. elegans</i> SS104	25 % rescue at 10 µM	50 % rescue at 10 µM

Despite a negative impact on enzymatic activity, the N-terminal fusion of this PK peptide was able to turn both endolysins in enzymes with a strong anti-Gram-negative activity, specifically towards Pseudomonads (*P. aeruginosa* and *P. putida*) and Burkholderiaceae family members. Of both fusion proteins, PK-OBPgp279 was the most active, significantly reducing *P. aeruginosa* PAO1, Br667, *P. putida* G1 and *B. pseudomallei* with 2.61, 1.56, 1.91 and 1.81 log units, respectively (Table 8.8). Addition of the outer membrane permeabilizer EDTA helped to improve the antibacterial activity of PK-OBPgp279 on *P. aeruginosa* PAO1 (5.38 log units) and extended the Gram-negative activity range of the enzyme with *E. coli* (1.71 log units) and *Salmonella* (0.91 log units) in only 30 minutes. This time-frame is generally much shorter than many antibiotics which reach their maximal *in vitro* reduction after hours of exposure (Ates et al, 2010; Mascio et al, 2012). For both PK fusion proteins, the antibacterial activity was more limited against *E. coli* and even more against *Salmonella*, most likely because their strong hydrophobic LPS layers are less stabilized by cationic interactions (Nikaido, 2003).

The apparent reason for the reduction in enzymatic activity of endolysins upon PK peptide fusion might be elucidated by small angle X-ray scattering (SAXS), which specifically enables the detection of conformational differences between the native and modified endolysins in solution. These structures might serve as a model for site-directed mutagenesis to increase the enzymatic activity of the modified endolysins up to the levels of the wild-type products and maybe beyond.

11.2.2 Biofilm-degrading potential of PK peptide fusion approach

Preliminary data showed that the PK-peptide fusion to PVP-SE1gp146 conferred biofilm-degrading activity of a 24-hour old *P. aeruginosa* PAO1 biofilm, in presence of EDTA (Figure 8.3). This might be due to (a) the higher intrinsic antibacterial activity of the PK-peptide fusion protein or (b) to the binding of biofilm-stabilizing extracellular DNA. If this observation could be extended towards other PK-modified endolysins in the future, this would greatly improve the therapeutic potential of the PK peptide fusion approach. The ability of cells to form biofilms facilitates colonization and the development of infections. The National Institute for Health (U.S.A) estimated that 65 to 80 % of the bacterial infections appears in

the form of biofilms, which are difficult to eradicate with conventional antibacterial compounds or antibiotics. Another aspect of the PK-fused endolysins still to be tested in addition to the biofilm-degrading activity is the possibility to inhibit biofilm formation.

Some phages, like the *Pseudomonas putida* phage $\phi 15$ (Cornelissen et al, 2011) or the *Shewanella oneidensis* MR-1 prophages MuSo1 and MuSo2 (Godeke et al, 2011), possess a tail-associated exopolysaccharide depolymerase enzyme that enables the phage to penetrate biofilms and to infect biofilm-encapsulated cells. These biofilm-degrading enzymes might help the PK-modified endolysins to break through polysaccharide capsules or biofilm barriers in a combinatorial approach. A major hurdle of the use of phage depolymerases in applications, however, is their high specificity towards the type of biofilm produced by their bacterial host, seriously narrowing the host range (Cornelissen et al, 2011; Sutherland, 1999). A better alternative may be the combination with Dornase alfa (Pulmozyme®), a DNase that cleaves the stabilizing extracellular DNA present in a biofilm, thereby lowering the biofilm viscosity (Bryson & Sorkin, 1994). Similar to a depolymerase, this could promote the diffusion of the PK-modified endolysins through the biofilm, leading to a higher antibacterial efficacy against biofilm-encapsulated cells. Dornase alfa is the most commonly used medication for treatment of cystic fibrosis patients (Jones & Wallis, 2010).

11.2.3 Safety and antibacterial efficacy in keratinocyte and *C. elegans* infection models

Endolysins are generally assumed to be safe compounds for eukaryotic or mammalian cells as their enzymatic substrate, the peptidoglycan layer, is exclusively present in bacterial cells (Borysowski et al, 2006). However, the excess of positive charges present in the PK peptide moiety of the fusion protein might be able to interact with the negatively charged eukaryotic or mammalian cell membranes, inducing pore formation as reported for the polycationic agents poly-L-lysine and polyethylenimine (Hong et al, 2006). Therefore, the cytotoxicity of the EDTA/PK-modified endolysin mixture was evaluated on growing human keratinocytes, on one hand, and on L4 stage-developed *C. elegans* nematodes, on the other hand. OBPgp279, (PK-)PVP-SE1gp146 and EDTA all turned out to be safe for *C. elegans*, but PK-OBPgp279 showed slightly toxic effects at 10 μM (Table 11.1). In contrast to the outcome for *C. elegans*, addition of OBPgp279 caused fast disintegration of growing keratinocytes.

Taken the observed intrinsic antibacterial activity of OBPgp279 on *P. aeruginosa* PAO1 into account, plausible explanations for this observation might be either LPS-binding or membrane-disrupting activity of the enzyme. LPS-binding could inhibit or neutralize the endotoxic effect of LPS due to the inability of bound LPS molecules to interact properly with the TLR4/MD-2/CD14 receptor complex (= anti-endotoxin activity), but could also promote the triggering of an inflammatory response in eukaryotic or mammalian cells, as showed for lactoferrin (Na et al, 2004) and proposed here for OBPgp279. In addition, LPS-binding might also destabilize and disrupt the outer membrane, explaining the observed intrinsic antibacterial activity of OBPgp279. Previously, another modular phage endolysin of Gram-negative origin, KZ144, has been reported to penetrate the cytoplasmic membrane (but not the eukaryotic membrane) (Cloutier et al, 2010). Specific physiochemical surface properties of OBPgp279 may be responsible for destabilization of the outer membrane, but also the eukaryotic membrane, explaining the observed keratinocyte disintegration. Currently, we cannot exclude either possibility or find an explanation why OBPgp279 is not toxic for *C. elegans*. This shows that a careful evaluation of the safety of each fusion protein on different models is of crucial importance in further preclinical and clinical studies. From an application point of view, topical administration of (PK-)OBPgp279/EDTA for local disinfection (e.g. ear infections with *P. aeruginosa*) would be still feasible. However, in its current state, OBPgp279 is not suitable for decontamination of burn wounds where wound healing is of crucial importance, and PVP-SE1gp146 derivatives are rather preferred there.

Human keratinocytes could be totally protected against an infection with cytotoxic *P. aeruginosa* PA14 (10^5 CFU/ml) by treatment with a (PK-)PVP-SE1gp146/EDTA (Chapter 9) (Table 11.1). At a hundred times higher bacterial cell density, the additional effect of the PK peptide fusion on keratinocyte survival became visible. In addition, the same mixture was able to induce a ± 50 % recovery of PA14-infected *C. elegans* nematodes after five days, which is considerably better than the antibiotic ciprofloxacin, at 5xMIC (Chapter 10) (Table 11.1). This last result emphasizes that endolysins also form a potential alternative for antibiotics as antibacterial compounds *in vivo*.

In a next step, the *in vivo* efficacy of the PK peptide fusion approach should be tested on other animals than the nematode *C. elegans*. A nose- or long-infection model in Balb/c mice

with bioluminescent *P. aeruginosa* cells to follow airway colonization (Debarbieux et al, 2010) offers an interesting approach in a next step to study *in vivo* efficacy in higher-order animals.

11.2.4 Taking the PK peptide fusion approach to a next level

Dependent on the endolysin used or the bacterial strain targeted, variation of the linker length (4-16 amino acids) and the position of the PK peptide (N- or C-terminal) could further improve or diminish the enzymatic and antibacterial activities. In case of PK-OBPgp279, enlarging the linker length further strengthened the antibacterial effect against *P. aeruginosa* (+ 0.80 log units, Link 1), *E. coli* (+ 0.71 log units, with EDTA, Link 4) and *Salmonella* (+ 0.61 log units, with EDTA, Link 4) (Table 8.7). In addition, an N-terminal PK peptide fusion, near the peptidoglycan binding domain of the endolysin, seemed favorable over the C-terminal variant, close to the catalytic domain, in case of OBPgp279 and PVP-SE1gp146. In general, however, the impact of these variations were empirical, no strict trends could be observed, emphasizing the need for a species-specific optimization. It is reasonable to assume that the optimization of the linker composition, further extension of the linker length and the improvement of hydrophobicity, amphipathicity or cationicity of the whole endolysin or specific endolysin domains by other peptide fusions, might further enhance or broaden the antibacterial efficacy and the Gram-negative activity range of the fusion proteins. To enhance the antibacterial efficacy on *Salmonella*, using other outer membrane permeabilizers that efficiently destabilize the *Salmonella* outer membrane, like lactate, malate, sorbate, benzoate or phenolic berry derivatives (Alakomi et al, 2007; Alakomi et al, 2000), instead of EDTA, could be a possible option.

11.2.5 Issues in future development of PK fusion approach

Multidrug-resistant superbugs have significantly raised the need for novel effective antibacterial compounds over the last couple of years. In addition to the ability to eradicate free-living bacterial cells and prevent biofilm formation, such a compound should also be more refractory to resistance development. In this light, resistance against the PK-modified endolysin is an important issue that should still be addressed. A commonly made assumption

is that due to millions of years of coevolution between phage and host, endolysins naturally were targeted towards essential bonds in the peptidoglycan structure. Therefore, resistance development against the endolysin by target modification is assumed to be unfavorable for the bacterial host cell and is not likely to occur (Fischetti, 2010). This assumption was confirmed in resistance studies for the *S. pneumoniae* Pal and *B. anthracis* PlyG endolysins, both from Gram-positive origin. Till date, studies on resistance of endolysins of Gram-negative origin remain absent. Despite the encouraging work on Gram-positive endolysins, resistant bacterial strains against non-phage peptidoglycan hydrolases, like human lysozyme and lysostaphin, have been identified. For these strains, resistance occurred by means of different cell wall modifications (O-acetylation, N-deacetylation of peptidoglycan, D-alanylation of teichoic acids in case of human lysozyme, modifications within the pentaglycine bridge in case of lysostaphin) (DeHart et al, 1995; Vollmer, 2008). The lysozyme and lysostaphin resistance illustrate that bacteria can harbor divers changes in their peptidoglycan structure. Therefore, there seems to be no fundamental reason why bacteriophage endolysins would be less susceptible to resistance development than peptidoglycan hydrolases from other origins (Callewaert et al, 2011). It is difficult to give a definitive answer on the resistance development question, due to the limited data available so far.

Unlike the endolysin itself, the PK peptide interacts with the outer membrane, more specifically with the negative phosphate groups in the LPS moiety. This part of the outer membrane is prone to divers alterations of modifications, which help the bacterial cell adapting to changing environments. In clinical isolates or multidrug-resistant strains of different Gram-negative species, addition of positively charged, amine-containing residues (4-amino-4-deoxy-l-arabinose or phosphoethanolamine) to the lipid A or core polysaccharide parts of the LPS, confers resistance against cationic antimicrobial peptides or polycationic antibiotics (polymyxin B), that have a similar mode of action as the PK peptide (Loutet & Valvano, 2011; Tran et al, 2005). It is therefore reasonable to assume that, in addition to the enzyme itself, resistance might also occur to the PK moiety. However, this assumption should still be confirmed.

To improve the antibacterial potential, broadening the host range and in the same time reducing the chance on resistance development for the PK peptide fusion approach, a combination with other antibacterial compounds, including antibiotics, or the creation of chimeric endolysins by fusion of the PK-fused endolysin with specific catalytic or peptidoglycan binding domains, are two possible options. A combination of a modified endolysin with another antibacterial compound (e.g. antibiotic) may reveal unexpected synergistic effects in antibacterial activity, as observed for the phage-encoded endolysin LysH5 and the bacteriocin nisin on the Gram-positive bacteria *S. aureus* (Garcia et al, 2010) or the pneumococcal lysin Cpl-1 and penicillin on *S. pneumonia* (Djurkovic et al, 2005). In addition, a synergistic effect would potentially extend the clinical half-life of overused antibiotics and slow down the resistance development. For the second option, the fusion engineering of chimeric endolysins, Becker and coworkers (2009) constructed triple-lytic-domain constructs with a stronger anti-staphylococcal activity than the corresponding single domains. It is expected to be a rare event that a pathogen can become resistant against three simultaneous lytic activities exerted by these triple-fusion constructs.

Another issue that should be considered for therapeutic use of a mixture of EDTA and a PK-modified endolysin is the extensive release of pyrogenic LPS molecules upon EDTA- and PK peptide-induced outer membrane permeabilization. The pyrogenicity is particularly caused by the lipid A part (endotoxin) that triggers the TLR4/MD-2/CD14 receptor-mediated pathway, leading to the production of proinflammatory components, including cytokines and chemokines (Hajjar et al, 2002). Eventually, these components may lead to a severe septic shock and multiple organ failure in the treated patient. To reduce potential endotoxic effects, it is important to work with endotoxin-free enzyme and EDTA solutions, *in vivo*. However, the release of bacterial antigens which is intrinsically related to cell lysis can hardly be avoided and is common with cell wall acting antibiotics, from which many were successful in the past.

With our PK peptide fusion approach, we envisage topical applications in human health, veterinary and food industry. The mixture of a PK-modified endolysin with EDTA might be a suitable tool to prevent or cure opportunistic *P. aeruginosa* and *A. baumannii* infections of skin, burn wounds, eyes, ears and lung areas; and to decontaminate surfaces used for the

preparation and/or preservation of broiler eggs (to prevent *Salmonella*-infections) and meat (*E. coli*-infections). Systemic applications are not intended due to immunogenicity, lower instability and fast clearance of an endolysin in the blood stream. In case of Cpl-1, the triggered immune response resulted in a partial inactivation of the enzyme by the raised antibodies (Loeffler et al, 2003). In addition, the half-life of endolysins, and enzymes in general, in the bloodstream is rather short (+/- 20 min), so repeated administration would be necessary to retain the same concentration level for a longer period. Possible strategies to elongate the half-life of Cpl-1 that prove successful were binding to polyethyleneglycol (PEGylation) (Walsh et al, 2003) and dimerization by introduction of cysteine residues (Resch et al, 2011). Normally, the second component of the PK fusion peptide approach, EDTA, is not expected to cause problems at the test concentration of 0.5 mM, if systemically administrated. EDTA only inhibits blood coagulation at concentrations above 1.3 mM (Triantaphyllopoulos et al, 1955). Furthermore, EDTA is also used in chelation therapy to recover from intoxications with heavy metals. Ideally, further optimization of the fusion approach, making an outer membrane permeabilizer unnecessary, would be the best option to improve safety of systemic applications.

11.3 Widening the possibilities: from phage therapy to natural predators

In this dissertation, we specifically focused on the development of bacteriophage endolysins into effective anti-Gram-negative agents which are both able to disrupt the outer membrane and lyse the peptidoglycan layer. During evolution, these enzymes have been evolved into highly efficient tools to perform their task with high redundancy. Bacteriophage therapy, the use of whole phages, cocktails of phages or phage-antibiotic mixtures for the treatment of bacterial infections, offers an additional approach to combat worrisome Gram-negative infections. Nowadays, phage therapy knows diverse applications in biocontrol of plant diseases caused by phytopathogenic bacteria (e.g. soft rot in potatoes by *Dickeya solani* phages) (Adriaenssens et al, 2012b) or in prophylaxis or treatment of clinical infections (Matsuzaki et al, 2005; Miedzybrodzki et al, 2012). Advantages of phage therapy compared to endolysins of Gram-negative origin are the high specificity of a phage towards a certain bacterial species or strain, leaving the normal flora unharmed, the continuous replenishment due to multiplication in the host and the targeted action. In multiple infections, a narrow

host range is less desirable. In addition, the faster appearance of phage resistance, ethical burdens due to potential horizontal transfer of toxic genes from the phage to mammalian cells and an enigmatic intellectual property protection hinder the commercialization of phage therapy.

Some small, single stranded DNA or RNA phages, like ϕ X174 or Q β , encode inhibitors (gpE and gpA2, respectively) of specific steps in peptidoglycan synthesis (MraY and MurA-catalyzed pathways, respectively) as a general approach to release their virions, instead of using endolysins or holins (Bernhardt et al, 2001a; Bernhardt et al, 2001b). These inhibitory proteins can be used as bacteriostatic “phage antibiotics” to control bacterial growth, if a way is found to transfer them to the cytoplasm (Bernhardt et al, 2002). In addition, these known lysis proteins could potentially serve as a model for the development of non-peptide small molecules that mimic their action.

Besides phages, bacteria are also attacked by other natural predators, including protists like free-living soil amoebae (e.g. *Acanthamoeba castellanii*) (Anderson et al, 2005) and other bacteria, like the obligate predatory bacterium *Bdellovibrio bacteriovorus* or members of the facultative predatory Myxobacterium family (Jurkevitch, 2012). All these predators secrete specific cell wall degrading enzymes and secondary metabolites (e.g. antibiotics) that are necessary for evasion of the host bacterium. Amoebae specifically devour a variety of Gram-negative and Gram-positive bacteria by phagocytosis and subsequent digestion in their phagolysosomes using a whole spectrum of peptidoglycan lytic enzymes including muramidases, glucosaminidases or amidases (Braun et al, 1972). *Bdellovibrio bacteriovorus* is able to attack almost all Gram-negative species, including many prominent pathogens, which they need for survival, and is therefore an interesting species from an anti-Gram-negative point of view. *Bdellovibrio* possesses a whole arsenal of hydrolytic and proteolytic enzymes needed for its predatory life style, including exopolysaccharide depolymerases (Martinez et al, 2012) and specialized broad-range peptidoglycan hydrolases (Lerner et al, 2012). It is an attractive idea to tap the pool of these interesting hydrolytic enzymes encoded by amoebae, *Bdellovibrio* and other natural predators, and to gain insight in their predator mechanisms, as a starting point for development of new classes of antibacterial compounds.

The work on endolysins from Gram-negative origin, that once started in an era of general disbelief in their applicability due to the outer membrane, has now reached the stage that ready-to-use, tailored enzymes against a wide range of Gram-negative pathogens are on the avenue for commercialization. At this moment, the phage lysin community finally seems to have embraced the potential of tailored strategies to target Gram-negative bacteria (Nelson et al, 2012; Schmelcher et al, 2012a).

References

Web references

European Medicines Agency (EMA): The bacterial challenge: time to react. http://www.ema.europa.eu/docs/en_GB/document_library/Report/2009/11/WC500008770.pdf

R.E.W. Hancock Laboratory webpage: <http://cmdr.ubc.ca/bobh/uptake.html>

Helical wheel projections: <http://cti.itc.virginia.edu/~cmg/Demo/wheel/wheelApp.html>

Peer-reviewed journals

Abaev I, Foster-Frey J, Korobova O, Shishkova N, Kiseleva N, Kopylov P, Pryamchuk S, Schmelcher M, Becker SC, Donovan DM (2012) Staphylococcal Phage 2638A endolysin is lytic for *Staphylococcus aureus* and harbors an inter-lytic-domain secondary translational start site. *Appl Microbiol Biotechnol* PMID:22777279

Aballay A, Yorgey P, Ausubel FM (2000) *Salmonella* Typhimurium proliferates and establishes a persistent infection in the intestine of *Caenorhabditis elegans*. *Curr Biol* **10**: 1539-1542

Adao R, Seixas R, Gomes P, Pessoa JC, Bastos M (2008) Membrane structure and interactions of a short Lycotoxin I analogue. *J Pept Sci* **14**: 528-534

Adriaenssens EM, Mattheus W, Cornelissen A, Shaburova O, Krylov VN, Kropinski AM, Lavigne R (2012a) Complete genome sequence of the giant *Pseudomonas* phage Lu11. *J Virol* **86**: 6369-6370

Adriaenssens EM, Van Vaerenbergh J, Vandenhoevel D, Dunon V, Ceysens PJ, De Proft M, Kropinski AM, Noben JP, Maes M, Lavigne R (2012b) T4-related bacteriophage LIMEstone isolates for the control of soft rot on potato caused by '*Dickeya solani*'. *PLoS One* **7**: e33227

Aertsen A, Vanoirbeek K, De Spiegeleer P, Sermon J, Hauben K, Farewell A, Nystrom T, Michiels CW (2004) Heat shock protein-mediated resistance to high hydrostatic pressure in *Escherichia coli*. *Appl Environ Microbiol* **70**: 2660-2666

Alakomi HL, Skytta E, Saarela M, Mattila-Sandholm T, Latva-Kala K, Helander IM (2000) Lactic acid permeabilizes Gram-negative bacteria by disrupting the outer membrane. *Appl Environ Microbiol* **66**: 2001-2005

Alakomi HL, Puupponen-Pimia R, Aura AM, Helander IM, Nohynek L, Oksman-Caldentey KM, Saarela M (2007) Weakening of *salmonella* with selected microbial metabolites of berry-derived phenolic compounds and organic acids. *J Agric Food Chem* **55**: 3905-3912

Alcantara EH, Kim DH, Do SI, Lee SS (2007) Bi-functional activities of chimeric lysozymes constructed by domain swapping between bacteriophage T7 and K11 lysozymes. *J Biochem Mol Biol* **40**: 539-546

Alekshun MN, Levy SB (2007) Molecular mechanisms of antibacterial multidrug resistance. *Cell* **128**: 1037-1050

Alexander C, Rietschel ET (2001) Bacterial lipopolysaccharides and innate immunity. *J Endotoxin Res* **7**: 167-202

Altschul SF, Madden TL, Schaffer AA, Zhang J, Zhang Z, Miller W, Lipman DJ (1997) Gapped BLAST and PSI-BLAST: a new generation of protein database search programs. *Nucleic Acids Res* **25**: 3389-3402

Anaya-Lopez JL, Lopez-Meza JE, Ochoa-Zarzosa A (2012) Bacterial resistance to cationic antimicrobial peptides. *Crit Rev Microbiol* PMID:22799636

Anderson IJ, Watkins RF, Samuelson J, Spencer DF, Majoros WH, Gray MW, Loftus BJ (2005) Gene discovery in the *Acanthamoeba castellanii* genome. *Protist* **156**: 203-214

Andersson M, Gunne H, Agerberth B, Boman A, Bergman T, Olsson B, Dagerlind A, Wigzell H, Boman HG, Gudmundsson GH (1996) NK-lysin, structure and function of a novel effector molecule of porcine T and NK cells. *Vet Immunol Immunopathol* **54**: 123-126

Andersson M, Girard R, Cazenave P (1999) Interaction of NK lysin, a peptide produced by cytolytic lymphocytes, with endotoxin. *Infect Immun* **67**: 201-205

Andra J, Leippe M (1999) Candidacidal activity of shortened synthetic analogs of amoebapores and NK-lysin. *Med Microbiol Immunol* **188**: 117-124

Archibald AR, Hancock IC, Harwood CR (1993) Cell wall structure, synthesis and turnover. In: Hoch JA, Losick R (eds.) *Bacillus subtilis* and other Gram-positive bacteria, biochemistry, physiology and molecular genetics, American Society for Microbiology, Washington DC. pp. 381-410.

- Arima H, Ibrahim HR, Kinoshita T, Kato A (1997) Bactericidal action of lysozymes attached with various sizes of hydrophobic peptides to the C-terminal using genetic modification. *FEBS Lett* **415**: 114-118
- Arima H, Kinoshita T, Ibrahim HR, Azakami H, Kato A (1998) Enhanced secretion of hydrophobic peptide fused lysozyme by the introduction of N-glycosylation signal and the disruption of calnexin gene in *Saccharomyces cerevisiae*. *FEBS Lett* **440**: 89-92
- Arnusch CJ, Pieters RJ, Breukink E (2012) Enhanced membrane pore formation through high-affinity targeted antimicrobial peptides. *PLoS One* **7**: e39768
- Ates L, Hanssen-Hubner C, Norris DE, Richter D, Kraiczky P, Hunfeld KP (2010) Comparison of in vitro activities of tigecycline, doxycycline, and tetracycline against the spirochete *Borrelia burgdorferi*. *Ticks Tick Borne Dis* **1**: 30-34
- Atrih A, Bacher G, Allmaier G, Williamson MP, Foster SJ (1999) Analysis of peptidoglycan structure from vegetative cells of *Bacillus subtilis* 168 and role of PBP 5 in peptidoglycan maturation. *J Bacteriol* **181**: 3956-3966
- Baker MA, Maloy WL, Zasloff M, Jacob LS (1993) Anticancer efficacy of Magainin2 and analogue peptides. *Cancer Res* **53**: 3052-3057
- Bakker-Woudenberg IA, ten Kate MT, Stearne-Cullen LE, Woodle MC (1995) Efficacy of gentamicin or ceftazidime entrapped in liposomes with prolonged blood circulation and enhanced localization in *Klebsiella pneumoniae*-infected lung tissue. *J Infect Dis* **171**: 938-947
- Bakker-Woudenberg IA (2002) Long-circulating sterically stabilized liposomes as carriers of agents for treatment of infection or for imaging infectious foci. *Int J Antimicrob Agents* **19**: 299-311
- Beaulac C, Sachetelli S, Lagace J (1998) In-vitro bactericidal efficacy of sub-MIC concentrations of liposome-encapsulated antibiotic against Gram-negative and gram-positive bacteria. *J Antimicrob Chemother* **41**: 35-41
- Becker SC, Foster-Frey J, Donovan DM (2008) The phage K lytic enzyme LysK and lysostaphin act synergistically to kill MRSA. *FEMS Microbiol Lett* **287**: 185-191
- Becker SC, Dong S, Baker JR, Foster-Frey J, Pritchard DG, Donovan DM (2009a) LysK CHAP endopeptidase domain is required for lysis of live staphylococcal cells. *FEMS Microbiol Lett* **294**: 52-60
- Becker SC, Foster-Frey J, Stodola AJ, Anacker D, Donovan DM (2009b) Differentially conserved staphylococcal SH3b_5 cell wall binding domains confer increased staphylolytic and streptolytic activity to a streptococcal prophage endolysin domain. *Gene* **443**: 32-41
- Bernhardt TG, Struck DK, Young R (2001a) The lysis protein E of phi X174 is a specific inhibitor of the MraY-catalyzed step in peptidoglycan synthesis. *J Biol Chem* **276**: 6093-6097
- Bernhardt TG, Wang IN, Struck DK, Young R (2001b) A protein antibiotic in the phage Qbeta virion: diversity in lysis targets. *Science* **292**: 2326-2329
- Bernhardt TG, Wang IN, Struck DK, Young R (2002) Breaking free: "protein antibiotics" and phage lysis. *Res Microbiol* **153**: 493-501
- Bhatia SR, Miedel MT, Chotoo CK, Graf NJ, Hood BL, Conrads TP, Silverman GA, Luke CJ (2011) Using *C. elegans* to identify the protease targets of serpins in vivo. *Methods Enzymol* **499**: 283-299
- Bienkowska-Szewczyk K, Taylor A (1980) Murein transglycosylase from phage lambda lysate. Purification and properties. *Biochim Biophys Acta* **615**: 489-496
- Bierbaum G, Sahl HG (1985) Induction of autolysis of staphylococci by the basic peptide antibiotics Pep 5 and nisin and their influence on the activity of autolytic enzymes. *Arch Microbiol* **141**: 249-254
- Bishop RE, Gibbons HS, Guina T, Trent MS, Miller SI, Raetz CR (2000) Transfer of palmitate from phospholipids to lipid A in outer membranes of Gram-negative bacteria. *EMBO J* **19**: 5071-5080
- Blasi U, Chang CY, Zagotta MT, Nam KB, Young R (1990) The lethal lambda S gene encodes its own inhibitor. *EMBO J* **9**: 981-989
- Bolton SJ, Jones DN, Darker JG, Eggleston DS, Hunter AJ, Walsh FS (2000) Cellular uptake and spread of the cell-permeable peptide penetratin in adult rat brain. *Eur J Neurosci* **12**: 2847-2855
- Boman HG (1995) Peptide antibiotics and their role in innate immunity. *Annu Rev Immunol* **13**: 61-92
- Borysowski J, Weber-Dabrowska B, Gorski A (2006) Bacteriophage endolysins as a novel class of antibacterial agents. *Exp Biol Med (Maywood)* **231**: 366-377
- Borysowski J, Gorski A (2010) Fusion to cell-penetrating peptides will enable lytic enzymes to kill intracellular bacteria. *Med Hypotheses* **74**: 164-166
- Boyce ST, Warden GD, Holder IA (1995) Noncytotoxic combinations of topical antimicrobial agents for use with cultured skin substitutes. *Antimicrob Agents Chemother* **39**: 1324-1328

- Brade L (2000) Assay of anti-endotoxin antibodies. *Methods Mol Med* **36**: 27-35
- Braun V, Hantke K, Wolff H, Gerisch G (1972) Degradation of the murein-lipoprotein complex of *Escherichia coli* cell walls by *Dictyostelium amoebae*. *Eur J Biochem* **27**: 116-125
- Brenner S (1974) The genetics of *Caenorhabditis elegans*. *Genetics* **77**: 71-94
- Breukink E, de Kruijff B (2006) Lipid II as a target for antibiotics. *Nat Rev Drug Discov* **5**: 321-332
- Brewer D, Lajoie G (2002) Structure-based design of potent histatin analogues. *Biochemistry* **41**: 5526-5536
- Briers Y, Lavigne R, Plessers P, Hertveldt K, Hanssens I, Engelborghs Y, Volckaert G (2006) Stability analysis of the bacteriophage phiKMV lysin gp36C and its putative role during infection. *Cell Mol Life Sci* **63**: 1899-1905
- Briers Y, Lavigne R, Volckaert G, Hertveldt K (2007a) A standardized approach for accurate quantification of murein hydrolase activity in high-throughput assays. *J Biochem Biophys Methods* **70**: 531-533
- Briers Y, Volckaert G, Cornelissen A, Lagaert S, Michiels CW, Hertveldt K, Lavigne R (2007b) Muralytic activity and modular structure of the endolysins of *Pseudomonas aeruginosa* bacteriophages phiKZ and EL. *Mol Microbiol* **65**: 1334-1344
- Briers Y, Cornelissen A, Aertsen A, Hertveldt K, Michiels CW, Volckaert G, Lavigne R (2008) Analysis of outer membrane permeability of *Pseudomonas aeruginosa* and bactericidal activity of endolysins KZ144 and EL188 under high hydrostatic pressure. *FEMS Microbiol Lett* **280**: 113-119
- Briers Y, Schmelcher M, Loessner MJ, Hendrix J, Engelborghs Y, Volckaert G, Lavigne R (2009) The high-affinity peptidoglycan binding domain of *Pseudomonas* phage endolysin KZ144. *Biochem Biophys Res Commun* **383**: 187-191
- Briers Y, Peeters LM, Volckaert G, Lavigne R (2011a) The lysis cassette of bacteriophage varphiKMV encodes a signal-arrest-release endolysin and a pinholin. *Bacteriophage* **1**: 25-30
- Briers Y, Walmagh M, Lavigne R (2011b) Use of bacteriophage endolysin EL188 and outer membrane permeabilizers against *Pseudomonas aeruginosa*. *J Appl Microbiol* **110**: 778-785
- Brogden KA (2005) Antimicrobial peptides: pore formers or metabolic inhibitors in bacteria? *Nat Rev Microbiol* **3**: 238-250
- Brogden KA, Guthmiller JM, Taylor CE (2005) Human polymicrobial infections. *Lancet* **365**: 253-255
- Brown EA, Hardwidge PR (2007) Biochemical characterization of the enterotoxigenic *Escherichia coli* LeoA protein. *Microbiology* **153**: 3776-3784
- Bryson HM, Sorkin EM (1994) Dornase alfa. A review of its pharmacological properties and therapeutic potential in cystic fibrosis. *Drugs* **48**: 894-906
- Bullas LR, Mostaghimi AR, Arensdorf JJ, Rajadas PT, Zuccarelli AJ (1991) Salmonella phage PSP3, another member of the P2-like phage group. *Virology* **185**: 918-921
- Bustamante N, Campillo NE, Garcia E, Gallego C, Pera B, Diakun GP, Saiz JL, Garcia P, Diaz JF, Menendez M (2010) Cpl-7, a Lysozyme Encoded by a Pneumococcal Bacteriophage with a Novel Cell Wall-binding Motif. *Journal of Biological Chemistry* **285**: 33184-33196
- Butler ET, Chamberlin MJ (1982) Bacteriophage SP6-specific RNA polymerase. I. Isolation and characterization of the enzyme. *J Biol Chem* **257**: 5772-5778
- Callewaert L, Walmagh M, Michiels CW, Lavigne R (2011) Food applications of bacterial cell wall hydrolases. *Curr Opin Biotechnol* **22**: 164-171
- Carty SM, Sreekumar KR, Raetz CR (1999) Effect of cold shock on lipid A biosynthesis in *Escherichia coli*. Induction At 12 degrees C of an acyltransferase specific for palmitoleoyl-acyl carrier protein. *J Biol Chem* **274**: 9677-9685
- Casteels P, Ampe C, Jacobs F, Vaeck M, Tempst P (1989) Apidaecins: antibacterial peptides from honeybees. *EMBO J* **8**: 2387-2391
- Ceri H, Olson ME, Stremick C, Read RR, Morck D, Buret A (1999) The Calgary Biofilm Device: new technology for rapid determination of antibiotic susceptibilities of bacterial biofilms. *J Clin Microbiol* **37**: 1771-1776
- Chang TW, Lin YM, Wang CF, Liao YD (2012a) Outer membrane lipoprotein Lpp is Gram-negative bacterial cell surface receptor for cationic antimicrobial peptides. *J Biol Chem* **287**: 418-428
- Chang Y, Gu W, McLandsborough L (2012b) Low concentration of ethylenediaminetetraacetic acid (EDTA) affects biofilm formation of *Listeria monocytogenes* by inhibiting its initial adherence. *Food Microbiol* **29**: 10-17
- Cheng X, Zhang X, Pflugrath JW, Studier FW (1994) The structure of bacteriophage T7 lysozyme, a zinc amidase and an inhibitor of T7 RNA polymerase. *Proc Natl Acad Sci U S A* **91**: 4034-4038

- Chihara S, Okuzumi K, Yamamoto Y, Oikawa S, Hishinuma A (2011) First case of New Delhi metallo-beta-lactamase 1-producing *Escherichia coli* infection in Japan. *Clin Infect Dis* **52**: 153-154
- Christensen B, Fink J, Merrifield RB, Mauzerall D (1988) Channel-forming properties of cecropins and related model compounds incorporated into planar lipid membranes. *Proc Natl Acad Sci U S A* **85**: 5072-5076
- Christie GE, Haggard-Ljungquist E, Calendar R The complete genome of bacteriophage P2. Unpublished.
- Cloutier I, Paradis-Bleau C, Giroux AM, Pigeon X, Arseneault M, Levesque RC, Auger M (2010) Biophysical studies of the interactions between the phage varphiKZ gp144 lytic transglycosylase and model membranes. *Eur Biophys J* **39**: 263-276
- Collins BS (2011) Gram-negative outer membrane vesicles in vaccine development. *Discov Med* **12**: 7-15
- Cooper JF, Hochstein HD, Seligmann EB, Jr. (1972) The Limulus test for endotoxin (Pyrogen) in radiopharmaceuticals and biologicals. *Bull Parenter Drug Assoc* **26**: 153-162
- Cornelissen A, Ceysens PJ, T'Syen J, Van Praet H, Noben JP, Shaburova OV, Krylov VN, Volckaert G, Lavigne R (2011) The T7-related *Pseudomonas putida* phage phi15 displays virion-associated biofilm degradation properties. *PLoS One* **6**: e18597
- Cornelissen A, Hardies SC, Shaburova OV, Krylov VN, Mattheus W, Kropinski AM, Lavigne R (2012) Complete genome sequence of the giant virus OBP and comparative genome analysis of the diverse PhiKZ-related phages. *J Virol* **86**: 1844-1852
- Courtin P, Miranda G, Guillot A, Wessner F, Mezange C, Domakova E, Kulakauskas S, Chapot-Chartier MP (2006) Peptidoglycan structure analysis of *Lactococcus lactis* reveals the presence of an L,D-carboxypeptidase involved in peptidoglycan maturation. *J Bacteriol* **188**: 5293-5298
- Cruciani RA, Barker JL, Zasloff M, Chen HC, Colamonici O (1991) Antibiotic magainins exert cytolytic activity against transformed cell lines through channel formation. *Proc Natl Acad Sci U S A* **88**: 3792-3796
- Czihal P, Knappe D, Fritsche S, Zahn M, Berthold N, Piantavigna S, Muller U, Van Dorpe S, Herth N, Binas A, Kohler G, De Spiegeleer B, Martin LL, Nolte O, Strater N, Alber G, Hoffmann R (2012) Api88 is a novel antibacterial designer Peptide to treat systemic infections with multidrug-resistant Gram-negative pathogens. *ACS Chem Biol* **7**: 1281-1291
- de Breijl A, Haisma EM, Rietveld M, El Ghalbzouri A, van den Broek PJ, Dijkshoorn L, Nibbering PH (2012) Three-dimensional human skin equivalent as a tool to study *Acinetobacter baumannii* colonization. *Antimicrob Agents Chemother* **56**: 2459-2464
- Debarbieux L, Leduc D, Maura D, Morello E, Criscuolo A, Grossi O, Balloy V, Touqui L (2010) Bacteriophages can treat and prevent *Pseudomonas aeruginosa* lung infections. *J Infect Dis* **201**: 1096-1104
- DeHart HP, Heath HE, Heath LS, LeBlanc PA, Sloan GL (1995) The lysostaphin endopeptidase resistance gene (epr) specifies modification of peptidoglycan cross bridges in *Staphylococcus simulans* and *Staphylococcus aureus*. *Appl Environ Microbiol* **61**: 1475-1479
- Del Sal G, Storici P, Schneider C, Romeo D, Zanetti M (1992) cDNA cloning of the neutrophil bactericidal peptide indolicidin. *Biochem Biophys Res Commun* **187**: 467-472
- Desvaux M (2012) Contribution of holins to protein trafficking: secretion, leakage or lysis? *Trends Microbiol* **20**: 259-261
- Desvaux M, Hebraud M, Talon R, Henderson IR (2009) Secretion and subcellular localizations of bacterial proteins: a semantic awareness issue. *Trends Microbiol* **17**: 139-145
- d'Hérelle F (1917) Sur un microbe invisible antagoniste des bacilles dysentériques. *Compt Rend Acad Sci* **165**: 373-375
- d'Herelle F (1921) Le bactériophage. Son rôle dans l'immunité. *La Presse méd* **29**: 463-464
- Djurkovic S, Loeffler JM, Fischetti VA (2005) Synergistic killing of *Streptococcus pneumoniae* with the bacteriophage lytic enzyme Cpl-1 and penicillin or gentamicin depends on the level of penicillin resistance. *Antimicrob Agents Chemother* **49**: 1225-1228
- Donovan DM, Dong S, Garrett W, Rousseau GM, Moineau S, Pritchard DG (2006a) Peptidoglycan hydrolase fusions maintain their parental specificities. *Appl Environ Microbiol* **72**: 2988-2996
- Donovan DM, Foster-Frey J, Dong S, Rousseau GM, Moineau S, Pritchard DG (2006b) The cell lysis activity of the *Streptococcus agalactiae* bacteriophage B30 endolysin relies on the cysteine, histidine-dependent amidohydrolase/peptidase domain. *Appl Environ Microbiol* **72**: 5108-5112
- Donovan DM, Foster-Frey J (2008) LambdaSa2 prophage endolysin requires Cpl-7-binding domains and amidase-5 domain for antimicrobial lysis of streptococci. *FEMS Microbiol Lett* **287**: 22-33
- Donovan DM, Becker SC, Dong S, Baker JR, Foster-Frey J, Pritchard DG (2009) Peptidoglycan hydrolase enzyme fusions for treating multi-drug resistant pathogens. *Biotech* **3**: 6-10

- Dortet L, Poirel L, Anguel N, Nordmann P (2012) New Delhi Metallo-beta-Lactamase 4-producing *Escherichia coli* in Cameroon. *Emerg Infect Dis* **18**: 1540-1542
- Doughty CC, Hayashi JA (1962) Enzymatic properties of a phage-induced lysin affecting group A streptococci. *J Bacteriol* **83**: 1058-1068
- Drago-Serrano ME, de la Garza-Amaya M, Luna JS, Campos-Rodriguez R (2012) Lactoferrin-lipopolysaccharide (LPS) binding as key to antibacterial and antiendotoxic effects. *Int Immunopharmacol* **12**: 1-9
- Drulis-Kawa Z, Dorotkiewicz-Jach A (2010) Liposomes as delivery systems for antibiotics. *Int J Pharm* **387**: 187-198
- Drulis-Kawa Z, Maciaszczyk-Dziubinska E, Bocer T Genomic sequence and analysis of *Klebsiella* sp. KP32 bacteriophage. Unpublished.
- During K, Porsch P, Mahn A, Brinkmann O, Gieffers W (1999) The non-enzymatic microbicidal activity of lysozymes. *FEBS Lett* **449**: 93-100
- Ehrenstein G, Lecar H (1977) Electrically gated ionic channels in lipid bilayers. *Q Rev Biophys* **10**: 1-34
- Ellis TN, Kuehn MJ (2010) Virulence and immunomodulatory roles of bacterial outer membrane vesicles. *Microbiol Mol Biol Rev* **74**: 81-94
- Erijman L, Clegg RM (1998) Reversible stalling of transcription elongation complexes by high pressure. *Biophys J* **75**: 453-462
- Ernst RK, Yi EC, Guo L, Lim KB, Burns JL, Hackett M, Miller SI (1999) Specific lipopolysaccharide found in cystic fibrosis airway *Pseudomonas aeruginosa*. *Science* **286**: 1561-1565
- Ernst RK, Adams KN, Moskowitz SM, Kraig GM, Kawasaki K, Stead CM, Trent MS, Miller SI (2006) The *Pseudomonas aeruginosa* lipid A deacylase: selection for expression and loss within the cystic fibrosis airway. *J Bacteriol* **188**: 191-201
- Ernst RK, Moskowitz SM, Emerson JC, Kraig GM, Adams KN, Harvey MD, Ramsey B, Speert DP, Burns JL, Miller SI (2007) Unique lipid A modifications in *Pseudomonas aeruginosa* isolated from the airways of patients with cystic fibrosis. *J Infect Dis* **196**: 1088-1092
- Evrard C, Fastrez J, Declercq JP (1998) Crystal structure of the lysozyme from bacteriophage lambda and its relationship with V and C-type lysozymes. *J Mol Biol* **276**: 151-164
- Ewbank JJ, Zugasti O (2011) *C. elegans*: model host and tool for antimicrobial drug discovery. *Disease Models & Mechanisms* **4**: 300-304
- Fernandes S, Proenca D, Cantante C, Silva FA, Leandro C, Lourenco S, Milheirico C, de Lencastre H, Cavaco-Silva P, Pimentel M, Sao-Jose C (2012) Novel Chimerical Endolysins with Broad Antimicrobial Activity Against Methicillin-Resistant *Staphylococcus aureus*. *Microb Drug Resist* **18**: 333-343
- Finn RD, Mistry J, Tate J, Coghill P, Heger A, Pollington JE, Gavin OL, Gunasekaran P, Ceric G, Forslund K, Holm L, Sonnhammer EL, Eddy SR, Bateman A (2010) The Pfam protein families database. *Nucleic Acids Res* **38**: D211-222
- Fischer MJ (2010) Amine coupling through EDC/NHS: a practical approach. *Methods Mol Biol* **627**: 55-73
- Fischetti VA, Gotschlich EC, Bernheimer AW (1971) Purification and physical properties of group C streptococcal phage-associated lysin. *J Exp Med* **133**: 1105-1117
- Fischetti VA (2001) Phage antibacterials make a comeback. *Nat Biotechnol* **19**: 734-735
- Fischetti VA (2005) Bacteriophage lytic enzymes: novel anti-infectives. *Trends Microbiol* **13**: 491-496
- Fischetti VA (2010) Bacteriophage endolysins: a novel anti-infective to control Gram-positive pathogens. *Int J Med Microbiol* **300**: 357-362
- Fokine A, Battisti AJ, Bowman VD, Efimov AV, Kurochkina LP, Chipman PR, Mesyanzhinov VV, Rossmann MG (2007) Cryo-EM study of the *Pseudomonas* bacteriophage phiK2. *Structure* **15**: 1099-1104
- Fokine A, Miroshnikov KA, Shneider MM, Mesyanzhinov VV, Rossmann MG (2008) Structure of the bacteriophage phi K2 lytic transglycosylase gp144. *J Biol Chem* **283**: 7242-7250
- Galvez A, Abriouel H, Lopez RL, Ben Omar N (2007) Bacteriocin-based strategies for food biopreservation. *Int J Food Microbiol* **120**: 51-70
- Ganzle MG, Vogel RF (2001) On-line fluorescence determination of pressure mediated outer membrane damage in *Escherichia coli*. *Syst Appl Microbiol* **24**: 477-485
- Garcia-del Portillo F, Foster JW, Maguire ME, Finlay BB (1992) Characterization of the micro-environment of Salmonella Typhimurium-containing vacuoles within MDCK epithelial cells. *Mol Microbiol* **6**: 3289-3297
- Garcia E, Garcia JL, Garcia P, Arraras A, Sanchez-Puelles JM, Lopez R (1988) Molecular evolution of lytic enzymes of *Streptococcus pneumoniae* and its bacteriophages. *Proc Natl Acad Sci U S A* **85**: 914-918
- Garcia P, Martinez B, Rodriguez L, Rodriguez A (2010) Synergy between the phage endolysin LysH5 and nisin to kill *Staphylococcus aureus* in pasteurized milk. *Int J Food Microbiol* **141**: 151-155

- Garsin DA, Villanueva JM, Begun J, Kim DH, Sifri CD, Calderwood SB, Ruvkun G, Ausubel FM (2003) Long-lived *C. elegans* daf-2 mutants are resistant to bacterial pathogens. *Science* **300**: 19-21
- Gasteiger E, Hoogland C, Gattiker A, Duvaud S, Wilkins MR, Appel RD, Bairoch A (2005) Protein Identification and Analysis Tools on the ExPASy Server. In: Walker JM (ed.) *The Proteomics Protocols Handbook*, Humana Press. pp. 571-607.
- Gazit E, Boman A, Boman HG, Shai Y (1995) Interaction of the mammalian antibacterial peptide cecropin P1 with phospholipid vesicles. *Biochemistry* **34**: 11479-11488
- Geier G, Banaj HJ, Heid H, Bini L, Pallini V, Zwilling R (1999) Aspartyl proteases in *Caenorhabditis elegans*. Isolation, identification and characterization by a combined use of affinity chromatography, two-dimensional gel electrophoresis, microsequencing and databank analysis. *Eur J Biochem* **264**: 872-879
- Gendrin C, Contreras-Martel C, Bouillot S, Elsen S, Lemaire D, Skoufias DA, Huber P, Attree I, Dessen A (2012) Structural basis of cytotoxicity mediated by the type III secretion toxin ExoU from *Pseudomonas aeruginosa*. *PLoS Pathog* **8**: e1002637
- Gibbons HS, Lin S, Cotter RJ, Raetz CR (2000) Oxygen requirement for the biosynthesis of the S-2-hydroxymyristate moiety in *Salmonella* Typhimurium lipid A. Function of LpxO, A new Fe²⁺/alpha-ketoglutarate-dependent dioxygenase homologue. *J Biol Chem* **275**: 32940-32949
- Godeke J, Paul K, Lassak J, Thormann KM (2011) Phage-induced lysis enhances biofilm formation in *Shewanella oneidensis* MR-1. *ISME J* **5**: 613-626
- Govind R, Dupuy B (2012) Secretion of *Clostridium difficile* Toxins A and B Requires the Holin-like Protein TcdE. *PLoS Pathog* **8**: e1002727
- Green H, Kehinde O, Thomas J (1979) Growth of cultured human epidermal cells into multiple epithelia suitable for grafting. *Proc Natl Acad Sci U S A* **76**: 5665-5668
- Groisman EA (2001) The pleiotropic two-component regulatory system PhoP-PhoQ. *J Bacteriol* **183**: 1835-1842
- Grundling A, Manson MD, Young R (2001) Holins kill without warning. *Proc Natl Acad Sci U S A* **98**: 9348-9352
- Guha A, Choudhury A, Unni BG, Roy MK (2002) Effect of outer-membrane permeabilizers on the activity of antibiotics and plant extracts against *Pseudomonas aeruginosa*. *Folia Microbiol (Praha)* **47**: 379-384
- Gunn JS, Lim KB, Krueger J, Kim K, Guo L, Hackett M, Miller SI (1998) PmrA-PmrB-regulated genes necessary for 4-aminoarabinose lipid A modification and polymyxin resistance. *Mol Microbiol* **27**: 1171-1182
- Guo L, Lim KB, Gunn JS, Bainbridge B, Darveau RP, Hackett M, Miller SI (1997) Regulation of lipid A modifications by *Salmonella* Typhimurium virulence genes phoP-phoQ. *Science* **276**: 250-253
- Guo L, Lim KB, Poduje CM, Daniel M, Gunn JS, Hackett M, Miller SI (1998) Lipid A acylation and bacterial resistance against vertebrate antimicrobial peptides. *Cell* **95**: 189-198
- Hajjar AM, Ernst RK, Tsai JH, Wilson CB, Miller SI (2002) Human Toll-like receptor 4 recognizes host-specific LPS modifications. *Nat Immunol* **3**: 354-359
- Halwani M, Mugabe C, Azghani AO, Lafrenie RM, Kumar A, Omri A (2007) Bactericidal efficacy of liposomal aminoglycosides against *Burkholderia cenocepacia*. *J Antimicrob Chemother* **60**: 760-769
- Hancock RE (1984) Alterations in outer membrane permeability. *Annu Rev Microbiol* **38**: 237-264
- Hancock RE, Wong PG (1984) Compounds which increase the permeability of the *Pseudomonas aeruginosa* outer membrane. *Antimicrob Agents Chemother* **26**: 48-52
- Hancock RE, Farmer SW, Li ZS, Poole K (1991) Interaction of aminoglycosides with the outer membranes and purified lipopolysaccharide and OmpF porin of *Escherichia coli*. *Antimicrob Agents Chemother* **35**: 1309-1314
- Hancock RE, Farmer SW (1993) Mechanism of uptake of deglucoteicoplanin amide derivatives across outer membranes of *Escherichia coli* and *Pseudomonas aeruginosa*. *Antimicrob Agents Chemother* **37**: 453-456
- Hancock RE (2001) Cationic peptides: effectors in innate immunity and novel antimicrobials. *Lancet Infect Dis* **1**: 156-164
- Handa H, Gurchynski S, Jackson MP, Mao G (2010) Immobilization and molecular interactions between bacteriophage and lipopolysaccharide bilayers. *Langmuir* **26**: 12095-12103
- Hauben KJA, Wuytack EY, Soontjens CCF, Michiels CW (1996) High-pressure transient sensitization of *Escherichia coli* to lysozyme and nisin by disruption of outer-membrane permeability. *J Food Protect* **59**: 350-355
- Haun RS, Serventi IM, Moss J (1992) Rapid, reliable ligation-independent cloning of PCR products using modified plasmid vectors. *Biotechniques* **13**: 515-518

- Helander IM, Mattila-Sandholm T (2000) Fluorometric assessment of Gram-negative bacterial permeabilization. *J Appl Microbiol* **88**: 213-219
- Hong S, Leroueil PR, Janus EK, Peters JL, Kober MM, Islam MT, Orr BG, Baker JR, Jr., Banaszak Holl MM (2006) Interaction of polycationic polymers with supported lipid bilayers and cells: nanoscale hole formation and enhanced membrane permeability. *Bioconjug Chem* **17**: 728-734
- Hornsey M, Phee L, Wareham DW (2011) A novel variant, NDM-5, of the New Delhi metallo-beta-lactamase in a multidrug-resistant *Escherichia coli* ST648 isolate recovered from a patient in the United Kingdom. *Antimicrob Agents Chemother* **55**: 5952-5954
- Huang HW (2000) Action of antimicrobial peptides: two-state model. *Biochemistry* **39**: 8347-8352
- Hughes KA, Sutherland IW, Jones MV (1998) Biofilm susceptibility to bacteriophage attack: the role of phage-borne polysaccharide depolymerase. *Microbiology* **144**: 3039-3047
- Ibrahim HR, Yamada M, Matsushita K, Kobayashi K, Kato A (1994) Enhanced bactericidal action of lysozyme to *Escherichia coli* by inserting a hydrophobic pentapeptide into its C terminus. *J Biol Chem* **269**: 5059-5063
- Irvin RT, MacAlister TJ, Costerton JW (1981) Tris(hydroxymethyl)aminomethane buffer modification of *Escherichia coli* outer membrane permeability. *J Bacteriol* **145**: 1397-1403
- Ito Y, Kwon OH, Ueda M, Tanaka A, Imanishi Y (1997) Bactericidal activity of human lysozymes carrying various lengths of polyproline chain at the C-terminus. *FEBS Lett* **415**: 285-288
- Jacob F, Fuerst CR (1958) The mechanism of lysis by phage studied with defective lysogenic bacteria. *J Gen Microbiol* **18**: 518-526
- Jones AP, Wallis C (2010) Dornase alfa for cystic fibrosis. *Cochrane Database Syst Rev*: CD001127
- Junn HJ, Youn J, Suh KH, Lee SS (2005) Cloning and expression of *Klebsiella* phage K11 lysozyme gene. *Protein Expr Purif* **42**: 78-84
- Jurkevitch E (2012) Isolation and classification of *Bdellovibrio* and like organisms. *Curr Protoc Microbiol* **Chapter 7**: Unit7B 1
- Kadurugamuwa JL, Beveridge TJ (1996) Bacteriolytic effect of membrane vesicles from *Pseudomonas aeruginosa* on other bacteria including pathogens: conceptually new antibiotics. *J Bacteriol* **178**: 2767-2774
- Kadurugamuwa JL, Beveridge TJ (1997) Natural release of virulence factors in membrane vesicles by *Pseudomonas aeruginosa* and the effect of aminoglycoside antibiotics on their release. *J Antimicrob Chemother* **40**: 615-621
- Kagan BL, Selsted ME, Ganz T, Lehrer RI (1990) Antimicrobial defensin peptides form voltage-dependent ion-permeable channels in planar lipid bilayer membranes. *Proc Natl Acad Sci U S A* **87**: 210-214
- Karch H, Denamur E, Dobrindt U, Finlay BB, Hengge R, Johannes L, Ron EZ, Tonjum T, Sansonetti PJ, Vicente M (2012) The enemy within us: lessons from the 2011 European *Escherichia coli* O104:H4 outbreak. *EMBO Mol Med* **4**: 841-848
- Kawasaki K, Ernst RK, Miller SI (2004a) 3-O-deacylation of lipid A by PagL, a PhoP/PhoQ-regulated deacylase of *Salmonella* Typhimurium, modulates signaling through Toll-like receptor 4. *J Biol Chem* **279**: 20044-20048
- Kawasaki K, Ernst RK, Miller SI (2004b) Deacylation and palmitoylation of lipid A by *Salmonella* outer membrane enzymes modulate host signaling through Toll-like receptor 4. *J Endotoxin Res* **10**: 439-444
- Kaya S, Araki Y, Ito E (1989) The structure of the O-polysaccharide from *Pseudomonas aeruginosa* IID 1009 (ATCC 27585). *J Biochem* **105**: 35-38
- Kempf M, Rolain JM (2012) Emergence of resistance to carbapenems in *Acinetobacter baumannii* in Europe: clinical impact and therapeutic options. *Int J Antimicrob Agents* **39**: 105-114
- Kim J-Y, Doody AM, Chen DJ, Cremona GH, Shuler ML, Putnam D, DeLisa MP (2008) Engineered Bacterial Outer Membrane Vesicles with Enhanced Functionality. *Journal of Molecular Biology* **380**: 51-66
- Kim SH, Wei CI (2007) Biofilm formation by multidrug-resistant *Salmonella enterica* serotype Typhimurium phage type DT104 and other pathogens. *J Food Prot* **70**: 22-29
- Klemens SP, Cynamon MH, Swenson CE, Ginsberg RS (1990) Liposome-encapsulated-gentamicin therapy of *Mycobacterium avium* complex infection in beige mice. *Antimicrob Agents Chemother* **34**: 967-970
- Knirel YA, Bystrova OV, Kocharova NA, Zahringer U, Pier GB (2006) Conserved and variable structural features in the lipopolysaccharide of *Pseudomonas aeruginosa*. *J Endotoxin Res* **12**: 324-336
- Kokryakov VN, Harwig SS, Panyutich EA, Shevchenko AA, Aleshina GM, Shamova OV, Korneva HA, Lehrer RI (1993) Protegrins: leukocyte antimicrobial peptides that combine features of corticostatic defensins and tachyplesins. *FEBS Lett* **327**: 231-236

- Koo YS, Kim JM, Park IY, Yu BJ, Jang SA, Kim KS, Park CB, Cho JH, Kim SC (2008) Structure-activity relations of parasin I, a histone H2A-derived antimicrobial peptide. *Peptides* **29**: 1102-1108
- Korndorfer IP, Kanitz A, Danzer J, Zimmer M, Loessner MJ, Skerra A (2008) Structural analysis of the L-alanyl-D-glutamate endopeptidase domain of *Listeria* bacteriophage endolysin Ply500 reveals a new member of the LAS peptidase family. *Acta Crystallogr D Biol Crystallogr* **64**: 644-650
- Kragol G, Lovas S, Varadi G, Condie BA, Hoffmann R, Otvos L, Jr. (2001) The antibacterial peptide pyrrocoricin inhibits the ATPase actions of DnaK and prevents chaperone-assisted protein folding. *Biochemistry* **40**: 3016-3026
- Krause RM (1958) Studies on the bacteriophages of hemolytic streptococci. II. Antigens released from the streptococcal cell wall by a phage-associated lysin. *J Exp Med* **108**: 803-821
- Kristian SA, Durr M, Van Strijp JA, Neumeister B, Peschel A (2003) MprF-mediated lysinylation of phospholipids in *Staphylococcus aureus* leads to protection against oxygen-independent neutrophil killing. *Infect Immun* **71**: 546-549
- Kropinski AM, Kovalyova IV, Billington SJ, Patrick AN, Butts BD, Guichard JA, Pitcher TJ, Guthrie CC, Sydlaske AD, Barnhill LM, Havens KA, Day KR, Falk DR, McConnell MR (2007) The genome of epsilon15, a serotype-converting, Group E1 *Salmonella enterica*-specific bacteriophage. *Virology* **369**: 234-244
- Krylov VN, Dela Cruz DM, Hertveldt K, Ackermann HW (2007) "phiKZ-like viruses", a proposed new genus of myovirus bacteriophages. *Arch Virol* **152**: 1955-1959
- Kuehn MJ, Kesty NC (2005) Bacterial outer membrane vesicles and the host-pathogen interaction. *Genes Dev* **19**: 2645-2655
- Kurz CL, Ewbank JJ (2003) *Caenorhabditis elegans*: an emerging genetic model for the study of innate immunity. *Nat Rev Genet* **4**: 380-390
- Kuty GF, Xu M, Struck DK, Summer EJ, Young R (2010) Regulation of a phage endolysin by disulfide caging. *J Bacteriol* **192**: 5682-5687
- Lai MJ, Lin NT, Hu A, Soo PC, Chen LK, Chen LH, Chang KC (2011) Antibacterial activity of *Acinetobacter baumannii* phage varphiAB2 endolysin (LysAB2) against both gram-positive and Gram-negative bacteria. *Appl Microbiol Biotechnol* **90**: 529-539
- Lai R, Liu H, Hui Lee W, Zhang Y (2001) A novel bradykinin-related peptide from skin secretions of toad *Bombina maxima* and its precursor containing six identical copies of the final product. *Biochem Biophys Res Commun* **286**: 259-263
- Lambert PA (2002) Mechanisms of antibiotic resistance in *Pseudomonas aeruginosa*. *J R Soc Med* **95 Suppl 41**: 22-26
- Larkin MA, Blackshields G, Brown NP, Chenna R, McGettigan PA, McWilliam H, Valentin F, Wallace IM, Wilm A, Lopez R, Thompson JD, Gibson TJ, Higgins DG (2007) Clustal W and Clustal X version 2.0. *Bioinformatics* **23**: 2947-2948
- Larose L, Gish G, Pawson T (1995) Construction of an SH2 domain-binding site with mixed specificity. *J Biol Chem* **270**: 3858-3862
- Lavigne R, Briers Y, Hertveldt K, Robben J, Volckaert G (2004) Identification and characterization of a highly thermostable bacteriophage lysozyme. *Cell Mol Life Sci* **61**: 2753-2759
- Lehrer RI, Lichtenstein AK, Ganz T (1993) Defensins: antimicrobial and cytotoxic peptides of mammalian cells. *Annu Rev Immunol* **11**: 105-128
- Leive L, Shovlin VK, Mergenhagen SE (1968) Physical, chemical, and immunological properties of lipopolysaccharide released from *Escherichia coli* by ethylenediaminetetraacetate. *J Biol Chem* **243**: 6384-6391
- Lerner TR, Lovering AL, Bui NK, Uchida K, Aizawa S, Vollmer W, Sockett RE (2012) Specialized peptidoglycan hydrolases sculpt the intrabacterial niche of predatory *Bdellovibrio* and increase population fitness. *PLoS Pathog* **8**: e1002524
- Leung AK, Duwel HS, Honek JF, Berghuis AM (2001) Crystal structure of the lytic transglycosylase from bacteriophage lambda in complex with hexa-N-acetylchitohexaose. *Biochemistry* **40**: 5665-5673
- Li Q, Zhang SH, Yu YH, Wang LP, Guan SW, Li PF (2012) Toxicity of sodium fluoride to *Caenorhabditis elegans*. *Biomed Environ Sci* **25**: 216-223
- Li XZ, Poole K, Nikaido H (2003) Contributions of MexAB-OprM and an EmrE homolog to intrinsic resistance of *Pseudomonas aeruginosa* to aminoglycosides and dyes. *Antimicrob Agents Chemother* **47**: 27-33
- Lin YM, Wu SJ, Chang TW, Wang CF, Suen CS, Hwang MJ, Chang MD, Chen YT, Liao YD (2010) Outer membrane protein I of *Pseudomonas aeruginosa* is a target of cationic antimicrobial peptide/protein. *J Biol Chem* **285**: 8985-8994
- Liu B, Knirel YA, Feng L, Perepelov AV, Senchenkova SN, Wang Q, Reeves PR, Wang L (2008) Structure and genetics of *Shigella* O antigens. *FEMS Microbiol Rev* **32**: 627-653

- Liu B, Perepelov AV, Li D, Senchenkova SN, Han Y, Shashkov AS, Feng L, Knirel YA, Wang L (2010) Structure of the O-antigen of *Salmonella* O66 and the genetic basis for similarity and differences between the closely related O-antigens of *Escherichia coli* O166 and *Salmonella* O66. *Microbiology* **156**: 1642-1649
- Liu YF, Yan JJ, Lei HY, Teng CH, Wang MC, Tseng CC, Wu JJ (2012) Loss of outer membrane protein C in *Escherichia coli* contributes to both antibiotic resistance and escaping antibody-dependent bactericidal activity. *Infect Immun* **80**: 1815-1822
- Lochnit G, Grabitzki J, Henkel B, Tavernarakis N, Geyer R (2006) First identification of a phosphorylcholine-substituted protein from *Caenorhabditis elegans*: isolation and characterization of the aspartyl protease ASP-6. *Biol Chem* **387**: 1487-1493
- Lodowska J, Wolny D, Weglarz L, Dzierzewicz Z (2007) The structural diversity of lipid A from Gram-negative bacteria. *Postepy Hig Med Dosw (Online)* **61**: 106-121
- Loeffler JM, Djurkovic S, Fischetti VA (2003) Phage lytic enzyme Cpl-1 as a novel antimicrobial for pneumococcal bacteremia. *Infect Immun* **71**: 6199-6204
- Loeffler JM, Fischetti VA (2003) Synergistic lethal effect of a combination of phage lytic enzymes with different activities on penicillin-sensitive and -resistant *Streptococcus pneumoniae* strains. *Antimicrob Agents Chemother* **47**: 375-377
- Loessner MJ, Wendlinger G, Scherer S (1995) Heterogeneous endolysins in *Listeria monocytogenes* bacteriophages: a new class of enzymes and evidence for conserved holin genes within the siphoviral lysis cassettes. *Mol Microbiol* **16**: 1231-1241
- Loessner MJ, Kramer K, Ebel F, Scherer S (2002) C-terminal domains of *Listeria monocytogenes* bacteriophage murein hydrolases determine specific recognition and high-affinity binding to bacterial cell wall carbohydrates. *Mol Microbiol* **44**: 335-349
- Loessner MJ (2005) Bacteriophage endolysins--current state of research and applications. *Curr Opin Microbiol* **8**: 480-487
- Lopez R, Garcia E, Garcia P, Garcia JL (1997) The pneumococcal cell wall degrading enzymes: a modular design to create new lysins? *Microb Drug Resist* **3**: 199-211
- Loutet SA, Valvano MA (2011) Extreme antimicrobial Peptide and polymyxin B resistance in the genus *Burkholderia*. *Front Microbiol* **2**: 159
- Low LY, Yang C, Perego M, Osterman A, Liddington RC (2005) Structure and lytic activity of a *Bacillus anthracis* prophage endolysin. *J Biol Chem* **280**: 35433-35439
- Luque-Ortega JR, van't Hof W, Veerman EC, Saugar JM, Rivas L (2008) Human antimicrobial peptide histatin 5 is a cell-penetrating peptide targeting mitochondrial ATP synthesis in *Leishmania*. *FASEB J* **22**: 1817-1828
- Maass D, Weidel W (1963) Final Proof for the Identity of Enzymic Specificities of Egg-White Lysozyme and Phage T2 Enzyme. *Biochim Biophys Acta* **78**: 369-370
- Mah TF (2012) Biofilm-specific antibiotic resistance. *Future Microbiol* **7**: 1061-1072
- Mahajan-Miklos S, Tan MW, Rahme LG, Ausubel FM (1999) Molecular mechanisms of bacterial virulence elucidated using a *Pseudomonas aeruginosa*-*Caenorhabditis elegans* pathogenesis model. *Cell* **96**: 47-56
- Martinez V, de la Pena F, Garcia-Hidalgo J, de la Mata I, Garcia JL, Prieto MA (2012) Identification and biochemical evidence of a medium-chain-length polyhydroxyalkanoate depolymerase in the *Bdellovibrio bacteriovorus* predatory hydrolytic arsenal. *Appl Environ Microbiol* **78**: 6017-6026
- Mascio CT, Mortin LI, Howland KT, Van Praagh AD, Zhang S, Arya A, Chuong CL, Kang C, Li T, Silverman JA (2012) In vitro and in vivo characterization of CB-183,315, a novel lipopeptide antibiotic for treatment of *Clostridium difficile*. *Antimicrob Agents Chemother* **56**: 5023-5030
- Masschalck B, Van Houdt R, Van Haver EG, Michiels CW (2001) Inactivation of Gram-negative bacteria by lysozyme, denatured lysozyme, and lysozyme-derived peptides under high hydrostatic pressure. *Appl Environ Microbiol* **67**: 339-344
- Matsushita K, Adachi O, Shinagawa E, Ameyama M (1978) Isolation and characterization of outer and inner membranes from *Pseudomonas aeruginosa* and effect of EDTA on the membranes. *J Biochem* **83**: 171-181
- Matsuzaki S, Rashed M, Uchiyama J, Sakurai S, Ujihara T, Kuroda M, Ikeuchi M, Tani T, Fujieda M, Wakiguchi H, Imai S (2005) Bacteriophage therapy: a revitalized therapy against bacterial infectious diseases. *J Infect Chemother* **11**: 211-219
- Matthews BW, Remington SJ (1974) The three dimensional structure of the lysozyme from bacteriophage T4. *Proc Natl Acad Sci U S A* **71**: 4178-4182
- Matthews BW (1995) In: Eisenberg DS, Richards FM (eds.) *Adv. Protein Chemistry*, Academic Press, San Diego. pp. 249-278
- Mayer MJ, Gasson MJ, Narbad A (2012) Genomic sequence of bacteriophage ATCC 8074-B1 and activity of its endolysin and engineered variants against *Clostridium sporogenes*. *Appl Environ Microbiol* **78**: 3685-3692

- Mayrand D, Grenier D (1989) Biological activities of outer membrane vesicles. *Can J Microbiol* **35**: 607-613
- McGowan S, Buckle AM, Mitchell MS, Hoopes JT, Gallagher DT, Heselpoth RD, Shen Y, Reboul CF, Law RH, Fischetti VA, Whisstock JC, Nelson DC (2012) X-ray crystal structure of the streptococcal specific phage lysin PlyC. *Proc Natl Acad Sci U S A* **109**: 12752-12757
- McPhee JB, Lewenza S, Hancock RE (2003) Cationic antimicrobial peptides activate a two-component regulatory system, PmrA-PmrB, that regulates resistance to polymyxin B and cationic antimicrobial peptides in *Pseudomonas aeruginosa*. *Mol Microbiol* **50**: 205-217
- Medina MB, VanHouten L, Cooke PH, Tu SI (1997) Real-time analysis of antibody binding interactions with immobilized E-coli O157:H7 cells using the BIAcore. *Biotechnol Tech* **11**: 173-176
- Miedzybrodzki R, Borysowski J, Weber-Dabrowska B, Fortuna W, Letkiewicz S, Szufnarowski K, Pawelczyk Z, Rogoz P, Klak M, Wojtasik E, Gorski A (2012) Clinical aspects of phage therapy. *Adv Virus Res* **83**: 73-121
- Moak M, Molineux IJ (2004) Peptidoglycan hydrolytic activities associated with bacteriophage virions. *Mol Microbiol* **51**: 1169-1183
- Monterroso B, Albert A, Martinez-Ripoll M, Garcia P, Garcia JL, Menendez M, Hermoso JA (2002) Crystallization and preliminary X-ray diffraction studies of the complete modular endolysin from Cp-1, a phage infecting *Streptococcus pneumoniae*. *Acta Crystallogr D Biol Crystallogr* **58**: 1487-1489
- Monzon M, Oteiza C, Leiva J, Lamata M, Amorena B (2002) Biofilm testing of Staphylococcus epidermidis clinical isolates: low performance of vancomycin in relation to other antibiotics. *Diagn Microbiol Infect Dis* **44**: 319-324
- Mor A, Hani K, Nicolas P (1994) The vertebrate peptide antibiotics dermaseptins have overlapping structural features but target specific microorganisms. *J Biol Chem* **269**: 31635-31641
- Morikawa N, Hagiwara K, Nakajima T (1992) Brevinin-1 and -2, unique antimicrobial peptides from the skin of the frog, *Rana brevipoda porsa*. *Biochem Biophys Res Commun* **189**: 184-190
- Morita M, Tanji Y, Mizoguchi K, Soejima A, Orito Y, Unno H (2001) Antibacterial activity of *Bacillus amyloliquefaciens* phage endolysin without holin conjugation. *J Biosci Bioeng* **91**: 469-473
- Moskowitz SM, Ernst RK (2010) The role of *Pseudomonas* lipopolysaccharide in cystic fibrosis airway infection. *Subcell Biochem* **53**: 241-253
- Moy TI, Ball AR, Anklesaria Z, Casadei G, Lewis K, Ausubel FM (2006) Identification of novel antimicrobials using a live-animal infection model. *Proc Natl Acad Sci U S A* **103**: 10414-10419
- Mugabe C, Halwani M, Azghani AO, Lafrenie RM, Omri A (2006) Mechanism of enhanced activity of liposome-entrapped aminoglycosides against resistant strains of *Pseudomonas aeruginosa*. *Antimicrob Agents Chemother* **50**: 2016-2022
- Murphy JS (1957) A phage-associated enzyme of *Bacillus megaterium* which destroys the bacterial cell wall. *Virology* **4**: 563-581
- Murray GL, Attridge SR, Morona R (2006) Altering the length of the lipopolysaccharide O antigen has an impact on the interaction of *Salmonella enterica* serovar Typhimurium with macrophages and complement. *J Bacteriol* **188**: 2735-2739
- Murzyn K, Pasenkiewicz-Gierula M (2003) Construction of a toroidal model for the magainin pore. *J Mol Model* **9**: 217-224
- Na YJ, Han SB, Kang JS, Yoon YD, Park SK, Kim HM, Yang KH, Joe CO (2004) Lactoferrin works as a new LPS-binding protein in inflammatory activation of macrophages. *Int Immunopharmacol* **4**: 1187-1199
- Nakamura T, Furunaka H, Miyata T, Tokunaga F, Muta T, Iwanaga S, Niwa M, Takao T, Shimonishi Y (1988) Tachyplesin, a class of antimicrobial peptide from the hemocytes of the horseshoe crab (*Tachypleus tridentatus*). Isolation and chemical structure. *J Biol Chem* **263**: 16709-16713
- Nakayama K, Kanaya S, Ohnishi M, Terawaki Y, Hayashi T (1999) The complete nucleotide sequence of phi CTX, a cytotoxin-converting phage of *Pseudomonas aeruginosa*: implications for phage evolution and horizontal gene transfer via bacteriophages. *Mol Microbiol* **31**: 399-419
- Nakimbugwe D, Masschalck B, Atanassova M, Zewdie-Bosuner A, Michiels CW (2006) Comparison of bactericidal activity of six lysozymes at atmospheric pressure and under high hydrostatic pressure. *Int J Food Microbiol* **108**: 355-363
- Nan YH, Park KH, Park Y, Jeon YJ, Kim Y, Park IS, Hahm KS, Shin SY (2009) Investigating the effects of positive charge and hydrophobicity on the cell selectivity, mechanism of action and anti-inflammatory activity of a Trp-rich antimicrobial peptide indolicidin. *FEMS Microbiol Lett* **292**: 134-140
- Nascimento JG, Guerreiro-Pereira MC, Costa SF, Sao-Jose C, Santos MA (2008) Nisin-triggered activity of Lys44, the secreted endolysin from *Oenococcus oeni* phage fOg44. *J Bacteriol* **190**: 457-461
- Navarre WW, Ton-That H, Faull KF, Schneewind O (1999) Multiple enzymatic activities of the murein hydrolase from staphylococcal phage phi11. Identification of a D-alanyl-glycine endopeptidase activity. *J Biol Chem* **274**: 15847-15856

- Nelson D, Schuch R, Chahales P, Zhu S, Fischetti VA (2006) PlyC: a multimeric bacteriophage lysin. *Proc Natl Acad Sci U S A* **103**: 10765-10770
- Nelson DC, Schmelcher M, Rodriguez-Rubio L, Klumpp J, Pritchard DG, Dong S, Donovan DM (2012) Endolysins as antimicrobials. *Adv Virus Res* **83**: 299-365
- Nicolas P (2009) Multifunctional host defense peptides: intracellular-targeting antimicrobial peptides. *FEBS J* **276**: 6483-6496
- Nikaido H (1998) The role of outer membrane and efflux pumps in the resistance of Gram-negative bacteria. Can we improve drug access? *Drug Resist Updat* **1**: 93-98
- Nikaido H (2003) Molecular basis of bacterial outer membrane permeability revisited. *Microbiol Mol Biol Rev* **67**: 593-656
- Nikaido H, Vaara M (1985) Molecular basis of bacterial outer membrane permeability. *Microbiol Rev* **49**: 1-32
- Oren Z, Shai Y (1998) Mode of action of linear amphipathic alpha-helical antimicrobial peptides. *Biopolymers* **47**: 451-463
- Orito Y, Morita M, Hori K, Unno H, Tanji Y (2004) *Bacillus amyloliquefaciens* phage endolysin can enhance permeability of *Pseudomonas aeruginosa* outer membrane and induce cell lysis. *Appl Microbiol Biotechnol* **65**: 105-109
- Otvos L, Jr., O I, Rogers ME, Consolvo PJ, Condie BA, Lovas S, Bulet P, Blaszczyk-Thurin M (2000) Interaction between heat shock proteins and antimicrobial peptides. *Biochemistry* **39**: 14150-14159
- Page RD (2002) Visualizing phylogenetic trees using TreeView. *Curr Protoc Bioinformatics* **Chapter 6**: Unit 6 2
- Paradis-Bleau C, Cloutier I, Lemieux L, Sanschagrin F, Laroche J, Auger M, Garnier A, Levesque RC (2007) Peptidoglycan lytic activity of the *Pseudomonas aeruginosa* phage phiKZ gp144 lytic transglycosylase. *FEMS Microbiol Lett* **266**: 201-209
- Park IY, Park CB, Kim MS, Kim SC (1998) Parasin I, an antimicrobial peptide derived from histone H2A in the catfish, *Parasilurus asotus*. *FEBS Lett* **437**: 258-262
- Park J, Yun J, Lim JA, Kang DH, Ryu S (2012) Characterization of an endolysin, LysBPS13, from a *Bacillus cereus* bacteriophage. *FEMS Microbiol Lett* **332**: 76-83
- Park SC, Kim JY, Shin SO, Jeong CY, Kim MH, Shin SY, Cheong GW, Park Y, Hahm KS (2006) Investigation of toroidal pore and oligomerization by melittin using transmission electron microscopy. *Biochem Biophys Res Commun* **343**: 222-228
- Parsons LM, Lin F, Orban J (2006) Peptidoglycan recognition by Pal, an outer membrane lipoprotein. *Biochemistry* **45**: 2122-2128
- Patrzykat A, Friedrich CL, Zhang L, Mendoza V, Hancock RE (2002) Sublethal concentrations of pleurocidin-derived antimicrobial peptides inhibit macromolecular synthesis in *Escherichia coli*. *Antimicrob Agents Chemother* **46**: 605-614
- Perez-Dorado I, Campillo NE, Monterroso B, Heseck D, Lee M, Paez JA, Garcia P, Martinez-Ripoll M, Garcia JL, Mobashery S, Menendez M, Hermoso JA (2007) Elucidation of the molecular recognition of bacterial cell wall by modular pneumococcal phage endolysin Cpl-1. *J Biol Chem* **282**: 24990-24999
- Petsch D, Deckwer WD, Anspach FB (1998) Proteinase K digestion of proteins improves detection of bacterial endotoxins by the Limulus amoebocyte lysate assay: application for endotoxin removal from cationic proteins. *Anal Biochem* **259**: 42-47
- Pier GB (2007) *Pseudomonas aeruginosa* lipopolysaccharide: a major virulence factor, initiator of inflammation and target for effective immunity. *Int J Med Microbiol* **297**: 277-295
- Piers KL, Brown MH, Hancock RE (1994) Improvement of outer membrane-permeabilizing and lipopolysaccharide-binding activities of an antimicrobial cationic peptide by C-terminal modification. *Antimicrob Agents Chemother* **38**: 2311-2316
- Pirnay JP, De Vos D, Cochez C, Bilocq F, Pirson J, Struelens M, Duinslaeger L, Cornelis P, Zizi M, Vanderkelen A (2003) Molecular epidemiology of *Pseudomonas aeruginosa* colonization in a burn unit: persistence of a multidrug-resistant clone and a silver sulfadiazine-resistant clone. *J Clin Microbiol* **41**: 1192-1202
- Pirnay JP, Bilocq F, Pot B, Cornelis P, Zizi M, Van Eldere J, Deschaght P, Vaneechoutte M, Jennes S, Pitt T, De Vos D (2009) *Pseudomonas aeruginosa* population structure revisited. *PLoS One* **4**: e7740
- Poirel L, Nordmann P (2006) Carbapenem resistance in *Acinetobacter baumannii*: mechanisms and epidemiology. *Clin Microbiol Infect* **12**: 826-836
- Polyansky AA, Vassilevski AA, Volynsky PE, Vorontsova OV, Samsonova OV, Egorova NS, Krylov NA, Feofanov AV, Arseniev AS, Grishin EV, Efremov RG (2009) N-terminal amphipathic helix as a trigger of hemolytic activity in antimicrobial peptides: a case study in laticins. *FEBS Lett* **583**: 2425-2428
- Poole K (2001) Multidrug resistance in Gram-negative bacteria. *Curr Opin Microbiol* **4**: 500-508

- Porter CJ, Schuch R, Pelzek AJ, Buckle AM, McGowan S, Wilce MC, Rossjohn J, Russell R, Nelson D, Fischetti VA, Whisstock JC (2007) The 1.6 Å crystal structure of the catalytic domain of PlyB, a bacteriophage lysin active against *Bacillus anthracis*. *J Mol Biol* **366**: 540-550
- Powell JR, Ausubel FM (2008) Models of *Caenorhabditis elegans* infection by bacterial and fungal pathogens. *Methods Mol Biol* **415**: 403-427
- Pritchard DG, Dong S, Kirk MC, Cartee RT, Baker JR (2007) LambdaSa1 and LambdaSa2 prophage lysins of *Streptococcus agalactiae*. *Appl Environ Microbiol* **73**: 7150-7154
- Qureshi N, Perera PY, Shen J, Zhang G, Lenschat A, Splitter G, Morrison DC, Vogel SN (2003) The proteasome as a lipopolysaccharide-binding protein in macrophages: differential effects of proteasome inhibition on lipopolysaccharide-induced signaling events. *J Immunol* **171**: 1515-1525
- Radermacher SW, Schoop VM, Schluesener HJ (1993) Bactenecin, a leukocytic antimicrobial peptide, is cytotoxic to neuronal and glial cells. *J Neurosci Res* **36**: 657-662
- Raetz CR, Whitfield C (2002) Lipopolysaccharide endotoxins. *Annu Rev Biochem* **71**: 635-700
- Ralston DJ, Lieberman M, Baer B, Krueger AP (1957) Staphylococcal virolysin, a phage-induced lysin; its differentiation from the autolysis of normal cells. *J Gen Physiol* **40**: 791-807
- Rashel M, Uchiyama J, Ujihara T, Uehara Y, Kuramoto S, Sugihara S, Yagyu K, Muraoka A, Sugai M, Hiramatsu K, Honke K, Matsuzaki S (2007) Efficient elimination of multidrug-resistant *Staphylococcus aureus* by cloned lysin derived from bacteriophage phi MR11. *J Infect Dis* **196**: 1237-1247
- Reiter B, Oram JD (1963) Group N Streptococcal Phage Lysin. *J Gen Microbiol* **32**: 29-32
- Resch G, Moreillon P, Fischetti VA (2011) A stable phage lysin (Cpl-1) dimer with increased antipneumococcal activity and decreased plasma clearance. *Int J Antimicrob Agents* **38**: 516-521
- Rice KC, Bayles KW (2008) Molecular control of bacterial death and lysis. *Microbiol Mol Biol Rev* **72**: 85-109
- Rocchetta HL, Burrows LL, Lam JS (1999) Genetics of O-antigen biosynthesis in *Pseudomonas aeruginosa*. *Microbiol Mol Biol Rev* **63**: 523-553
- Rodriguez-Rubio L, Martinez B, Rodriguez A, Donovan DM, Garcia P (2012) Enhanced staphylolytic activity of the *Staphylococcus aureus* bacteriophage vB_SauS-phiPLA88 HydH5 virion-associated peptidoglycan hydrolase: fusions, deletions, and synergy with LysH5. *Appl Environ Microbiol* **78**: 2241-2248
- Russel M, Linderoth NA, Sali A (1997) Filamentous phage assembly: variation on a protein export theme. *Gene* **192**: 23-32
- Rutten L, Geurtsen J, Lambert W, Smolenaers JJ, Bonvin AM, de Haan A, van der Ley P, Egmond MR, Gros P, Tommassen J (2006) Crystal structure and catalytic mechanism of the LPS 3-O-deacylase PagL from *Pseudomonas aeruginosa*. *Proc Natl Acad Sci U S A* **103**: 7071-7076
- Ryu J, Han K, Park J, Choi SY (2003) Enhanced uptake of a heterologous protein with an HIV-1 Tat protein transduction domains (PTD) at both termini. *Mol Cells* **16**: 385-391
- Sadovskaya I, Brisson JR, Lam JS, Richards JC, Altman E (1998) Structural elucidation of the lipopolysaccharide core regions of the wild-type strain PAO1 and O-chain-deficient mutant strains AK1401 and AK1012 from *Pseudomonas aeruginosa* serotype O5. *Eur J Biochem* **255**: 673-684
- Samuel G, Hogbin JP, Wang L, Reeves PR (2004) Relationships of the *Escherichia coli* O157, O111, and O55 O-antigen gene clusters with those of *Salmonella enterica* and *Citrobacter freundii*, which express identical O antigens. *J Bacteriol* **186**: 6536-6543
- Santos SB, Kropinski AM, Ceysens PJ, Ackermann HW, Villegas A, Lavigne R, Krylov VN, Carvalho CM, Ferreira EC, Azeredo J (2011) Genomic and Proteomic Characterization of the Broad-Host-Range *Salmonella* Phage PVP-SE1: Creation of a New Phage Genus. *Journal of Virology* **85**: 11265-11273
- Sao-Jose C, Parreira R, Vieira G, Santos MA (2000) The N-terminal region of the *Oenococcus oeni* bacteriophage fOg44 lysin behaves as a bona fide signal peptide in *Escherichia coli* and as a cis-inhibitory element, preventing lytic activity on oenococcal cells. *J Bacteriol* **182**: 5823-5831
- Sass P, Bierbaum G (2007) Lytic activity of recombinant bacteriophage phi11 and phi12 endolysins on whole cells and biofilms of *Staphylococcus aureus*. *Appl Environ Microbiol* **73**: 347-352
- Sass P, Jansen A, Szekat C, Sass V, Sahl HG, Bierbaum G (2008) The lantibiotic mersacidin is a strong inducer of the cell wall stress response of *Staphylococcus aureus*. *BMC Microbiol* **8**: 186
- Sato H, Feix JB (2006) Peptide-membrane interactions and mechanisms of membrane destruction by amphipathic alpha-helical antimicrobial peptides. *Biochim Biophys Acta* **1758**: 1245-1256

- Sato H, Feix JB (2008) Lysine-enriched cecropin-mellitin antimicrobial peptides with enhanced selectivity. *Antimicrob Agents Chemother* **52**: 4463-4465
- Savalia D, Severinov K, Molineux I Genomic sequences and analysis of several T7-like bacteriophages. Unpublished.
- Sawyer JG, Martin NL, Hancock RE (1988) Interaction of macrophage cationic proteins with the outer membrane of *Pseudomonas aeruginosa*. *Infect Immun* **56**: 693-698
- Schiffelers R, Storm G, Bakker-Woudenberg I (2001) Liposome-encapsulated aminoglycosides in pre-clinical and clinical studies. *J Antimicrob Chemother* **48**: 333-344
- Schindler PR, Teuber M (1978) Ultrastructural study of *Salmonella* Typhimurium treated with membrane-active agents: specific reaction dansylchloride with cell envelope components. *J Bacteriol* **135**: 198-206
- Schittek B (2012) The multiple facets of dermcidin in cell survival and host defense. *J Innate Immun* **4**: 349-360
- Schleifer KH, Kandler O (1972) Peptidoglycan types of bacterial cell walls and their taxonomic implications. *Bacteriol Rev* **36**: 407-477
- Schmelcher M, Tchang VS, Loessner MJ (2011) Domain shuffling and module engineering of *Listeria* phage endolysins for enhanced lytic activity and binding affinity. *Microb Biotechnol* **4**: 651-662
- Schmelcher M, Donovan DM, Loessner MJ (2012a) Bacteriophage endolysins as novel antimicrobials. *Future Microbiol* **7**: 1147-1171
- Schmelcher M, Powell AM, Becker SC, Camp MJ, Donovan DM (2012b) Chimeric phage lysins act synergistically with lysostaphin to kill mastitis-causing *Staphylococcus aureus* in murine mammary glands. *Appl Environ Microbiol* **78**: 2297-2305
- Schmelcher M, Waldherr F, Loessner MJ (2012c) *Listeria* bacteriophage peptidoglycan hydrolases feature high thermoresistance and reveal increased activity after divalent metal cation substitution. *Appl Microbiol Biotechnol* **93**: 633-643
- Schmidtchen A, Frick IM, Andersson E, Tapper H, Bjorck L (2002) Proteinases of common pathogenic bacteria degrade and inactivate the antibacterial peptide LL-37. *Mol Microbiol* **46**: 157-168
- Schroder-Borm H, Willumeit R, Brandenburg K, Andra J (2003) Molecular basis for membrane selectivity of NK-2, a potent peptide antibiotic derived from NK-lysin. *Biochim Biophys Acta* **1612**: 164-171
- Schroder-Borm H, Bakalova R, Andra J (2005) The NK-lysin derived peptide NK-2 preferentially kills cancer cells with increased surface levels of negatively charged phosphatidylserine. *FEBS Lett* **579**: 6128-6134
- Schuch R, Nelson D, Fischetti VA (2002) A bacteriolytic agent that detects and kills *Bacillus anthracis*. *Nature* **418**: 884-889
- Schulert GS, Feltman H, Rabin SD, Martin CG, Battle SE, Rello J, Hauser AR (2003) Secretion of the toxin ExoU is a marker for highly virulent *Pseudomonas aeruginosa* isolates obtained from patients with hospital-acquired pneumonia. *J Infect Dis* **188**: 1695-1706
- Schwarze SR, Dowdy SF (2000) *In vivo* protein transduction: intracellular delivery of biologically active proteins, compounds and DNA. *Trends Pharmacol Sci* **21**: 45-48
- Sertic V. (1929) Procédé d'obtention de variantes du bactériophage adaptées à lyser des formes bactériennes secondaires. *Compt Rend Soc Biol* **100**: 612-614
- Serwer P, Hayes SJ, Thomas JA, Hardies SC (2007) Propagating the missing bacteriophages: a large bacteriophage in a new class. *Virology* **4**: 21
- Shai Y, Oren Z (2001) From "carpet" mechanism to de-novo designed diastereomeric cell-selective antimicrobial peptides. *Peptides* **22**: 1629-1641
- Sifri CD, Begun J, Ausubel FM (2005) The worm has turned--microbial virulence modeled in *Caenorhabditis elegans*. *Trends Microbiol* **13**: 119-127
- Simmaco M, Mignogna G, Barra D, Bossa F (1994) Antimicrobial peptides from skin secretions of *Rana esculenta*. Molecular cloning of cDNAs encoding esculentin and brevinins and isolation of new active peptides. *J Biol Chem* **269**: 11956-11961
- Smith AW (2005) Biofilms and antibiotic therapy: is there a role for combating bacterial resistance by the use of novel drug delivery systems? *Adv Drug Deliv Rev* **57**: 1539-1550
- Smith MG, Des Etages SG, Snyder M (2004) Microbial synergy via an ethanol-triggered pathway. *Mol Cell Biol* **24**: 3874-3884
- Soares JA, Roque de Carvalho MA, Cunha Santos SM, Mendonca RM, Ribeiro-Sobrinho AP, Brito-Junior M, Magalhaes PP, Santos MH, de Macedo Farias L (2010) Effectiveness of chemomechanical preparation with alternating use of sodium hypochlorite and EDTA in eliminating intracanal *Enterococcus faecalis* biofilm. *J Endod* **36**: 894-898

- Sobko AA, Kotova EA, Antonenko YN, Zakharov SD, Cramer WA (2006) Lipid dependence of the channel properties of a colicin E1-lipid toroidal pore. *J Biol Chem* **281**: 14408-14416
- Sobral CS, Gragnani A, Morgan J, Ferreira LM (2007) Inhibition of proliferation of *Pseudomonas aeruginosa* by KGF in an experimental burn model using human cultured keratinocytes. *Burns* **33**: 613-620
- Soding J, Biegert A, Lupas AN (2005) The HHpred interactive server for protein homology detection and structure prediction. *Nucleic Acids Res* **33**: 244-248
- Son B, Yun J, Lim JA, Shin H, Heu S, Ryu S (2012) Characterization of LysB4, an endolysin from the *Bacillus cereus*-infecting bacteriophage B4. *BMC Microbiol* **12**: 33
- Song PI, Park YM, Abraham T, Harten B, Zivony A, Neparidze N, Armstrong CA, Ansel JC (2002) Human keratinocytes express functional CD14 and toll-like receptor 4. *J Invest Dermatol* **119**: 424-432
- Steiner H (1982) Secondary structure of the cecropins: antibacterial peptides from the moth *Hyalophora cecropia*. *FEBS Lett* **137**: 283-287
- Stewart PS, Costerton JW (2001) Antibiotic resistance of bacteria in biofilms. *Lancet* **358**: 135-138
- Stiernagle T (2006) Maintenance of *C. elegans*. *WormBook*
- Stover CK, Pham XQ, Erwin AL, Mizoguchi SD, Warrener P, Hickey MJ, Brinkman FS, Hufnagle WO, Kowalik DJ, Lagrou M, Garber RL, Goltry L, Tolentino E, Westbrook-Wadman S, Yuan Y, Brody LL, Coulter SN, Folger KR, Kas A, Larbig K, Lim R, Smith K, Spencer D, Wong GK, Wu Z, Paulsen IT, Reizer J, Saier MH, Hancock RE, Lory S, Olson MV (2000) Complete genome sequence of *Pseudomonas aeruginosa* PAO1, an opportunistic pathogen. *Nature* **406**: 959-964
- Subbalakshmi C, Sitaram N (1998) Mechanism of antimicrobial action of indolicidin. *FEMS Microbiol Lett* **160**: 91-96
- Summer EJ, Gonzalez CF, Bomer M, Carlile T, Embry A, Kucherka AM, Lee J, Mebane L, Morrison WC, Mark L, King MD, LiPuma JJ, Vidaver AK, Young R (2006) Divergence and mosaicism among virulent soil phages of the *Burkholderia cepacia* complex. *J Bacteriol* **188**: 255-268
- Sun Q, Kutyl GF, Arockiasamy A, Xu M, Young R, Sacchettini JC (2009) Regulation of a muralytic enzyme by dynamic membrane topology. *Nat Struct Mol Biol* **16**: 1192-1194
- Sutherland IW (1999) Microbial polysaccharide products. *Biotechnol Genet Eng Rev* **16**: 217-229
- Tabor S, Richardson CC (1985) A bacteriophage T7 RNA polymerase/promoter system for controlled exclusive expression of specific genes. *Proc Natl Acad Sci U S A* **82**: 1074-1078
- Tan MW, Mahajan-Miklos S, Ausubel FM (1999) Killing of *Caenorhabditis elegans* by *Pseudomonas aeruginosa* used to model mammalian bacterial pathogenesis. *Proc Natl Acad Sci U S A* **96**: 715-720
- Taneja J, Mishra B, Thakur A, Dogra V, Loomba P (2010) Nosocomial blood-stream infections from extended-spectrum-beta-lactamase-producing *Escherichia coli* and *Klebsiella pneumonia* from GB Pant Hospital, New Delhi. *J Infect Dev Ctries* **4**: 517-520
- Taylor A, Das BC, Van Heijenoort J (1975) Bacterial-cell-wall peptidoglycan fragments produced by phage λ or Vi II endolysin and containing 1,6-anhydro-N-acetylmuramic acid. *Eur J Biochem* **53**: 47-54
- Taylor D, Whatling C, Kearney JN, Matthews B, Holland KT (1990) The effect of bacterial products on human fibroblast and keratinocyte detachment and viability. *Br J Dermatol* **122**: 23-28
- Thomas JA, Rolando MR, Carroll CA, Shen PS, Belnap DM, Weintraub ST, Serwer P, Hardies SC (2008) Characterization of *Pseudomonas chlororaphis* myovirus 201varphi2-1 via genomic sequencing, mass spectrometry, and electron microscopy. *Virology* **376**: 330-338
- Tourville DR, Johnstone DB (1966) Lactic streptococcal phage-associated lysin. I. Lysis of heterologous lactic streptococci by a phage-induced lysin. *J Dairy Sci* **49**: 158-162
- Tran AX, Lester ME, Stead CM, Raetz CR, Maskell DJ, McGrath SC, Cotter RJ, Trent MS (2005) Resistance to the antimicrobial peptide polymyxin requires myristoylation of *Escherichia coli* and *Salmonella Typhimurium* lipid A. *J Biol Chem* **280**: 28186-28194
- Trent MS, Pabich W, Raetz CR, Miller SI (2001a) A PhoP/PhoQ-induced Lipase (PagL) that catalyzes 3-O-deacylation of lipid A precursors in membranes of *Salmonella Typhimurium*. *J Biol Chem* **276**: 9083-9092
- Trent MS, Ribeiro AA, Lin S, Cotter RJ, Raetz CR (2001b) An inner membrane enzyme in *Salmonella* and *Escherichia coli* that transfers 4-amino-4-deoxy-L-arabinose to lipid A: induction on polymyxin-resistant mutants and role of a novel lipid-linked donor. *J Biol Chem* **276**: 43122-43131
- Triantaphyllopoulos DC, Quick AJ, Greenwalt TJ (1955) Action of disodium ethylenediamine tetracetate on blood coagulation; evidence of the development of heparinoid activity during incubation or aeration of plasma. *Blood* **10**: 534-544
- Twort FW (1915) An investigation on the nature of ultra-microscopic viruses. *Lancet* **11**:1241-1243

- Tzeng YL, Ambrose KD, Zughair S, Zhou X, Miller YK, Shafer WM, Stephens DS (2005) Cationic antimicrobial peptide resistance in *Neisseria meningitidis*. *J Bacteriol* **187**: 5387-5396
- Uccelletti D, Zanni E, Marcellini L, Palleschi C, Barra D, Mangoni ML (2010) Anti-Pseudomonas Activity of Frog Skin Antimicrobial Peptides in a *Caenorhabditis elegans* Infection Model: a Plausible Mode of Action In Vitro and In Vivo. *Antimicrobial Agents and Chemotherapy* **54**: 3853-3860
- Udaya Prakash NA, Jayanthi M, Sabarinathan R, Kanguene P, Mathew L, Sekar K (2010) Evolution, Homology Conservation, and Identification of Unique Sequence Signatures in GH19 Family Chitinases. *Journal of Molecular Evolution* **70**: 466-478
- Vaara M, Vaara T, Sarvas M (1979) Decreased binding of polymyxin by polymyxin-resistant mutants of *Salmonella* Typhimurium. *J Bacteriol* **139**: 664-667
- Vaara M, Vaara T (1981) Outer membrane permeability barrier disruption by polymyxin in polymyxin-susceptible and -resistant *Salmonella* Typhimurium. *Antimicrob Agents Chemother* **19**: 578-583
- Vaara M (1992) Agents that increase the permeability of the outer membrane. *Microbiol Rev* **56**: 395-411
- van Etten EW, ten Kate MT, Stearne LE, Bakker-Woudenberg IA (1995) Amphotericin B liposomes with prolonged circulation in blood: *in vitro* antifungal activity, toxicity, and efficacy in systemic candidiasis in leukopenic mice. *Antimicrob Agents Chemother* **39**: 1954-1958
- Varea J, Monterroso B, Saiz JL, Lopez-Zumel C, Garcia JL, Laynez J, Garcia P, Menendez M (2004) Structural and thermodynamic characterization of Pal, a phage natural chimeric lysin active against pneumococci. *J Biol Chem* **279**: 43697-43707
- Veiga-Crespo P, Ageitos JM, Poza M, Villa TG (2007) Enzybiotics: a look to the future, recalling the past. *J Pharm Sci* **96**: 1917-1924
- Verkleij AJ, Zwaal RF, Roelofsen B, Comfurius P, Kastelij D, van Deenen LL (1973) The asymmetric distribution of phospholipids in the human red cell membrane. A combined study using phospholipases and freeze-etch electron microscopy. *Biochim Biophys Acta* **323**: 178-193
- Vinogradov EV, Knirel YA, Shashkov AS, Kochetkov NK (1987) Determination of the degree of amidation of 2-deoxy-2-formamido-D-galacturonic acid in O-specific polysaccharides of *Pseudomonas aeruginosa* O4 and related strains. *Carbohydr Res* **170**: 1-4
- Vollmer W (2008) Structural variation in the glycan strands of bacterial peptidoglycan. *FEMS Microbiol Rev* **32**: 287-306
- Vollmer W, Blanot D, de Pedro MA (2008a) Peptidoglycan structure and architecture. *FEMS Microbiol Rev* **32**: 149-167
- Vollmer W, Joris B, Charlier P, Foster S (2008b) Bacterial peptidoglycan (murein) hydrolases. *FEMS Microbiol Rev* **32**: 259-286
- Vukov N, Moll I, Blasi U, Scherer S, Loessner MJ (2003) Functional regulation of the *Listeria monocytogenes* bacteriophage A118 holin by an intragenic inhibitor lacking the first transmembrane domain. *Mol Microbiol* **48**: 173-186
- Walsh S, Shah A, Mond J (2003) Improved pharmacokinetics and reduced antibody reactivity of lysostaphin conjugated to polyethylene glycol. *Antimicrob Agents Chemother* **47**: 554-558
- Watt FM, Matthey DL, Garrod DR (1984) Calcium-induced reorganization of desmosomal components in cultured human keratinocytes. *J Cell Biol* **99**: 2211-2215
- Weaver LH, Gritter GI, Remington SJ, Gray TM, Isaacs NW (1985) Comparison of goose-type, chicken-type, and phage-type lysozymes illustrates the changes that occur in both amino acid sequence and three-dimensional structure during evolution. *J Mol Evol* **21**: 97-111
- Whitchurch CB, Tolker-Nielsen T, Ragas PC, Mattick JS (2002) Extracellular DNA required for bacterial biofilm formation. *Science* **295**: 1487
- Wiese A, Munstermann M, Gutschmann T, Lindner B, Kawahara K, Zahringer U, Seydel U (1998) Molecular mechanisms of polymyxin B-membrane interactions: direct correlation between surface charge density and self-promoted transport. *J Membr Biol* **162**: 127-138
- Wilks JC, Slonczewski JL (2007) pH of the cytoplasm and periplasm of *Escherichia coli*: rapid measurement by green fluorescent protein fluorimetry. *J Bacteriol* **189**: 5601-5607
- Willis M, Forssen E (1998) Ligand-targeted liposomes. *Adv Drug Deliv Rev* **29**: 249-271
- Wohlkonig A, Huet J, Looze Y, Wintjens R (2010) Structural relationships in the lysozyme superfamily: significant evidence for glycoside hydrolase signature motifs. *PLoS One* **5**: e15388
- Wren BW (1991) A family of clostridial and streptococcal ligand-binding proteins with conserved C-terminal repeat sequences. *Mol Microbiol* **5**: 797-803
- Wuthiekanun V, Peacock SJ (2006) Management of melioidosis. *Expert Rev Anti Infect Ther* **4**: 445-455
- Xu M, Struck DK, Deaton J, Wang IN, Young R (2004) A signal-arrest-release sequence mediates export and control of the phage P1 endolysin. *Proc Natl Acad Sci U S A* **101**: 6415-6420

- Xu M, Arulandu A, Struck DK, Swanson S, Sacchettini JC, Young R (2005) Disulfide isomerization after membrane release of its SAR domain activates P1 lysozyme. *Science* **307**: 113-117
- Xue D, Shaham S, Horvitz HR (1996) The *Caenorhabditis elegans* cell-death protein CED-3 is a cysteine protease with substrate specificities similar to those of the human CPP32 protease. *Genes Dev* **10**: 1073-1083
- Yan L, Adams ME (1998) Lycotoxins, antimicrobial peptides from venom of the wolf spider *Lycosa carolinensis*. *J Biol Chem* **273**: 2059-2066
- Yang L, Harroun TA, Weiss TM, Ding L, Huang HW (2001) Barrel-stave model or toroidal model? A case study on melittin pores. *Biophys J* **81**: 1475-1485
- Yin LM, Edwards MA, Li J, Yip CM, Deber CM (2012) Roles of hydrophobicity and charge distribution of cationic antimicrobial peptides in peptide-membrane interactions. *J Biol Chem* **287**: 7738-7745
- Yokoi KJ, Kawahigashi N, Uchida M, Sugahara K, Shinohara M, Kawasaki K, Nakamura S, Taketo A, Kodaira K (2005) The two-component cell lysis genes holWMY and lysWMY of the *Staphylococcus warneri* M phage varphiWMY: cloning, sequencing, expression, and mutational analysis in *Escherichia coli*. *Gene* **351**: 97-108
- Yoneyama F, Imura Y, Ohno K, Zendo T, Nakayama J, Matsuzaki K, Sonomoto K (2009) Peptide-lipid huge toroidal pore, a new antimicrobial mechanism mediated by a lactococcal bacteriocin, lacticin Q. *Antimicrob Agents Chemother* **53**: 3211-3217
- Yonezawa A, Kuwahara J, Fujii N, Sugiura Y (1992) Binding of tachyplesin I to DNA revealed by footprinting analysis: significant contribution of secondary structure to DNA binding and implication for biological action. *Biochemistry* **31**: 2998-3004
- Yoshino Y, Kitazawa T, Kamimura M, Tatsuno K, Ota Y, Yotsuyanagi H (2011) *Pseudomonas putida* bacteremia in adult patients: five case reports and a review of the literature. *J Infect Chemother* **17**: 278-282
- Young R (1992) Bacteriophage lysis: mechanism and regulation. *Microbiol Rev* **56**: 430-481
- Young R, Blasi U (1995) Holins: form and function in bacteriophage lysis. *FEMS Microbiol Rev* **17**: 191-205
- Zasloff M (1987) Magainins, a class of antimicrobial peptides from *Xenopus* skin: isolation, characterization of two active forms, and partial cDNA sequence of a precursor. *Proc Natl Acad Sci U S A* **84**: 5449-5453
- Zhou Z, Ribeiro AA, Lin S, Cotter RJ, Miller SI, Raetz CR (2001) Lipid A modifications in polymyxin-resistant *Salmonella* Typhimurium: PMRA-dependent 4-amino-4-deoxy-L-arabinose, and phosphoethanolamine incorporation. *J Biol Chem* **276**: 43111-43121

Other sources

Jaarverslag 2008-Lab MCT activiteiten 2007, Jean-Paul Pirnay

Peeters L (2009) De strategie van uw vijands grootste vijand ontrafeld. V.B.I.-Master thesis studentenprijs

FACULTEIT BIO-INGENIEURSWETENSCHAPPEN
DEPARTEMENT BIOSYSTEMEN
AFDELING GENTECHNOLOGIE
Kasteelpark Arenberg 21 box 2462
B-3001 HEVERLEE, BELGIUM
tel. + 32 16 32 96 72
maarten.walmagh@biw.kuleuven.be

